METAMORPHIC PETROLOGY, PRESSURE-TEMPERATURE PATHS, AND TECTONIC EVOLUTION OF THE MOUNT CUBE QUADRANGLE, NEW HAMPSHIRE AND VERMONT

by

DANIEL LEWIS ORANGE

S.B. Massachusetts Institute of Technology
(1985)

Submitted to the Department of
Earth, Atmospheric and Planetary Sciences
in Partial Fulfillment of the
Requirements of the Degree of

MASTER OF SCIENCE

at the

MASSACHUSETTS INSTITUTE OF TECHNOLOGY

May, 1985

Signature of Author ______________________________
Department of Earth, ~~Atmo~~spheric and
Planetary Sciences, May 14, 1985

Certified by ______________________________
Frank Spear
Thesis Supervisor

Accepted by ______________________________
Theodore Madden
Chairman, Departmental Committee on Graduate Students

Room 14-0551
77 Massachusetts Avenue
Cambridge, MA 02139
Ph: 617.253.5668 Fax: 617.253.1690
Email: docs@mit.edu
http://libraries.mit.edu/docs

DISCLAIMER OF QUALITY

Due to the condition of the original material, there are unavoidable flaws in this reproduction. We have made every effort possible to provide you with the best copy available. If you are dissatisfied with this product and find it unusable, please contact Document Services as soon as possible.

Thank you.

Some pages in the original document contain text /figures
That runs off the edge of the page.

(Pages A-100 & A-101)

METAMORPHIC PETROLOGY, PRESSURE-TEMPERATURE PATHS, AND TECTONIC EVOLUTION

OF THE MOUNT CUBE QUADRANGLE, NEW HAMPSHIRE AND VERMONT

by

DANIEL LEWIS ORANGE

Submitted to the Department of Earth, Atmospheric and Planetary Sciences
in Partial Fulfillment of the Requirements for the Degree of
Master of Science in Geology
May 14, 1985

ABSTRACT

The metamorphic history of a traverse across the Mount Cube Quadrangle and Rumney Quadrangle, New Hampshire and Vermont, is investigated using optical petrology, geothermometry, geobarometry, and a garnet zoning technique for calculating pressure-temperature paths. A variety of pelitic assemblages are present across 15 kilometers of strike; these range from garnet-staurolite-kyanite rocks in the Archertown Brook (AB) and Cottonstone Mountain (CM) localities to the west to garnet-chlorite-chloritoid grade rocks along the Northey Hill Line (NHL) to garnet-cordierite-sillimanite grade rocks in the Baker Pond (BP) locality to the east.

Pressure-temperature calculations indicate peak metamorphic conditions in the CM locality of 3.75-5.25 kb and 460-510°C. The AB locality presents peak conditions of 3-5 kb and 425-500°C. The NHL has lower peak conditions of 2-3 kb and 450-490°C. Samples from the Jacobs Brook Recumbant Syncline (JBRS) have a peak temperature of 490-575°C and the pressure is not constrained. The BP locality has peak conditions of 3-5 kb and 490-550°C.

The garnets analyzed from the NHL exhibit small zoning gradients. In contrast, garnets from the other localities have steep zoning profiles. Quantitative P-T paths are presented for all but the JBRS and BP localities. Pressure-temperature paths computed from samples west of the NHL suggest up to two nappe-stage compressional events, a near-isothermal dome-stage decompression, and a late-stage isobaric cooling correlative with the development of the Sunday Mountain Cleavage Belt. The NHL samples show an isothermal decompression associated with the Sunday Mountain Cleavage Belt. The isobaric cooling seen west of the NHL is thought to be due either to thrusting of hot rocks over cold rocks or the folding of isosotherms during a late stage back-folding event. Neither of these hypotheses can accomodate the isothermal decompression seen in the NHL samples. A structural break is inferred along the Northey Hill Line, where detailed mapping shows drastic thinning of beds and the highest intensity of the Sunday Mountain Cleavage Belt. To create the P-T path geometry seen in the NHL, this locality must have experienced differential uplift with respect to the samples to the west. In this interpretation, the isobaric cooling in the samples to the west is produced prior to the uplift along the NHL.

Thesis Supervisor: Frank Spear
Title: Associate Professor of Geology

ACKNOWLEDGEMENTS

First and foremost, I would like to thank my father for four years of financial and emotional support. I would like to thank my advisor, Frank Spear, for his enthusiasm and support all along, and for the insight he has given me towards metamorphic processes. Don Hickmott deserves special note, for without his constant availability and untiring fielding of my many questions, this thesis would never have been completed. I would also like to thank Dr. Douglas Rumble III for the many days he spent with me in the field explaining the structures of the Mount Cube Quadrangle, and also for providing thin sections for the Cottonstone Mountain and Archertown Brook localities. I would like to thank Larry McKenna for his field assistance. Doug Chor (MIT) and Dave Lange (Harvard) provided many hours of instruction and assistance in the use of the electron microprobe.

Matt Kohn typed the majority of this thesis, while Don Hickmott and Dr. Jane Selverstone provided thorough and thought-provoking commentaries on the rough drafts. Dr. Jane Selverstone also provided valuable insight into the role of fluids in metamorphic equilibria. Beatrice Silny assisted in putting the final draft together.

I wish to thank my fellow Masters student, Rosamond Kinzler, for the months of constant support and assistance. I wish to thank the Thursday Mandarin lunch/Thirsty Ear crowd for giving me something to look forward to every week, no matter how badly things were going. I wish to thank Baker House for the support in the tough times and three years of the good times.

Lastly, I would like to thank John Carl Adams, with whom I'm about to depart on a trip around the world. By consenting to this impending insanity, he has helped get through this year. Let the good times roll!

"Hoya Saxa!!"
(What Rocks!)

TABLE OF CONTENTS

TABLE OF CONTENTS (cont'd.)

LIST OF TABLES AND APPENDICES

LIST OF FIGURES

LIST OF FIGURES (cont'd.)

LIST OF FIGURES (cont'd.)

LIST OF FIGURES (cont'd.)

Chapter 1: INTRODUCTION

With the advent and development of quantitative metamorphic petrology, the study of ancient mountain belts has taken a giant step forward. The use of geothermometers, geobarometers, and garnet zoning techniques have given geologists a strong tool for deciphering the tectonic evolution of orogenic events. The purpose of this thesis is to bring together quantitative and qualitative metamorphic petrology with detailed structural mapping in order to solve structural controversies and provide information about the tectonic evolution of a region in west-central New Hampshire.

The rocks studied in this thesis come from the Mount Cube Quadrangle, New Hampshire and Vermont, and the Rumney Quadrangle, New Hampshire. The location of these quadrangles is shown in Figure 1. This region was chosen for a study of this type for several reasons. First of all, the metamorphic grade is appropriate. Secondly, garnet-bearing pelitic rocks are abundant in the area in all structural and stratigraphic levels. Lastly, there is a complex interplay of structural styles throughout the area.

The next chapter of this thesis covers the regional geology and geologic setting. The third chapter discusses the methods of investigation. The fourth chapter describes the five localities chosen for in-depth study. Optical petrology is covered in the fifth chapter. The purpose of this chapter is to relate porphyroblast growth to fabric development, and, from regional and outcrop analysis, to structural development. Chapter six investigates the "peak" metamorphic conditions by the use of geothermometers and geobarometers. The different "peak" conditions experienced by the five localities are then discussed. Chapter seven presents the microprobe analyses, with special attention given to garnet zoning. In chapter eight the garnet zoning profiles are combined with matrix and inclusion mineral analyses, geothermometry, and geobarometry in order to determine pressure-temperature paths. Chapter nine synthesizes the qualitative and quantitative petrologic data into a regional framework.

In addition, to the author's knowledge, few studies of this sort have been carried out -- ie: looking specifically at the pressure-temperature-growth paths of porphyroblastic crystals in order to resolve andnd define the contrasting thermal/tectonic histories of a series of rocks across strike in a metamorphic belt. This thesis also attempts this analysis on a cross-sectional scale smaller than that which has been analyzed before.

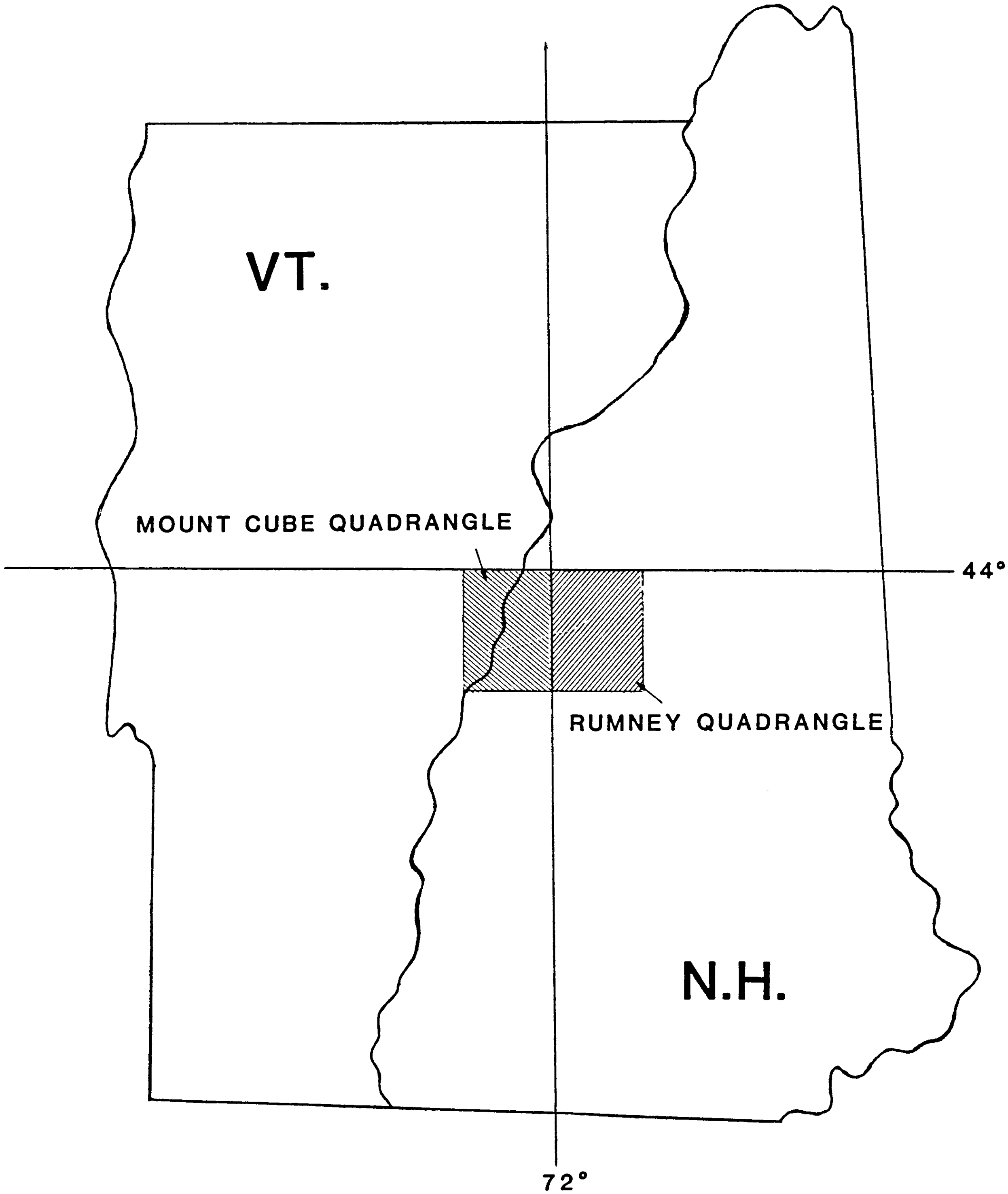

Figure 1: Map of New Hampshire and Vermont, showing the location of the Mount Cube and Rumney Quadrangles.

Chapter 2: REGIONAL GEOLOGY

The majority of the study area lies west of the Bronson Hill Anticlinorium and east of the Ammonoosuc Fault. Detailed mapping has been carried out by Hadley (1938, 1942) and more recently by Rumble (1969), thus the regional geology and structure are fairly well understood. Additionally, P-T path investigations have been carried out in the southwest corner of the Mount Cube Quadrangle by Spear and Rumble (1985). A detailed geologic map of the area is presented as Figure 2. The cross-section of Thompson, et al. (1968) is extrapolated north to the Mount Cube Quadrangle and is included as Figure 3.

The metasedimentary rocks found in the study area range in age from mid-Ordovician to lower Devonian, and comprise two distinct stratigraphic successions separated by the late Ordovician-early Silurian Taconic unconformity (Rumble, 1969). The older of the two successions is made up of the Cambrian (?) to Ordovician Albee Formation, the Middle Ordovician Ammonoosuc Volcanics, and the Middle Ordovician Partridge Formation. These underlie the Taconic unconformity in the western and central part of the Mount Cube Quadrangle at angles varying from sub-parallel to relatively shallow. In the eastern part of the quadrangle, the Taconic unconformity is underlain by the Ammonoosuc volcanics and the Mascoma Granite (Rumble, 1969). Pre-Silurian rocks of these types occur from southern New England to central Quebec, and their paleogeography has been interpreted to be that of a volcanic arc with associated volcaniclastic and deep-sea sediments (Berry, 1968).

Above the Taconic unconformity the stratigraphic succession consists of the Silurian Clough Formation, the Silurian Fitch Formation, and the Devonian Littleton Formation. These rocks represent the metasedimentary

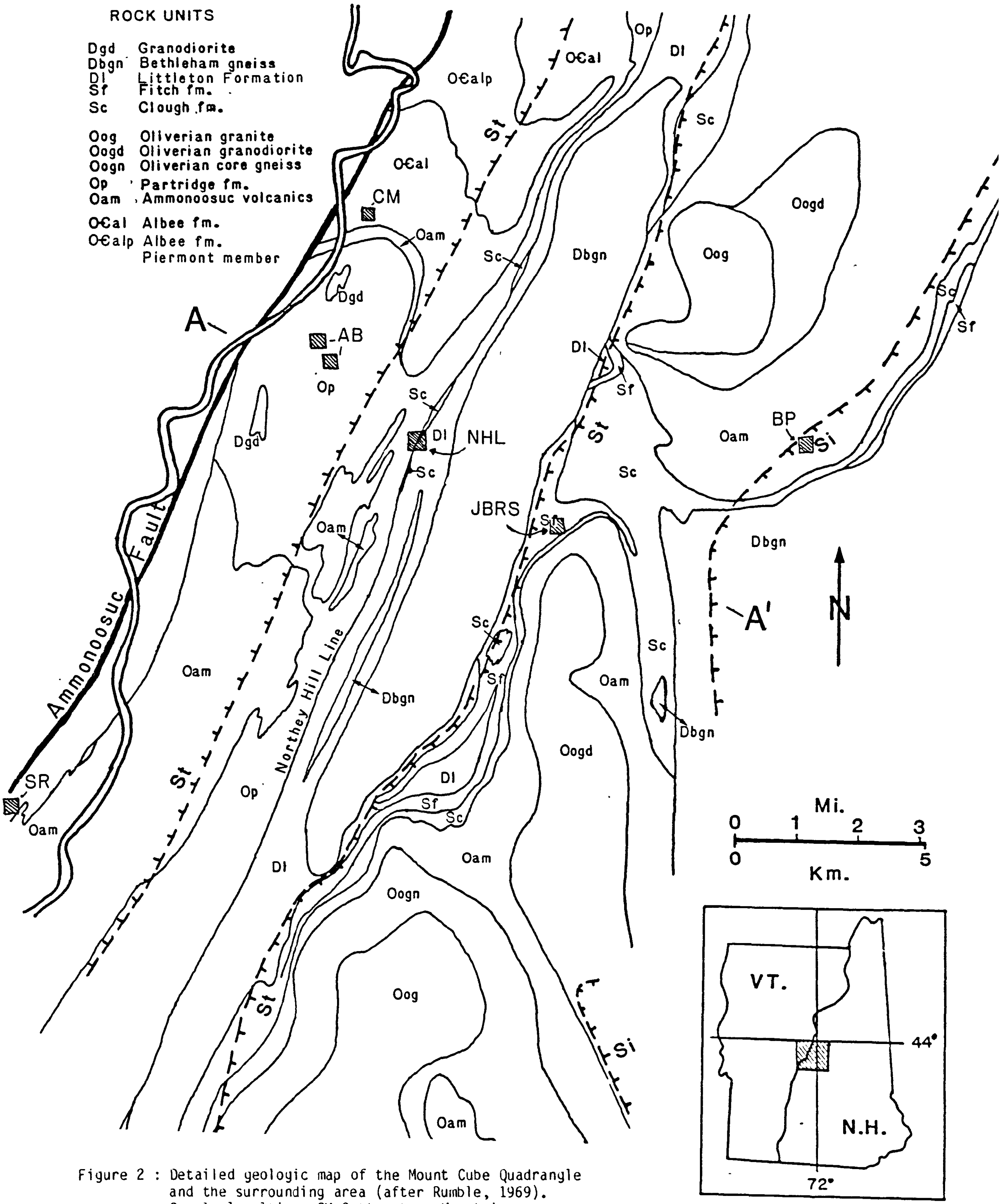

Figure 2 : Detailed geologic map of the Mount Cube Quadrangle and the surrounding area (after Rumble, 1969). Sample localties: CM=Cottonstone Mountain, AB=Archertown Brook, SR=Spear and Rumble (1985), NHL=Northey Hill Line, JBRS=Jacobs Brook Recumbant Syncline, BP=Baker Pond. Cross-section A-A' is shown in Figure 3.

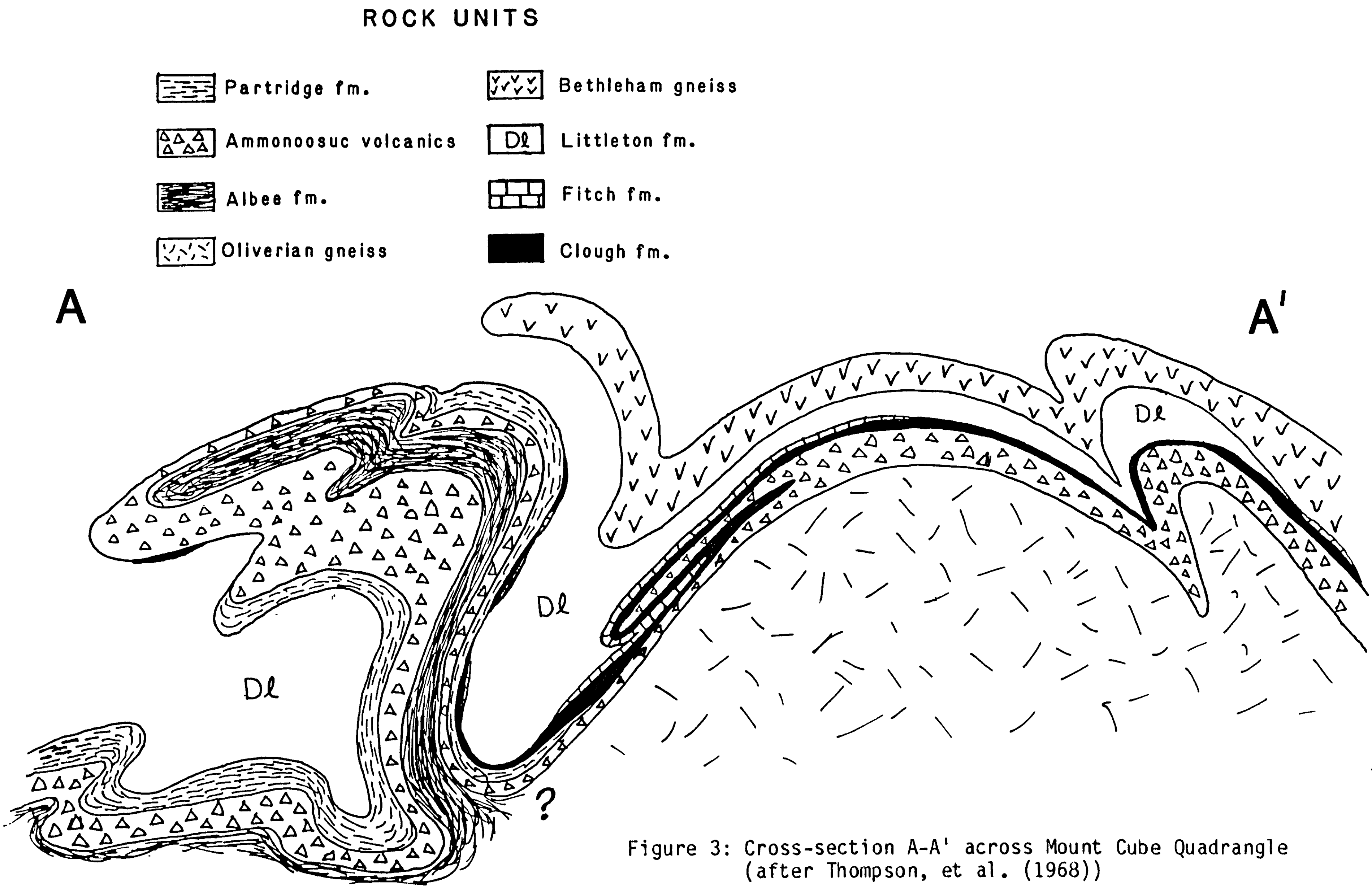

Figure 3: Cross-section A-A' across Mount Cube Quadrangle (after Thompson, et al. (1968))

equivalents of the classic transgressive sequence: conglomerates and sandstones grading up to shallow water carbonates and deep water sands and shales. Figure 4 illustrates the stratigraphic relationships and descriptions of these formations.

Rumble (1969) presents evidence for at least five phases of deformation in the Mount Cube Quadrangle, of which three are discussed in a regional context by Thompson, et. al. (1968). The first phase of deformation is recorded by the angular Taconic unconformity. In the core of the Sunday Mountain Anticline, rocks of the Littleton Formation truncate the contact between the conformable Ammonoosuc Volcanics and the Partridge Formation (Rumble, 1969). It is unclear whether the rocks of Ordovician age were metamorphosed prior to the Taconic unconformity. Rumble (1969) found no structures in the Ordovician meta-sediments that were not related to the multi-phase Acadian events. This, coupled with the sub-parallel unconformity, suggests that if the Ordovician section were metamorphosed, it was probably to a low degree, and any metamorphism and structure that developed has been obliterated by the strong Acadian metamorphism and deformation.

The second phase of deformation manifests itself in the existence of small to large scale recumbant and reclined isoclinal folds. The larger scaled structures of this kind are called nappes. This stage was first recognized by Thompson (1954, 1956) with the discovery of inverted stratigraphic sections on Skitchewaug Mountain. Since then Thompson, et al. (1968) and Robinson, et al. (1979) have recognized four westerly facing nappes in Massachusetts and southern New England. In ascending order, these are known as the Cornish Nappe, the Bernardston Nappe, the Skitchewaug Nappe, and the Fall Mountain Nappe. The Skitchewaug Nappe has been recognized in the Mount Cube Quadrangle, and may possibly exist as far

SUMMARY OF THE STRATIGRAPHY OF THE IN THE
MOUNT CUBE QUADRANGLE

Only Ordovician through Devonian metasediments and metavolcanics.
(After Rumble, 1969, and Lyons, 1983)

AGE	NAME	LITHOGRAPHIC DESCRIPTION
Lower Devonian	Littleton Formation	Grey to greenish-grey pelitic schist, graded-bedded metapelite, minor felsic volcanics, and occasional calc-siliscates.
Upper Silurian (?)	Fitch Foramtion	Calc-silicate granulite, quartz-feldspar granofels, calcareous quartz-mica schist, interbedded quartzite, minor coticule.
Lower Silurian	Clough Formation	Quartzite quartz-mica schist, quartz meta-conglomerate.
	UNCONFORMITY	
Middle Ordovician (?)	Partridge Formation	Black, rusty-weathering, sulfidic-graphitic schist.
Middle Ordovician (?)	Ammonoosuc Volcanics	Amphibolite, amphibole gneiss, minor fine-grained biotite gneiss
Ordovician and Cambrian (?)	Albee Foramtion	Interlayered quartzite, quartz-mica schist, and mica schist, giving the characteristic "pinstriped" appearance. Piermont member consists of dark grey, graphitic mica schist.

Figure 4: Stratigraphy of the Mount Cube Area

north as the Moosilauke Quadrangle (north of the Owls Head Dome) (Rumble, 1969). In the Mount Cube Quadrangle, the Skitchewaug Nappe is folded over the Smarts Mountain Dome in the core of the Bronson Hill Anticlinorium (Rumble, 1969). The recumbantly folded outcrops of the Clough and Fitch Formations lying west of the dome have been interpreted to be in or near the nose or anticlinal hinge of the nappe (Rumble, 1969). The nappe stage fold axes in the Mount Cube Quadrangle may trend to the northwest (in the western part, near the Connecticut River) or to the north-east (eastern Mount Cube, adjacent to the Rumney Quadrangle) (Rumble, 1969).

The third phase of deformation resulted in the dominant structural style seen in the Mount Cube Quadrangle. This phase, termed the Dome Stage, produced the major anticline and syncline pair (Cottonstone Mountain Anticline and Hardscrabble Syncline) as well as the Bronson Hill Anticlinorium (Rumble, 1969). The name is derived from the en echelon configuration of the Oliverian gneiss domes occupying the core of the Bronson Hill zone from west-central Massachusetts to southern Maine. This deformational phase is responsible for New Hampshire's prominent northeast trending structural and topographic fabric. In the Mount Cube Quadrangle, the Dome Stage deformation is responsible for the large scale anticline and syncline, as well as smaller scale tight folds, all of these having axes gently plunging to the northeast or southwest (Rumble, 1969).

The fourth deformational feature recognized in the Mount Cube Quadrangle is the Sunday Mountain cleavage belt. This deformational feature produces a foliation that strikes northeasterly and dips vertically. This foliation folds the earlier dome stage foliation. The Sunday Mountain cleavage belt varies in intensity across strike, reaching a maximum along the Northey Hill Line and dying out rapidly to the east and west.

The fifth phase of deformation recognized by Rumble consists of the high angle faulting along the Ammonoosuc fault and its associated retrograde metamorphism. Thompson, et al. (1968) consider this fault to be Mesozoic in age, based on correlation with definitive Mesozoic faults in western Massachusetts. Deformation is localized to within 150 meters of the fault and consists of small kink folds and conjugate folds. The metamorphism is manifested by intense retrogradation of porphyroblastic crystals, specifically kyanite, staurolite, garnet and biotite by muscovite and chlorite (Rumble, 1969). Mylonite zones also occur along the fault Hadley (1942) and Rumble (1969) report that this is the only mylonite found in the Mount Cube Quadrangle.

Chapter 3: METHODS OF INVESTIGATION

Field work for this thesis was carried out for ten weeks during the summer of 1984. The field work consisted of regional reconnaissance of structural and stratigraphic relations, sample collection, and detailed tape and compass mapping of a small section of the Northey Hill Line. Eighty samples were collected, of which 75 were chosen for thin section study. Addition samples and thin sections were provided by Prof. Spear and Dr. Rumble. These samples were concentrated in four suites occurring perpendicular to strike across the Mount Cube Quadrangle and the Rumney Quadrangle.

For the purposes of this thesis, the term 'matrix mineral' will be used to describe any porphyroblast that appears to be in contact with the major matrix phases of the rock, as opposed to 'inclusion mineral,' which will be used to describe phases that appear to be completely encased in other minerals.

Most of microprobe analyses were performed on the MIT in-house three spectrometer Materials Analysis Corporation automated electron microprobe. Two types of analyses were made, conventional oxide analyses and garnet "turbo-probe" analyses. Oxide analyses were made using a 15 kV accelerating voltage and a 30 nanoamp beam flag current. The beam size was approximately 4-6 microns in diameter (T. Grove, pers. comm.). The electron beam was defocussed slightly when analyzing plagioclase so that the sodium was not boiled away. The LiF diffraction crystal was used for analyzing iron, manganese, and chromium. The PET crystal was used for potassium, calcium, and titanium. Finally, the TAP crystal was used for sodium, magnesium, aluminum, and silicon. Counts were made for twenty seconds or 100,000 counts.

"Turbo-probe" garnet analyses were made using a 15 kV accelerating voltage and a beam flag current of 60 nanoamps. These analyses were carried out to obtain detailed maps of garnet zoning. Iron, manganese, calcium, and magnesium were the only elements analyzed for, whereas silicon and aluminum were assumed to occur in stoichiometric proportions. Since iron and manganese were both on the LiF crystal, this routine analyzed a single spot twice--once for iron, calcium, and magnesium, and a second time for manganese, calcium, and magnesium. The two values for calcium and magnesium were averaged. Counts were made for ten seconds or 100,000 counts. This accelerated method allowed for a large number of analyses to be made in a short time. Indeed, it was found that each analysis took less than forty seconds. Several spots in the garnet in 79-449f were investigated using both the normal oxide routine and turbo-probe. Most analyses varied by less than 0.5% (ie: well within counting statistics); a maximum error of 1.0% was observed.

Empirical oxide corrections were made using the method of Bence-Albee (1968) and the improved alpha corrections of Albee and Ray (1970). On-line corrections were made using a Tracor Norther TN-2000 microcomputer equipped with Flextran.

MIT's MAC probe was dismantled in January, 1985 to make way for a new JEOL-73 superprobe. As a result, all analyses carried out after January were performed using Harvard University's 3 spectrometer CAMECA probe. This probe used a 15 kV accelerating voltage and a 15 nanoamp beam flag current. The minerals analyzed using the Harvard probe characteristically gave low weight percent totals. The reason for this is unknown. In comparison, however, analyses from the same sample gave similar values for

An content in plagioclase as well as for almandine-pyrope-spessartine-grossular components in garnet. Because of this, low total Harvard analyses are considered acceptable.

Chapter 4: SAMPLE LOCALITIES

The samples investigated and analyzed for this thesis come from five major locations in the Mount Cube Quad and environs. These will be discussed from west to east, covering the exact location, description, physiography, and mineralogy of each. Figure 5 shows the Mount Cube Quadrangle, the neighboring Rumney Quadrangle, and a blow-up of the area of interest, including the location and number of each sample collected. Figure 6 shows the sample localities with respect to the geologic map.

The most westerly locality is on the western ridge of Cottonstone Mountain (CM). The sample from this locality (67-82e) was provide by Dr. Rumble and comes from the pinstriped pelitic schists of the Albee Formation.

The next area of collection is termed Archertown Brook (AB). This locality, lying in the west-central ninth of the Mount Cube Quadrangle, covers 3 square kilometers, with the samples coming from the bed of Archertown Brook and Jacobs Brook. The samples are all from a grey muscovite-biotite-quartz (± staurolite) unit mapped as the Black Schist Member of the Orfordville Formation by Rumble (1969). This formation is now believed to be correlative with the Partridge Formation (Rumble, pers. comm.).

The third area of sample collection is located 4 kilometers to the east of the Archertown Brook locality, along the bed of Jacobs Brook near the Route 25a bridge. This sample location lies directly on the trace of the Northey Hill Line (NHL). This locality is in the central ninth of the Mount Cube Quadrangle, and covers an area of 1 square kilometer. The samples from this area consist of grey to black micaceous to graphitic schists of the Littleton and Partridge formations.

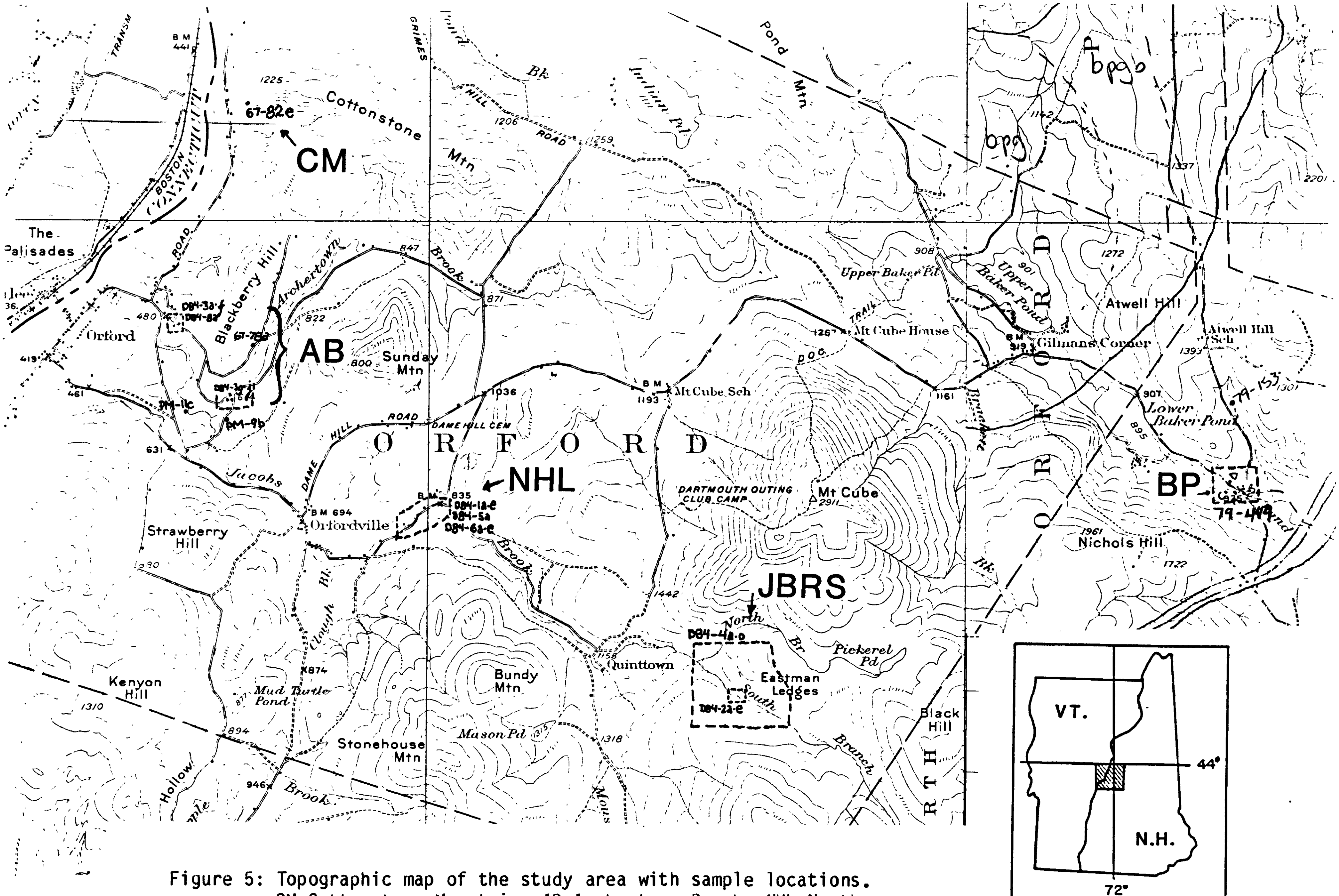

Figure 5: Topographic map of the study area with sample locations.
CM=Cottonstone Mountain, AB=Archertown Brook, NHL=Northey Hill Line, JBRS=Jacobs Brook Recumbant Syncline, BP=Baker Pond.

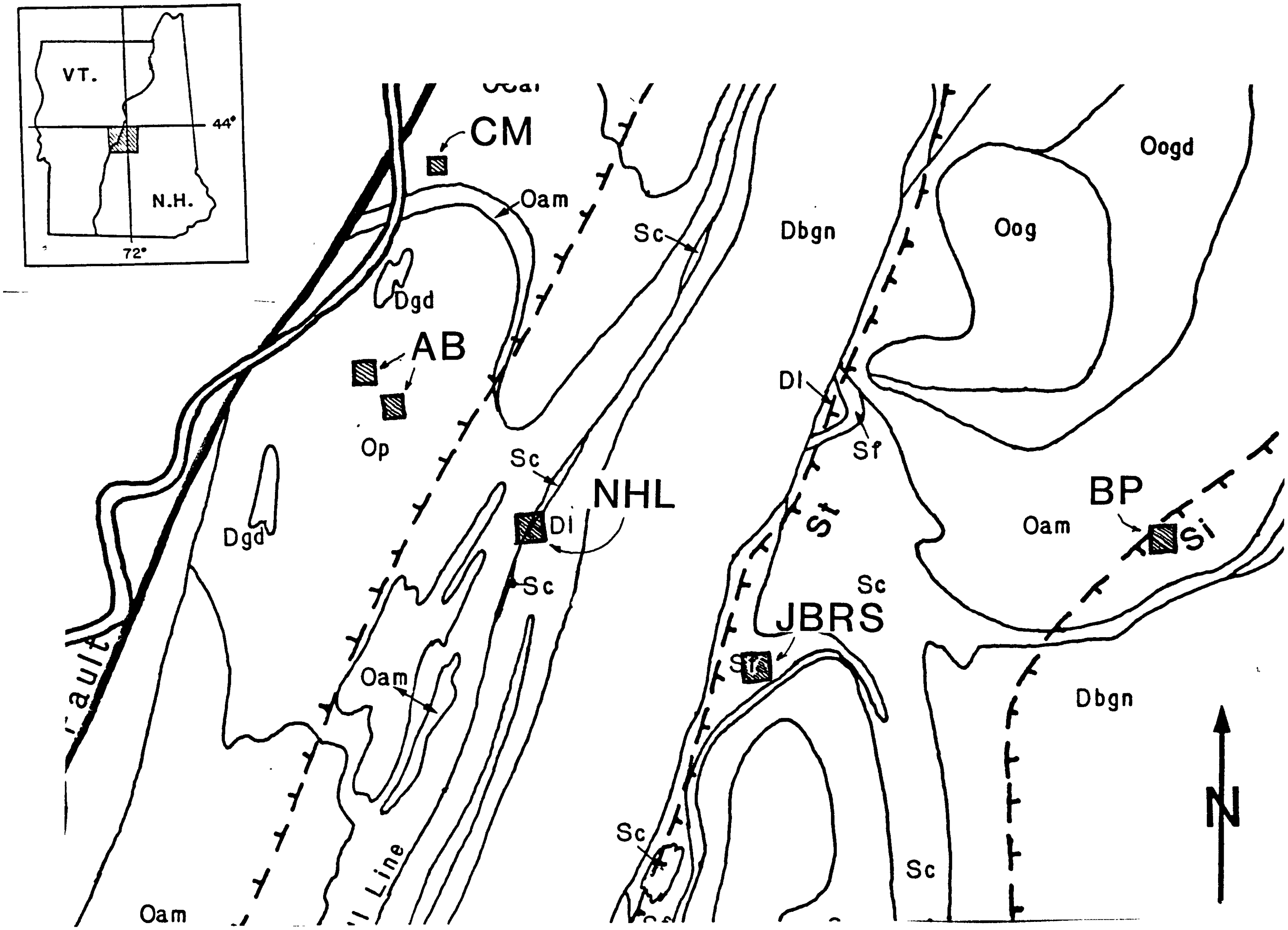

Figure 6: Geologic map of the study area with sample locations.
CM=Cottonstone Mountain, AB=Archertown Brook, NHL=Northey
Hill Line, JBRS=Jacobs Brook Recumbant Syncline, BP=Baker Pond.

The fourth area of collection lies on the southwest ridge of Mount Cube in the west-central ninth of the quadrangle. This locality lies in what Rumble (1969) has mapped as a recumbant syncline. The majority of the samples were collected in or near to Jacobs Brook, so this location will be termed the Jacobs Brook Recumbant Syncline (JBRS). The samples from this area consist of garnet bearing quartzites and muscovite-garnet schists of the Clough Formation.

The most easterly collection site lies 5 kilometers to the east, outside the Mount Cube Quadrangle in the Warren 7 1/2' Quadrangle (Rumney 15' quadrangle) in the vicinity of Baker Pond. For this reason, these shall be denoted as the Baker Pond (BP) samples. These samples were collected in the summer of 1979 by Prof. Spear and consist of the biotite-cordierite-garnet schists of the Ammonoosuc Volcanics.

Chapter 5: SYSTEMATIC MINERALOGY

The rocks in the study area include pelites, amphibolites and gneisses, all of medium to medium-high metamorphic grade. This thesis will concentrate only on the pelitic assemblages, because, in terms of reactions, geothermometry and geobarometry, and garnet zoning, these are the most well understood. The major prograde minerals recognized in the study area include: quartz, muscovite, biotite, garnet, plagioclase, chlorite, chloritoid, staurolite, cordierite, kyanite, and sillimanite (prismatic and fibrolite). The opaque minerals observed include graphite, ilmenite, rutile, and pyrrhotite. Common accessory minerals observed include zircon, sphene, apatite, and tourmaline. Retrograde chlorite and sericite are also observed. Due to differences in mineral assemblages as well as in morphological textures, the rocks from each different area will be discussed separately. A comparitive table of the systematic mineralogies from the five localities is included at the end of this chapter.

As was mentioned in the regional geology section, the rocks in the study area have been exposed to three phases of metamorphic deformation. These are the nappe stage, the dome stage, and the Sunday Mountain cleavage belt stage. To facilitate communication, these will be referred to as D1, D2, and D3; the associated folds will be termed F1, F2, and F3, and the resutant S-surfaces (foliations, schistosities, and cleavages) will be referred to as S1, S2, and S3.

COTTONSTONE MOUNTAIN

The sample from the Cottonstone Mountain locality have two evident schistosities. The first is weakly defined and occurs as small muscovite crenulations preserved in garnet shadows. The latter schistosity is the only one evident in outcrop, and is moderately developed in thin-section (Fig. 7). The early textural feature is interpreted to be due to the nappe stage (D1) deformation, while the latter schistosity is interpreted by Rumble (pers. comm.) to be due dome stage deformation (D2). The strong Sunday Mountain cleavage seen in the Archertown Brook and Northey Hill Line localities does not appear in the Cottonstone Mountain sample. This cleavage belt reaches a maximum in the Northey Hill Line and dies out both to the east and west.

One sample (67-82e) was studied in detail from the Cottonstone Mountain locality. The assemblage found in this sample is garnet-biotite-staurolite-kyanite-plagioclase-quartz-muscovite.

Garnet

Garnets from sample 67-82e are rolled and have the dominant schistosity (S2) warped around them. Garnets are rotated 10-50° as evidenced by opaque inclusion trails. This implies that garnets were growing during the dome stage deformation, and may have also experienced earlier growth. Garnets from this sample contain inclusions of chlorite, biotite, plagioclase, and ilmenite. No chlorite occurs as a matrix phase in this sample.

Staurolite

The staurolites from this sample occur as large idioblastic to sub-idioblastic crystals. These staurolites always form after the latest foliation (F2) and are commonly 2-3 cm in length. Staurolites in 67-82e also mantle garnet. The inclusions present in these staurolites consist in

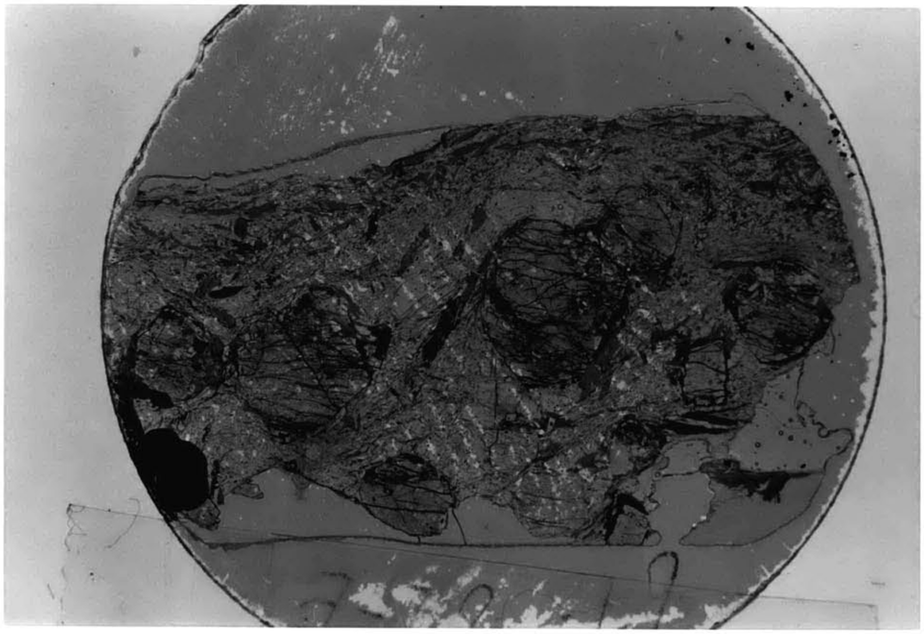

5 mm

a) plane light

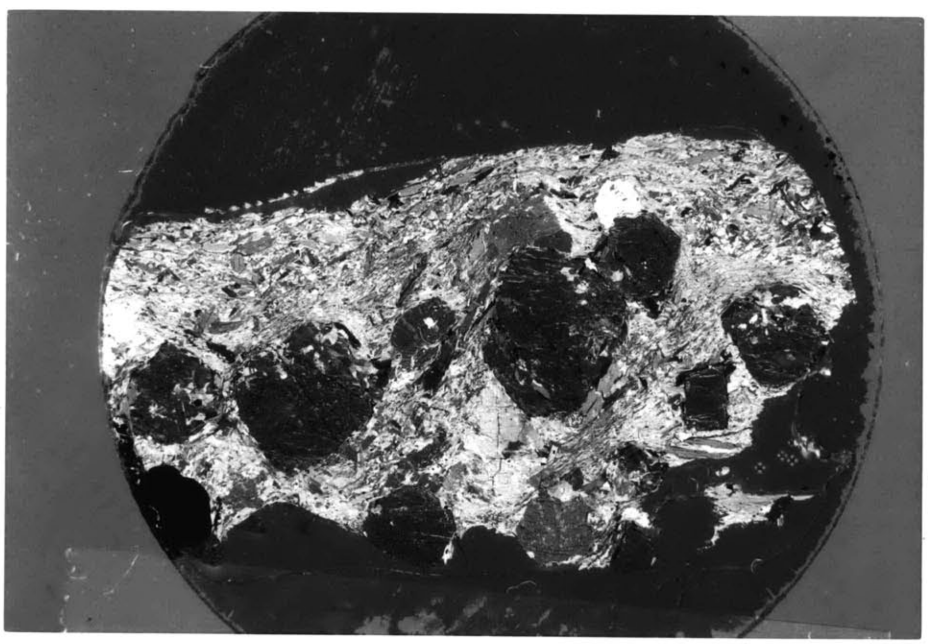

b) crossed polars

Figure 7: Cottonstone Mountain: Sample 67-82e; Showing representative fabric and porphyroblast morphology.

the most part of opaques, although quartz and plagioclase are also found. These inclusions lie parallel to the dominant schistosity.

Kyanite

Kyanite is found overprinting the dominant schistosity (S2) in sample 67-82e and contain inclusions that are parallel to the this schistosity. Kyanites also mantle garnets and are randomly oriented with respect to the schistosity.

PHASE EQUILIBRIA

The presence of chlorite as inclusions in garnet suggest that the Cottonstone Mountain sample has developed from a garnet-biotite-chlorite assemblage to garnet-biotite-chlorite-staurolite to garnet-biotite-staurolite-kyanite (Albee, 1972). The textural relations of porphyroblasts as well as inclusion relations are synthesized in the paragenesis diagram shown in Figure 8.

ARCHERTOWN BROOK

The Archertown Brook samples contain two visible schistosities. The first schistosity is visible in thin section as inclusion trails in rotated biotites, chlorites, staurolites and garnets. All of these phases have the latest schistosity wrapped around them. These samples occur at the edge of the region affected by the Sunday Mountain cleavage belt, and this feature is interpreted to be responsible for the prominent schistosity visible in thin-section (Fig. 9). The cleavage in the Sunday Mountain belt strikes northeast and dips steeply, with foliations becoming more vertical to the east. This foliation is parallel to the dome stage deformation in this area. As such, it is not clear whether the earlier schistosity evident in the Archertown Brook samples is due to dome stage or nappe stage deformation. Early folds are seen in the field, and these are tight, with

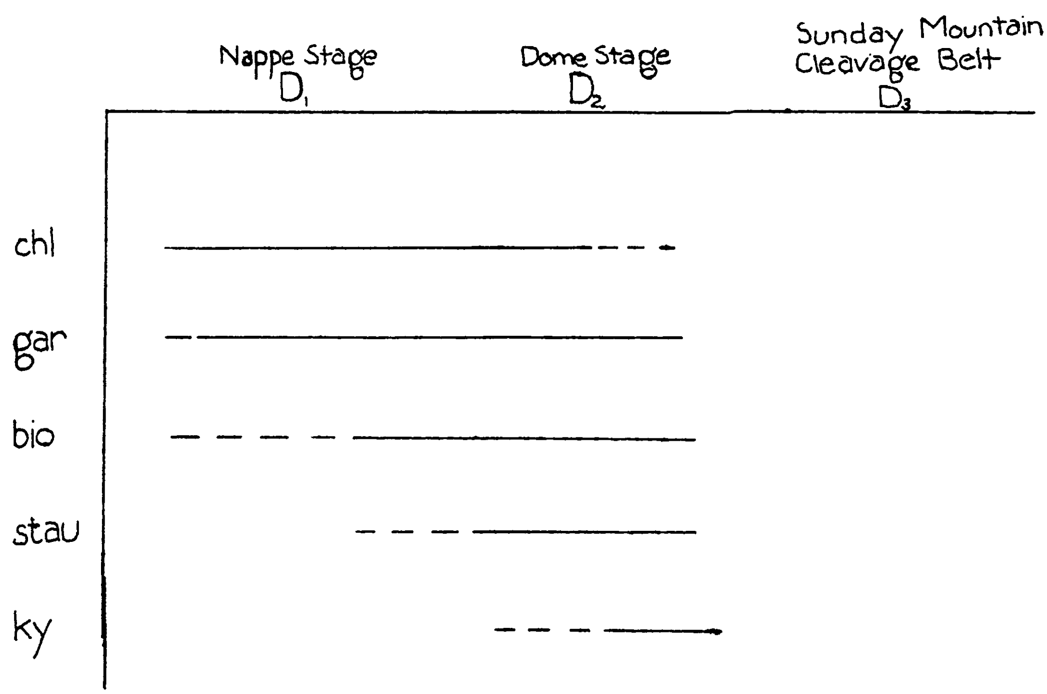

Figure 8: Paragenesis diagram, Cottonstone Mountain.

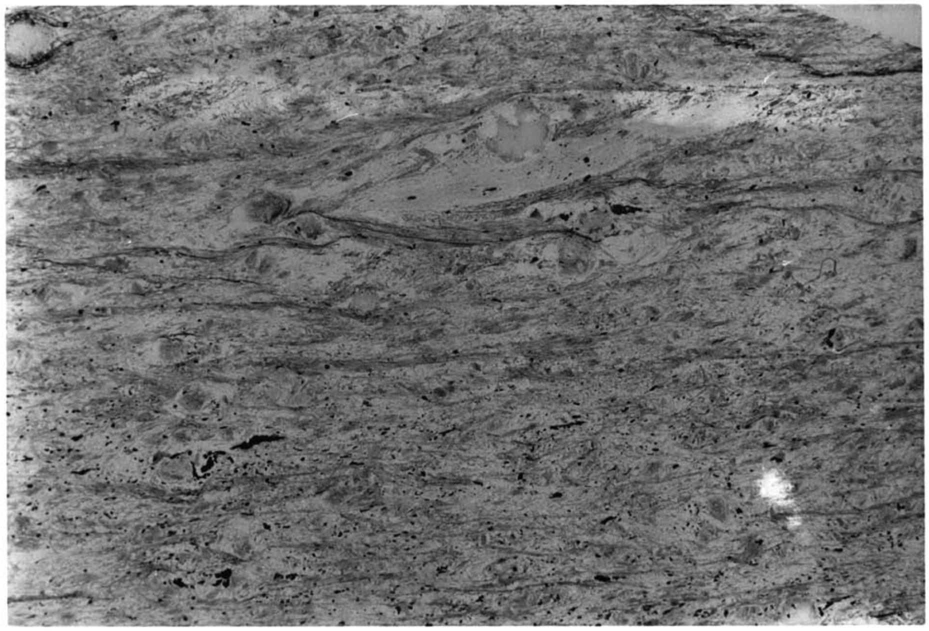

a) plane light

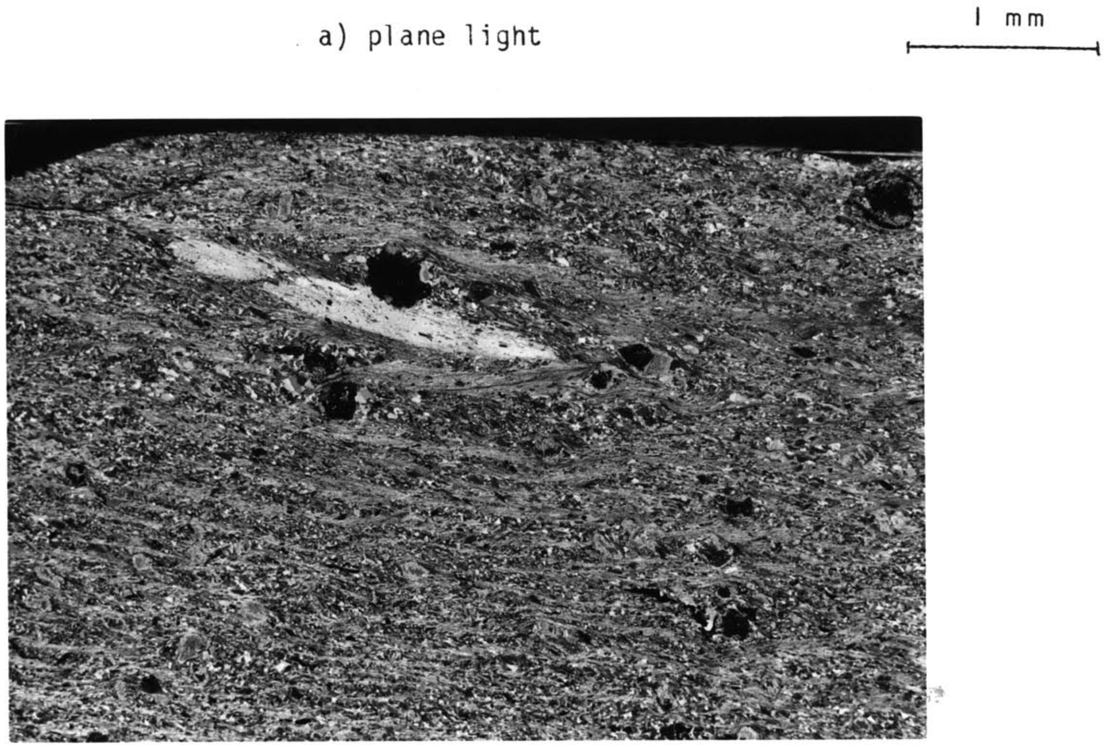

b)crossed polars

Figure 9: Archertown Brook: Sample D84-3d; Showing textural relations and porphyroblast growth features.

near vertical axial planes and noses that plunge slightly to the northeast (N15E 25). These folds are interpreted to be dome stage (D2) from similarities with folds reported by Rumble (1969). This interpretation suggests that the foliation folded in these early folds is nappe stage (F1) and the foliation overprinting these folds is Sunday Mountain stage (F3).

Plagioclase

Plagioclase occurs in one sample, D84-3a, as large (1.5-2.0 mm) poikiloblastic, twinned grains that occur in biotite clusters. These plagioclases contain dusty inclusion trails at high angle to the predominant foliation, indicative of formation prior to the development of the Sunday Mountain cleavage belt.

Biotite

The striking feature of the porphyroblastic biotites from Archertown Brook is the inclusion trails; dusty paths of opaques are seen in biotites in virtually every sample (Fig. 10). These inclusion trails, which are crenulated, define the earlier phases of deformation and occur within rotated biotites. These biotites have the latest foliation wrapping around them, suggesting that they grew early on in the second phase of deformation, absorbing the early crenulated foliation. As deformation continued, the biotites rotated and developed pressure shadows. Thus the crenulation cleavage exhibited within these biotites is at an angle to that of the matrix. The angle of the crenulation cleavage within the biotites to the dominant schistosity varies from 30° to sub-parallel. The interpretation of the latest schistosity in these samples as being due to the Sunday Mountain cleavage belt (S3) suggests that the crenulation preserved by these biotites is dome stage (S2).

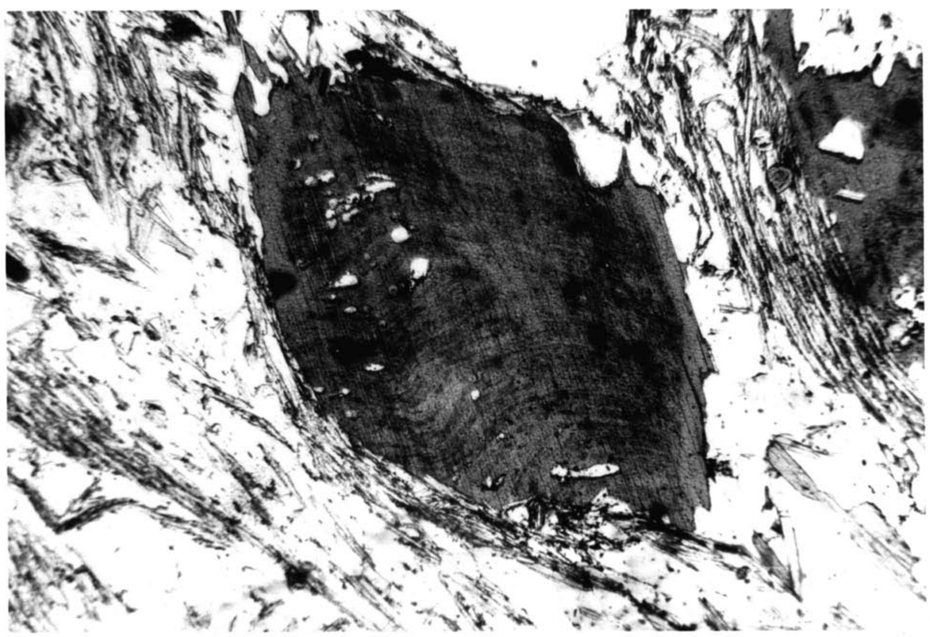

1 mm

Figure 10: Porphyroblastic biotites from Archertown Brook sample D84-3b. Dusty inclusion trails define early schistosity. Later schistosity is seen wrapping around biotites.

Garnet

The garnets from Archertown Brook clearly developed before or during the last deformational phase (D3). The latest foliation (F3) wraps around the garnet, and rotated garnets are common. The rotation observed in the Archertown Brook garnets varies from 90° to 20°, with a mean of approximately 35°. These textural relations indicate that garnet grew prior to or during the development of the Sunday Mountain cleavage belt. Due to the parallelism of this deformation to that of the dome stage deformation, these garnets may have formed and rolled during the dome stage and only have the Sunday Mountain cleavage warped around them.

Inclusions in garnet include quartz, biotite, chlorite, muscovite, a Ca-Al silicate, plagioclase, tourmaline, ilmenite, and other opaques. In one sample, 67-78a, garnet occurs as an inclusion in staurolite.

Some garnets also exhibit varying degrees of retrogradation. Sericite and chlorite overprint garnet in several samples--some almost to the point of complete retrogradation. In Sample D84-3g, the garnets are partially replaced by sericite and carbonate. The carbonate totally replaces the garnet, leaving a grain that is part garnet and sericite and part carbonate pseudomorph. No non-retrograde carbonate phases are seen in this sample. This suggests late stage CO_2-rich fluid infiltration of this sample.

Staurolite

Staurolites in Archertown Brook occur as poikiloblastic grains, whose inclusion trails of quartz and dusty opaques lie at odd angles to the latest foliation. The dominant schistosity (S3) is seen wrapping around the staurolite. In sample D84-3b the staurolites contain crenulations of an earlier schistosity (S2) and are rotated as much as 120° (Fig. 11). These syn-tectonic staurolites rarely exceed 3 mm in length, are always

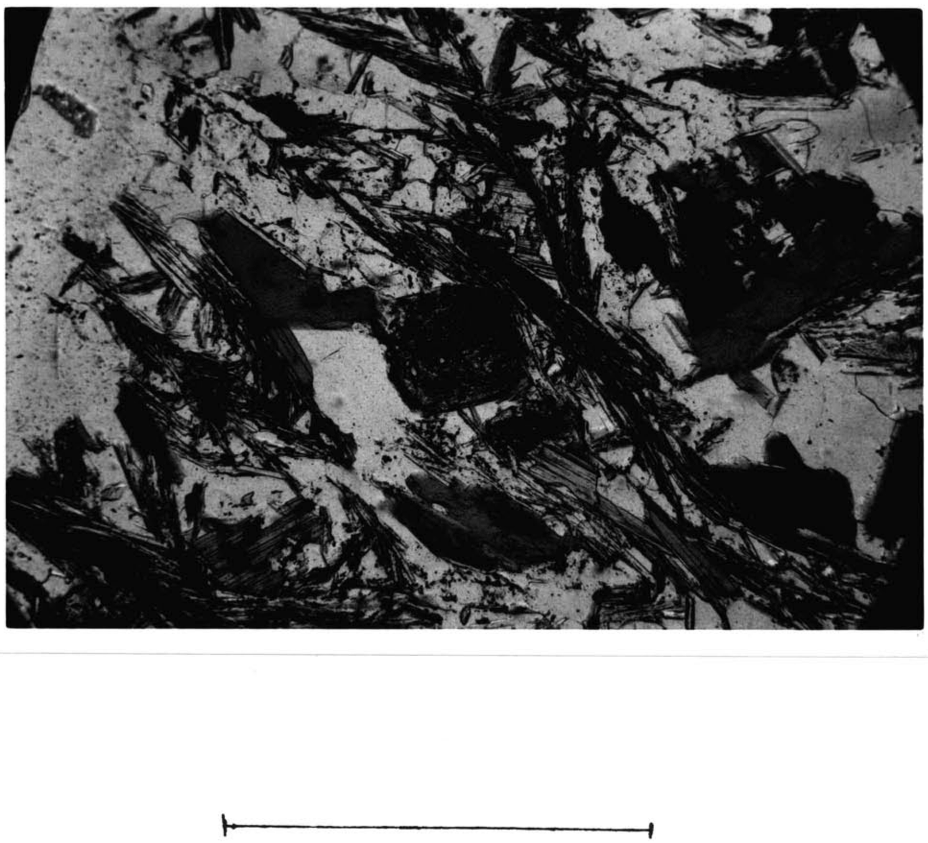

Figure 11: Archertown Brook: Sample D84-3b; Showing rotated staurolite containing crenulations of the earlier schistosity (S2).

poikilitic and always contain dusty inclusion trails of the previous foliation. The textural relations suggest that staurolite formed prior to or in the early phases of the development of the Sunday Mountain cleavage belt, thus absorbing the crenulated dome stage schistosity.

In Archertown Brook west of Sunday Mountain, large post-foliation staurolites exhibit partial to wholesale retrogradation. The grains, up to 4 cm long, contain, from rim to core, chlorite, muscovite, and a very small core of unaltered staurolite. This is the same sample with late replacement of garnet by sericite and carbonate. Clearly, this sample exhibits very late stage water and carbonate-rich fluid infiltration.

Chlorite

Prograde chlorite is present in four samples from Archertown Brook. In one of the samples, D84-3c, it occurs in the same thin section as staurolite. This relationship seems to be due to different bulk composition, and, therefore, different equilibria. In the three other samples, chlorite occurs as large (1.5-3.0 mm) grains rotated with respect to the latest foliation. These chlorites commonly contain dusty inclusion trails, with angles to the primary foliation of 30° to sub-parallel (Fig. 12). This texture indicates that chlorites formed prior to or contamporaneous with the late-stage Sunday Mountain cleavage belt.

Prograde chlorite also occurs as inclusions in garnet in sample 67-82e. No matrix chlorite appears in this sample; indeed, the matrix assemblage consists of garnet-staurolite-kyanite-biotite.

Kyanite

Kyanite is found in one of the samples from the Archertown Brook locality. It occurs as large (1.5-3.0 mm) bladed crystals that are folded in the latest schistosity. This suggests that kyanite formed prior to the development of the Sunday Mountain cleavage belt.

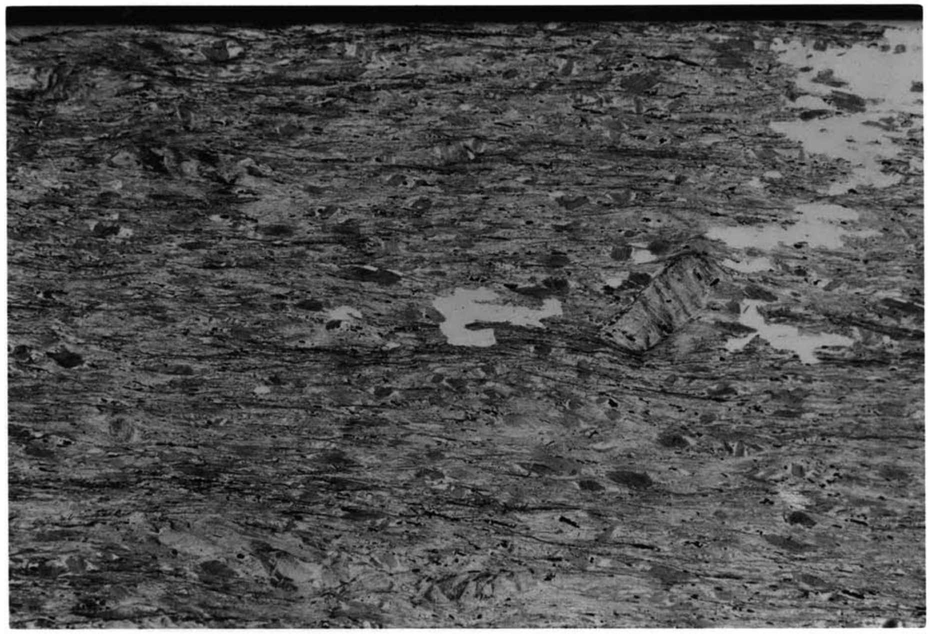

a) plane light

1 mm

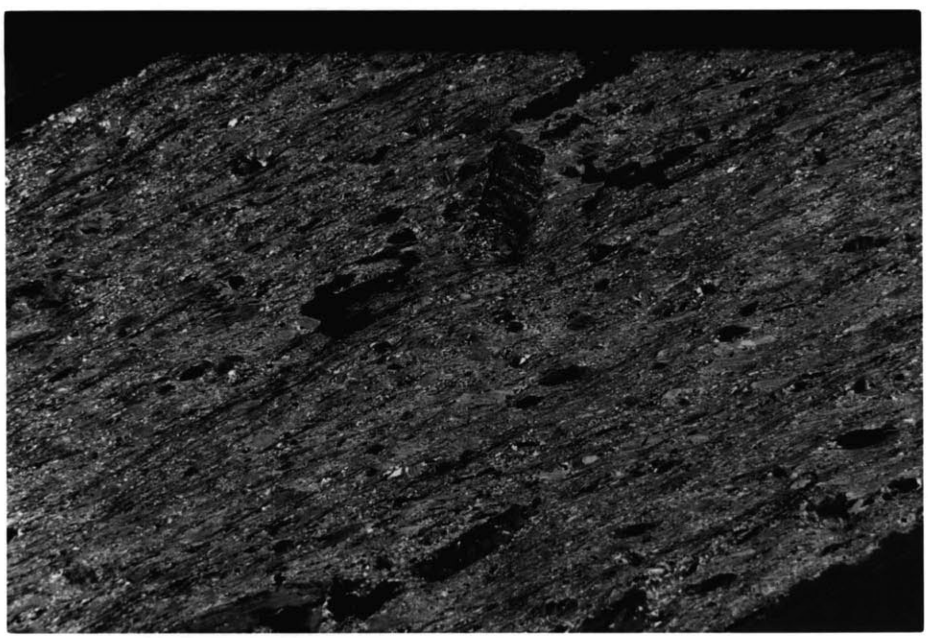

b) crossed polars

Figure 12: Archertown Brook: Sample D84-3g; Showing rotated chlorite.

PHASE EQUILIBRIA

The presence of chlorite as inclusions in the kyanite bearing samples, as well as textural information, suggest that the samples from the Archertown Brook locality have evolved as a series of assemblages starting with garnet-biotite-chlorite. A reasonable sequence of assemblages (Albee, in the evolution of these samples is garnet-biotite-chlorite to garnet-biotite-chlorite-staurolite to garnet-biotite-staurolite-kyanite. The relationships of porphyroblast growth to structural development is shown schematically in Figure 13.

NORTHEY HILL LINE

Rocks along the Northey Hill Line have experienced a profound late-stage deformation. The Northey Hill Line occurs at the maximum amplification of the Sunday Mountain cleavage belt. As such, the earlier phases of deformation are only seen in rare crenulations of muscovite or in rotated porphyroblasts, specifically plagioclase and garnet. Strong crenulations perpendicular to the latest foliation are seen in the field; these strike N85E and dip vertically, while the predominant foliation strikes north-northeasterly to northeasterly and dips within ten degress of vertical. The fabric evident in rotated crystals may be the early Sunday Mountain cleavage that has been progressively rotated or it may be the vestiges of dome-stage deformation. The combination of textures seen in the field and in rotated crystals suggests that the early deformation evident in thin section is dome stage, while the strong foliation is Sunday Mountain stage (Fig. 14).

In order to better constrain the structural interaction of the Northey Hill Line, a detailed geologic map was made during the summer field season. Mapping was carried out using tape and compass methods along a one

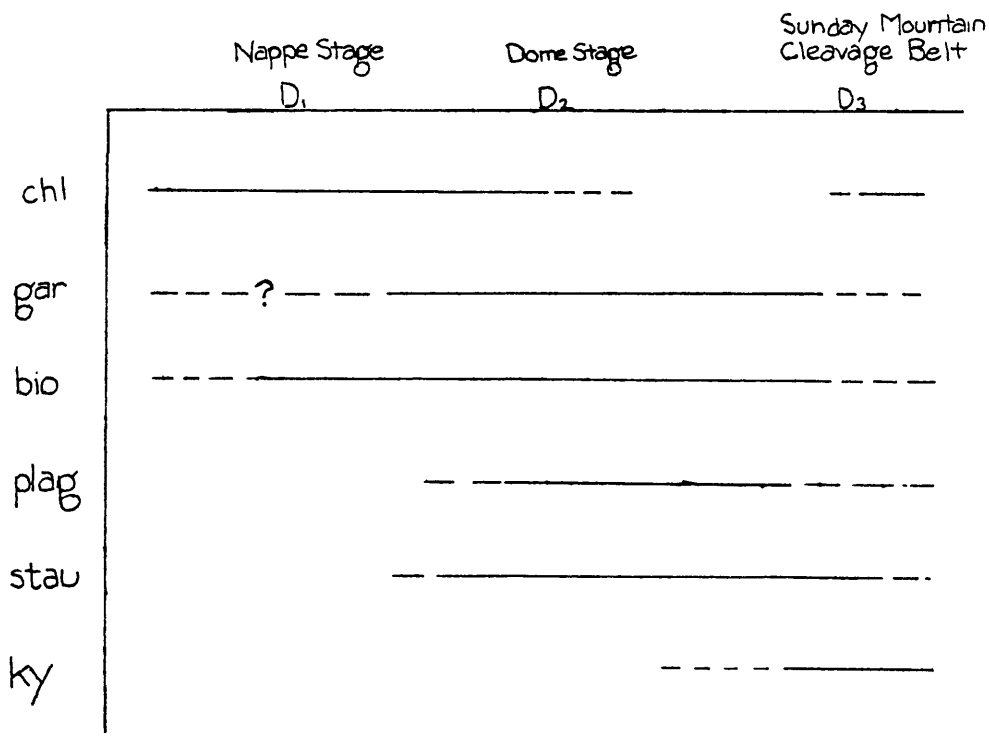

Figure 13: Paragenesis diagram, Archertown Brook.

a) plane light

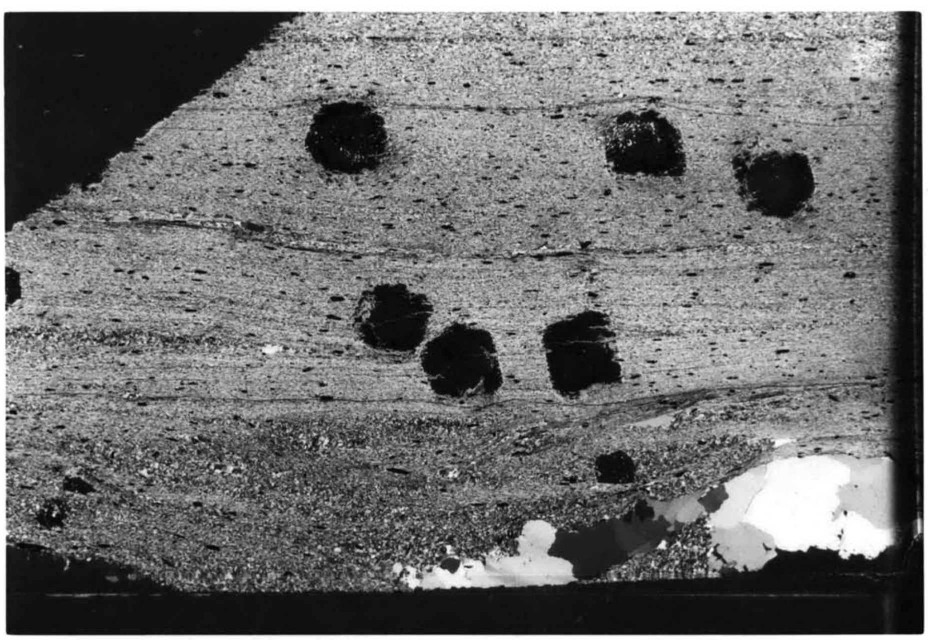

b) crossed polars

Figure 14: Northey Hill Line: Sample D84-6b; Showing textural and porphyroblast style in thin-section. Note garnet growth overprinting S3, and retainig the schistosity as inclusion trails.

kilometer stretch of Jacobs Brook where the Northey Hill Line crops out. The map is included as Figure 15. From west to east, this map shows an en echelon repetition of section, consisting of Littleton, Fitch, Clough and Partridge Formations. The sections present along this traverse have been drastically thinned. The Clough, when present, reaches a maximum thickness of 2 meters. Preliminary interpretation of the structure and morphology suggests that folding is responsible for the outcrop pattern. One fold nose is seen near the southwest portion of the outcrop. Continued strain along fold limbs may have been responsible for faulting out these noses as deformation continued. In this interpretation, the folding is due to the development of the Sunday Mountain cleavage belt, while the foliation that is folded is dome stage.

Individual crystals seen in thin sections collected from along the Northey Hill Line are also smaller on the average than samples from all of the other localities. Additionally, these samples contain an entirely different assemblage; all but one of the pelitic rocks contain no biotite, and the matrix assemblage is garnet-chlorite-chloritoid-graphite-muscovite.

Plagioclase

Plagioclase occurs as large (0.2 mm) rolled grains in sample D84-1e (Fig. 16). These plagioclases contain inclusions of quartz, k-spar, and ilmenite, and formed before or in the early stages of the Sunday Mountian cleavage formation.

Muscovite

Occasional crenulation cleavages of muscovite are found, although more often than not these have been destroyed by the later schistosity.

Garnet

Garnet habits vary from poikiloblastic to inclusion free idioblastic crystals. Initial garnet growth appears to be syntectonic; the latest

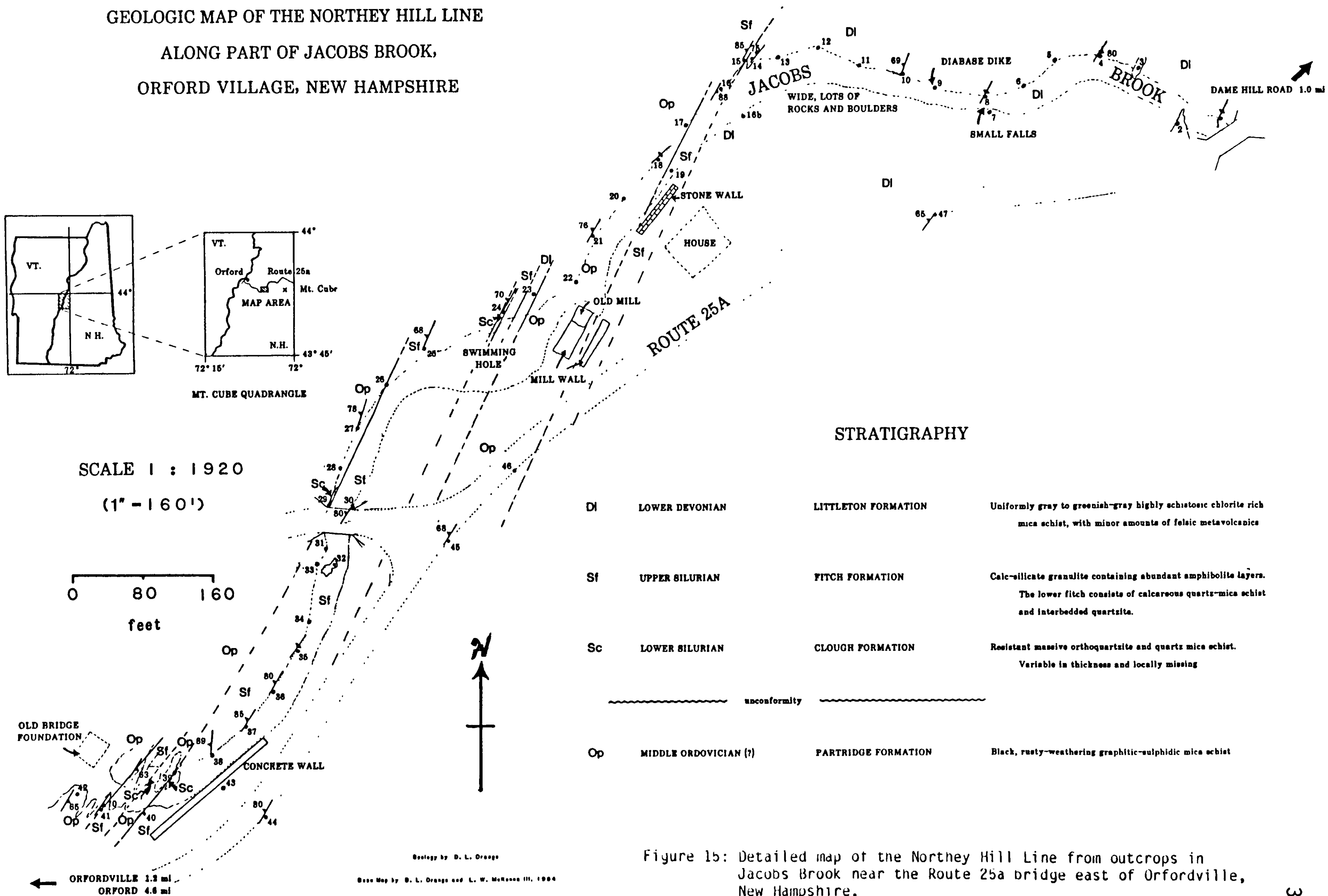

Figure 15: Detailed map of the Northey Hill Line from outcrops in Jacobs Brook near the Route 25a bridge east of Orfordville, New Hampshire.

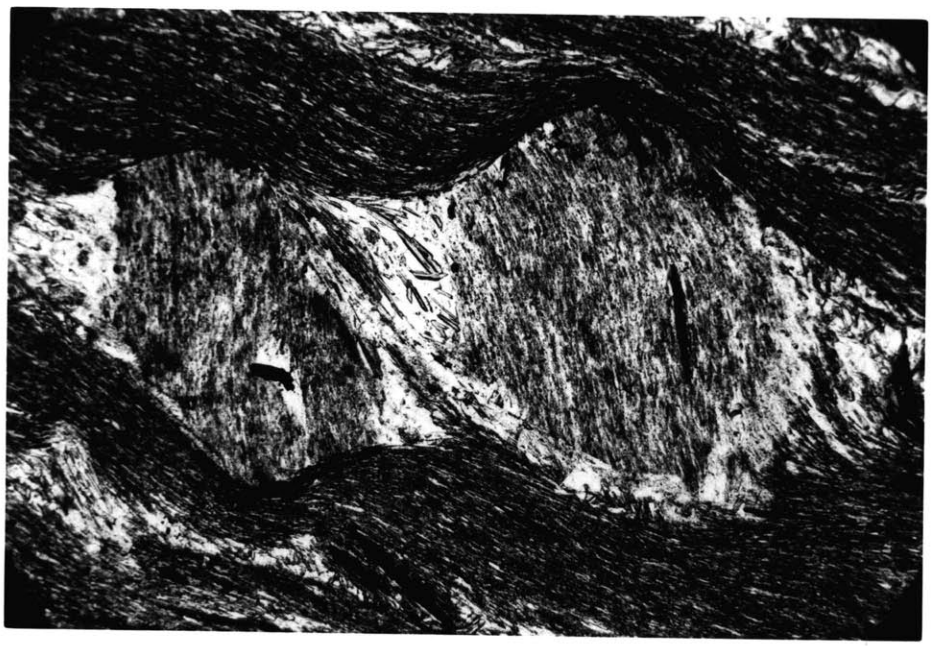

1 mm

Figure 16: Northey Hill Line: Sample D84-1e; Rotated plagioclase showing poikiloblastic habit.

schistosity is seen partially wrapped around garnet porphyroblasts. The majority of garnet growth, however, is post-tectonic; schistosity is terminated against crystal faces. In some cases, schistosity is preserved as trails of fine-grained opaque inclusions in the latter growth phases of garnet (see Fig. 14). These garnets suggest at least two distinct phases of growth.

Chlorite

Chlorite most commonly occurs as lepidoblastic grains 0.05-0.2 mm in length, but it is also found in rotated "clusters" of chlorite + chloritoid + opaques.

Retrograde chlorite is present in two samples from the Northey Hill Line. This chlorite is associated with garnet retrogradation, and is seen in the two samples exhibiting multiple phases of garnet crystalization.

Biotite

Biotite is found in one sample, D84-1c, from the Northey Hill Line. This biotite occurs as lepidoblastic crystals, and is usually 0.1-0.3 mm in length. These biotites are commonly intergrown with prograde chlorite, and they make up approximately 15% of this sample (D84-1c). D84-1c contains no chloritoid; the matrix assemblage is quartz-muscovite-garnet-biotite-chlorite-plagioclase. Biotites from this sample are exceptionally pleochroic with colors ranging from tan to very dark brown.

Chloritoid

Chloritoid can either be sub-parallel to the schistosity, or it can form in "clusters" with opaques, chlorite and quartz, which have the schistosity folded around them.

PHASE EQUILIBRIA

The two assemblages found in samples along the Northey Hill Line, garnet-chlorite-biotite and garnet-chlorite-chloritoid (+ muscovite + plagioclase + quartz + H_2O), can be represented on the same A-F-M diagram. A different bulk composition (less aluminous) in sample D84-1c places it below the garnet-chlorite tie line.

Several morphological and inclusion relationships allow for a petrologic history to be determined. In the garnet-chlorite-biotite rocks, garnets are rolled in the latest foliation, which contains lepidoblastic biotite and chlorite. In the garnet-chlorite-chloritoid samples, garnet is syn/post-deformational, chlorite is a lepidoblastic phase, chloritoid is rotated as well as with pressure shadows and hence clearly pre-S3, and large plagioclases are rolled and which contain quartz and K-feldspar inclusions.

At some point, when both assemblages were still on the more Fe-rich side of the A-F-M diagram, the chlorite solid solution reacted to form garnet and more magnesium-rich chlorite. Plagioclase formation at this point incorporated inclusions of K-feldspar. Crystallization of garnet (in the garnet-biotite-chlorite rocks) and plagioclase continued during the deformation which created the latest foliation (S3). As metamorphism continued, the chlorite solid solution becomes more magnesian, and the three-phase triangles continuously shifts toward magnesium. At this point, the bulk composition of the garnet-chlorite-chloritoid assemblage moves into its three-phase region, forming garnet by the reactions:

Chlorite + Chloritoid → Garnet + H_2O

Chlorite + Muscovite → Garnet + Biotite + H_2O

The relationships of porhyroblast growth to structural evolution is shown in Figure 17.

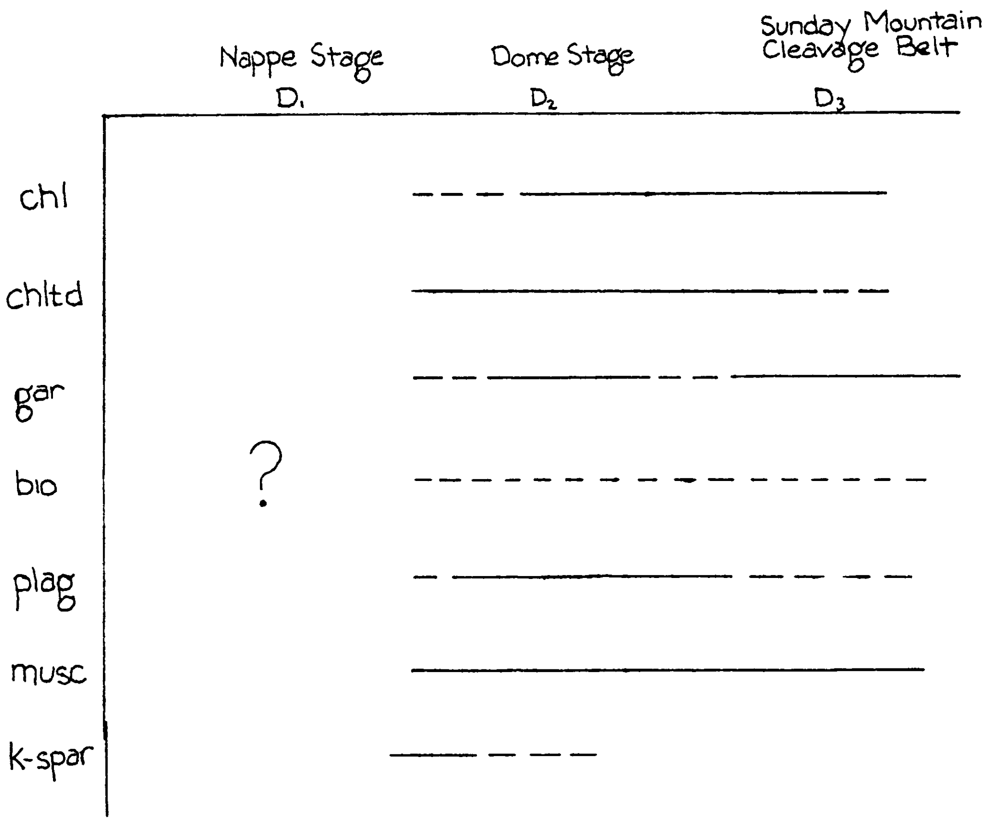

Figure 17: Paragenesis diagram, Northey Hill Line.

JACOBS BROOK RECUMBANT SYNCLINE

Samples from the Jacobs Brook Recumbant Syncline are from the Clough Formation, a Silurian quartzite unit. The deformation seen in these rocks appears similar to that at the other three localities; i.e. an early schistosity (not crenulated) cut by a later schistosity (Fig. 18). Late stage fold axes trend N20E and plunge 20 to 30 degrees to the northeast. Because of similarities between this and Rumble's (1969) findings, the early schistosity evident in thin section is interpreted to be nappe stage while the latter schistosity is interpreted to be dome stage. This is also consistent with the large scale structural features; ie: the nappe stage recumbant syncline itself. The cleavage from the Sunday Mountain cleavage belt to the west is not present in this locality. This may be due to a reduction in the magnitude of deformation spatially or it may be due to the greater rigidity of quartz-rich rocks. Whatever the reason, the magnitude of deformation is far less in the Jacobs Brook Recumbant Syncline samples. Samples from this locality contain the assemblages garnet-biotite-staurolite, garnet-biotite-chlorite and garnet-biotite-staurolite-chlorite.

Garnet

The larger garnets are frequently poikiloblastic and riddled with opaque inclusions. The schistosity wraps around these garnets, and inclusions commonly exhibit rotations of 30 to 120° . This suggests that garnets grew contemporaneously with the dome stage deformational event.

Staurolite

The large staurolite crystals found in the Jacobs Brook Recumbant Syncline are very poikiloblastic, with quartz and ilmenite being the most common inclusions. Some staurolites clearly overprint the latest schistosity, with inclusions of quartz and opaques lying parallel to and retaining the latest schistosity. Some poikiloblastic staurolites lie

a) plane light

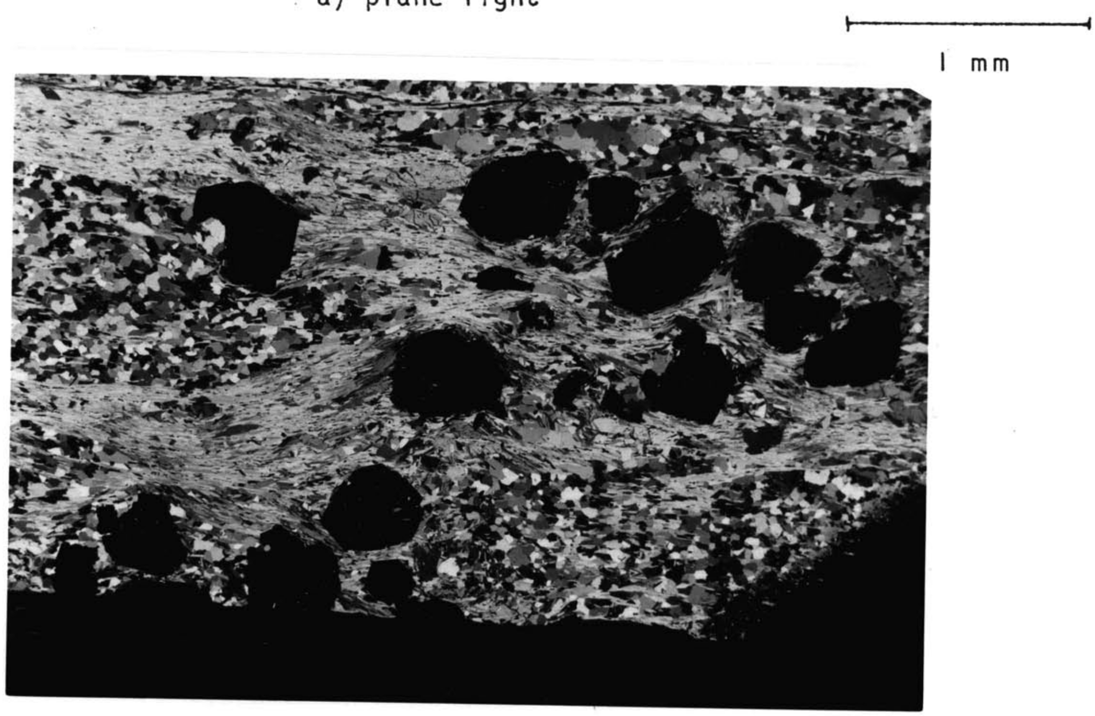

b) crossed polars

Figure 18: Jacobs Brook Recumbant Syncline: Sample D84-41; Showing textural features and relationships to porphyroblastic growth.

elongated in muscovite layers parallel to the latest schistosity (S2). This is more likely due to growth in a more favorable bulk composition layer than it is due to pre- or syn-tectonic growth. Staurolites are interpreted to have grown after the dome stage deformation. Staurolite also occurs as inclusions within garnet and muscovite.

The paragenesis diagram for the Jacobs Brook Recumbant Syncline samples is included as Figure 19.

BAKER POND

Six samples from the Baker Pond area were investigated. These samples display a weak schistosity and no crenulation cleavage (Fig. 20). The structural evolution of the Baker Pond samples is less well constrained than the other localities. The weak schistosity displayed by these samples is interpreted to be due to the doming along the Bronson Hill anticlinorium. The minerals present in the Baker Pond samples include: garnet, biotite, cordierite, plagioclase, kyanite, sillimanite, chlorite, staurolite, and quartz. No muscovite is found in the Baker Pond samples; they are from the Ammonoosuc Volcanics which have a low potassium bulk composition.

Cordierite

Cordierite is clearly one of the latest minerals to form in the Baker Pond samples. It contains inclusions of kyanite, staurolite, biotite and occurs as an inclusion in the mapped garnet in 79-449f.

Biotite

The small grains define the schistosity in the absence of muscovite.

Garnet

Garnets exhibit inclusion trails indicative of rotation of 0 to 20°. Schistosity is slightly warped, yet also overprinted. These textures

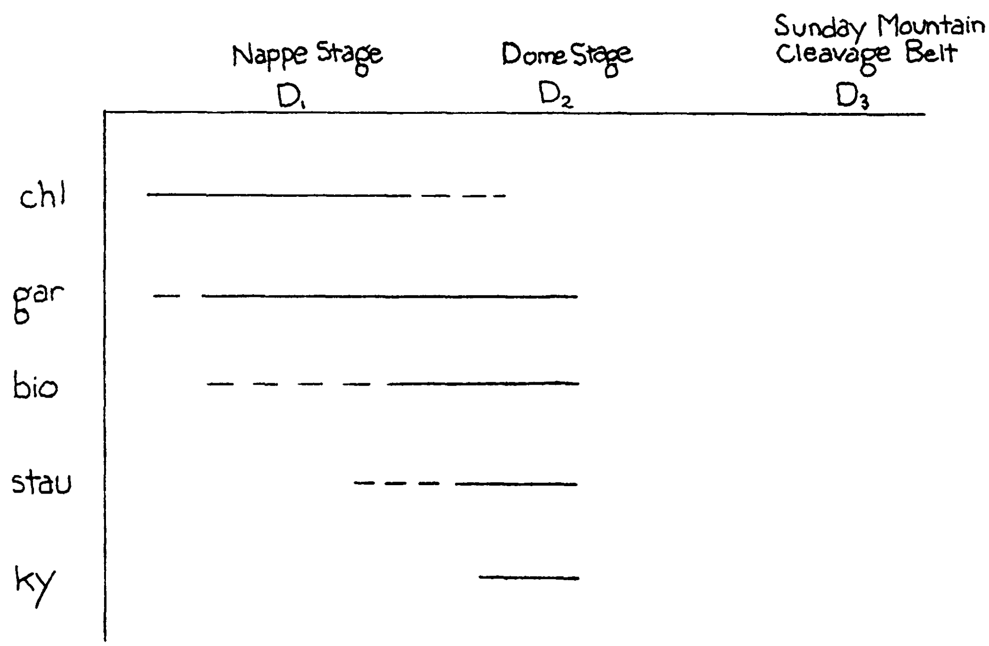

Figure 19: Paragenesis diagram, Jacobs Brook Recumbant Syncline.

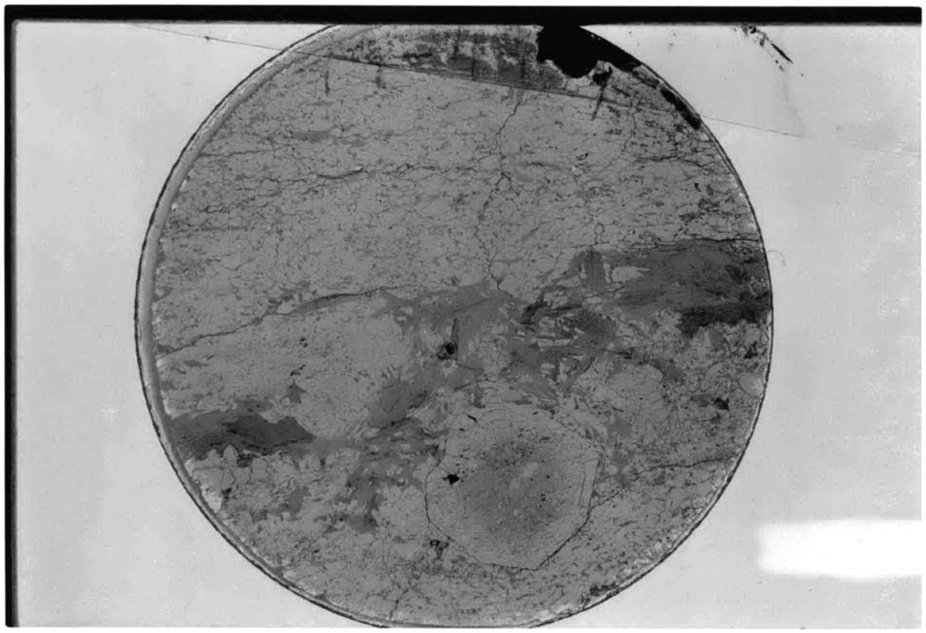

a) plane light

I cm

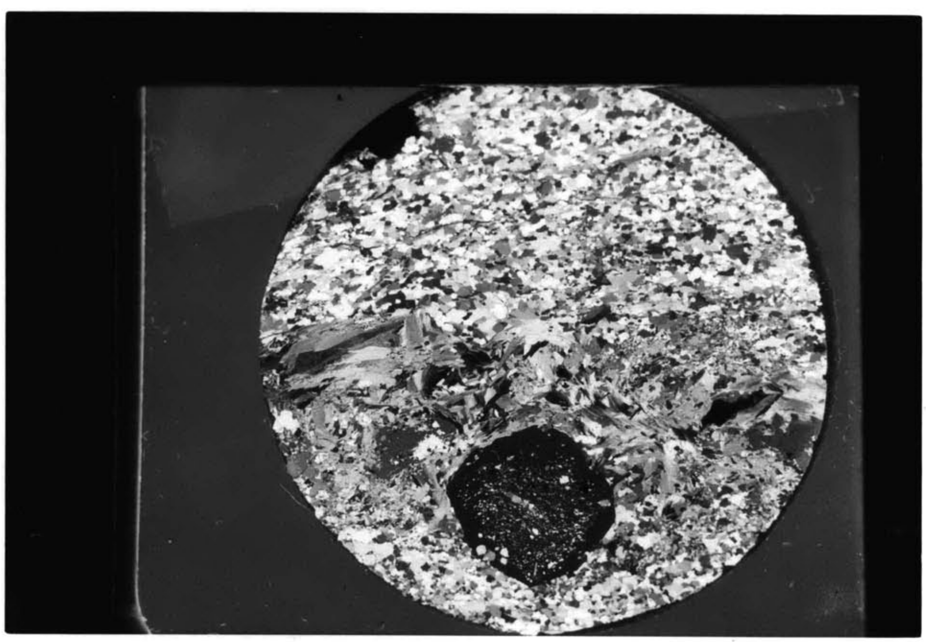

b) crossed polars

Figure 20: Baker Pond: Sample 79-449f; Showing porhyroblast growth and relationship to textural features.

suggest syn-deformational garnet growth during dome stage deformation.

Chlorite

In all garnet bearing samples prograde chlorite is preserved only as inclusions. These samples contain matrix chlorite, yet it is decussate and obviously late. Sample 79-449h contains lepidoblastic chlorites that could arguably be primary. This sample contains no garnet.

Staurolite

The staurolites from Baker Pond occur in a very discontinuous fashion--individual grains, identified by identical extinction angles, occur as a series of islands in a sea of matrix minerals, such as cordierite. Often the staurolite is found only as inclusions in cordierite.

Al_2SiO_5 Polymorphs

Aluminosilicate polymorphs occur in all of the samples from Baker Pond. Fibrolitic sillimanite is the most common polymorph, occurring in all of the samples. It occurs in knots from 1 to 5 mm long. Fibrolite is commonly associated with biotite, and there appears to be an inverse correlation between the amount of staurolite present and the amount of fibrolite present. This suggests that the fibrolite producing reaction is:

6 Staurolite + 4 Muscovite + 7 Quartz $\rightarrow$ 31 Fibrolite + 4 Biotite + 3 H_2O

(Rumble, 1973; Thompson and Norton, 1968; Chamberlain, 1981)

Xenoblastic sillimanite crystals are also seen in sample 79-449G--they reach a maximum dimension of 0.2 mm.

Kyanite is also observed in the Baker Pond samples, occurring in three of the six samples. In the samples with abundant fibrolite, kyanite occurs only as inclusions in staurolite, quartz, and cordierite. These crystals occur as bladed prisms 0.1 to 0.5 mm long exhibiting low birefringence and one good cleavage. Prismatic sillimanite also contains inclusions of prismatic kyanite. All textural relations indicate that sillimaite clearly postdates kyanite.

The paragenesis diagram for the Baker Pond samples is shown in Figure 21.

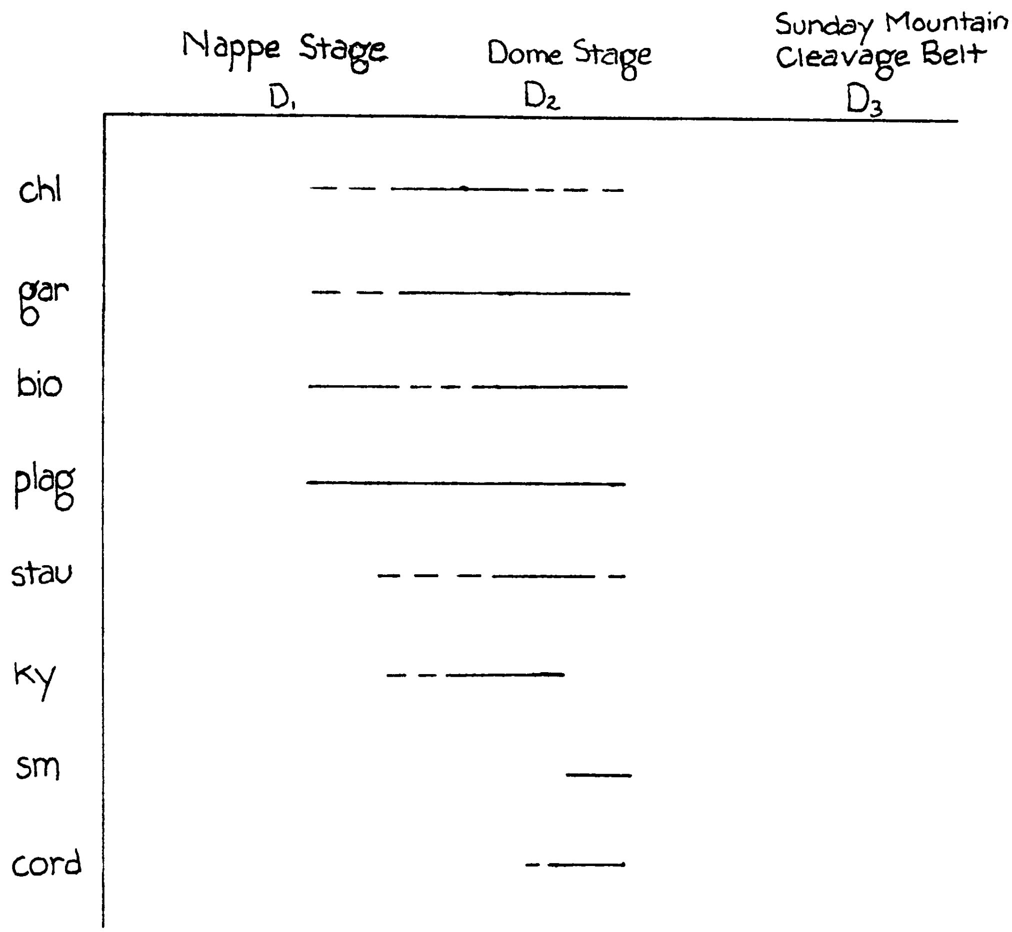

Figure 21: Paragenesis diagram, Baker Pond.

Taole 1: Comparitive Systematic Mineralogy

COTTONSTONE MOUNTAIN

	present	features	textural relations	inclusions
quartz	X	10-15% 0.1-0.5 mm non-uniform size	associated with plag	
plagioclase	X	10-15% 0.5-1 mm	twinned, zoned, opaques along grain boundaries.	
muscovite	X	35-50% 0.5 mm	lepidoblastic.	
biotite	X	5-10% 0.5-3 mm	lepidoblastic with musc or at angles to schistosity.	zir
chlorite				
chloritoid				

Table 1: (cont'd.)

COTTONSTONE MOUNTAIN

	present	features	textural relations	inclusions
garnet	X	20-30% 2-5 mm	rolled poikoblastic xytls with schistosity wrapped around it.	bio, chl plag, ilm qtz, opaq
staurolite	X	5-10% 1.5-3 mm not v. pleo.	idioblastic to sub- idioblastic. Over prints schist.	qtz, plag opaques
cordierite				
kyanite	X	10-15% 2-3 mm	overprints schist. slightly pleo.	qtz, palg opaques
sillimanite				
graphite				
accessory minerals and opaques	zircon opaques: ilmenite			

Table 1: (cont'd.)

ARCHERTOWN BROOK

	present	features	textural relations	inclusions
quartz	X	20-50% 0.5-0.8 mm uniform size	120° grain boudaries more common: sutured grain boundaries	tour, musc biotite
plagioclase	X	-15% 0.25-1.5 mm Ab twinning (5 samples) minimal sericitization	fine grained plag in qtzitic layers D84-3a: lg(1.5-2.0 mm) poikoblastic twinned grains. Contain dusty incl trails at high angle to schistosity. Ass. w/ bio clusters	
muscovite	X	25-50% 0.05-0.5 mm subtle pleo.: red to green	lepidoblastic. Also retro. min'l cross cutting schistosity at hi-angle*. Also in pseudomorphs of stau	
biotite	X	15-30% a) 0.1-0.5 mm b) 0.5-2.5 mm	a) lepidoblastic w/ white mica. b) contain dusty incl trail at angles to schistosity (seen in all samples). Also have shistosity wrapped arond them. Rotated as much as 30°.	qtz, tour, staurolite zircon opaques
chlorite	4/11	1-5% a) 0.1-0.3 mm b) 0.5-3.0 mm	a) in same thin-section as gar-stau-bio; diff't bulk comp. b) contain dusty incl trail at angle to dominant schistosity (10-30°). Schistosity also wrapped around it.	
chloritoid				

Table 1: (cont'd.)

ARCHERTOWN BROOK

	present	features	textural relations	inclusions
garnet	X	5-15% 0.3-5 mm	a) small idioblastic xytls. b) lg. poikoblastic (sub-idioblastic to xenoblastic). b) more common. Rotated garnets common (20-90°). schistosity wrapped around garnet. textural relations similar to bio	qtz, bio, chl, musc, marg, plag tour, ilm opaques
staurolite	X	2-10% a) 0.5-3 mm yellow, very slightly pleo. a)commonly retro:	a) poikoblastic, irregular xytls. Incl trails of qtz+dusty opaques at angle to schistosity. Schist. also wraps around stau commonly exhibit oblique penetration twinning. sericite replacing 10-50% of orig. xytl.	qtz, plag, opaques
		b) 2-4 cm	b) lg. idioblastic to sub-idioblastic. Over-print schistosity. Contain fewer incl. fewer incl. than a). 30-95% replaced by rim of chl, interior of sericite or musc., v. small core of staurolite	qtz, plag, opaques, sub-euhedral garnet
cordierite				
kyanite	2/11	2-10% 1.5-3.0 mm	usually overprints latest schistosity one of two kyanites in D84-3d folded	qtz, plag
sillimanite				
graphite				
accessory minerals and opaques		tour (up to 1%), apatite zircon (up to 0.05 mm), sphene. opaques: graphite (<1%), rutile, ilmenite, pyrrhotite		

Table 1: (cont'd.)

NORTHEY HILL LINE

	present	features	textural relations	inclusions
quartz	X	30-50% < 0.1 mm (< 0.05 mm common)	bimodally as veins and as disseminated xytls. Non-vein grain boundaries commonly sutured.	
plagioclase	X	< 5% a) 0.2 mm b) 0.1-0.3 mm c) 0.05-0.1 mm	a) poikoblastic twinned rolled crystals. b) sub-idioblastic grains in qtz veins. a) and b) Ab twinned c) sm. xenoblastic grains ingrown in the schistosity the schistosity. Rarely twinned.	qtz, k-spar, graphite, opaques, ilm
muscovite	X	- 50% 0.05-0.1 mm	lenticular lepidoblastic xytls defining multiple schistosities (occasional crenulation cleavages)	
biotite	1 sample (D84-1c)	15% 0.1-0.3 mm	lepidoblastic very pleo: tan to very dark brown	
chlorite	X	1-5% 0.05-0.2 mm pleochroic	lepidoblastic. Also in rotated "clusters" with chltd+opaques+qtz Distinguished from chltd by lower refractive index lt. green to lime green	
chloritoid	X (except D84-1c)	1-3% a) 0.1-0.2 mm b) 0.5 mm pleo: lt. green to pale blue	a) sub-idioblastic b) twinned idioblastic xytls. Sub-parallel to schistosity or in clusters w/ chl+op+qtz	

Table 1: (cont'd.)

NORTHEY HILL LINE

	present	features	textural relations	inclusions
garnet	X	- 5% 0.5-1.5 mm	poikoblastic to inclusion free idioblastic xytls. Initial growth syn-tectonic schistosity wrapped around garnet (also rotated 30°). Final Final growth post tectonic: warped schistosity preserved by graphite + quartz incl trails.	qtz,tour, ilm, graph
staurolite				
cordierite				
kyanite				
sillimanite				
graphite	X	20-30% 0.25-0.1 mm	lepidoblastic xytls along with chl+musc. Minimal graph in D84-1c.	

Accessory minerals and opaques	toumaline most common (< 2%) minimal zircon opaques: graphite + ilmenite

Table 1: (cont'd.)

JACOBS BROOK RECUMBANT SYNCLINE

	present	features	textural relations	inclusions
quartz	XX	50-80% 0.1-0.5 mm (mean 0.3 mm)	very uniform grain size sutured grain bdys less common	
plagioclase	7/15	2-20% (est.) (mean 5%) a) 0.1-0.3 mm b) 2-4 mm	a) sericitized, Albite twinning common b) sericitized	
muscovite	X	5-20% 0.1-0.5 mm pleo.	elongate lepidoblastic xytls defining multiple schistosities subtle yet pronounced red to green	
biotite	13/15	1-20% (mean 15%) 0.1-0.5 mm pleo. varies retrograded	lepidoblastic or rotated grains lt. orange brown to dk. reddish brown replaced by chlorite	bio
chlorite				
chloritoid				

Table 1: (cont'd.)

JACOBS BROOK RECUMBANT SYNCLINE

	present	features	textural relations	inclusions
garnet	13/15	1-5 mm (D84-2c: 3 cm)	sub-idioblastic, poikoblastic, schistosity wraps around. Rotated 30-120°. [v. small (0.05-0.15 mm) garnets in coticule layer seen in sample D84-4d]	qtz, ilm, marg, musc, bio, tour, staur
		retrograded	replaced 10-100% by bio, musc, plag, sericite and ilmenite.	
staurolite	8/15	2-10%		qtz, ilmenite
		a) 0.1 mm	a) xenoblastic grains in musc-rich layers (favorable bulk comp)	
		b) 0.5-3.0 mm	b) idio- to sub-idioblastic xytls, pokoblastic. Most overprint latest schistosity w/incl of qtz+opaques parallel to and retaining latest schistosity.	
cordierite				
kyanite	1/15	1% 0.2-0.3 mm	Note: abundant kyanite "veins" seen in the field	qtz, tour, opaques
sillimanite				
graphite				
accessory minerals and opaques	tourmaline (up to 1%), sphene, zircon, apatite, margarite in garnet. opaques: ilmenite, rutile, pyrite			

Table 1: (cont'd.)

BAKER POND

	present	features	textural relations	inclusions
quartz	X	30-65% 0.1-0.4 mm	equi-dimensional. Undulose extinction far less prevalent than in other areas.	
plagioclase	3/6	2-7% 0.1-2.0 mm	visible zoning. Ab twinning common. Occurs as clusters w/schistosity wrapped around it in 79-450c. Difficult to discern from qtz, cord.	
muscovite				
biotite	X	5-20% a) 0.1-1.0 mm b) 1.0-7.0 mm	a) lepidoblastic; define schistosity in absence of muscovite. b) decussate grains	lg. zircon (0.1-0.2 mm)
chlorite	X	3-5% 0.5-2.0 mm	lepidoblastic. No garnet in this sample. In all gar-bearing samples, chl is preserved only as incl in garnet.	
chloritoid				

Table 1: (cont'd.)

BAKER POND

	present	features	textural relations	inclusions
garnet	4/6	1-20% 2-15 mm	rotated up to 20°. Very poikoblastic. Schistosity warped, yet also overprinteted.	qtz, plag, bio, chl, cord, ilm, epid, apatite rutile
staurolite	5/6	2-5% 0.1-4.0 mm	poikoblastic; occurs in very discontinuous grains (identified by identical extinction angle). Occurs as series of islands in sea of matrix minerals, commonly cordierite	qtz, ilm, ky
		very pleo.	to bright canary yellow	
cordierite	X	-5% 0.1-0.6 mm (as lg. as 1.5 mm ?)	yellow pleochroic haloes around zircon lg. grains often twinned, very poikoblastic	zir, ky, stau, bio
kyanite	3/6	1-5% 0.1-0.5 mm	bladed prisms. In samples w/abundant fibrolite, occurs only as incl in stau, qtz, cord. In 79-449f, minimal fibrolite, ky questionably mx. phase.	
sillimanite	X	1-15% (mean 4%) 1.0-5.0 mm	occurs in knots. Commonly associated with biotite.	
graphite				
accessory minerals and opaques		lg. zircon (0.1-0.2 mm) seen in chl and bio apatite, ilmentite, epidote, rutile.		

CHAPTER 5: ELECTRON MICROPROBE ANALYSES

Introduction

Twenty, round (2.5 cm diameter) thin sections were made for electron microprobe (= 'probe') analysis from samples throughout the Mount Cube Quadrangle. Of these, thirteen were chosen for further study. These included one from the Cottonstone Mountain locality, four from Archertown Brook, two from the Northey Hill Line, three from the Jacobs Brook Recumbant Syncline, and two from Baker Pond. These samples were examined for garnet zoning, matrix mineral compositions and zoning, and mineral inclusion composition and zoning. Geothermometry and geobarometry will be discussed in the following section.

Most minerals were analyzed three times, twice on the rim and once in the core. If significant zoning was not observed, these analyses were averaged. Minerals displaying complex zoning were probed in more detail. Plagioclase grains were routinely analyzed with two to fifteen points. Garnets were analyzed using the turbo-probe technique at 100 to 350 points, depending on size and zoning gradients.

Garnet maps are contoured in intervals of $X_{0.01}$ or $X_{0.02}$ where X is the component of interest. This interval well exceeds the limits of error in the microprobe analysis, allowing for confident and realistic interpretation. Where changes in the direction of zoning occur, ticks are marked on the lower valued side. The location of the compositional traverse across the garnet is indicated on the Fe/Fe+Mg map by the line A-A'.

Where plagioclase inclusions were found in garnets other than the one mapped, several garnet analyses were made adjacent to the inclusion and its possible correlative location in the mapped garnet has been plotted on the traverse. If the garnet compositions did not correlate closely, the inclusion was ignored. All inclusions found in the mapped garnet are sketched in on the maps with their approximate shape and size indicated. This is accompanied by the analysis number, included in the appendix, and the anorthite content. All inclusions discussed in the text are marked with their approximate compositional location on the garnet traverses. The analysis number and anorthite composition is also included. Inclusions from correlative garnets are marked with dashed lines. Where multiple compositional correlations are possible, the range of possibilitites is indicated with brackets and a question mark.

Electron Microprobe--Results

COTTONSTONE MOUNTAIN

Sample 67-82E was analyzed for garnet zoning, plagioclase zoning (matrix and inclusion), biotite (matrix and inclusion), muscovite, staurolite, and chlorite. Individual analyses are listed in Appendix 1.

Garnet Map

The Cottonstone Mountain garnet was analyzed at 167 points. 145 of these points were concentrated in one quadrant of the garnet. The remaining 22 points continued across the garnet to investigate a biotite inclusion. It was found that, due to a series of cracks, this latter area of the garnet has experienced varying amounts of re-equilibration. For this reason, discussion will concentrate on the non-retrograded section.

The garnet investigated has an almandine-rich rim with approximately 15% pyrope component. Pyrope and almandine decrease toward the core while spessartine and grossular increase. The garnet maps are included as Figure 22. Traverse A-A' across the garnet is illustrated in Figure 23. Note that the initial zoning (the first three points) is consistently in the opposite direction from the rest of the garnet.

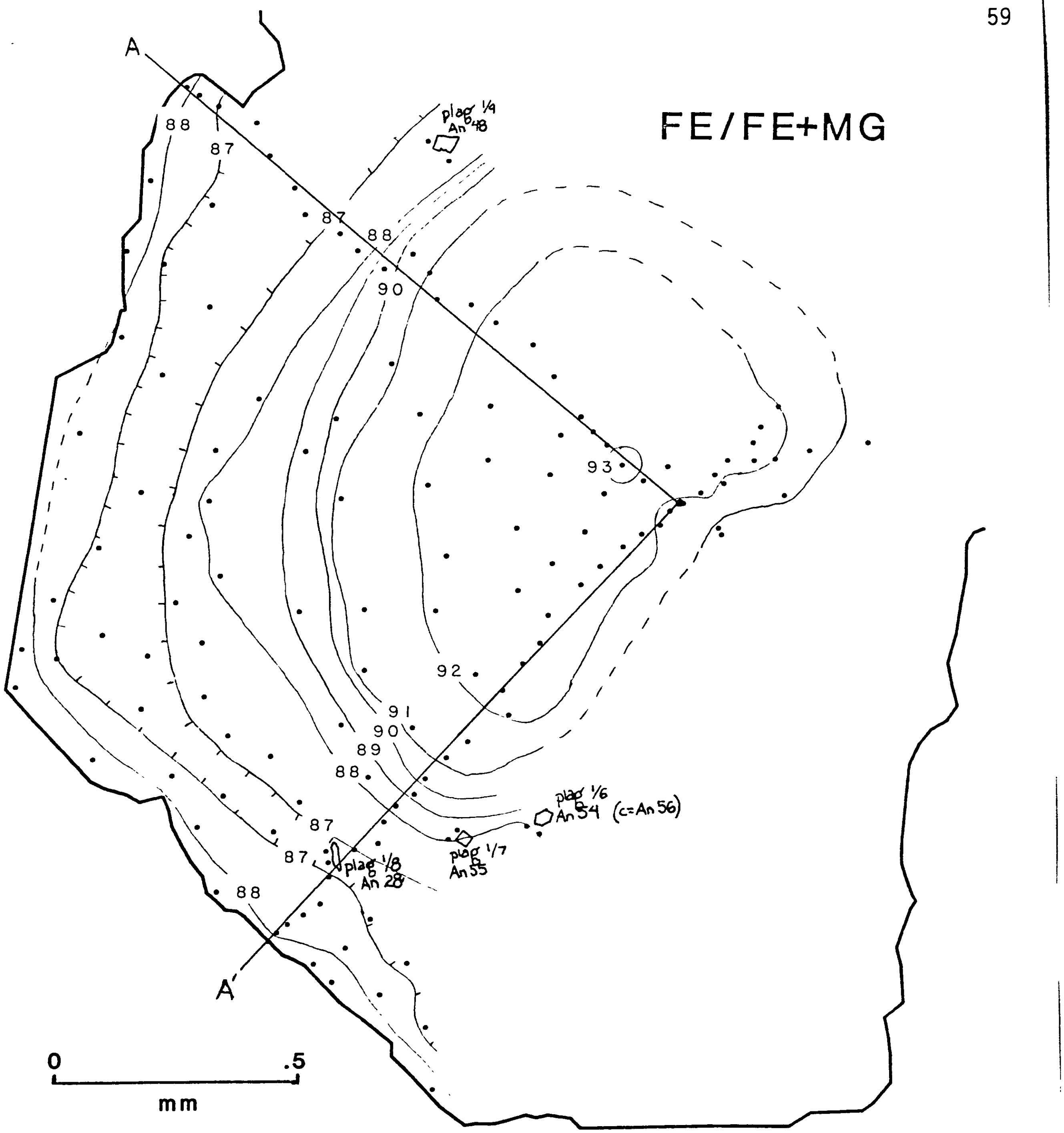

Figure 22: Cottonstone Mountain: Sample 67-82e; Garnet Maps

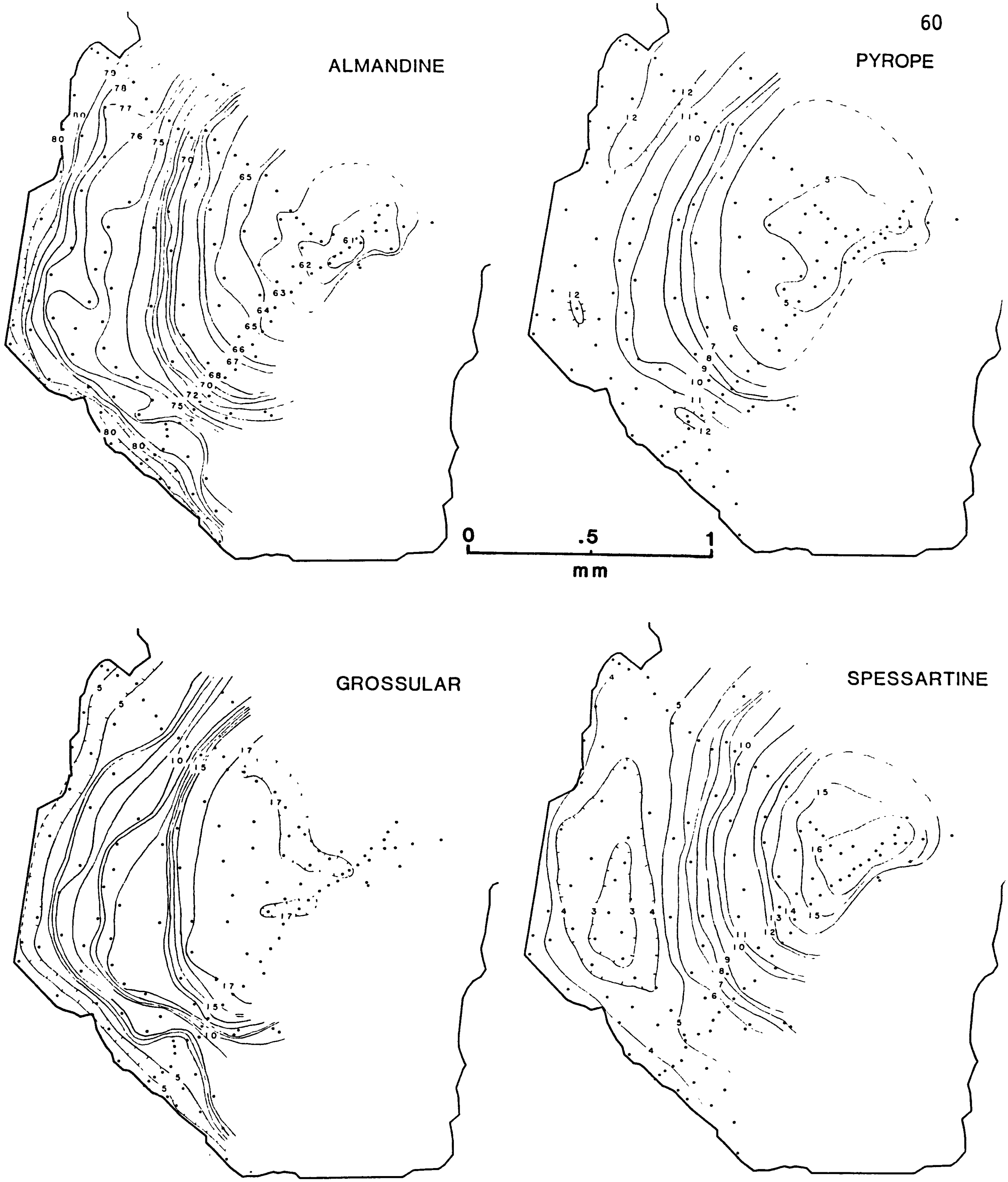

Figure 22: Sample 67-82e; Garnet Maps (cont'd.)

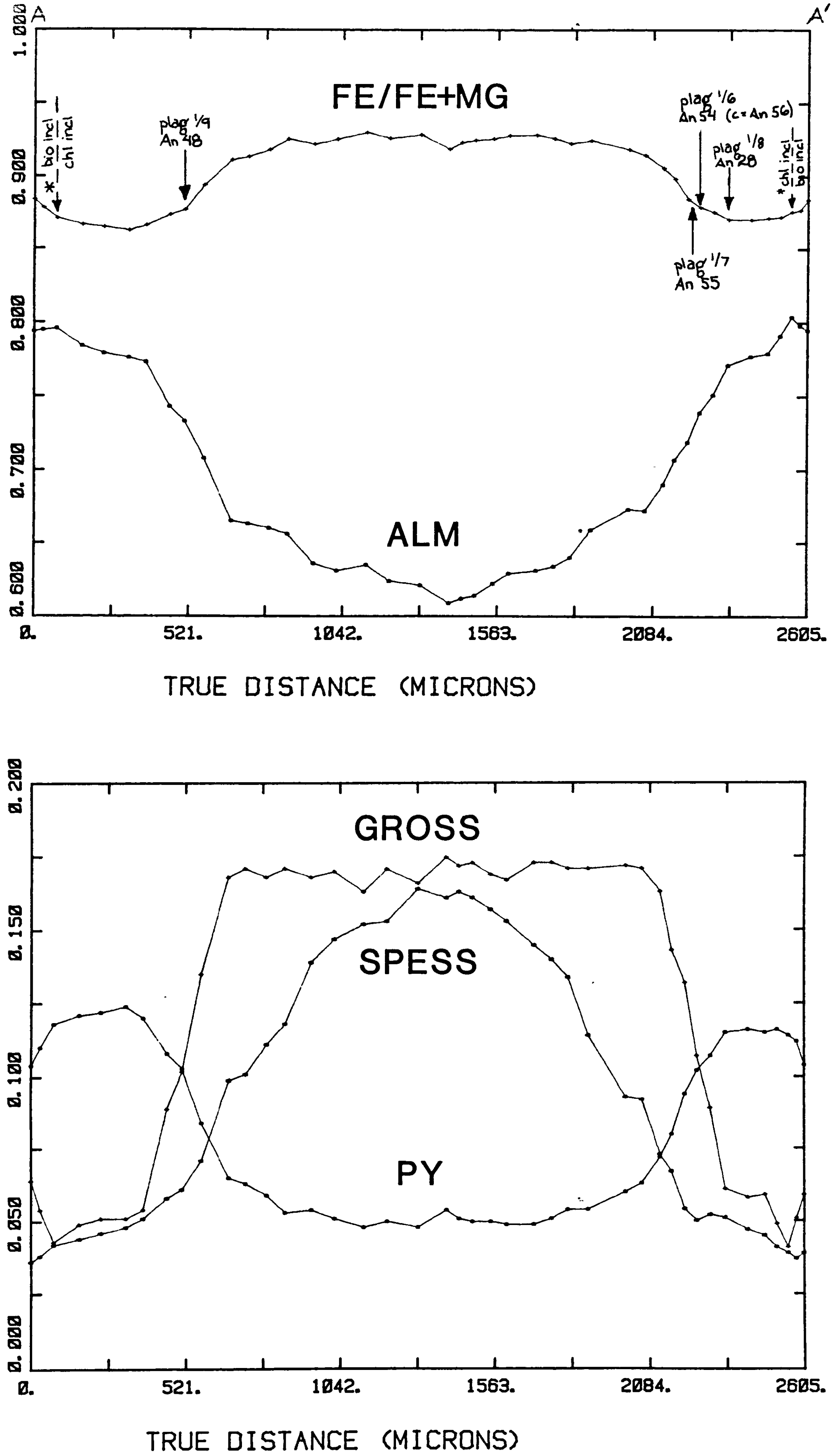

Figure 23: Cottonstone Mountain: Sample 67-82e; Garnet Traverse

Matrix plagioclases in this sample have rim compositions varying from An_{20} to An_{23}, with the vast majority of analyses clustering around An_{20}. These matrix plagioclases display higher anorthitic cores with zoning increases of An_{1-2}. Plagioclase inclusions in kyanite are $An_{23.5}$ while inclusions in staurolite have rim values of An_{22-24} and a core composition of An_{25}. Plagioclase inclusions analyzed in the garnets from 67-82e vary from An_{28-55}, with the more anorthitic plagioclases occurring closer to the core (see FE/FE+MG map for location of inclusions in mapped garnet, Fig. 22). In addition, inclusions occuring in the mapped garnet are plotted with inclusions in correlative garnets on the traverse in Figure 23.

A neighboring garnet to the one mapped contains chlorite inclusions in the core, biotite inclusions in the rim, and a chlorite+biotite inclusion near the rim. The rim and core compositions of this garnet correlated within a few percent of the mapped garnet, although the near-rim zoning changes observed in the mapped garnet are not seen. It is felt that a biotite grain mantling the garnet at this rim has kept the garnet rim from finishing its growth. This biotite to chlorite transition is also mapped on the traverse in Figure 23.

ARCHERTOWN BROOK

Four samples from Archertown Brook were extensively analyzed (D84-3d, PM-9b, PM-11c, and 67-78A) for garnet zoning, plagioclase, biotite, staurolite, muscovite and chlorite. Microprobe analyses from these samples are listed in Appendix 2.

<u>Garnet Zoning</u>

Detailed garnet maps were obtained from samples D84-3d (207 points), PM-9b (251 points), and PM-11c (100 points). D84-3d and PM-11c were contoured at $X_{0.02}$, while PM-9b is contoured at $X_{0.01}$. The garnet maps follow as Figures 24 (D84-3d), 26 (PM-9b) , and 28 (Pm-11c). Linear traverses across each of these garnets are included as Figures 25 (D84-3d), 27 (PM-9b), and 29 (PM-11c). These three garnets all show similar zoning patterns, although the details and magnitudes of compositional gradients differ. These garnets exhibit an almandine-pyrope-rich rim with grossular and spessartine increasing towards the core while almandine and pyrope decrease. The Fe/Fe+Mg profiles are almost identical for the three samples, with a near-rim decrease changing to a increase and a levelling off approximately half way from the rim to the core. The zoning direction fluctuates at the rim, with pyrope first increasing and then decreasing on all six rims (two per profile). The other garnet components are less consistent from sample to sample; ie: not every rim has the same character. The reader is reminded that these garnets are all of different size, with PM-11c substantially smaller in width than the other two. Thus, while the zoning is the same in PM-11c, the gradient is steeper.

The garnet map from D84-3d, Figure 24, exhibits some differences from the other garnets in this locality. Here, a high grossular core (X_{Gr}>0.200) occurs rather than a grossular plateau as seen in the other samples. Also, the general shape is more irregular, with the "center" of the garnet skewed to one side. This results in a steeper contour gradient on one side than the other. Inclusions of plagioclase and chlorite were analyzed in this garnet. No prograde chlorite occurs in the matrix. Three plagioclase inclusions were identified. Compositions range from An_{37-40} near the rim with An_2 found near the core. These inclusions are shown on the Fe/Fe+Mg map in Figure 24 and on the traverse in Figure 25. A plagioclase inclusion from another garnet is also shown at its correlative point on the garnet traverse (Fig. 25).

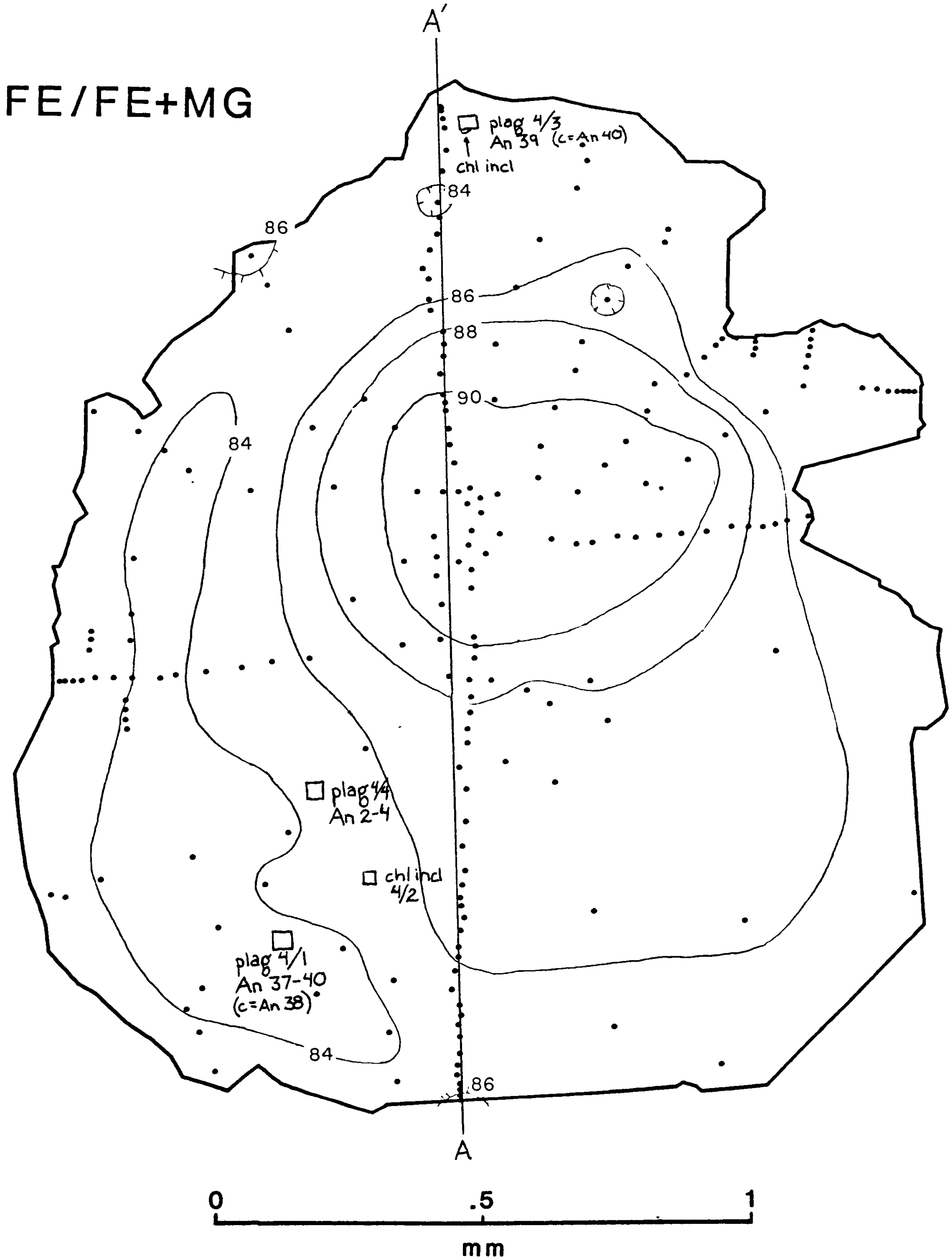

Figure 24: Archertown Brook: Sample D84-3d; Garnet Maps

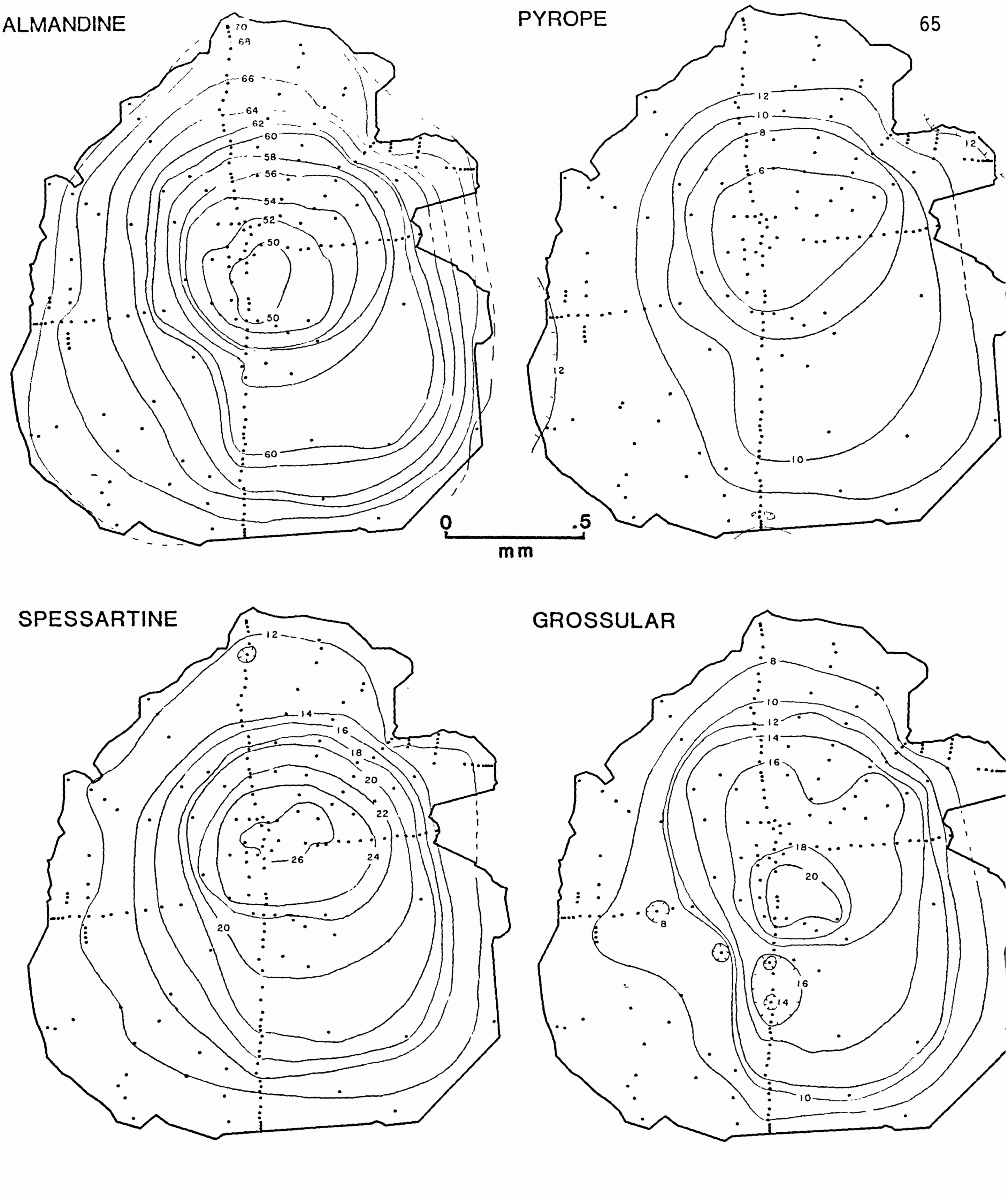

Figure 24: Sample D84-3d; Garnet Maps (cont'd.)

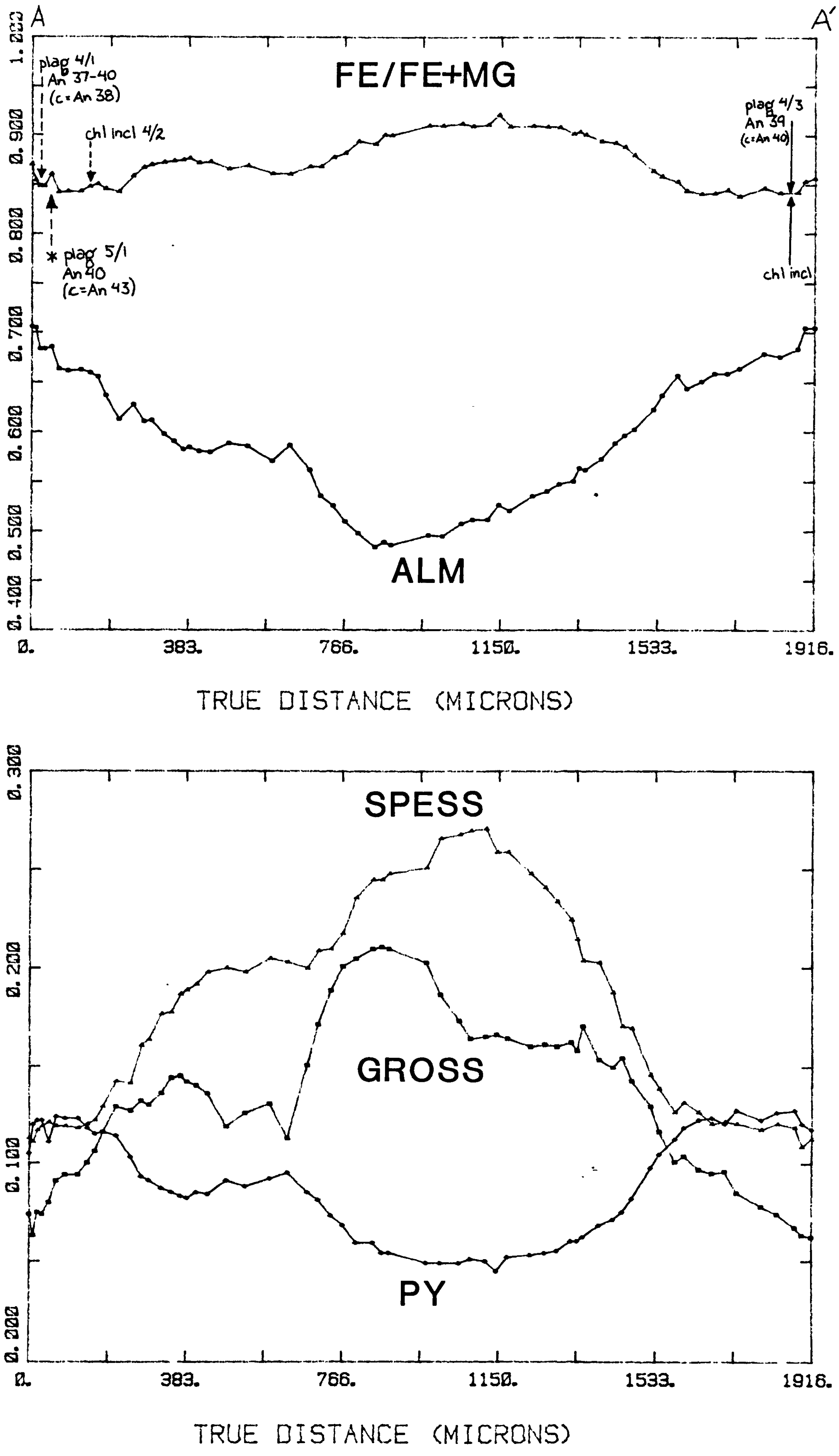

Figure 25: Archertown Brook: Sample D84-3d; Garnet Traverse

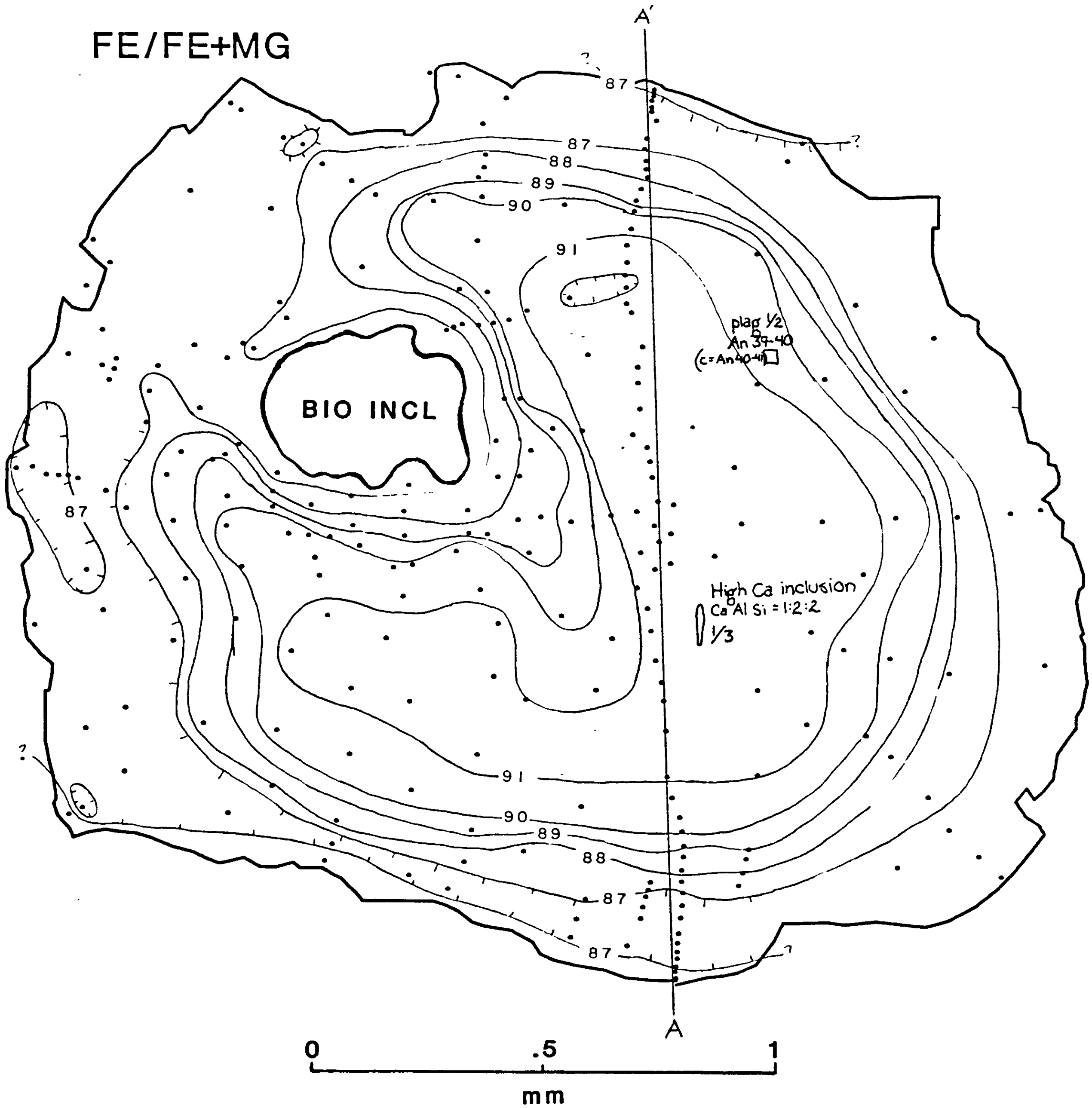

Figure 26: Archertown Brook: Sample PM-9b; Garnet Maps

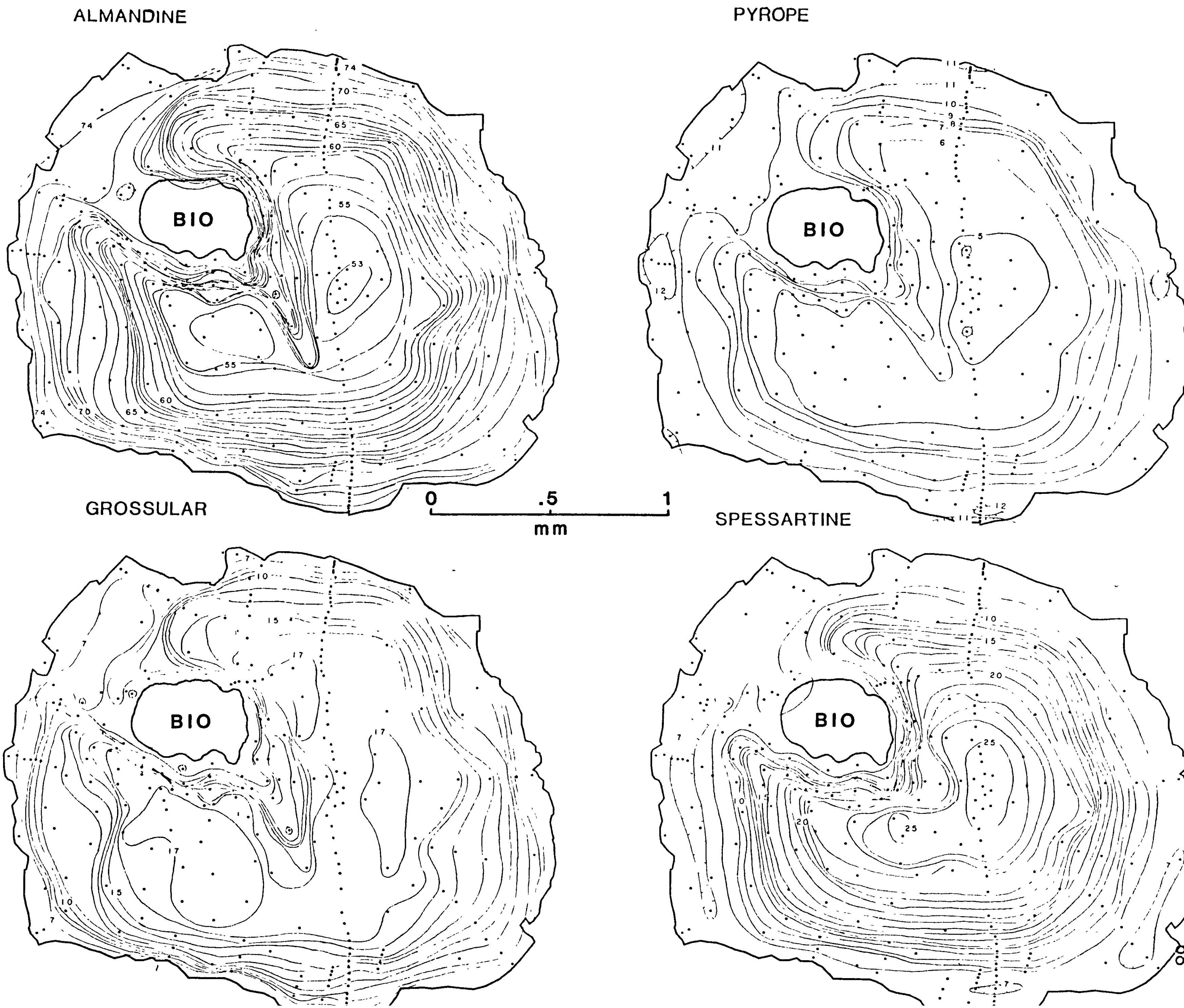

Figure 26: Sample PM-9b; Garnet Maps (cont'd.)

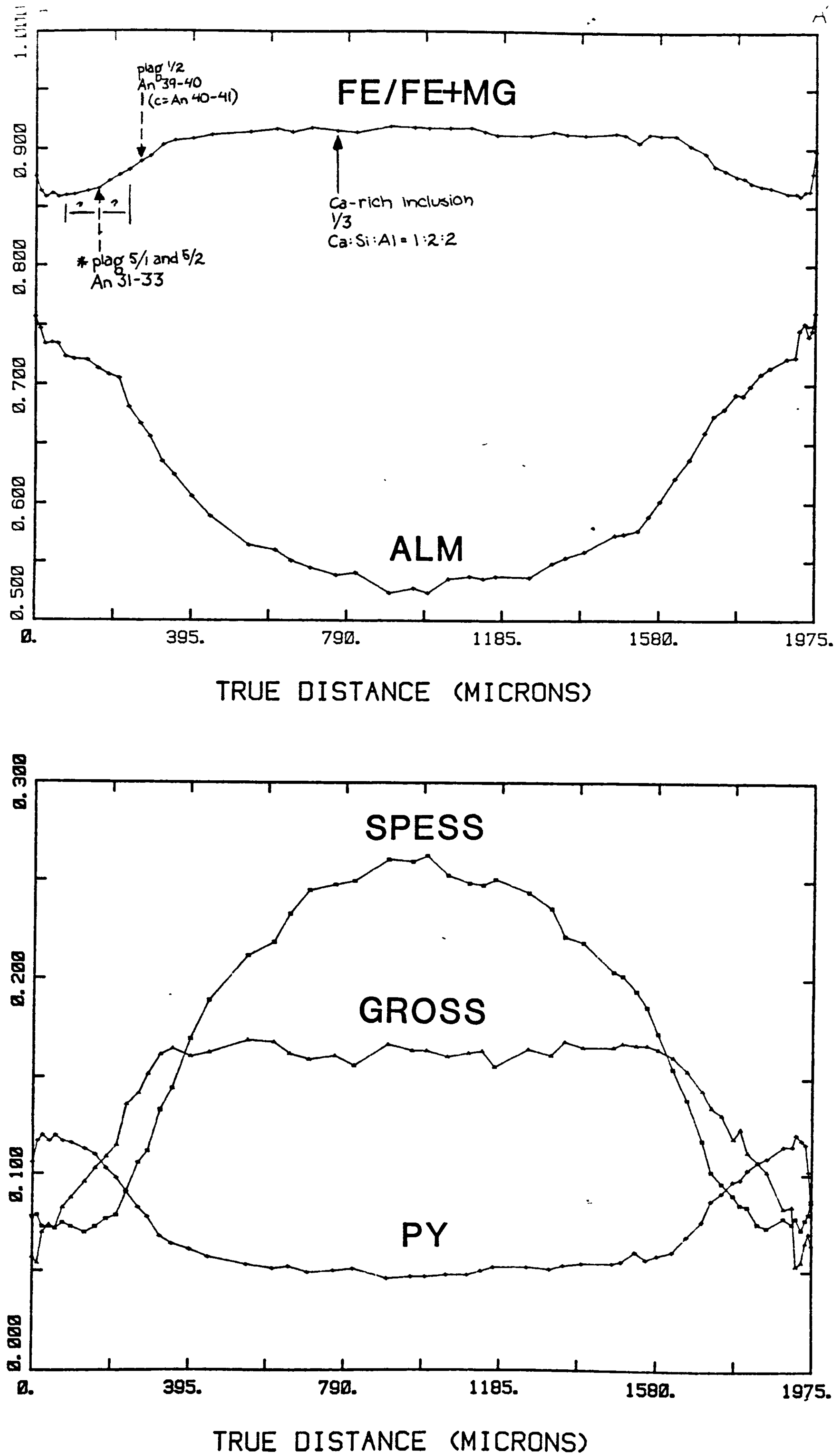

Figure 27: Archertown Brook: Sample PM-9b; Garnet Traverse

FE/FE+MG

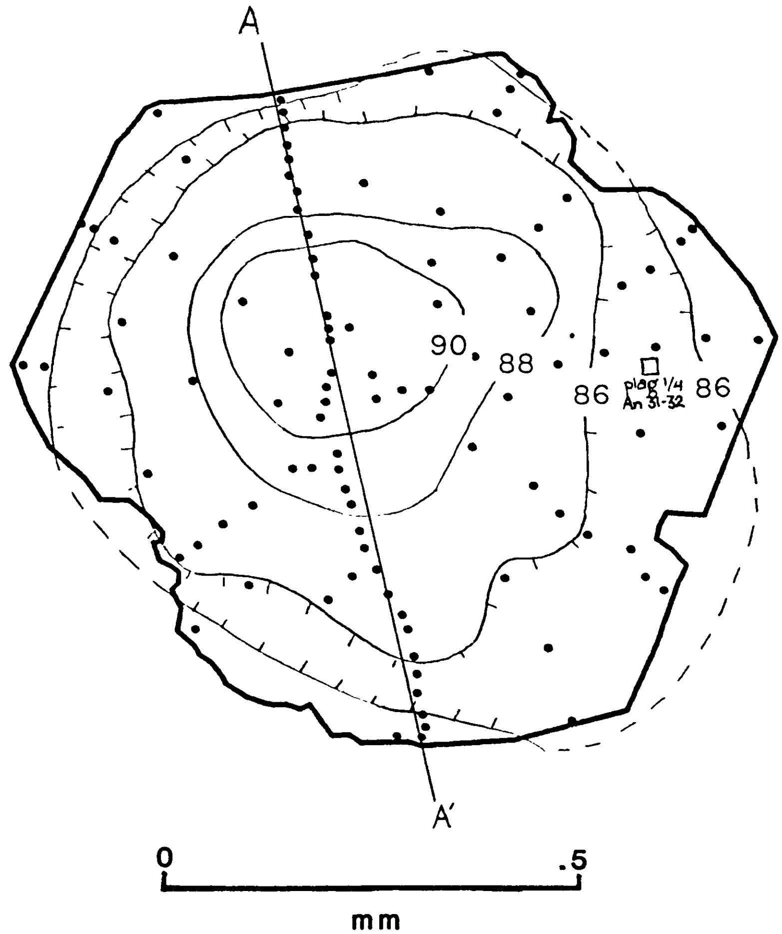

Figure 28: Archertown Brook: Sample PM-11c; Garnet Maps

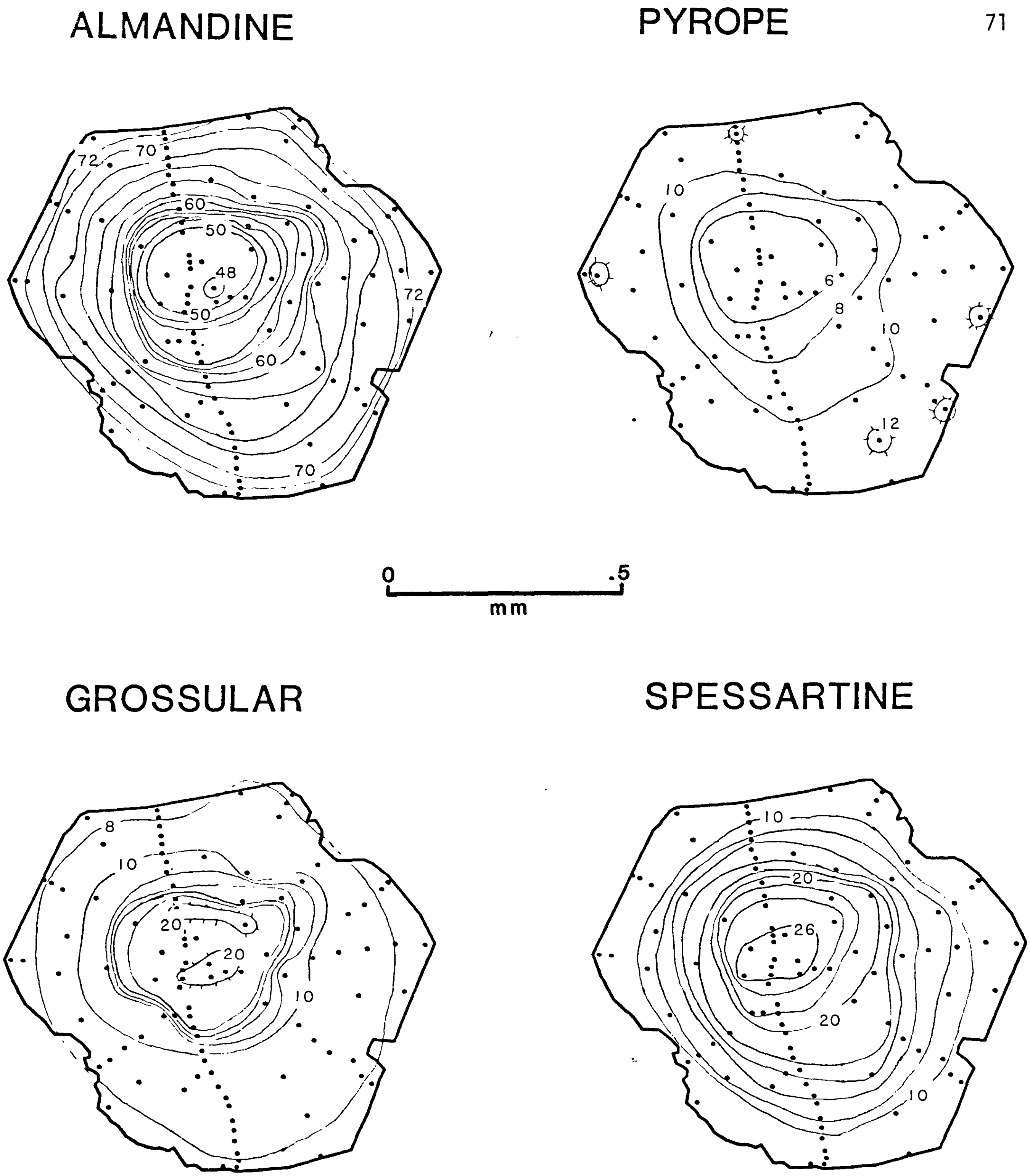

Figure 28: Sample PM-11c; Garnet Maps (cont'd.)

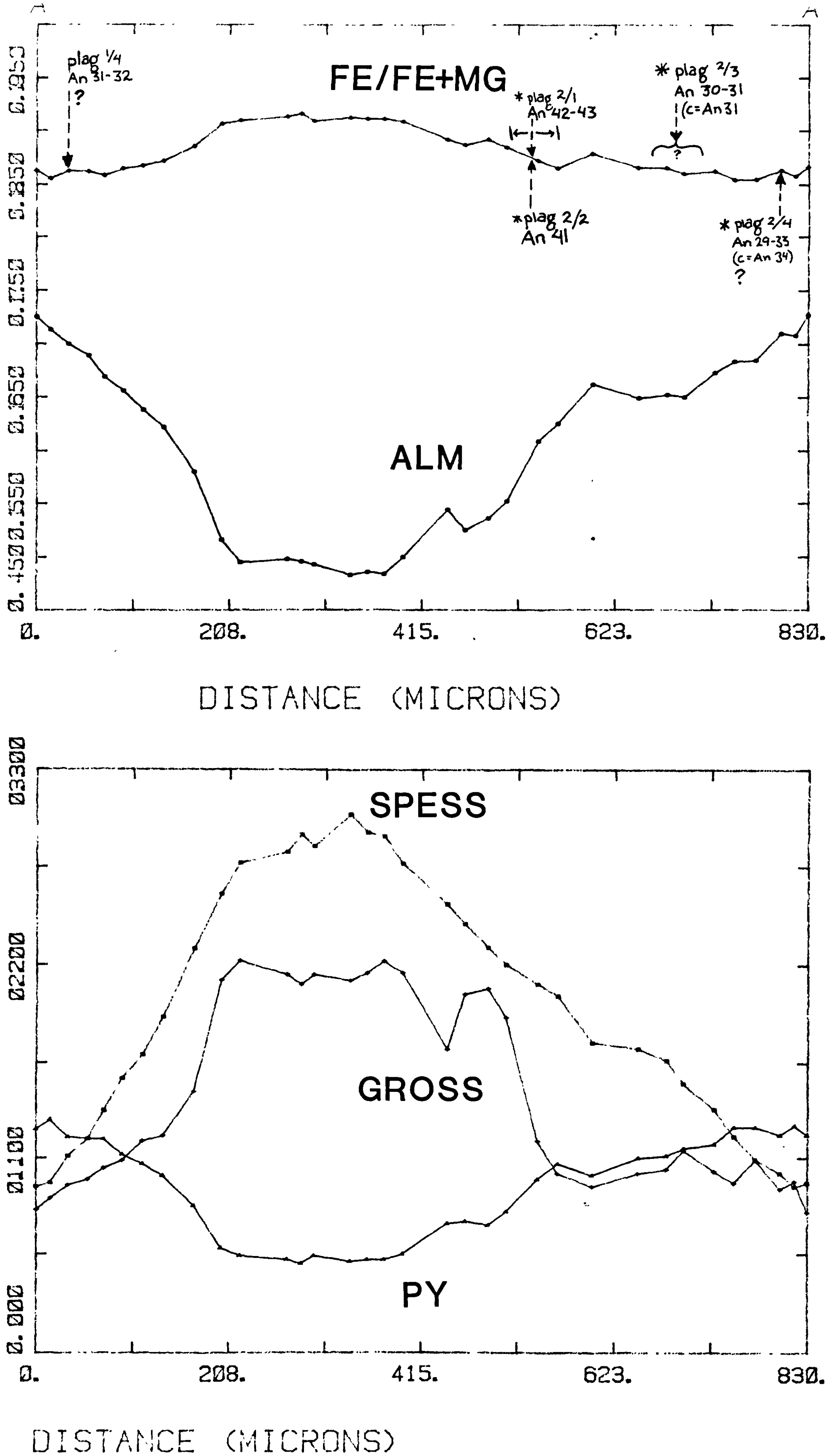

Figure 29: Archertown Brook: Sample PM-11c; Garnet Traverse

The garnet map from PM-9b, Figure 26, exhibits some interesting characteristics. The odd shape of the contours corresponds to garnet compositional changes around a large biotite inclusion. Since changes in grossular component are also seen, this is not likely to be just from iron-magnesium diffusional re-equilibration. Grossular values all decrease to a reasonably consistent value of X_{Gr}=0.075. Additionally, the grossular composition between the inclusion and the rim has values in this neighborhood. This suggests that as the garnet was growing around the biotite, grain boundary diffusion allowed continual re-equilibration of the garnet with the matrix (similar to crack-induced re-equilibration).

This biotite was analyzed and compared to matrix biotites. The Fe/Fe+Mg values determined for several biotites are as follows:

	Fe/Fe+Mg	Average
Biotite inclusion	.419-.447	.434
Biotite in rim (matrix)	.427-.437	.431
Biotite near garnet	.416-.456	.437
Matrix biotite	.430-.442	.436

If there is any difference, the inclusion is more magnesian by a very small amount. Statistically speaking, however, these are identical.

Matrix plagioclases were determined to have rim compositions ranging from An_{22} to An_{28}. A plagioclase inclusion was also identified in PM-9b. The rim composition was determined to be An_{39-40} and the core An_{40-41}. The location of this inclusion is shown on the map (Fig. 26) and on the traverse (Fig. 27). A palgioclase inclusion was found in another garnet from this sample. It does not correlate perfectly with the mapped garnet; the range of possible locations for this inclusion in the mapped garnet is shown on the traverse (Fig. 27). No other plagioclase inclusions were found.

An inclusion of a calcium-aluminum silicate was identified in the core of the mapped garnet. This inclusion was analyzed using the Harvard Cameca probe and yielded a low percentage total, but a Ca:Si:Al ratio of 1:2:2. The analysis was made on an oxygen basis of eight, and the analysis is included in Appendix 1. Based on the stoichiometry, the inclusion could be either anorthite ($CaAl_2Si_2O_8$) or lawsonite ($CaAl_2Si_2O_7(OH)_2 \cdot H_2O$). Lawsonite ideally contains 16% H_2O; tne low weight percent total (95%) is too low for plagioclase, whereas it is also too high for lawsonite. Due to the fact that it is easier to get a low weight percent total than a high weight percent total, this inclusion is praobably not lawsonite. Unfortunately, the grain is too small to obtain definitive optical data.

Sample PM-11c, Figure 28, exhibits some truncated contours where biotite occurs at the rim. In addition, it exhibits a higher grossular plateau in the core than PM-9b. Matrix plagioclases from this sample yielded compositions of An_{27-28}, with minimal zoning between rims and cores. Several plagioclase inclusions were found in garnets from this sample, never more than one to a garnet. The one inclusion found in the mapped garnet is shown on the map, while all of the plagioclase inclusions are show at their correlative compositional points on the traverse in Figure 29. Several of these inclusions are suspect, however, due to the fact that they lie next to cracks in the garnet. These inclusions are marked with a question mark in Figure 29.

In sample 67-78a, a 0.5 mm crystal of subhedral garnet occurs as an inclusion in staurolite. Microprobe analyses of the inclusion's rim show that the staurolite grew towards the very end of garnet growth, with the inclusion's rim composition corresponding to 5-10 microns from the rim of the matrix garnet.

NORTHEY HILL LINE

Two samples from the Northey Hill Line (D84-1c and D84-1d-2) were investigated for garnet zoning, as well as plagioclase, chlorite, chloritoid, muscovite, and biotite compositions. Microprobe analyses from these samples are listed in Appendix 3.

Garnet Zoning

The garnet in D84-1c was probed at 273 points and D84-1d-2 was probed at 154 points using the "turbo-probe" technique. A problem was encountered with a bad carbon coat on D84-1c. Thus analyses 1-72 are on the poorly coated sample while 100-300 are on the better coated sample. Discrepencies between identical points in the two sets exist, yet the earlier data is of some use. The earlier analyses are left on the plot, but disregarded when large differences are found. Contoured garnet maps of D84-1c and D84-1d-2 are included as Figures 30 and 32. Additionally, linear traverses across both of these garnets are included as Figures 31 and 33.

The most striking feature of these garnets is their incredibly flat zoning profile. The most variable component is spessartine, which varies from 0.036 to 0.072 in D84-1d-2. The two garnets show similar zoning patterns, yet they formed in different bulk compositions. D84-1d-2 has more grossular, far less spessartine, similar pyrope, and more almandine than D84-1c.

Another distinctive feature about the D84-1c garnet is its curious comma shape. The garnet map suggests that the core is in the middle of the lower half. The contours of the west half, however, continue on into the arm. The only low grossular values inside the arm are found on a small garnet island. The area inside this arm is composed almost entirely of quartz. This suggests that some resorption has taken place. Due to the existence of several other garnet islands inside this arm, this morphology is interpreted to be due to resorption. Rotated inclusion trails of ilmenite and quartz suggest that the garnet formed syn-tectonically.

Matrix palgioclases from this sample were analyzed using both MIT's MAC probe and Harvard's Cameca probe. Analyses made with the MIT probe

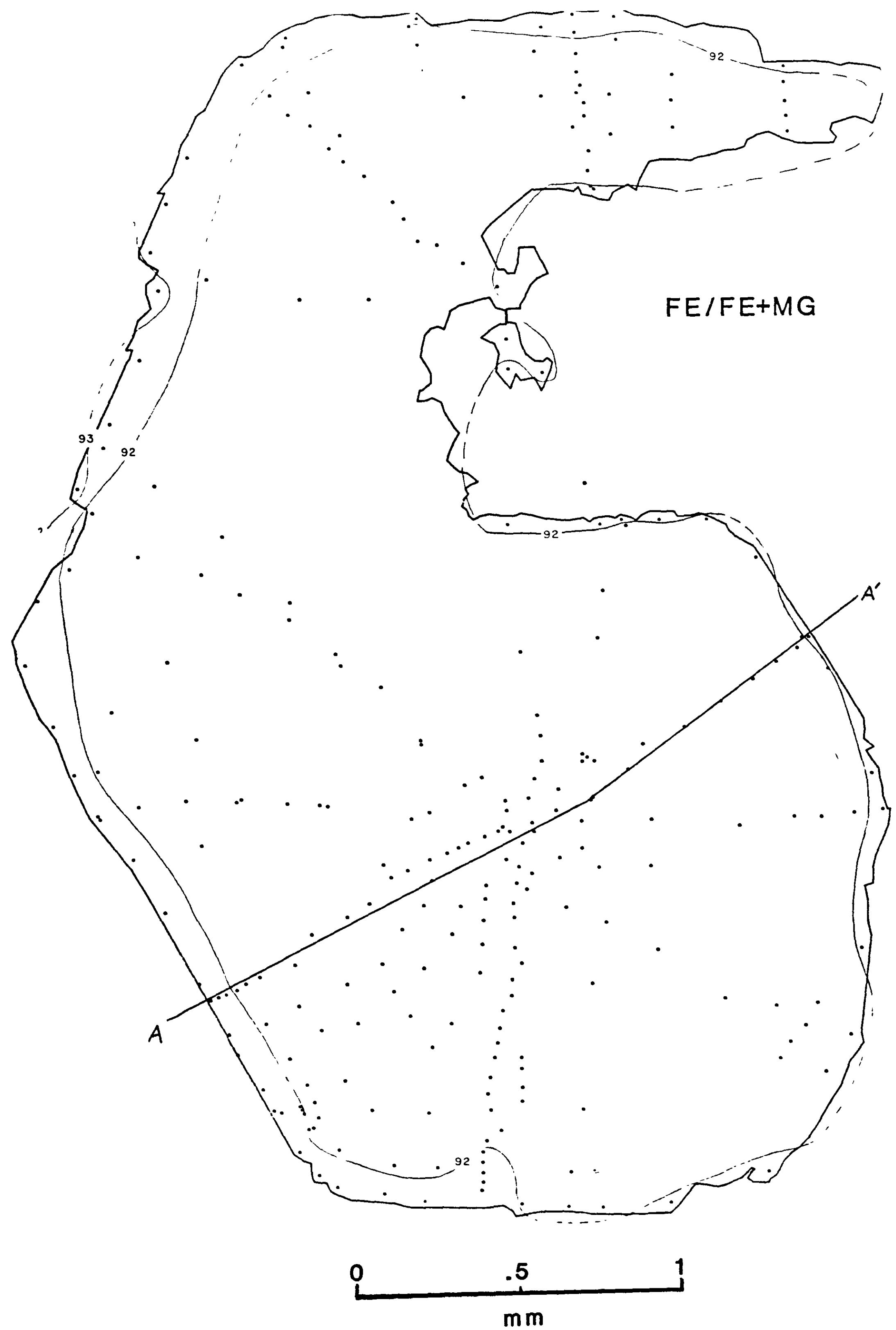

Figure 30: Northey Hill Line: Sample D84-1c; Garnet Maps

Figure 30: Sample D84-1c; Garnet Maps (cont'd.)

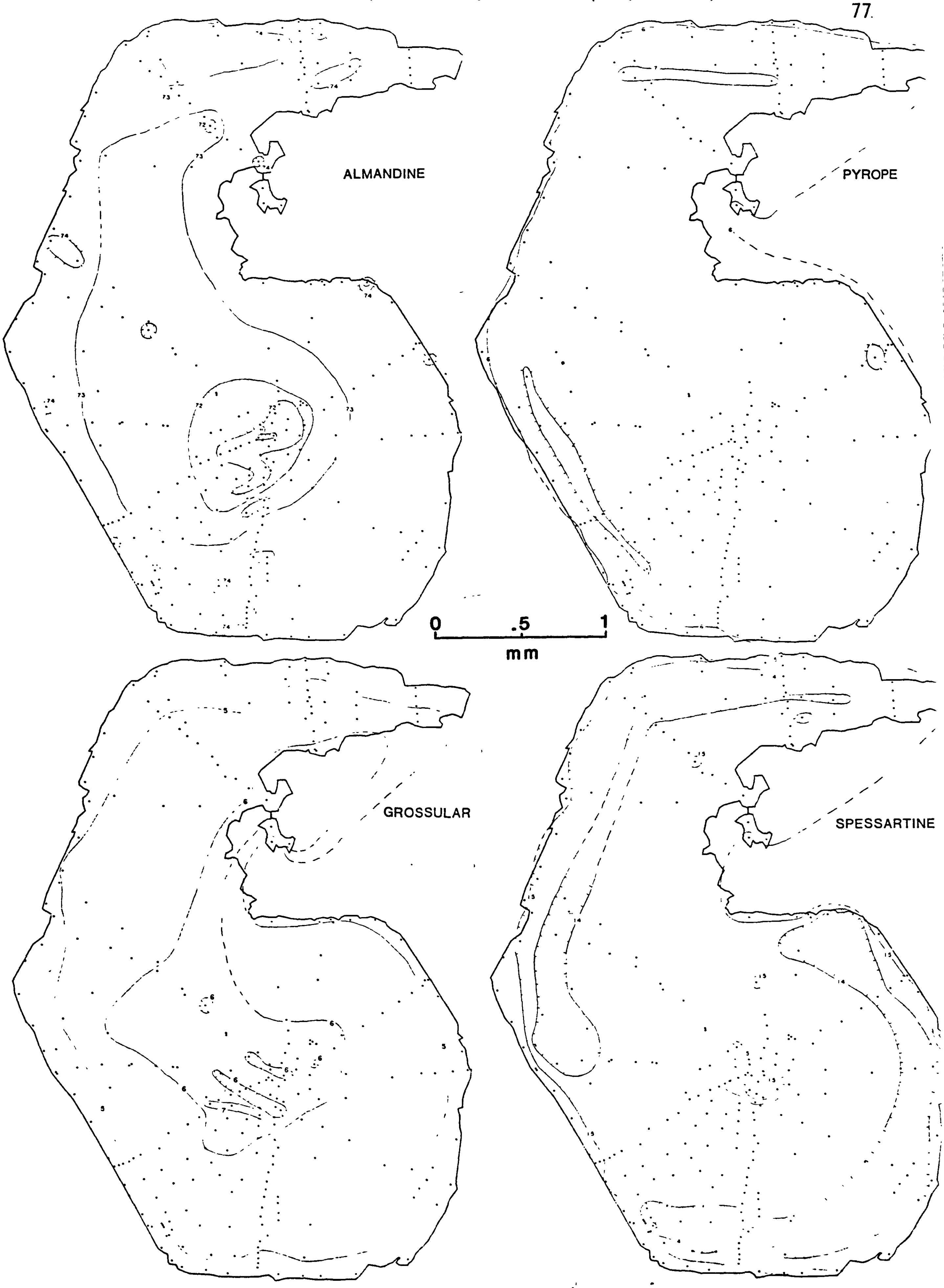

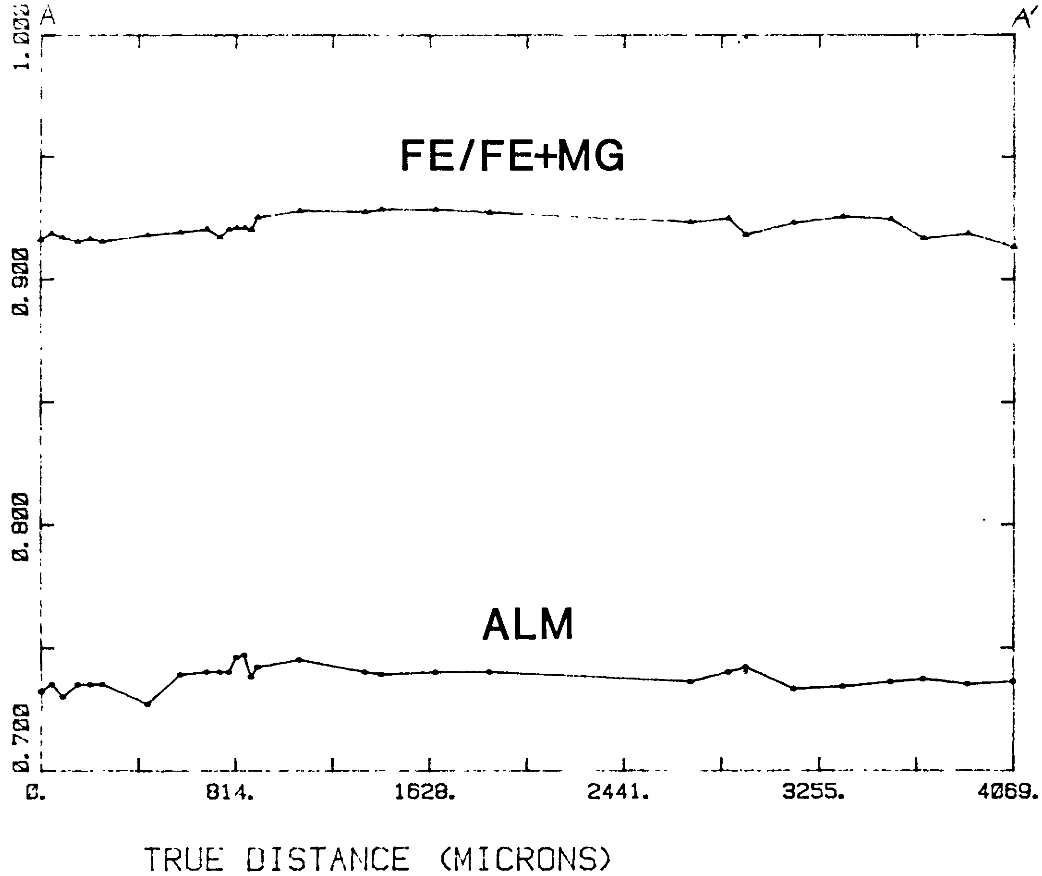

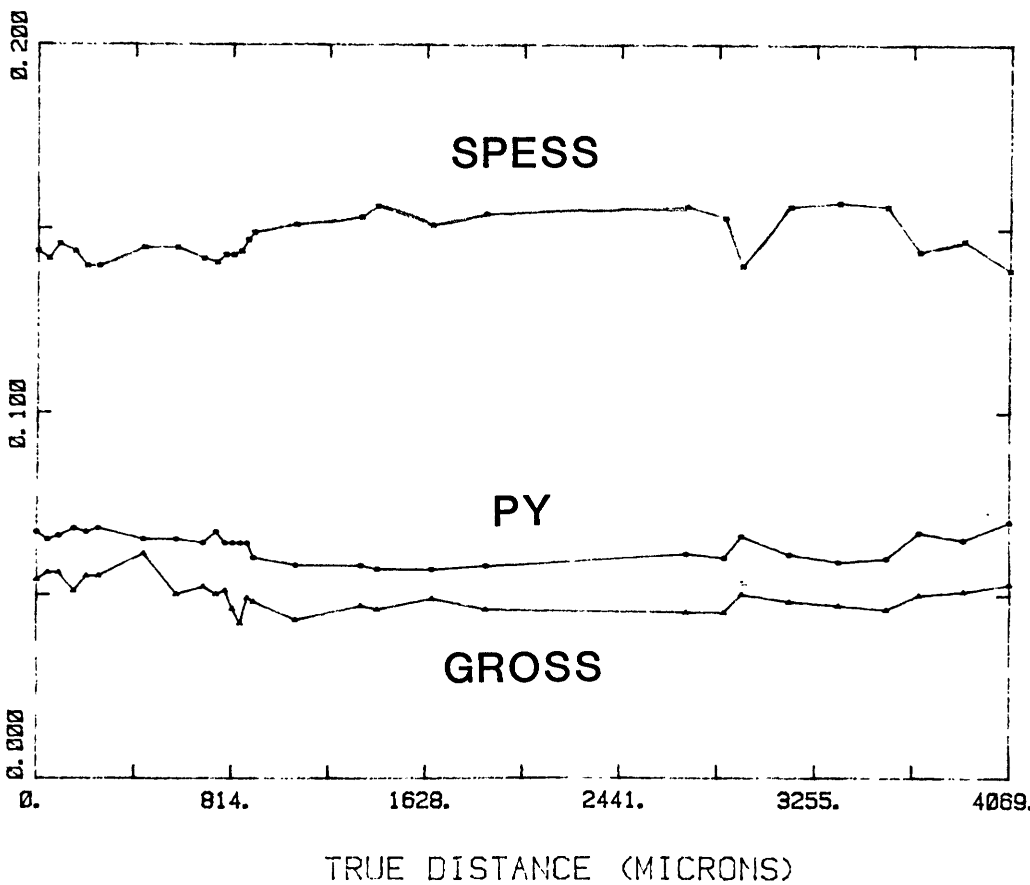

Figure 31: Northey Hill Line: Sample D84-1c; Garnet Traverse

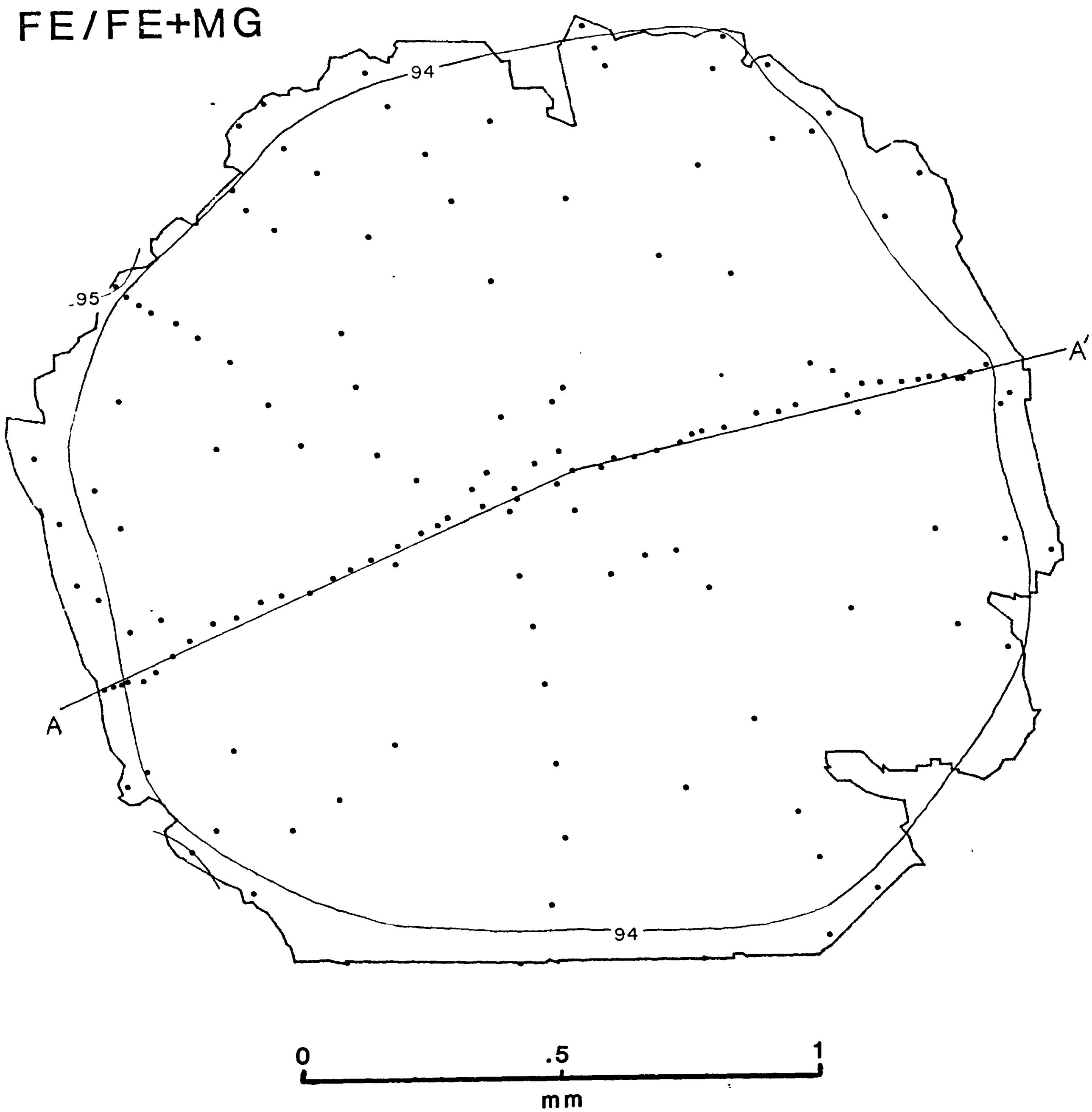

Figure 32: Northey Hill Line: Sample D84-1d-2; Garnet Maps

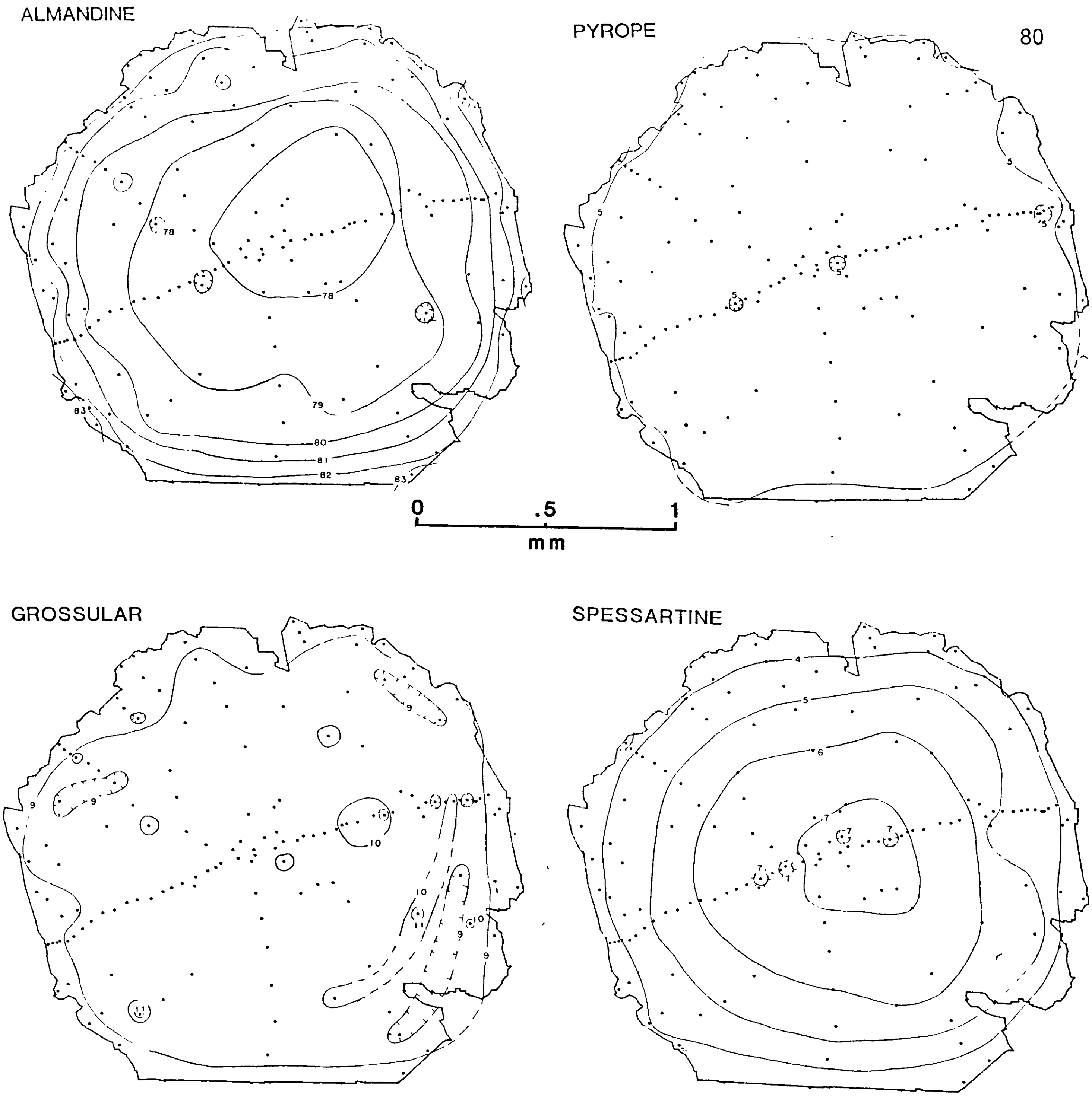

Figure 32: Sample D84-1d-2; Garnet Maps (cont'd.)

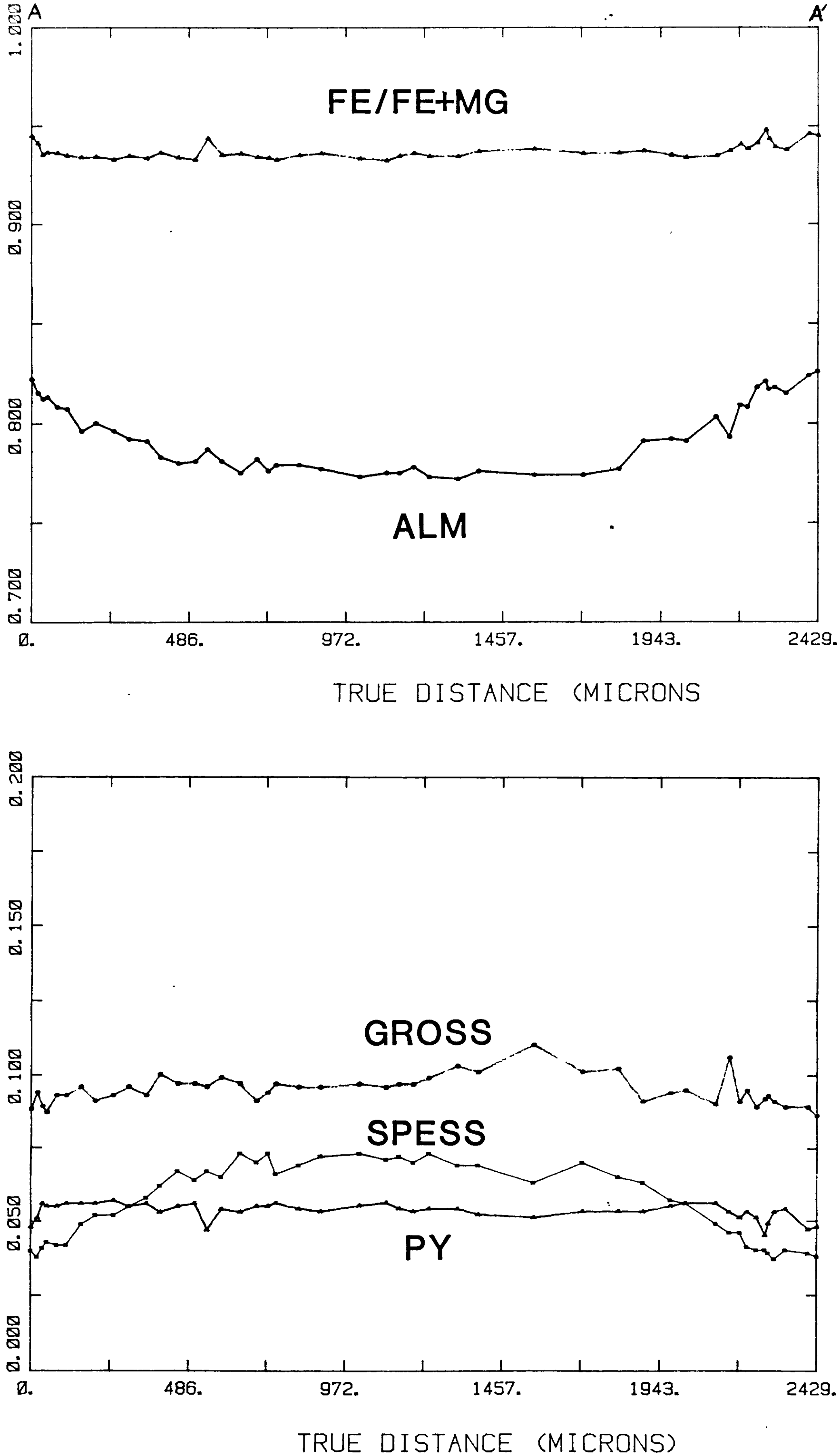

Figure 33: Northey Hill Line: Sample D84-1d-2; Garnet Traverse

fall into the range of An_{19-23} with grains having more anorthitic cores (zoning of An_2). Analyses made with the Harvard probe fall into the range of An_{13-14}. No plagioclase inclusions were found in this sample. Inclusions in this sample consist entirely of quartz and ilmenite.

Sample D84-1d-2 shows higher magnitude zoning than D84-1c. The pyrope component is basically unzoned while the grossular component is very slightly zoned. In contrast, almandine and spessartine are antithetically zoned. With pyrope constant and almandine changing, the Fe/Fe+Mg also changes. The grossular compositions fluctuate slightly from the rim to the core.

Matrix plagioclases from D84-1d-2 have rim compositions ranging from An_{33} to An_{36}. Core compositions range from An_{37} to An_{38}. The maximum zoning seen in any one grain is An_4. These analyses come from both the MIT microprobe and the Harvard microprobe. No plagioclase inclusions are present in this sample. Abundant ilmenite inclusions were found, as well as quartz and apatite. Ilmenite inclusions were investigated using EDS spectrometry and were found to have higher manganese contents toward the core of the garnet.

JACOBS BROOK RECUMBANT SYNCLINE

In the Jacobs Brook Recumbant Syncline, four samples (D84-2e, D84-4k, D84-4e, and D84-2c) were analyzed for garnet compositions, biotite, chlorite, staurolite, muscovite, and margarite. No plagioclase was found in these samples. Microprobe analyses from these samples are listed in Appendix 4.

Garnet Zoning

Two of the four garnets were extensively analyzed for garnet maps. D84-4k was analyzed at 200 points using the turbo-probe technique, while D84-2e was analyzed at 100 points. D84-4k is contoured at $X_{0.02}$ while D84-2e is contoured at $X_{0.01}$. The garnet maps follow as Figures 34 and 36. Linear traverses were made across these garnets, and these follow as Figures 35 and 37.

Sample D84-4k exhibits an unusual shape and a steep zoning profile. In contrast to the Northey Hill Line sample D84-1c, the contours on this garnet continue on both sides of this "horse-head" shape. All contours except the last one continue around the head. The shape is also mirrored by elongated inclusions parallel to the contours and rim. This appears to be a garnet that has grown syntectonically. The truncated contours seen at the very nose of the horse head can be attributed to resorption. Another possibility is that there has been a lack of communication between the garnet and the matrix due to this area being occupied by only two large quartz grains. This garnet exhibits an almandine-pyrope-rich rim with spessartine and grossular increasing toward the core. One curious feature is that the grossular core is skewed slightly with respect to the other phases.

No plagioclase inclusions were found in D84-4k. One staurolite inclusion was found near the rim, and abundant margarite and ilmenite inclusions were found throughout the garnet. Ilmenite inclusions were investigated using EDS spectrometry techniques and the manganese contents increase toward the core.

Several margarite inclusions were analyzed quantitatively; calcium contents were found to increase towards the core of the garnet. Individual margarite grains, however, have higher calcic rims and lower calcic cores.

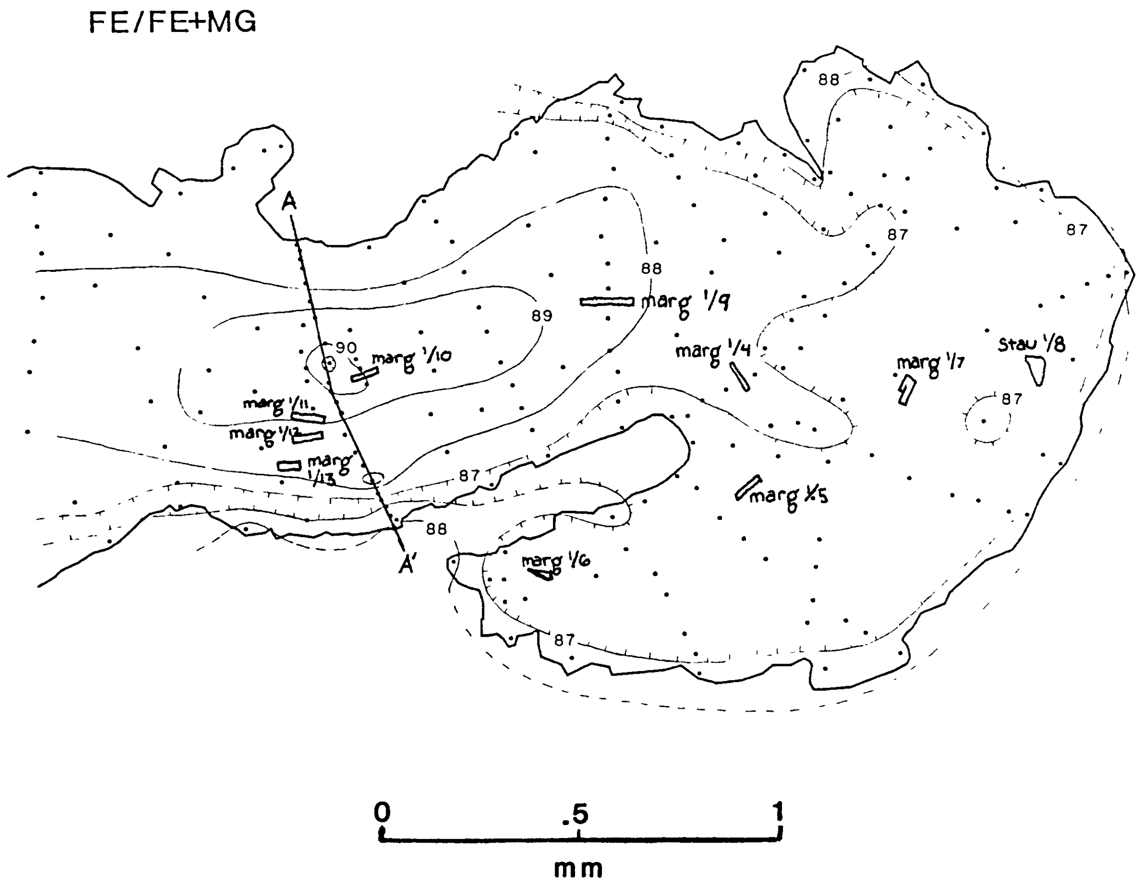

Figure 34: Jacobs Brook Recumbant Syncline: Sample D84-4k; Garnet Maps

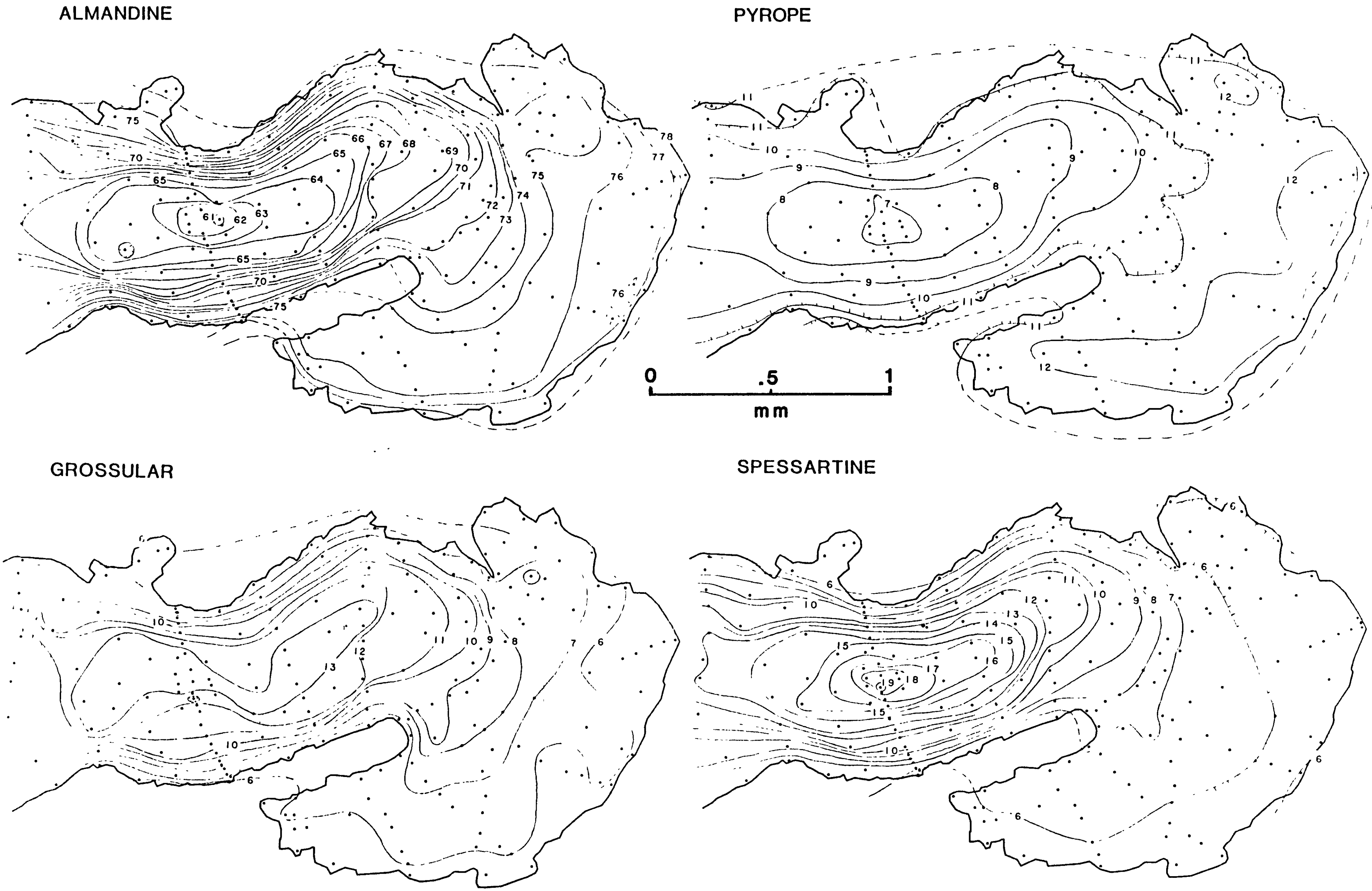

Figure 34: Sample D84-4k; Garnet Maps (cont'd.)

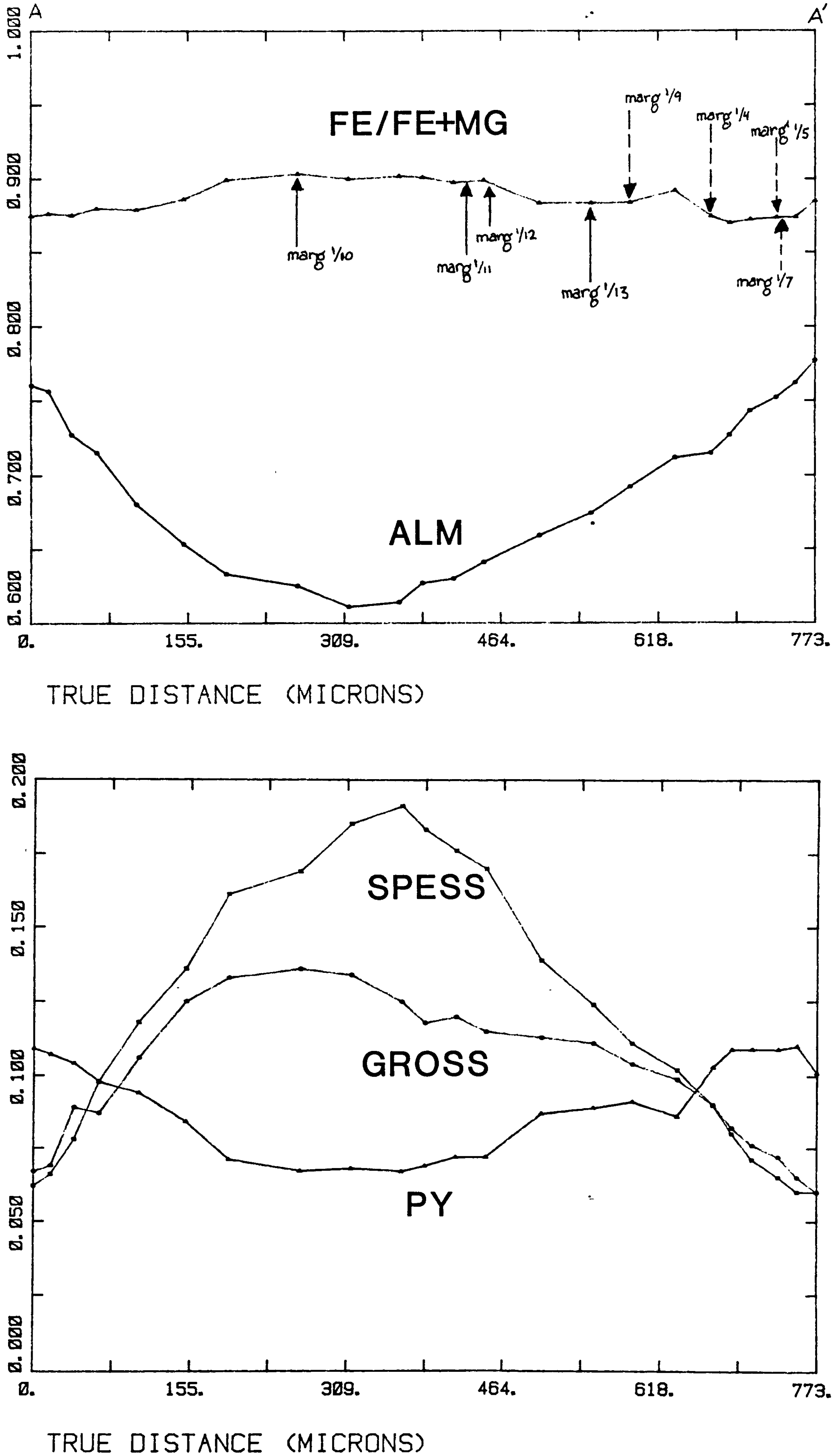

Figure 35: Jacobs Brook Recumbant Syncline: Sample D84-4k; Garnet Traverse

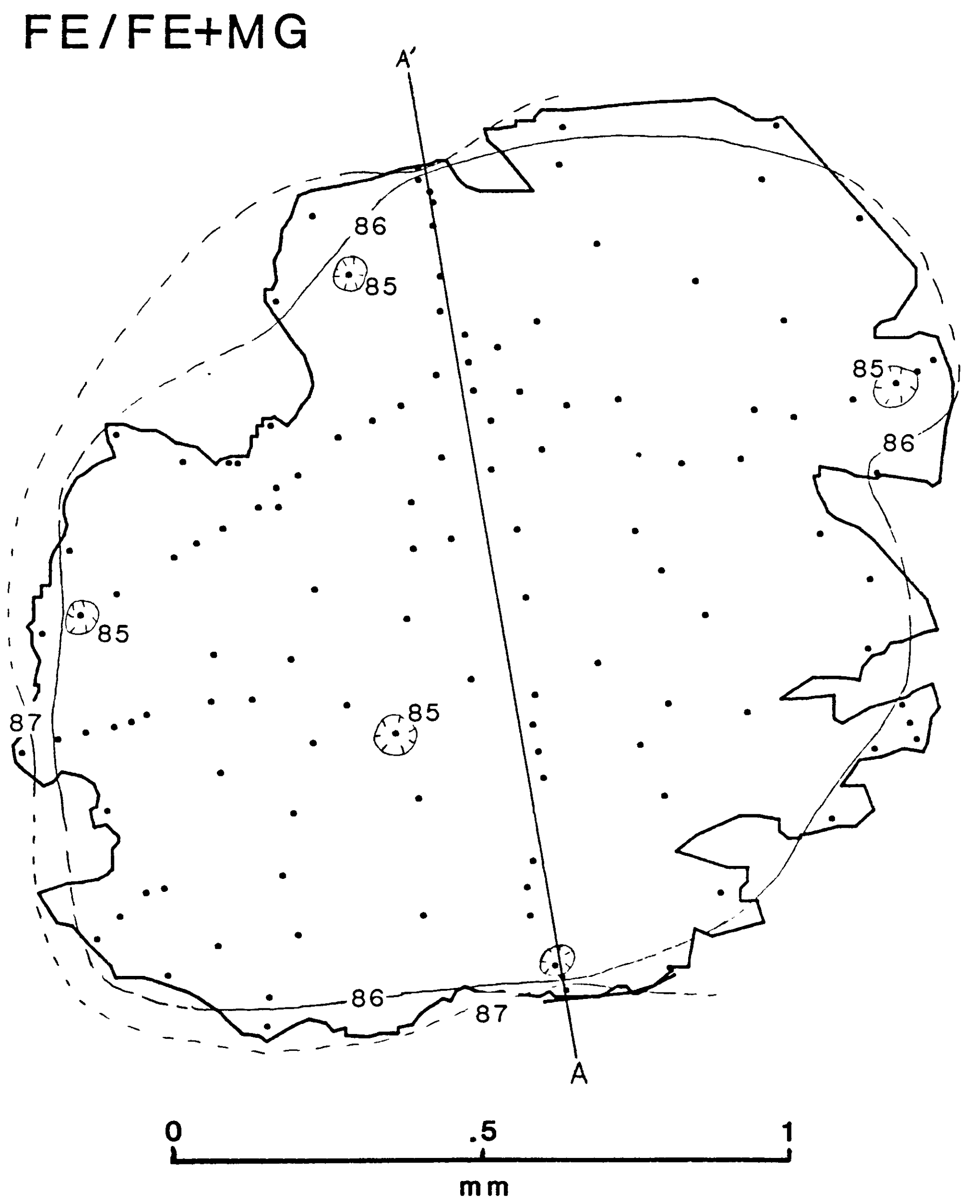

Figure 36: Jacobs Brook Recumbant Syncline: Sample D84-2e; Garnet Maps

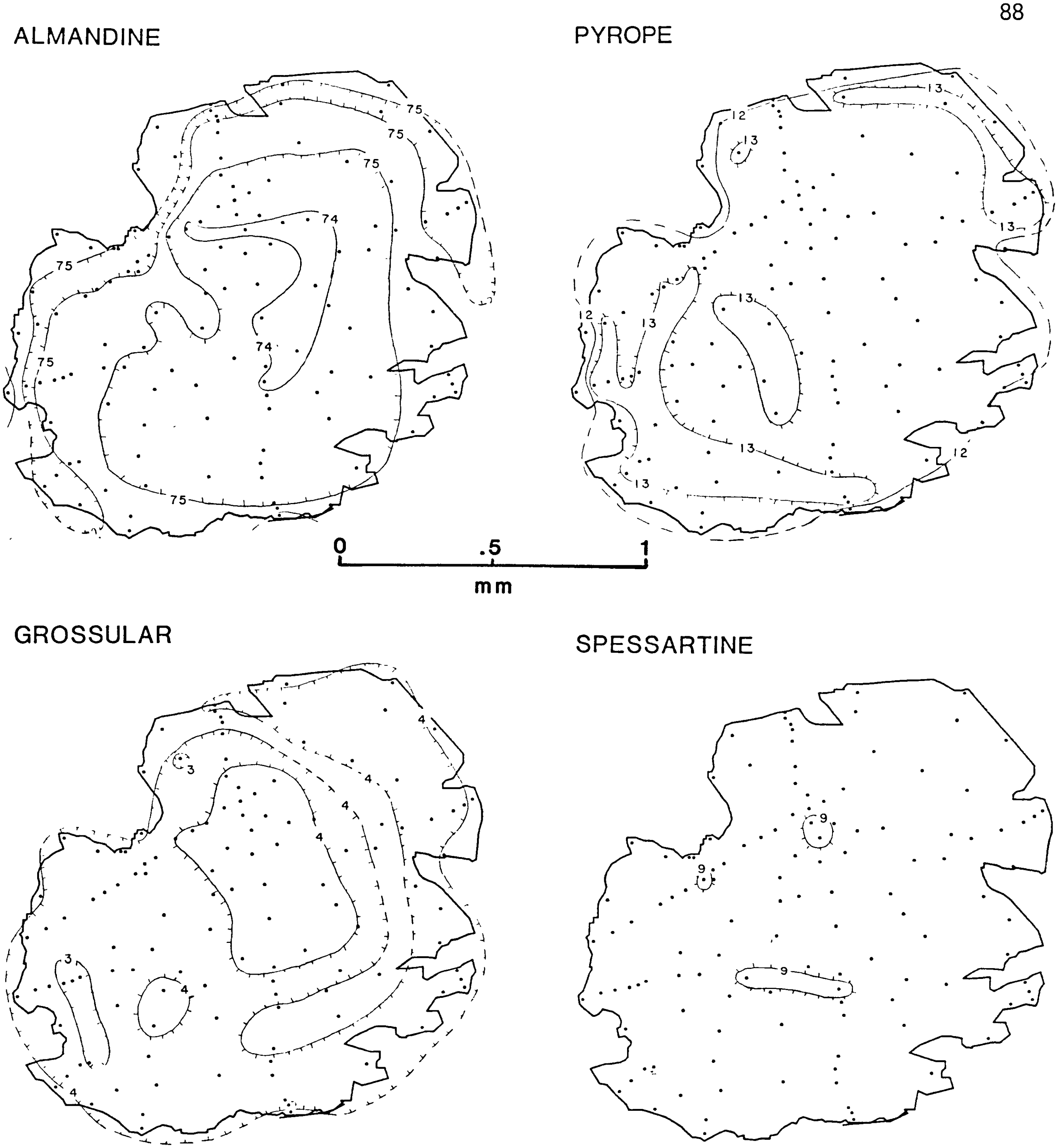

Figure 36: Sample D84-2e; Garnet Maps (cont'd.)

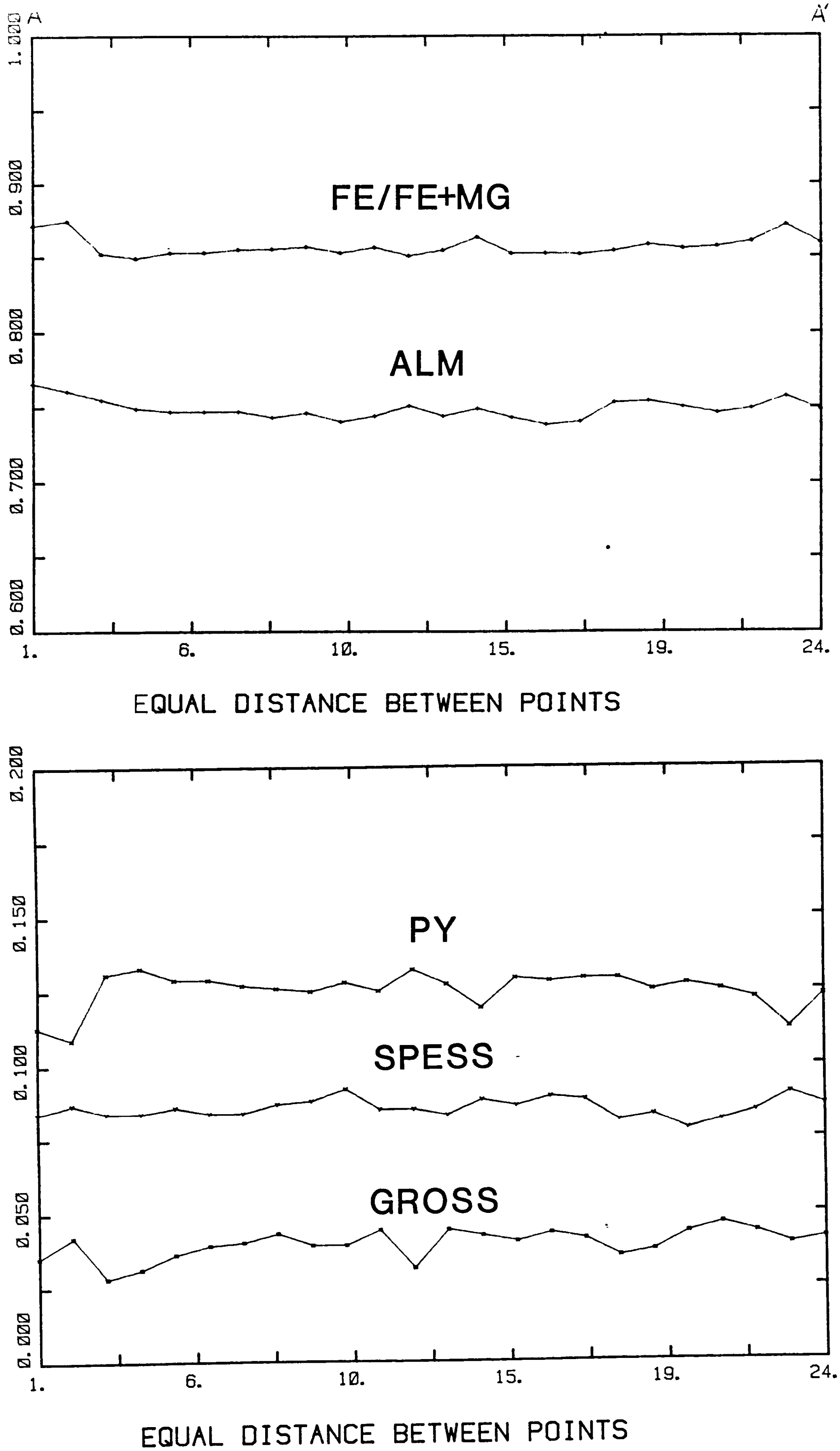

Figure 37: Jacobs Brook Recumbant Syncline: Sample D84-2e; Garnet Traverse

Sample D84-2e has a dramatically different character than D84-4k. This garnet displays far less compositional zoning, with almandine exhibiting a maximum difference of 0.02. Pyrope has a 0.02 maximum difference while spessartine and grossular are less than 0.01.

No plagioclase or margarite inclusions were found in this garnet. All but one non-opaque inclusion in this poikilitic garnet are quartz. The one exception is a tourmaline. Inclusions of rutile and ilmenite were identified, but none was analyzed with the probe.

BAKER POND

For the Baker Pond locality, one sample (79-449f) was analyzed using the electron microprobe for garnet, plagioclase, staurolite, biotite, cordierite, muscovite, and chlorite. Microprobe analyses from this samples are listed in Appendix 5.

Garnet Zoning

Several different techniques were used to collect 270 data points on the garnet from 79-449f. This is the sample that the "turbo-probe" technique was developed on. Twenty full oxide analyses were collected. These gave an indication of the magnitude of zoning. The analysis time was cut to ten seconds, and another 97 points were collected analyzing all six components for the shorter time. The remaining 154 points were collected using the "turbo-probe" technique: short time and four elements.

The garnet was mapped in contours of $X_{0.01}$. The garnet maps follow as Figure 38. Due to the higly irregular zoning in 79-449f, a traverse is not shown.

This garnet exhibits an almandine-pyrope-rich rim. Grossular and spessartine increase toward the core while almandine and pyrope decrease. The contours in 79-449f exhibit a non-symmetrical character. Garnet spans

FE/FE+MG

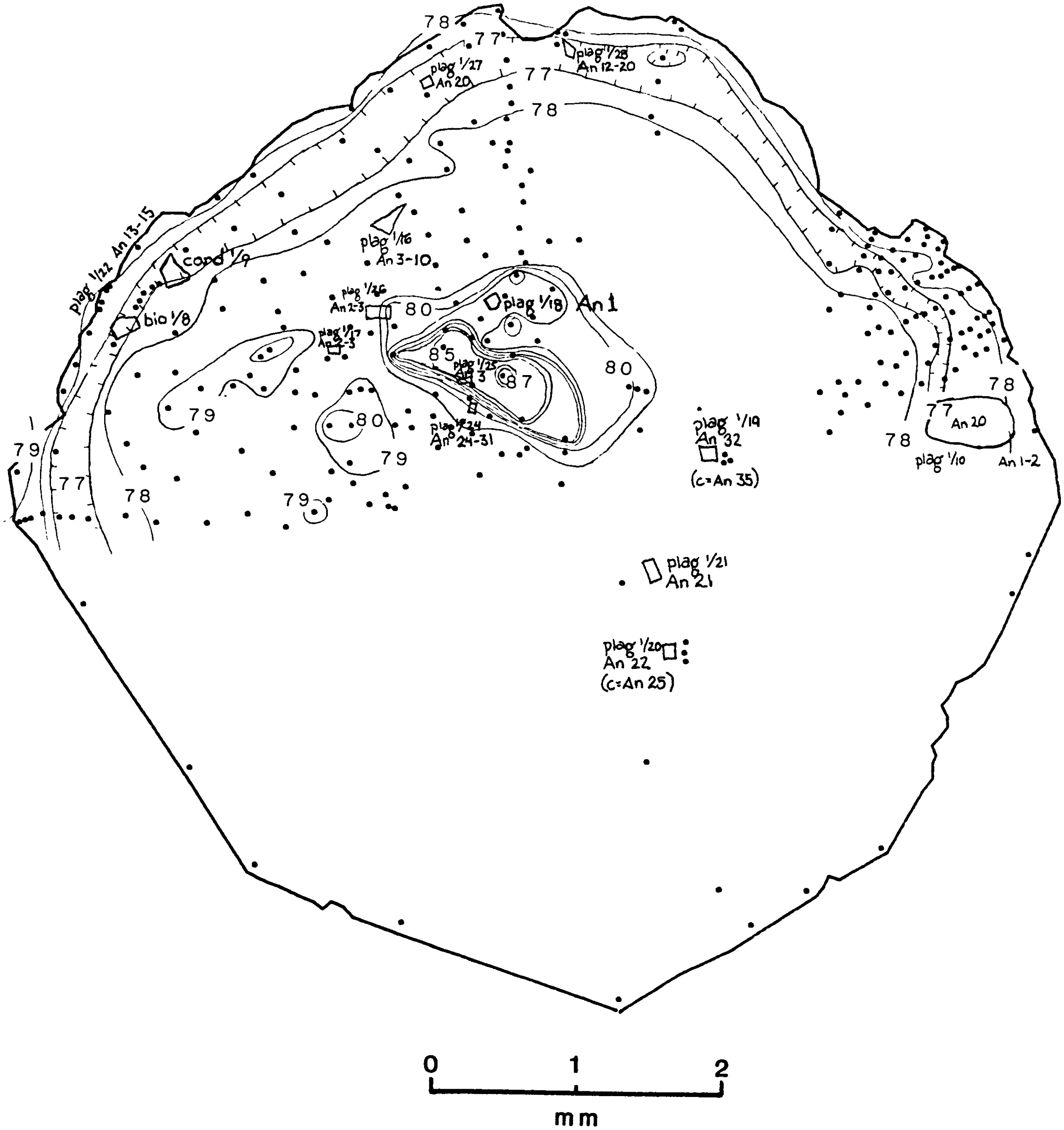

Figure 38: Baker Pond: Sample 79-449f; Garnet Maps

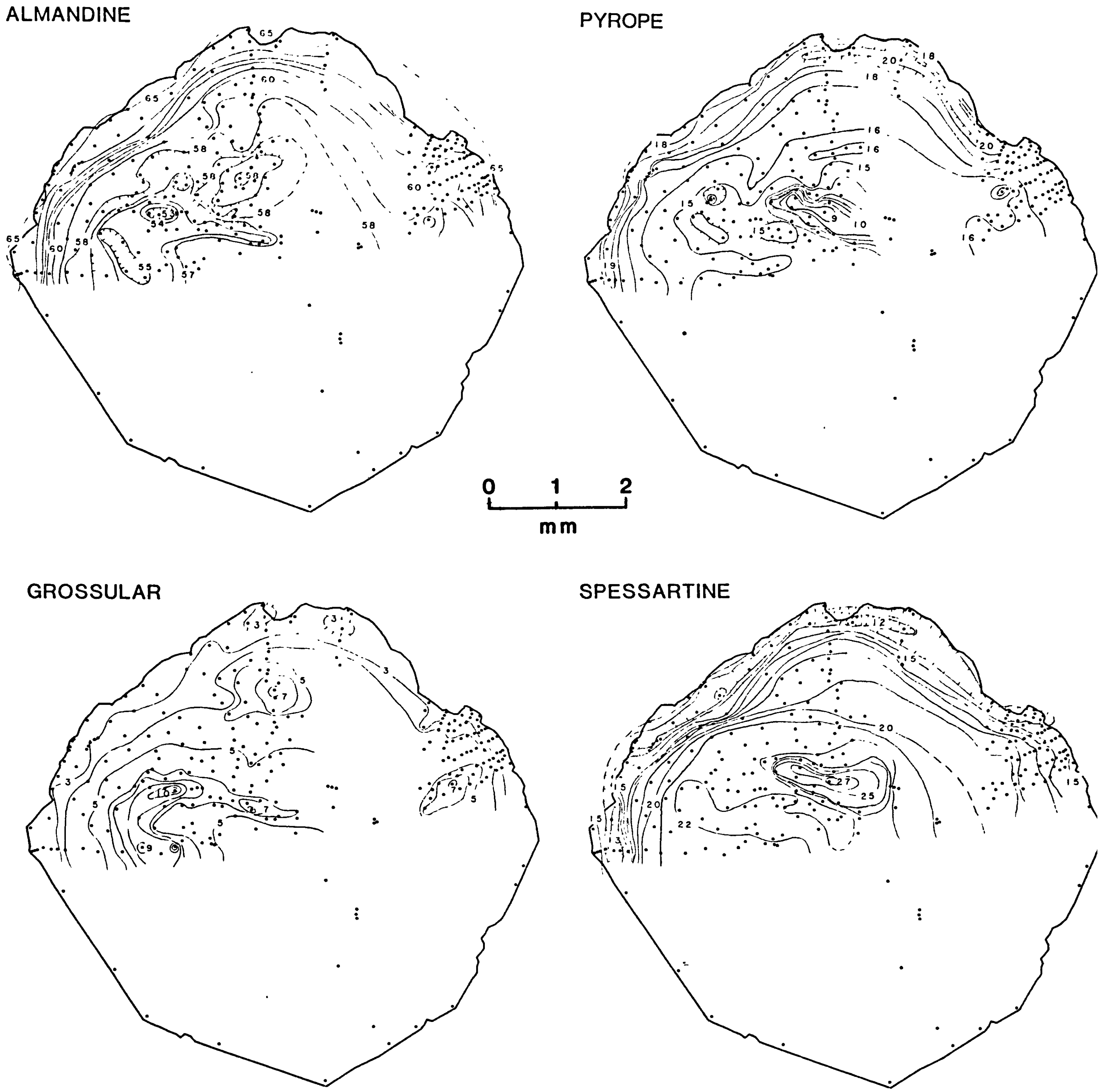

Figure 38: Sample 79-449f; Garnet Maps (cont'd.)

two different layers--one with far more cordierite + staurolite + biotite than the other. A syn-deformational garnet growing in two bulk compositions would be expected to have an odd contour character. This garnet also exhibits a small number of truncated contours. In these areas, the garnet is resorbed and it is rimmed by a thin layer of plagioclase (An_{13-15}).

The location of the "core" is difficult to discern. The highest grossular values coincide with the lowest almandine values, yet these are in a totally different location than the highest spessartine and lowest pyrope values. The grossular-almandine "core" occurs in a section of the garnet that appears to be rotated around from the other bulk composition area (Fig. 39). Due to this relationship, as well as the very steep contours of pyrope and spessartine as compared to grossular and almandine, the core is considered to be at the high-spessartine, low-pyrope location.

In sample 79-449f, three matrix plagioclases were analyzed. Rim compositions vary from An_{11} to An_{15}. The maximum observed zoning was An3 with the core more calcic than the rim. Plagioclase inclusions in matrix biotites had rim compositions of $An_{7.5}$ and core compositions of $An_{8.5}$. These analyses are puzzling due to the fact that they fall into the middle of the peristerite gap. It is possible that these are "mixed" analyses where the electron beam spanned two different plagioclase compositions.

Many inclusions were investigated in this garnet. Plagioclase, biotite, cordierite, and chlorite were analyzed, while ilmenite was observed using EDS analysis techniques. The locations and compositions of the analyzed inclusions are shown on the Fe/Fe+Mg map in Figure 38. Biotite and cordierite occur close to the rim, and have Fe/Fe+Mg values less than their matrix counterparts, although the values are similar. Plagioclase inclusions near the rim vary from An_{12} to An_{20}. From one-third

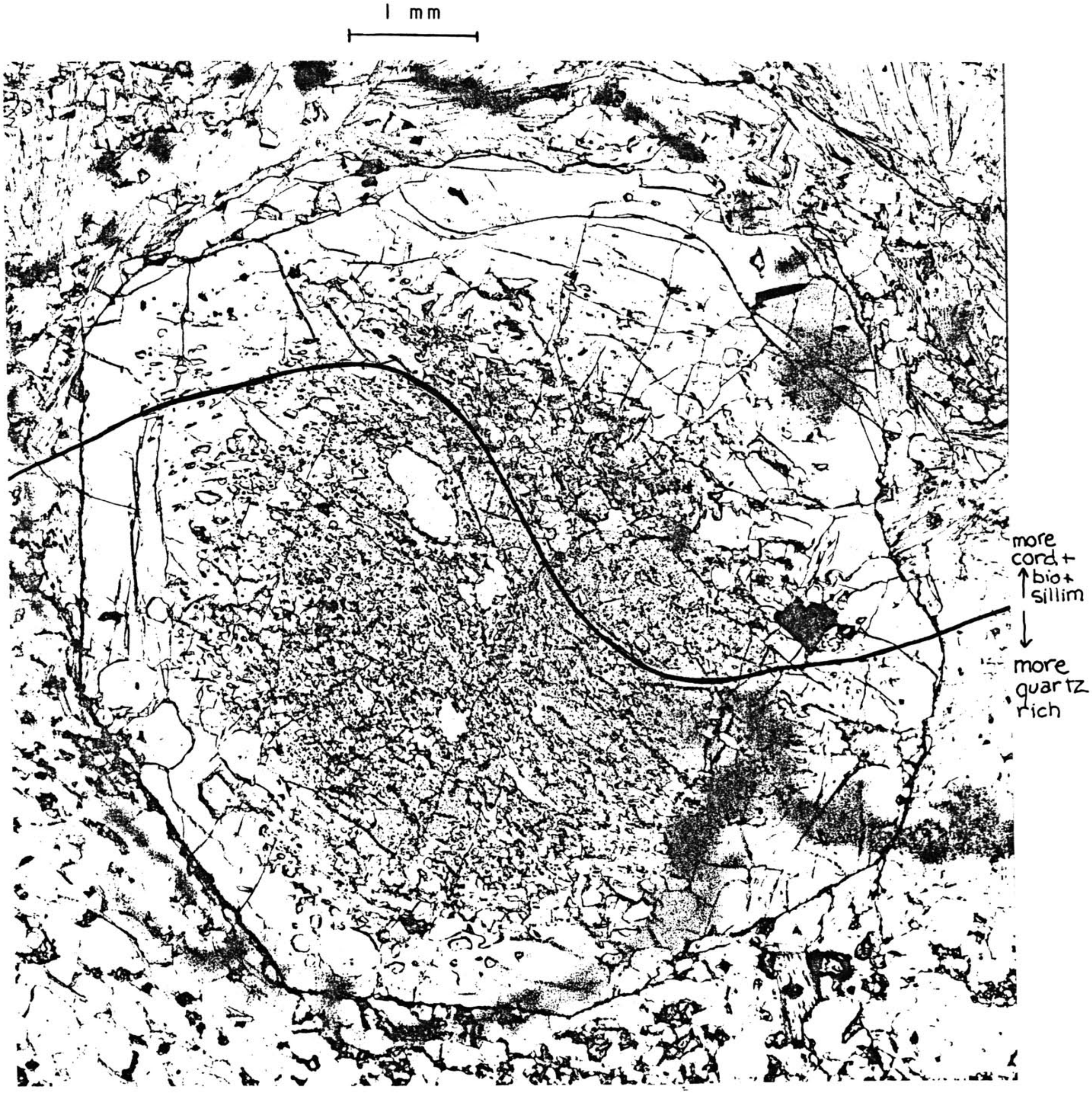

Figure 39: Baker Pond: Sample 79-449f; Exhibiting rotated garnet spanning different bulk compositions.

of the way in to just near the core, every plagioclase is albite. Plagioclase in the core is An_{25-32}. A large number of chlorite inclusions were analyzed. Unfortunately no definitive systematic change in their compositions can be identified. Investigation of backscatter photographs suggest re-equilibration along cracks as the major reason for variability. Figure 40 shows one such chlorite, its visible compositional differences, and the Fe/Fe+Mg values at certain points. Different crack densities, matrix communication rates, and initial chlorite values are probably responsible for the variability seen in these samples. Ilmenites were found to have higher manganese values towards the core of the garnet.

GARNET ZONING: DISCUSSION

The garnets from the various localities in the study area show a wide variety of garnet zoning trends. The most dramatic difference is seen in the Northey Hill Line samples, which exhibit zoning profiles of a far smaller magnitude than the other areas. The traverses across these garnets are basically flat. The Cottonstone Mountain sample (67-82e) appears very similar to the Archertown Brook samples in zoning morphology. It is possible that both grew syn-tectonically with the dome stage (F2) deformation and the latest foliation (F3) merely overprints the garnets from the Archertown Brook locality. One of the garnets (D84-4k) from the Jacobs Brook Recumbant Syncline exhibit a similar character to the garnets from Archertown Brook and Cottonstone Mountain, even though this garnet comes from an entirely different bulk composition. The other garnet from the Jacobs Brook Recumbant Syncline (D84-2e) appears similar to those from the Northey Hill Line; ie: it exhibits minimal zoning. The garnet from Baker Pond (79-449f) exhibits very unusual features, although in zoning style it is more similar to the Cottonstone Mountain/Archertown Brook/ Jacobs Brook Recumbant Syncline samples.

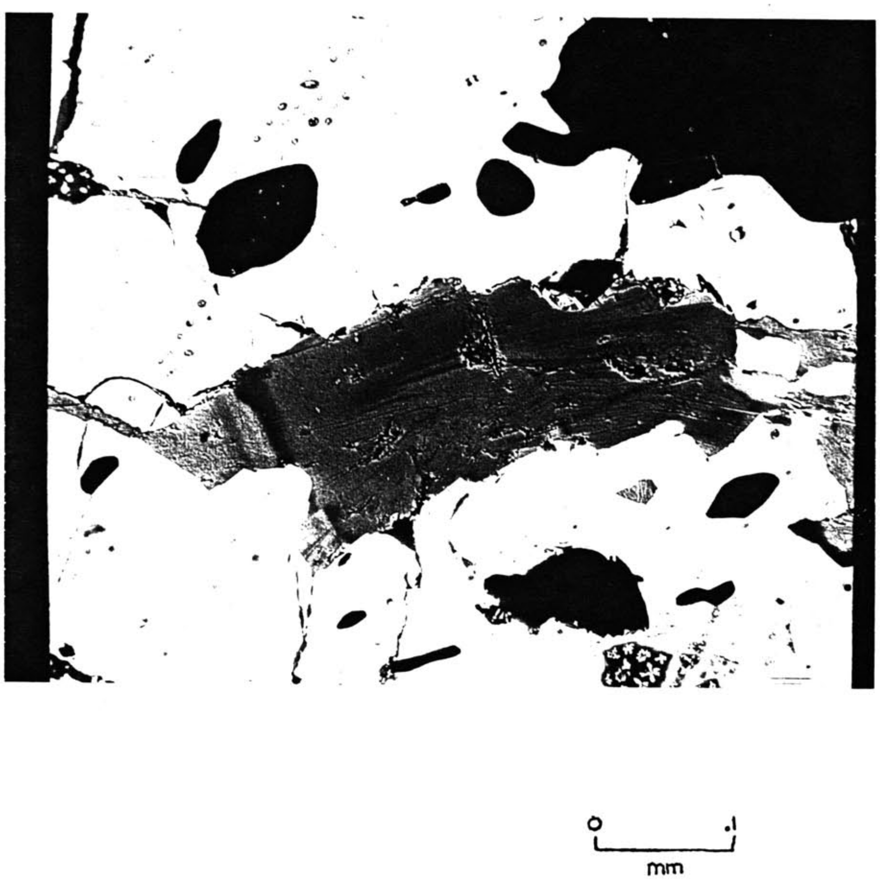

Figure 40: Baker Pond: Sample 79-449f; Chlorite #1/23 showing re-equilibration in the vicinity of cracks.

Chapter 7: GEOTHERMOMETRY AND GEOBAROMETRY

Geothermometry and geobarometry provide a means of comparing the different peak metamorphic conditions experienced by the localities in the study area, as well as providing a point in P-T space for the start of garnet zoning calculations. To investigate the temperature of final equilibration in the samples from the study area, the iron-magnesium exchange K_D between co-existing garnet and biotite has been computed using the calibration of Ferry and Spear (1978). The result of this geothermometer is a line of constant K_D in P-T space for each garnet-biotite pair. All temperatures computed from the five localities are in the range of 400-550°C. Retrograde iron-magnesium re-equilibration is unlikely to be of importance in this temperature range (Hodges and Spear, 1981). Temperature estimates using this experimentally determined geothermometer are accurate to whithin $\pm$50°C.

Pressure estimates have been computed using two geobarometers. In samples containing aluminosilicate and quartz, pressures are calculated from the net transfer reaction between garnet, plagioclase, aluminosilicate, and quartz using the method of Ghent, et al. (1979), with modified activity models for garnet and plagioclase as discussed by Hodges and Spear (1982). Due to the slow diffusion rates of plagioclase, retrograde re-equilibration is thought to be negligible, especially in this range of temperatures (Grove, et al., 1985). This experimentally determined geobarometer is accurate to whithin $\pm$1000 bars. Samples containing aluminosilicate+garnet+plagioclase+quartz were also investigated using the Ghent, et al. (1979) calibration (without the revised activity models of Hodges and Spear (1982)) and the results of this calibration often plotted below the aluminosilicate field of Holdaway (1971) of the polymorph present in the sample. It should be pointed out that even though the Ghent, et al. (1979) calibration plotted with low pressures, the inherent uncertainties in the geobarometer could more than compensate for this.

The other net transfer reaction involves the phases garnet, plagioclase, biotite, and muscovite (Ghent and Stout, 1981). In this thesis, the more recent calibration of Hodges and Crowley (1985) has been used. In samples containing aluminosilicate phases, both geobarometers have been computed, and the garnet-plagioclase-biotite-muscovite calibration is shown to be consistent with the garnet-plagioclase-aluminosilicate-quartz calibration of Hodges and Spear (1982). Uncertainties for the garnet-plag-bio-musc geobarometer have been estimated to be $\pm$2500 bars (Hodges and Crowley, 1985) although the scatter in calculated pressures in samples from the study area is considerably less.

COTTONSTONE MOUNTAIN

Five analyses from the rim of 67-82E garnet were chosen for P-T computations. These analyses span the range of garnet rim values. Six biotite analyses were used for computations. These include three analyses (rim and core) from two biotites, one at the garnet rim and one farther away. __ plagioclase rim analyses were used in the pressure calculations. These span the rim compositions of An_{20} and An_{24}. Due to the presence of kyanite, the garnet-plagioclase-kyanite-quartz (Hodges and Spear, 1982) geobarometer was used. As a comparison to this parallelogram, the garnet-plagioclase-biotite-muscovite geobarometer was also used. Four muscovite analyses were obtained; due to their similarity, the average was used in these calculations. Figure 41 shows the resultant P-T region as well as all of the computated K_D lines. Figure 42 presents the P-T parallelogram from the garnet-plagioclase-kyanite-quartz (Hodges and Spear, 1982) geobarometer and the garnet-biotite (Ferry and Spear, 1978) as well as the garnet-plagioclase-biotite-muscovite K_D lines. Matrix conditions indicated by the garnet-biotite geothermometer and the garent-plagioclase-aluminosilicate-quartz geothermomomemeter are 490±15°C and 4800±700 bars. The garnet-plagioclase-biotite-muscovite geobarometer corresponds favorably with these values, lying for a large part within the parallelogram and to a small degree below it.

ARCHERTOWN BROOK

D84-3d: Sample D84-3d also allowed the use and comparison of several geobarometers. For this kyanite bearing sample, six representative garnet rim compositions were used, along with eight biotite compositions, four muscovite, and eighteen plagioclase analyses (rim composition = An31-An37). Figure 43 shows the results of the garnet-biotite geothermometer (Ferry and Spear, 1978) (48 combinations) and the garnet-plagioclase-kyanite-quartz geobarometer (Hodges and Spear, 1982) (108 combinations). The diagram suggests temperatures of 485±25°C and pressures of 3800±900 bars. Figure 44 presents the results of the garnet-plagioclase-biotite-muscovite geobarometer in comparison to the parallelogram from Figure 43. In order to avoid using all combinations available (3456), the extremal garnet-biotite analyses were coupled with the extremal garnet-plagioclase analyses. It was also found that changes in muscovite had no effect on the geobarometer; as a result, the average of three muscovite analyses was used.

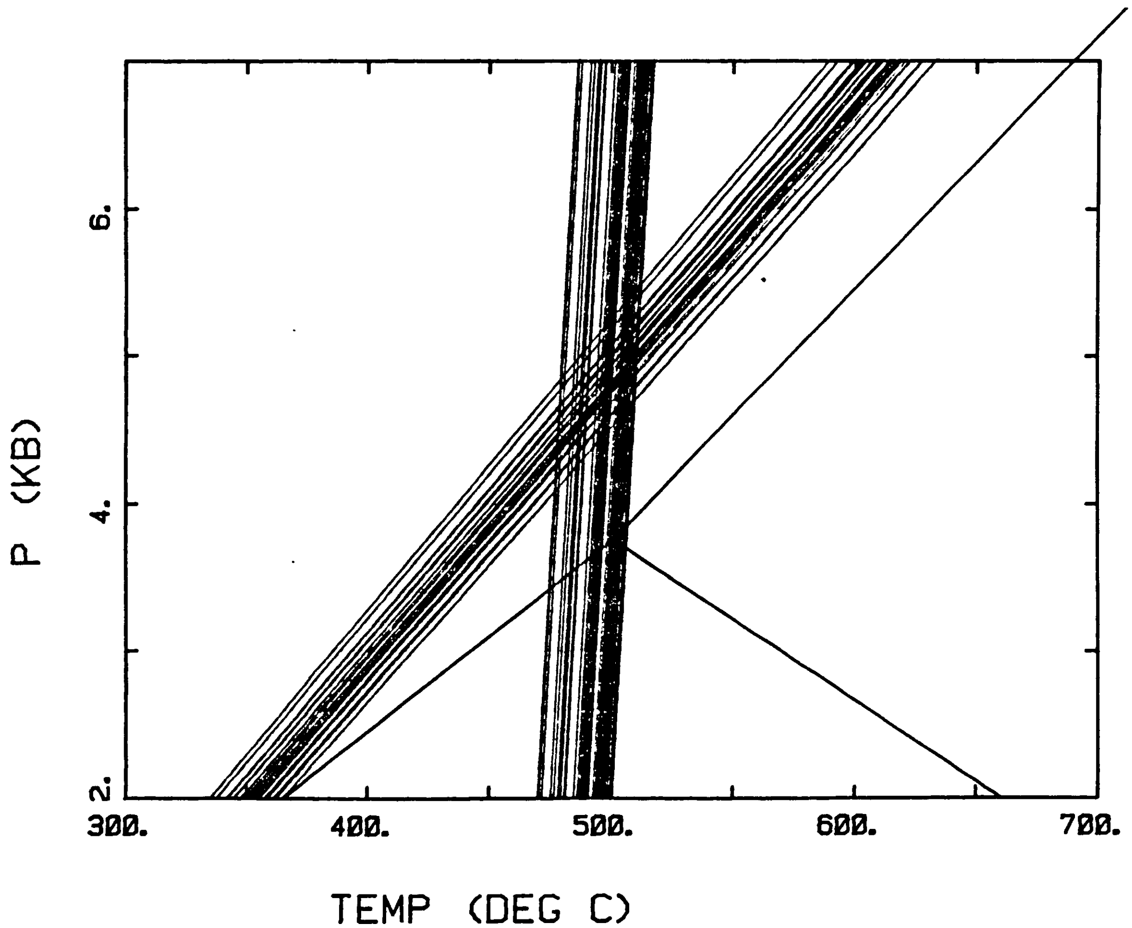

Figure 41: Cottonstone Mountain: Sample 67-82e; P-T calculations using the garnet-biotite geothermometer (Ferry and Spear, 1978) and the garnet-plagioclase-kyanite-quartz geobarometer (Hodges and Spear, 1982).

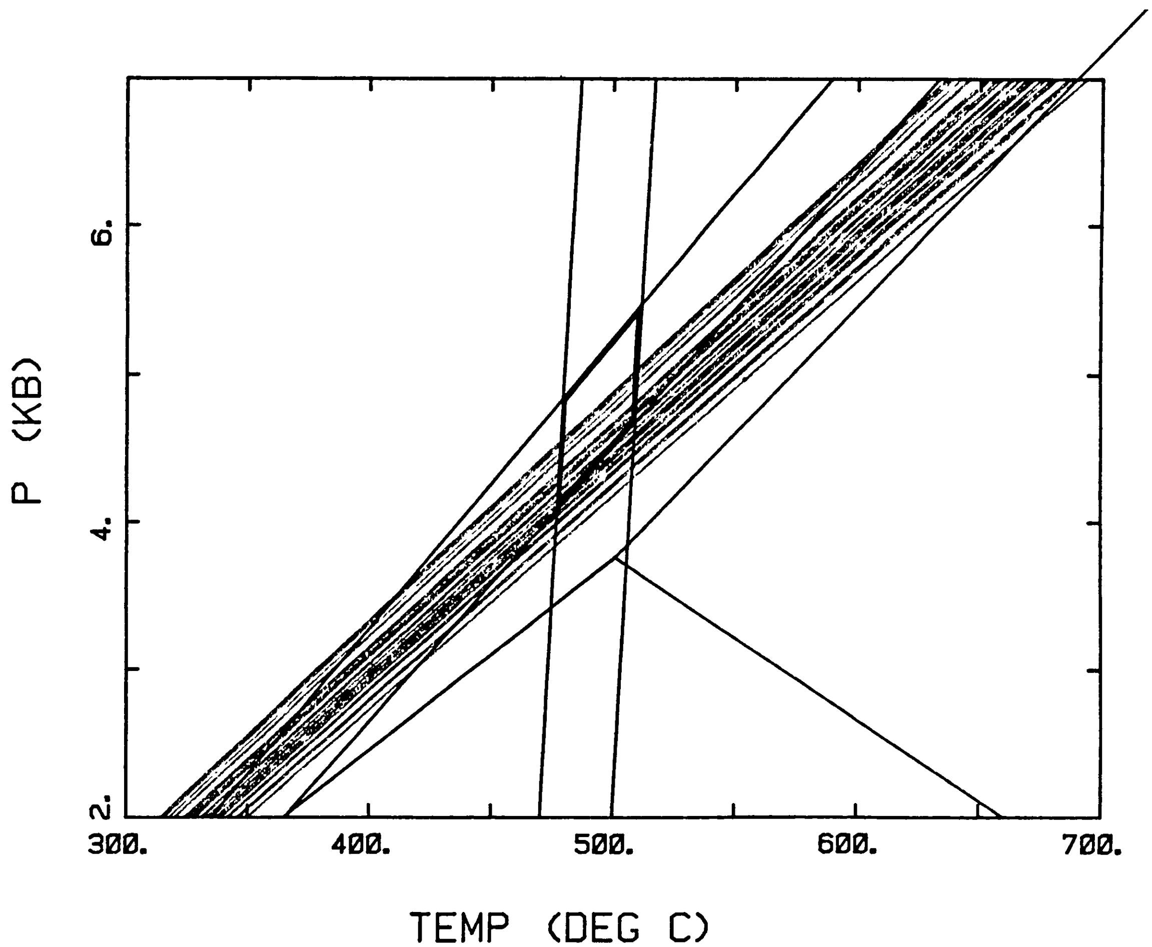

Figure 42: Cottonstone Mountain: Sample 67-82e; Comparison between P-T parallelogram from Figure 41 with garnet-plagioclase-biotite -muscovite geobarometer.

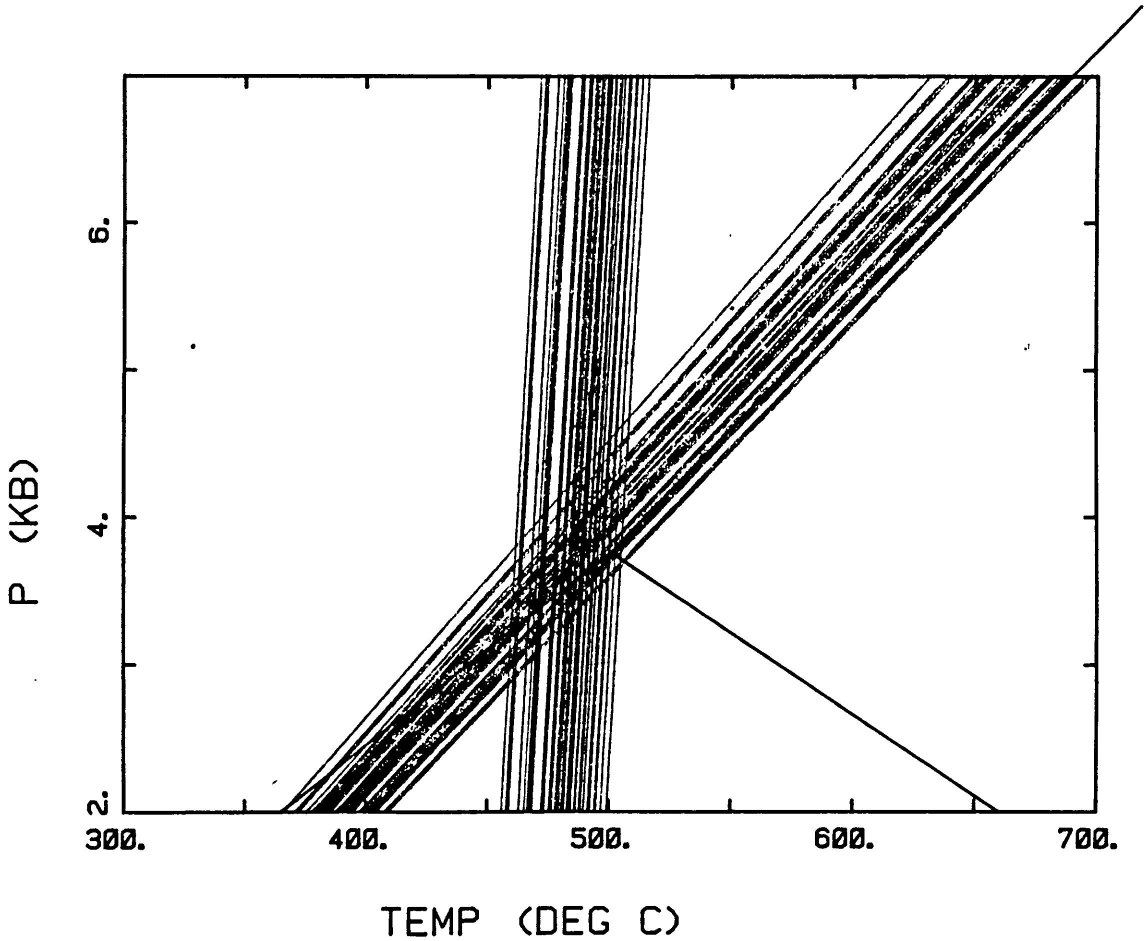

Figure 43: Archertown Brook: Sample D84-3d; Matrix conditions as determined by garnet-biotite geothermometry and garnet-plagioclase-kyanite-quartz geobarometry.

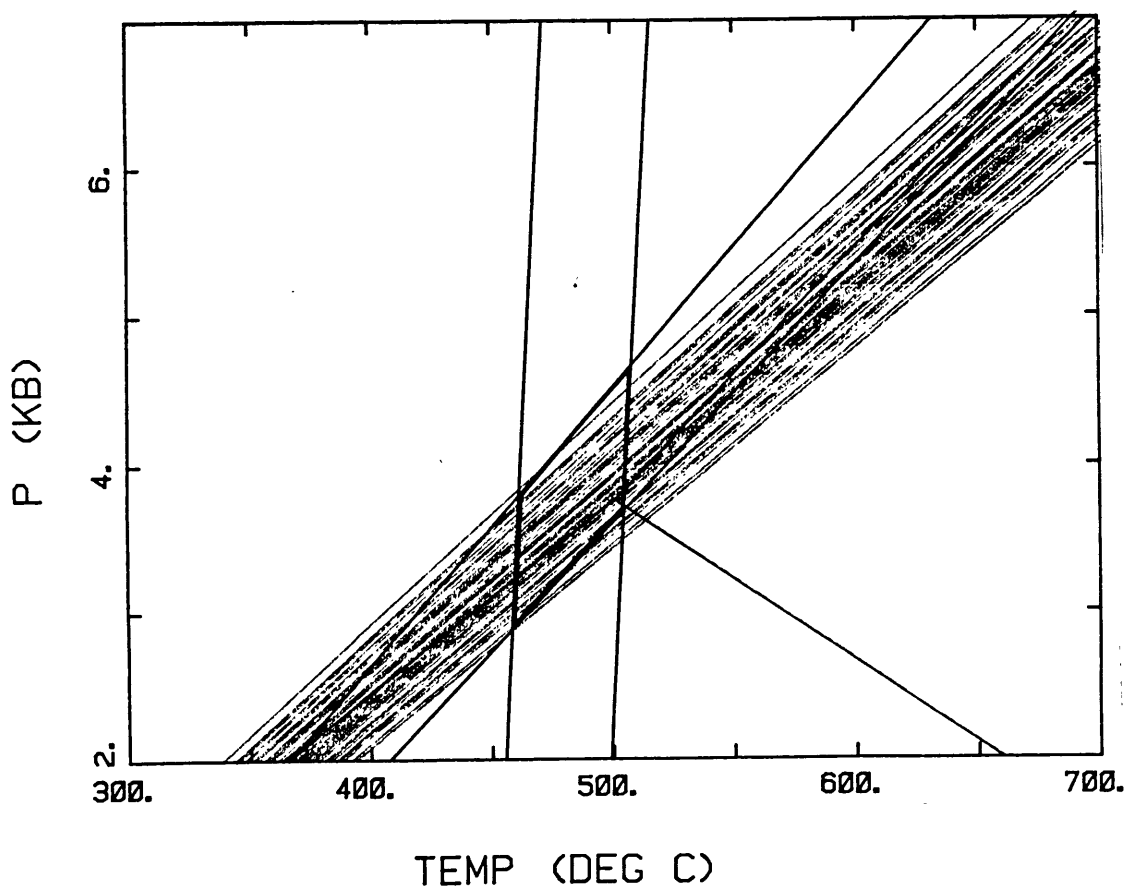

Figure 44: Archertown Brook: Sample D84-3d; Compares P-T parallelogram from Figure 43 with garnet-plagioclase-biotite-muscovite geobarometry

The garnet-biotite-plagioclase-muscovite geobarometer has basically the same upper limit as the garnet-plagioclase-kyanite-quartz geobarometer; the lower limit, however, is shifted to lower pressures by approximately 300 bars.

PM-9b: For sample PM-9b, five garnet rim compositions were used, as well as ten biotite analyses, nine plagioclases (An_{24-32}) and four muscovites. No aluminosilicate phases occur in this sample. Figure 45 contains the computed garnet-biotite geothermometer K_D lines, as well as the garnet-plagioclase-biotite-muscovite geobarometer K_D lines. Not every available combination was used; instead, garnet rim compositions were paired with nearby or adjacent plagioclase and biotite grains. The resultant parallelogram has temperature values ranging from 420 to 480°C and pressures ranging from 3000 to 4850 bars. To acquire the geobarometric lines, the extremal geothermometer pairs were matched with the average muscovite analysis and this group of three analyses was combined with each plagioclase, in turn, to produce one K_D line. Temperatures from PM-9b are slightly lower than those computed for D84-3d.

PM-11c: This sample also contains no aluminosilicate phases. Ten garnet rims were used, along with seven biotites, six plagioclases (An_{26-29}) and four muscovites. Three of the garnet rim analyses occur where biotite mantles the garnet extensively. These garnets were used only as geothermometers. Plagioclase also occurs at the garnet rim. These garnets were only used in the geobarometric calculations. Figure 46 contains the plot of all the geothermometer and geobarometer K_D lines. This sample has experienced peak conditions of 465±25°C and 4000±750 bars, similar to those from the other Archertown Brook samples.

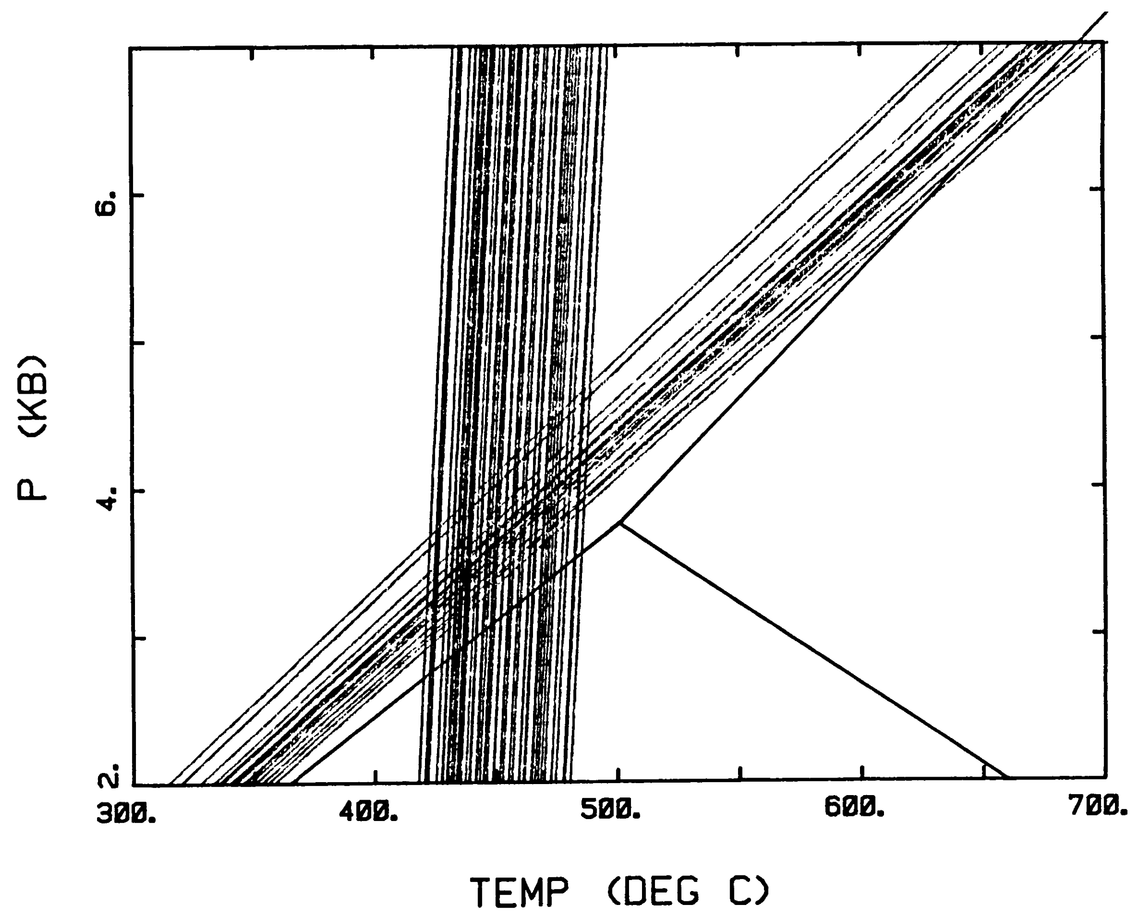

Figure 45: Archertown Brook: Sample PM-9b; Rim P-T conditions from garnet-biotite geothermometry and garnet-plagioclase-biotite-muscovite geobarometry.

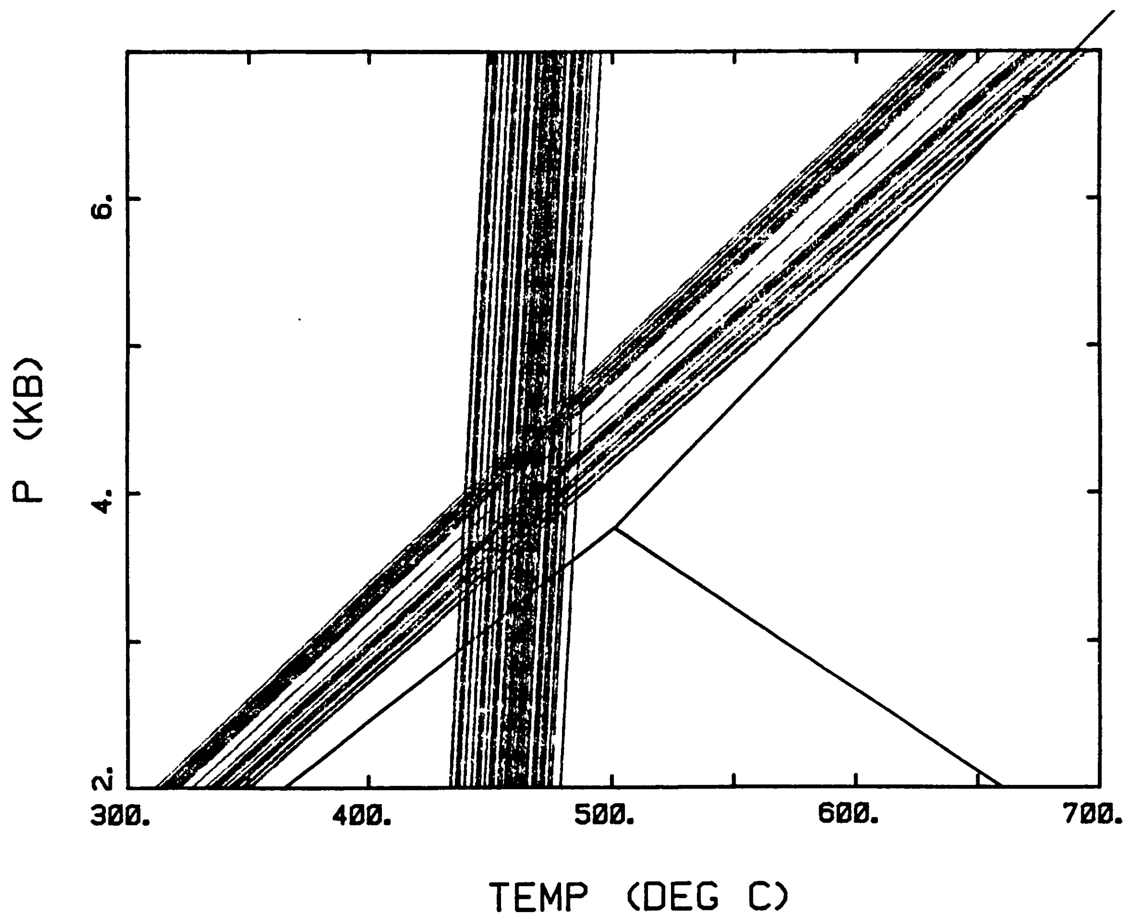

Figure 46: Archertown Brook: Sample PM-11c; Resultant Kd lines from the garnet-biotite geothermometer (Ferry and Spear, 1978) and the garnet-plagioclase-biotite-muscovite geobarometer.

67-78A: The primary purpose for studying sample 67-78A was to investigate when staurolite entered the assemblage. As a result, only two matrix garnet rim analyses were gathered, along with three biotite analyses and three plagioclase rim analyses (An_{26-31}). Because muscovite was not analyzed in this sample, the garnet, plagioclase, and biotite analyses were combined with a muscovite analysis from PM-11c to compute the K_D lines. This procedure is valid for geobarometers because the computation is only weakly sensitive to changes in muscovite composition The computations are illustrated in Figure 47. The resultant small parallelogram suggests rim conditions of 455-480°C and 3100 to 4100 bars.

Archertown Brook: Comparison

Statistically speaking, samples PM-9b, PM-11c, and 67-78A have all experienced similar peak P-T conditions. The P-T parallelogram for sample PM-11c is almost exactly the same as PM-9b and 67-78A lies (for the most part) inside these parallelograms. Sample D84-3d, from along Archertown Brook but one kilometer to the northwest, has a slightly lower pressure but a considerably higher (30-50°C) temperature at its peak. In comparison, 67-82E, occuring three kilometers to the north, has the same (or slightly higher) temperature as D84-3d, but a pressure that is one kilobar higher. These relationships are shown in Figure 48.

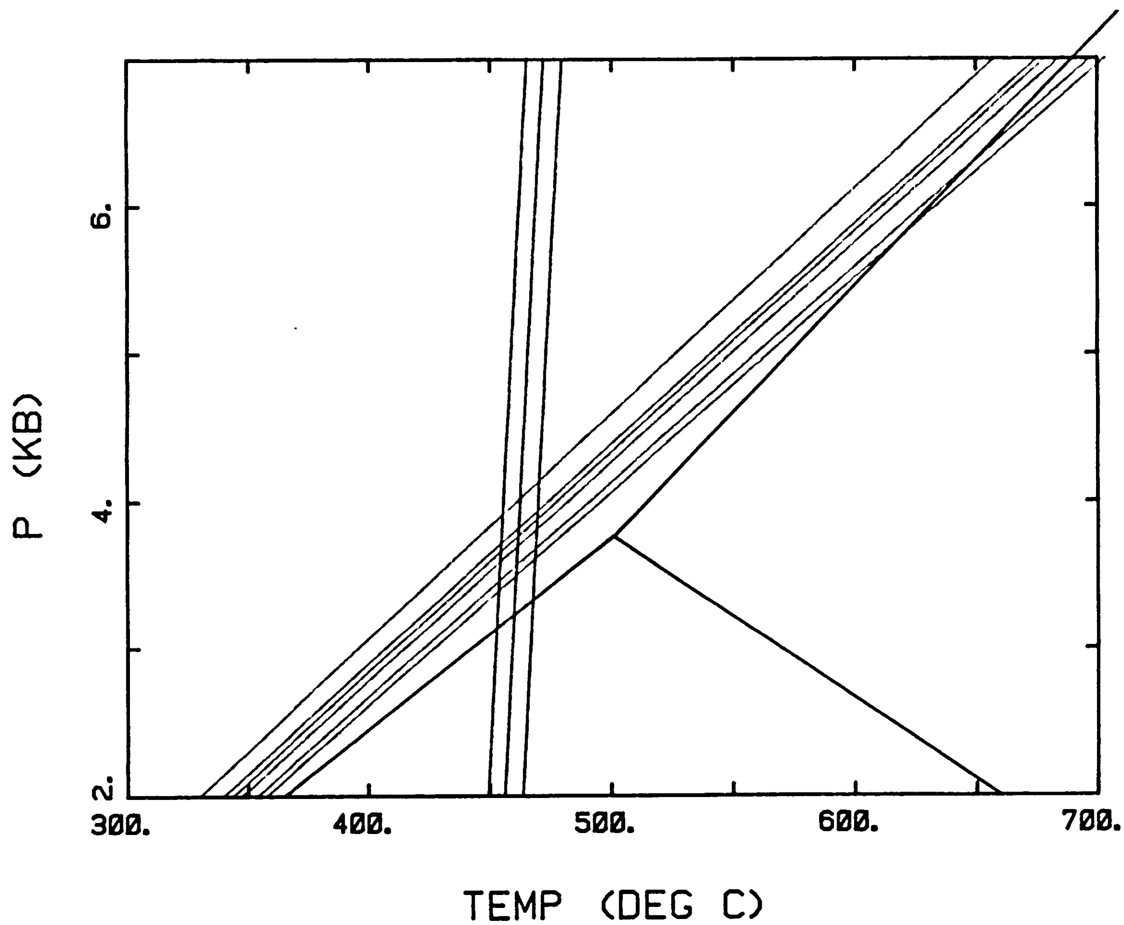

Figure 47: Archertown Brook: Sample 67-78a; P-T conditions from the garnet-biotite geothermometer (Ferry and Spear, 1978) and garnet-plagioclase-biotite-muscovite geobarometer.

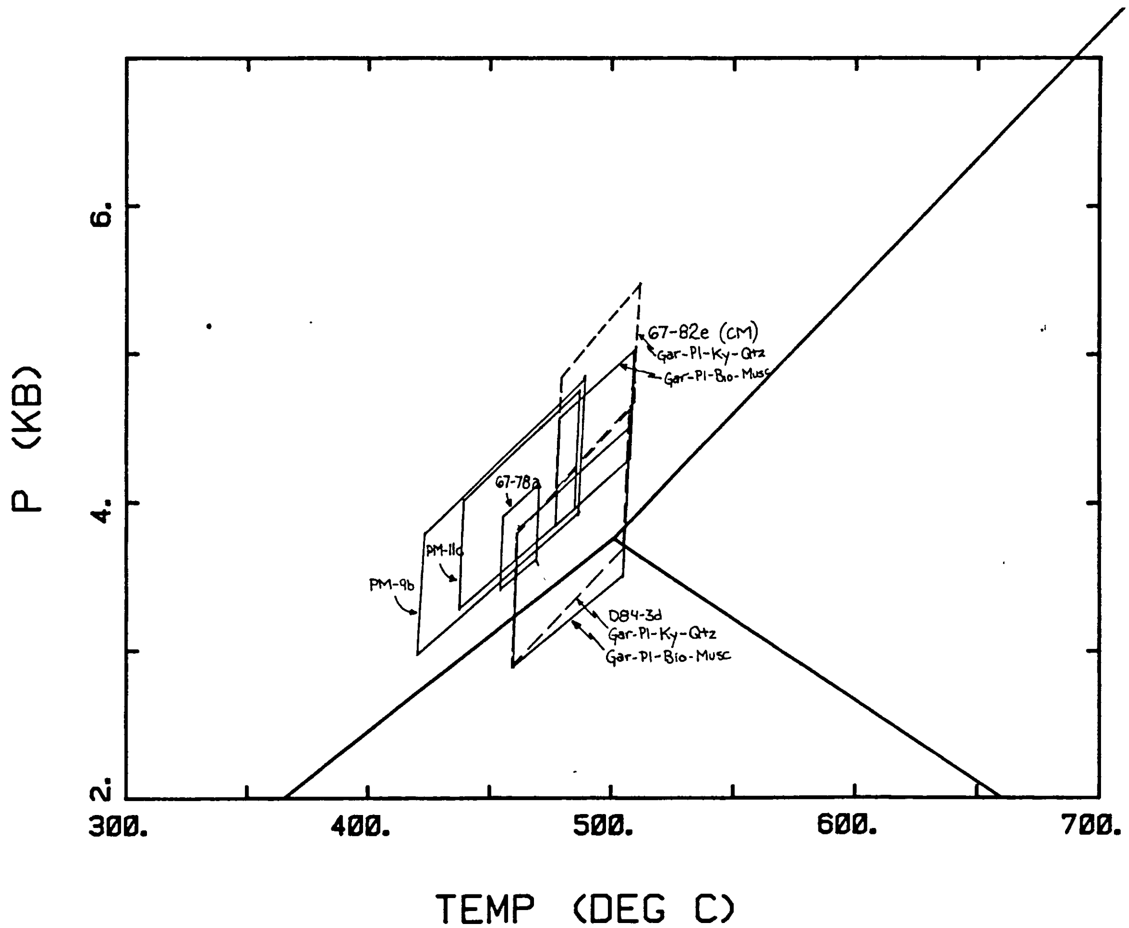

Figure 48: Comparison of rim P-T conditions for Archertown Brook and Cottonstone Mountain samples.

NORTHEY HILL LINE

D84-1c: For this sample, seven garnet rim compositions were used, as well as twenty plagioclase analyses (An_{13}-An_{24}), seven biotites, and four muscovites. There is no Al_2SiO_5 phase in this sample. These analyses are input into the garnet-biotite geothermometer and garnet-biotite-plagioclase-muscovite geobarometer, and the results are plotted in Figure 49a. Discounting suspect analyses, all of the plagioclase rim analyses (16) collected with the MIT probe fall in the range An_{19}-An_{24}. The four Harvard plagioclase rim analyses, however, lie in the region An_{13}-An_{14}. The analyses appear good, and analyses taken on the same grain in other samples have compared favorably in other samples (e.g. 67-82E, 79-449f). The reasons for this systematic difference are unclear but may simply result from sampling bias. Figure 49b shows the P-T lines produced by considering all possible combinations without the Harvard data. Since this garnet has biotite and plagioclase very near the rim, another P-T plot was constructed using only the data from neighboring phases (Fig. 49c). Figure 50 shows the comparative parallelograms of the three P-T approaches.

Figure 49a suggests rim conditions of 480±30° C and 3450±1450 bars. The parallelogram computed without using the Harvard plagioclase analyses has a peak P-T of 480±30°C and 3050±890 bars. The peak conditions suggested from considering only the neighboring minerals (excluding the Harvard analyses) are 470±20°C and 2700±500 bars.

It is possible that these three parallelograms represent actual "peak" conditions along a single decompression path. In this scenario, separate plagioclase crystals stop growth at different points along the P-T path. The older (lower An) plagioclases might not have been able to re-equilibrate due to slow kinetics.

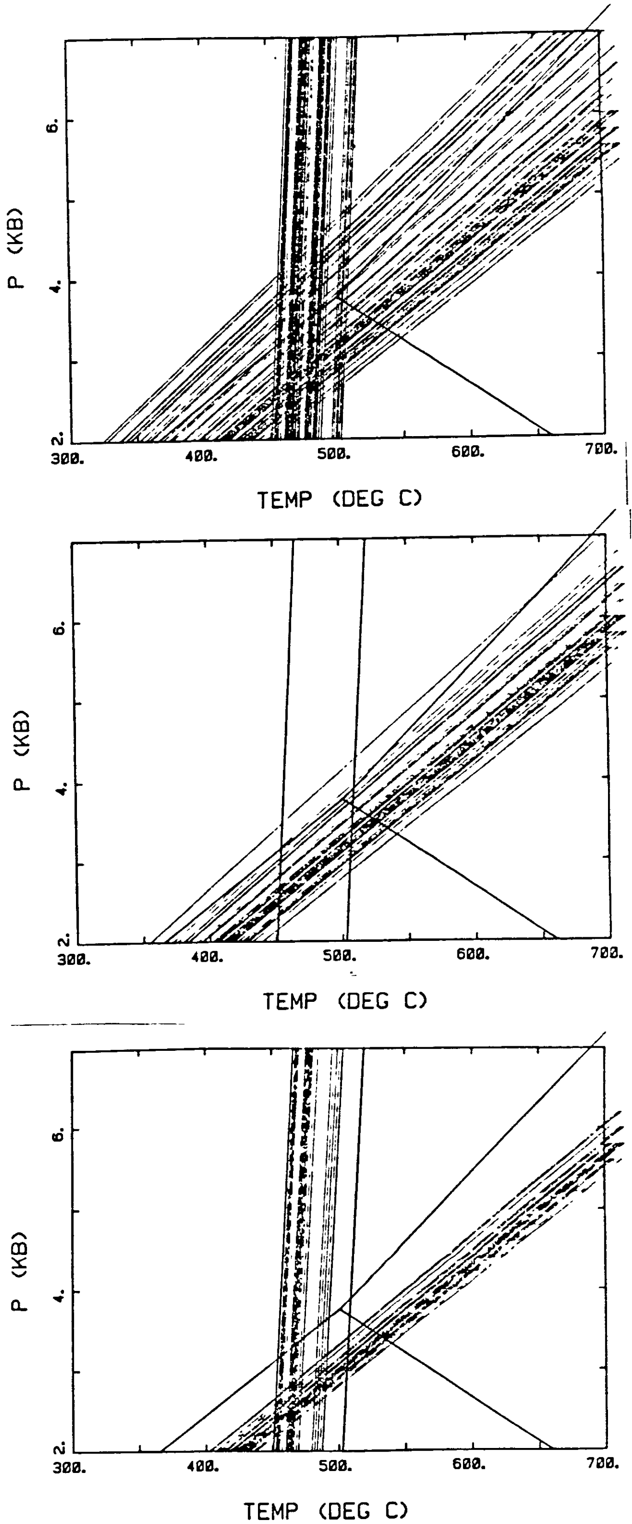

Figure 49: Northey Hill Line: Sample D84-1c; Garnet-biotite geothermometry and garnet-plagioclase-biotite-muscovite geobarometry. a) using all available data. b) without data collected on Harvard probe. c) considers only neighboring phases.

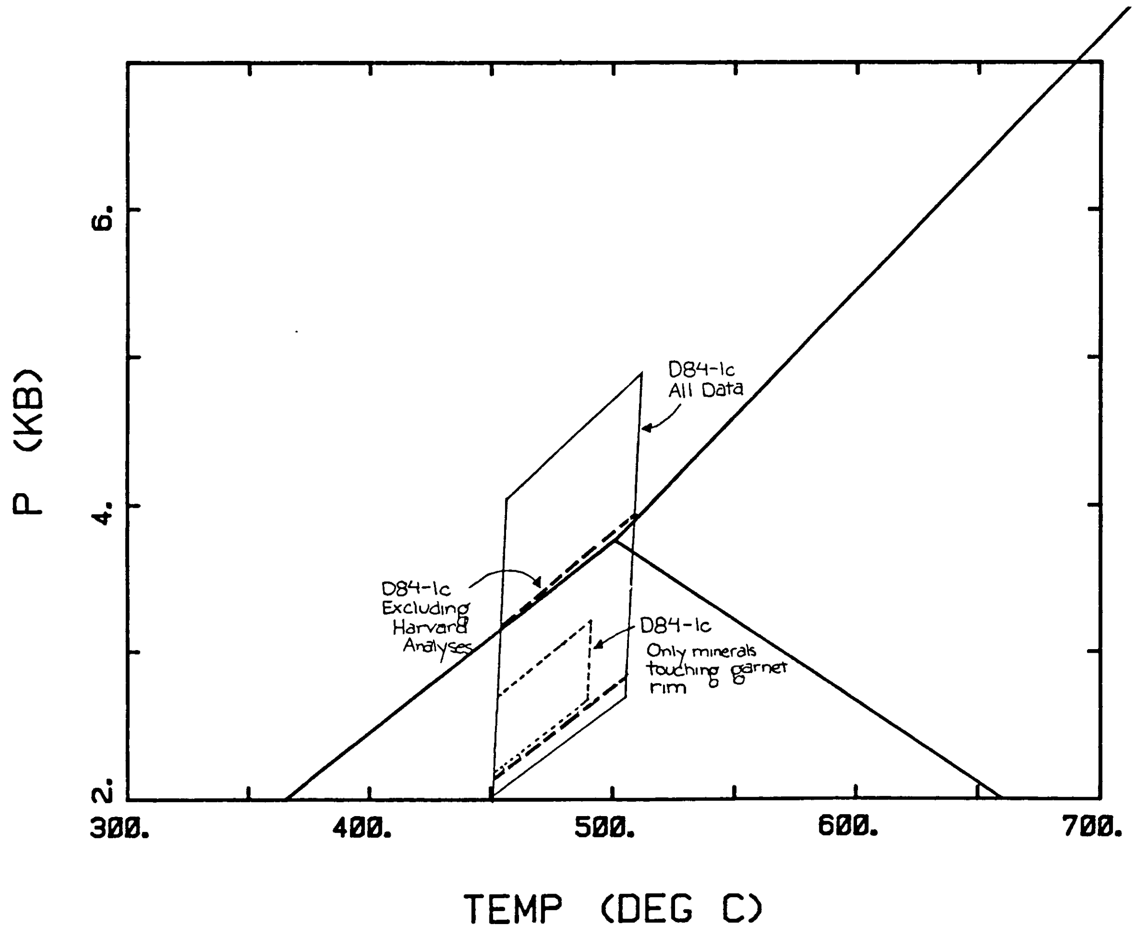

Figure 50: Northey Hill Line: Sample D84-1c; Compares three parallelograms from P-T approaches illustrated in Figure 49.

D84-1d-2: the sample contains no aluminosilicate phase nor any biotite. No geobarometer or geothermometer can be applied to this sample.

JACOBS BROOK RECUMBANT SYNCLINE

No plagioclase was analyzed in any of the samples from this locality. As a result, only temperatures will be reported.

D84-2e: Seven representative garnet analyses were used along with nine biotite analyses. Biotite analyses near the garnet show systematically higher Fe/Fe+Mg values (0.541 vs. 0.515) with respect to matrix biotites. This conclusion is by no means certain, due to the fact that all of the analyses taken near the garnet have low totals. To remain consistent, all biotite analyses with totals less than 93.50 weight percent are ignored. This limits the geothermometry to the matrix biotites. The results of the geothermometry calculations are shown in Figure 51. The peak temperature experienced by this sample is 555±35°C.

D84-4k: For this sample, eight representative garnet rim compositions were used in conjunction with eight biotite analyses. All of the 64 resultant K_D lines lie in the range of 480-580°C, with the vast majority in the range of 530-580°C. This is shown graphically on Figure 52.

D84-2c: This sample was not extensively analyzed. Only a traverse across the garnet was analyzed, so there were only two rim analyses. These were combined with three biotite analyses to get six geothermometer lines. These are shown in Figure 53. The two rim compositions have identical Fe/Fe+Mg values, so only three distinct lines appear. These occur in the narrow range of 500-510°C.

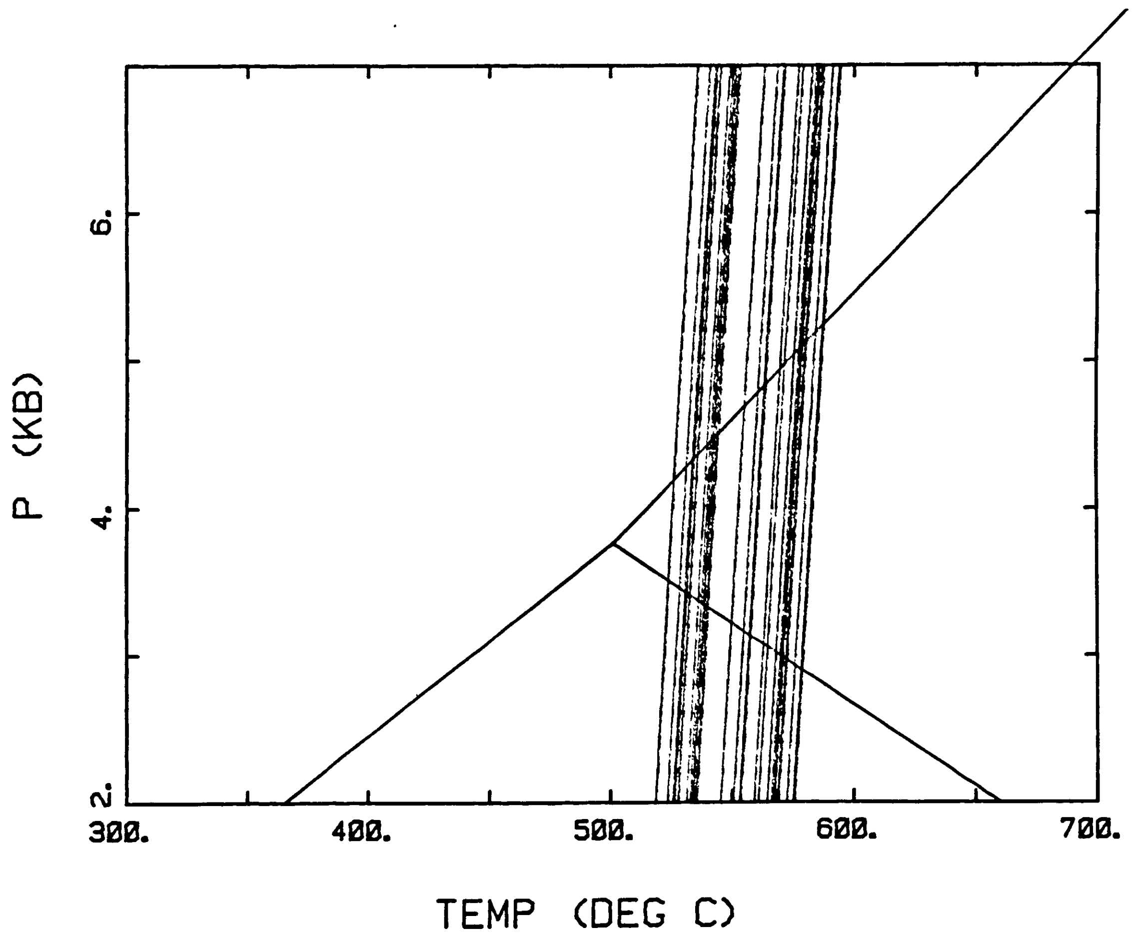

Figure 51: Jacobs Brook Recumbant Syncline: Sample D84-2e; Results of garnet-biotite geothermometry (Ferry and Spear, 1978).

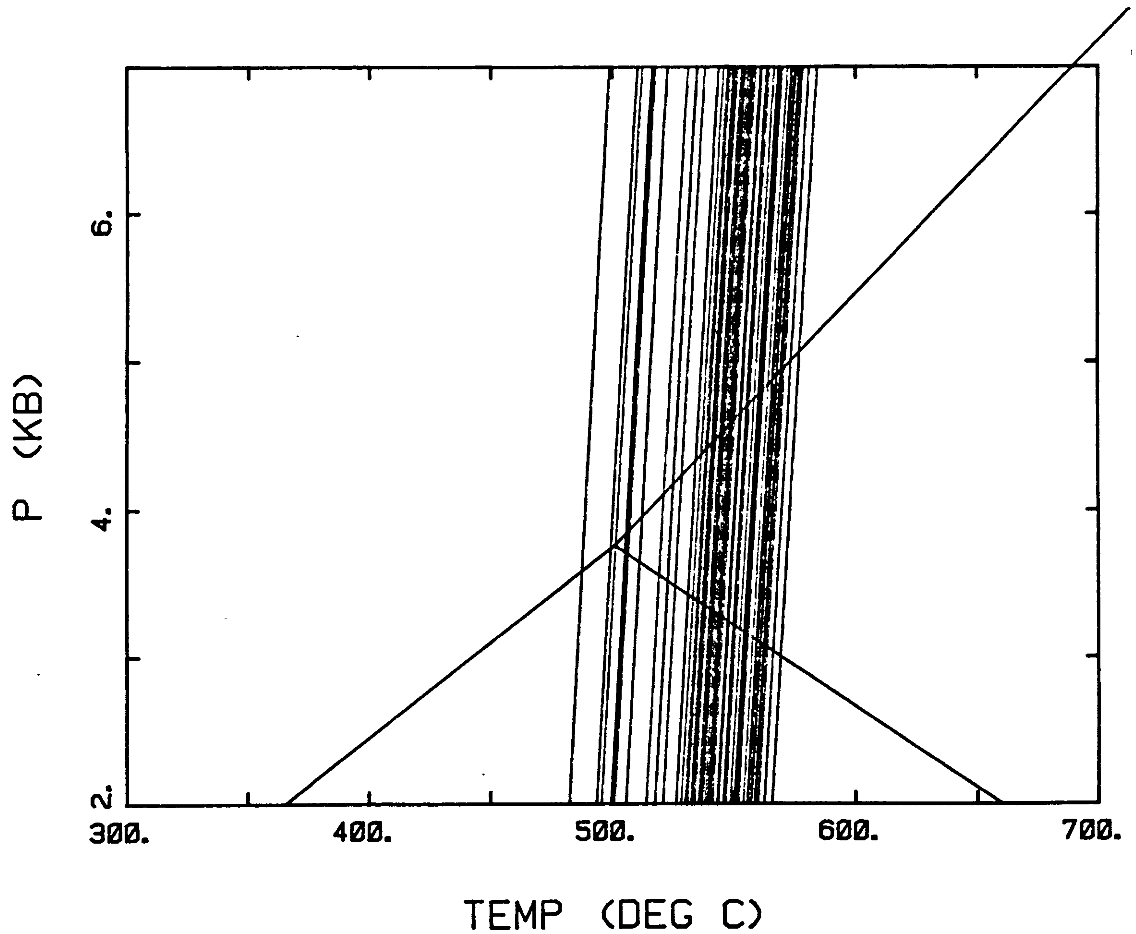

Figure 52: Jacobs Brook Recumbant Syncline: Sample D84-4k; Results of garnet-biotite geothermometry (Ferry and Spear, 1978).

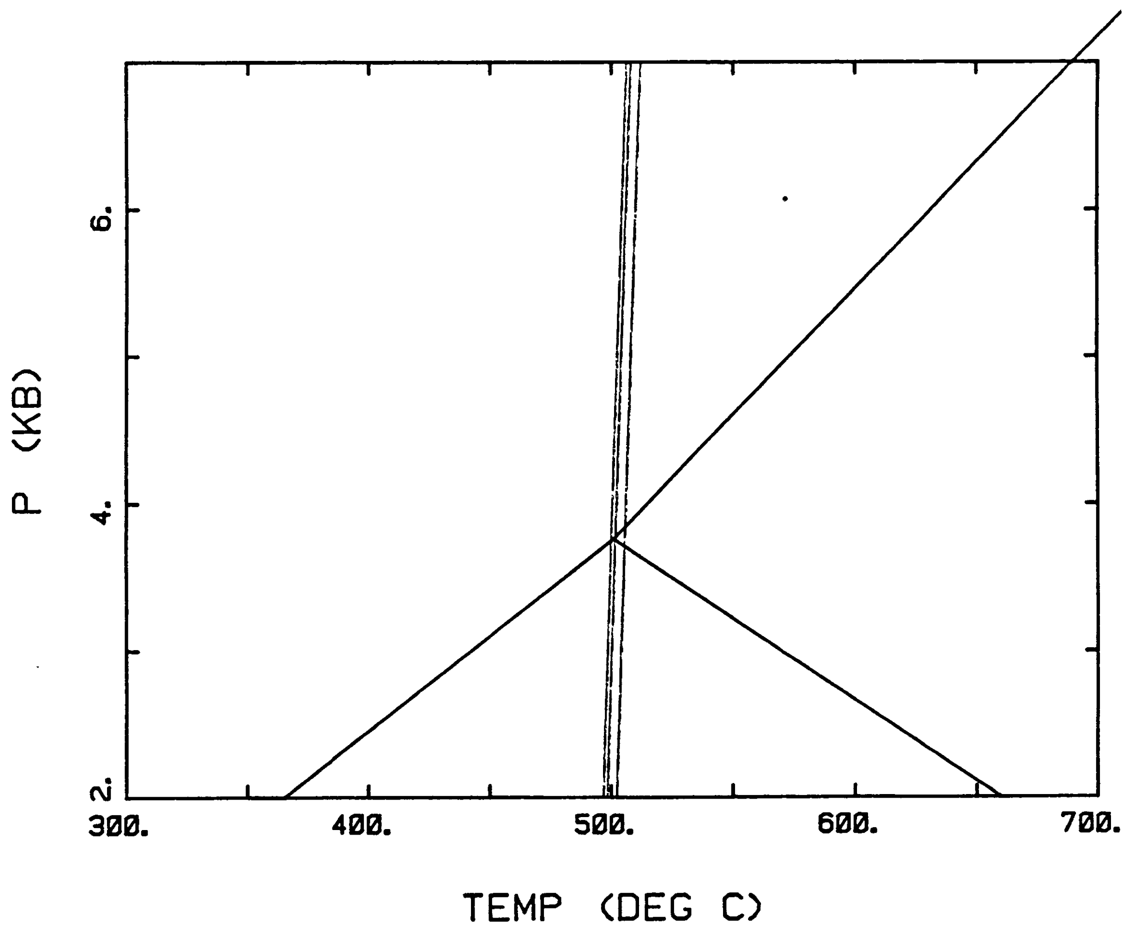

Figure 53: Jacobs Brook Recumbant Syncline: Sample D84-2c; Results of garnet-biotite geothermometry (Ferry and Spear, 1978)

Discussion: The presence of kyanite in thin section and outcrop adds some pressure constraints to the Jacobs Brook Recumbant Syncline samples. Assuming that the Holdaway (1971) triple point is correct, then these samples have experienced "peak" temperatures of 530±50°C and a peak pressure greater than 3800 bars (ie: approx. 4500 bars at 530°C). This is shown graphically in Figure 54. The presence of sillimanite only 5 kilometers to the east suggests pressures near the kyanite-sillimanite boundary.

BAKER POND

79-449J: 79-449J contains abundant fibrolitic sillimanite. On this sample, a single traverse across the garnet was the extent of garnet analysis, thus, there were only two garnet rim analyses. These were combined with eight biotite analyses and thirteen plagioclase analyses (An_{15-17}). The resultant geothermometers and geobarometers (26) are illustrated in Figure 55. The results of the garnet-biotite temperatures and the garnet-plagioclase-sillimanite-quartz pressures are 530±20°C and 3400±550 bars. The region intersected by the Hodges-Spear (1982) calibration is shown with a stippled border in Figure 56.

79-449f: Extensive analyses were made on sample 79-449f on garnet rims, biotites, plagioclases, and cordierites. In this sample, kyanite occurs as inclusions in cordierite. Additionally, sillimanite is observed associated with biotite in the matrix. The garnet fortunately has biotite and plagioclase touching its rim. For the geothermometry and geobarometry calculations, nine representative garnet rim compositions were used, as well as three biotites and three plagioclase analyses from grains near the garnet. All three plagioclases had nearly identical compositions (An_{13}).

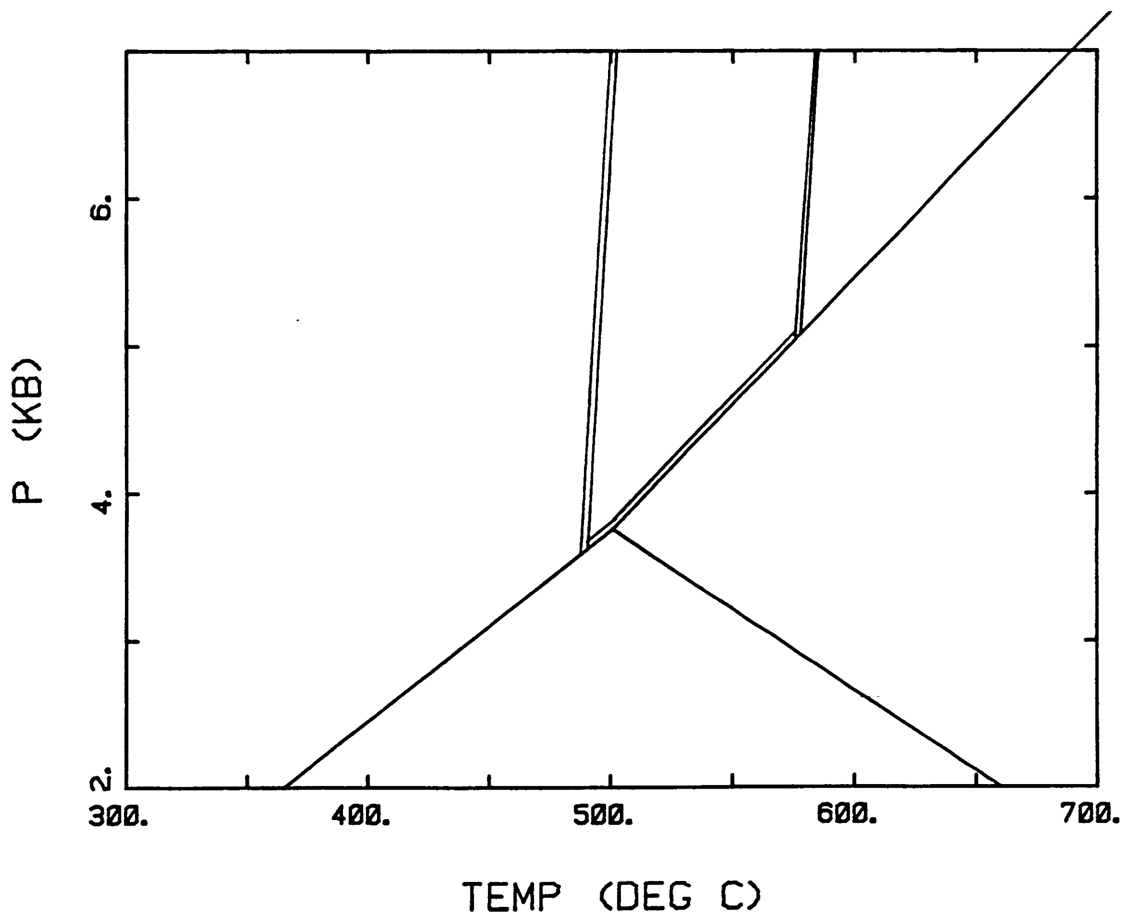

Figure 54: Jacobs Brook Recumbant Syncline; Results of all geothermometry calculations coupled with observation of kyanite.

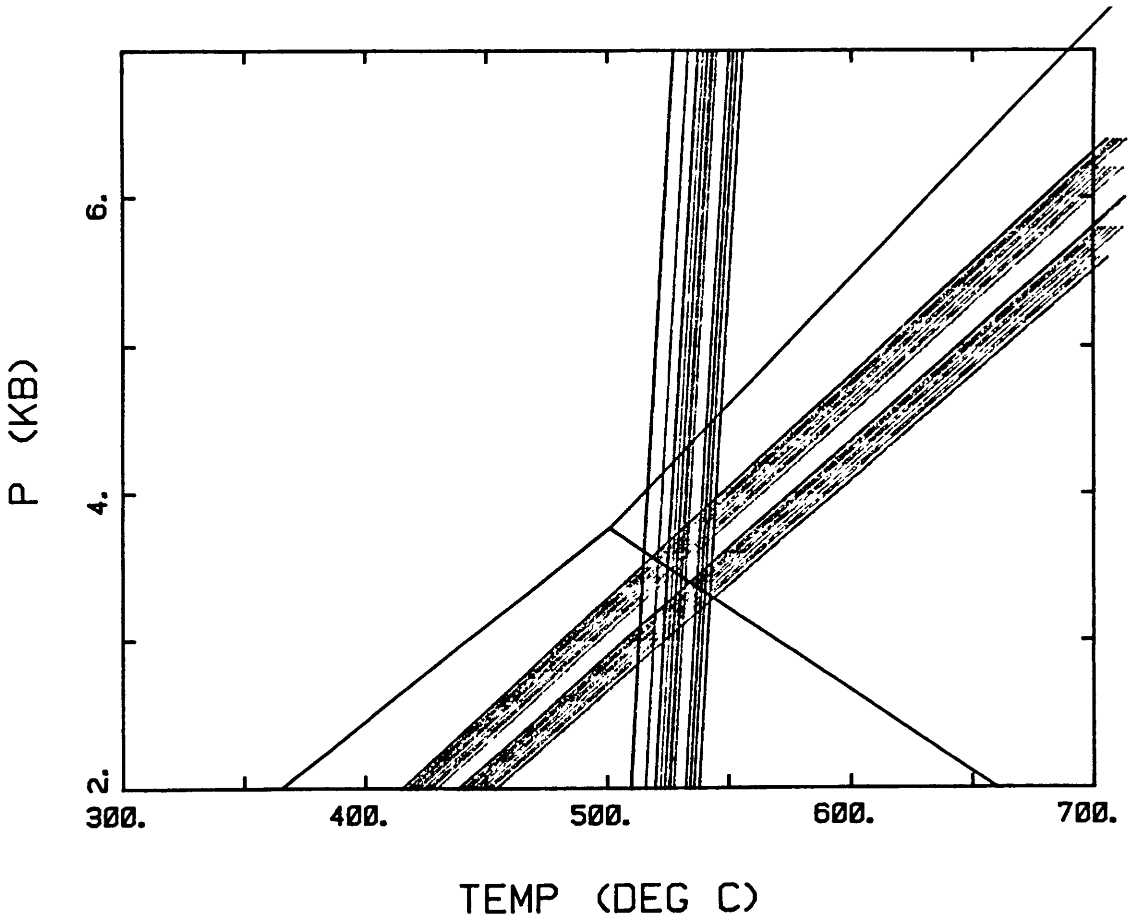

Figure 55: Baker Pond: Sample 79-449j; Rim P-T conditions from garnet-biotite geothermometer (Ferry and Spear, 1978) and garnet-plagioclase sillimanite-quartz geobarometer (Hodges and Spear, 1982).

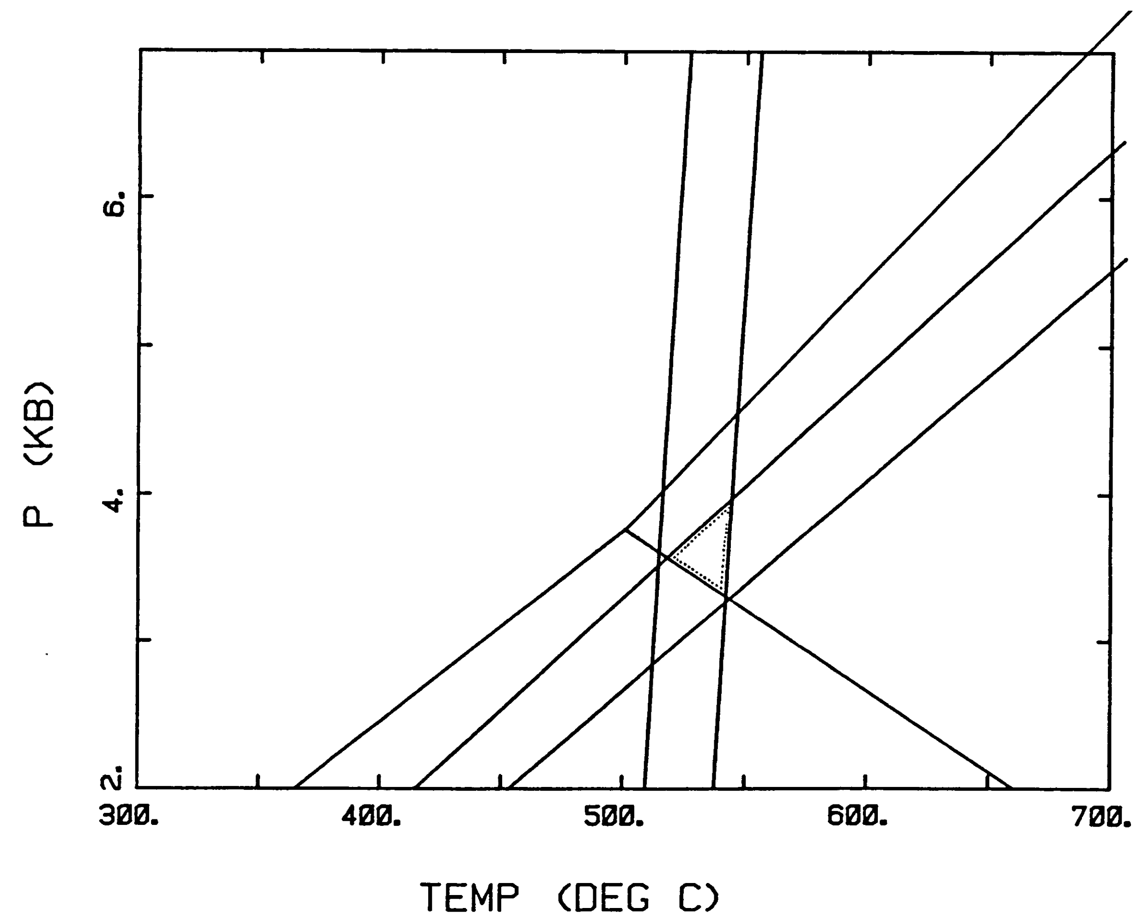

Figure 56: Baker Pond: Sample 79-449j; Comparison of P-T parallelogram with the additional constraint of abundant matrix fibrolite.

The K_D lines computed from all of the possible combinations are shown in Figure 57. The peak conditions suggested by the resultant extremal parallelogram are 500±30°C and 3675±425 bars. Several other plagioclases and biotites were probed from this sample. The difference in Fe/Fe+Mg ranges in the matrix biotites vs. the biotites touching the garnet are minimal--thus the temperature range is hardly affected. The matrix plagioclase grains, on the other hand, have quite a large variation in An-content with respect to the grains at the garnet rim (max An_{17} vs. max An_{13}). Thus the pressures computed using the matrix plagioclases were lower than for the plagioclases touching the garnet rim. The resultant P-T parallelogram produced from considering all of the biotites and plagioclase analyses (matrix and touching) is shown dashed in with the parallelogram from the limited consideration in Figure 58. Approximately one-half of the dashed parallelogram lies in the andalusite field of Holdaway (1971). Since this sample contains kyanite inclusions and fibrolitic sillimanite, the P-T parallelogram from the analyses near the garnet rim is far more reasonable. As a result, this parallelogram will be used for further discussion.

Discussion: Samples from the Baker Pond locality contain abundant fibrolitic sillimanite, prismatic sillimanite, and common kyanite preserved as inclusions in staurolite and cordierite. One sample contains fibrolitic sillimanite cored by kyanite, and another contains overgrowths of prismatic sillimanite on kyanite (F. Spear, pers. comm.). All evidence suggests a "peak" P-T condition at or near the kyanite-sillimanite boundary. The two extremal parallelograms from samples 79-449f and 79-449J are plotted together in Figure 59. The two do not overlap, but they lie within the maximum errors inherent to the geothermometer and geobarometer. A maximum

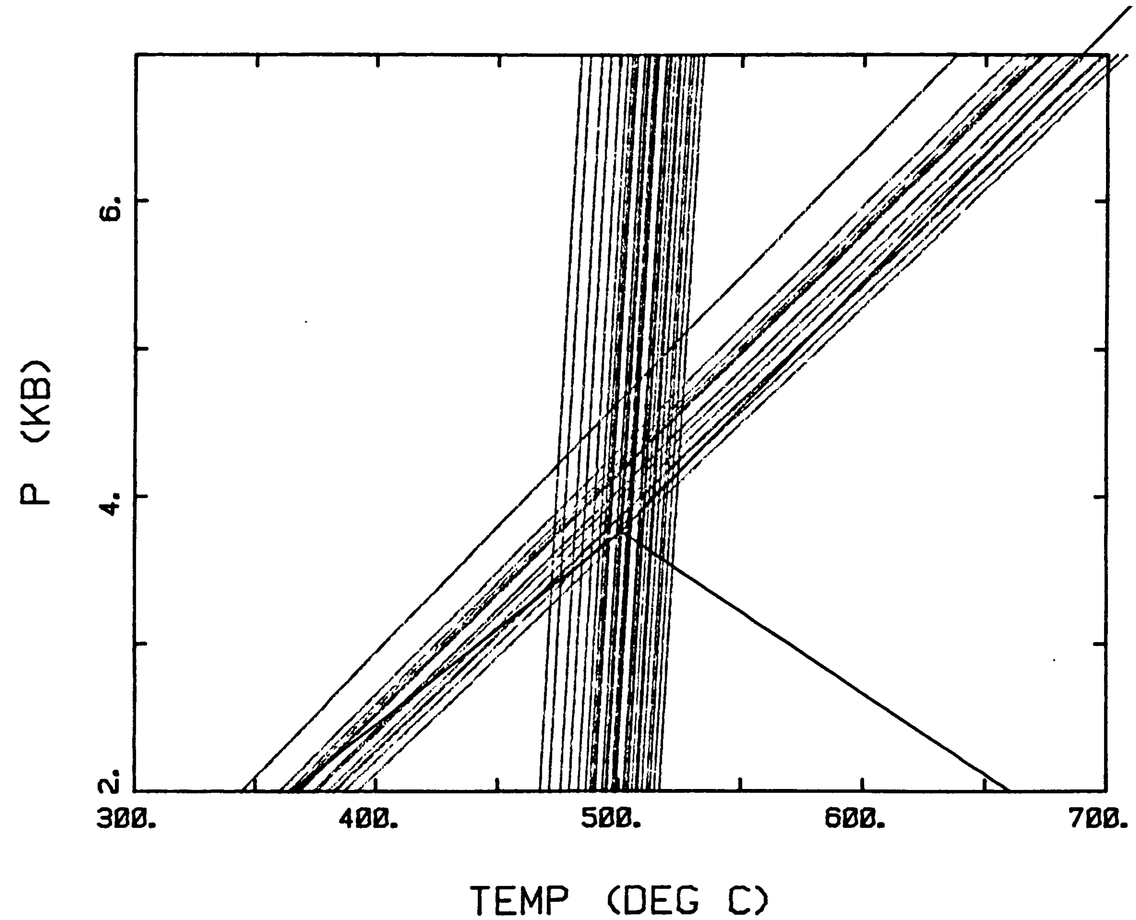

Figure 57: Baker Pond: Sample 79-449f; Resultant Kd lines from garnet-biotite (Ferry and Spear, 1978) and garnet-plagioclase-sillimanite-quartz (Hodges and Spear, 1982) equilibria.

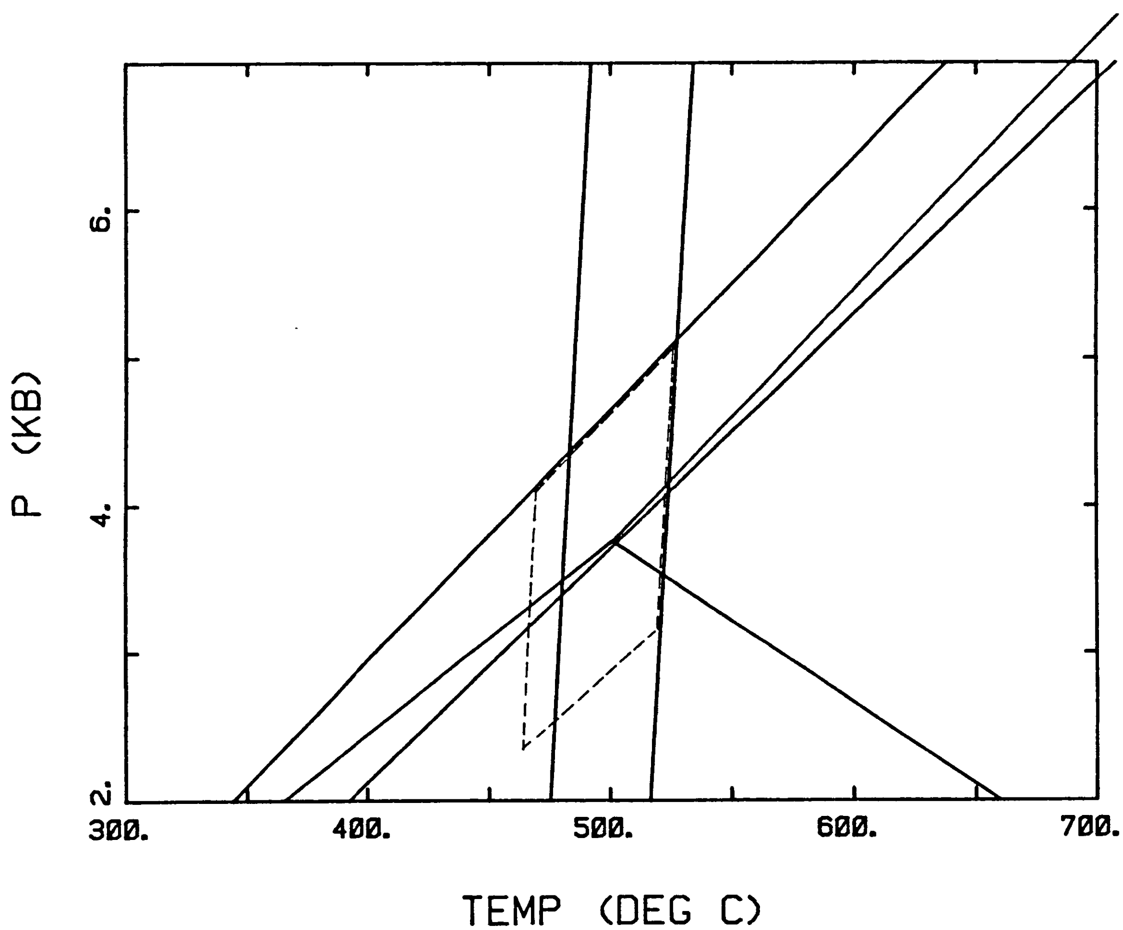

Figure 58: Baker Pond: Sample 79-449f; Dashed line indicates extremal parallelogram produced by considering all possible plagioclase and biotite compositions.

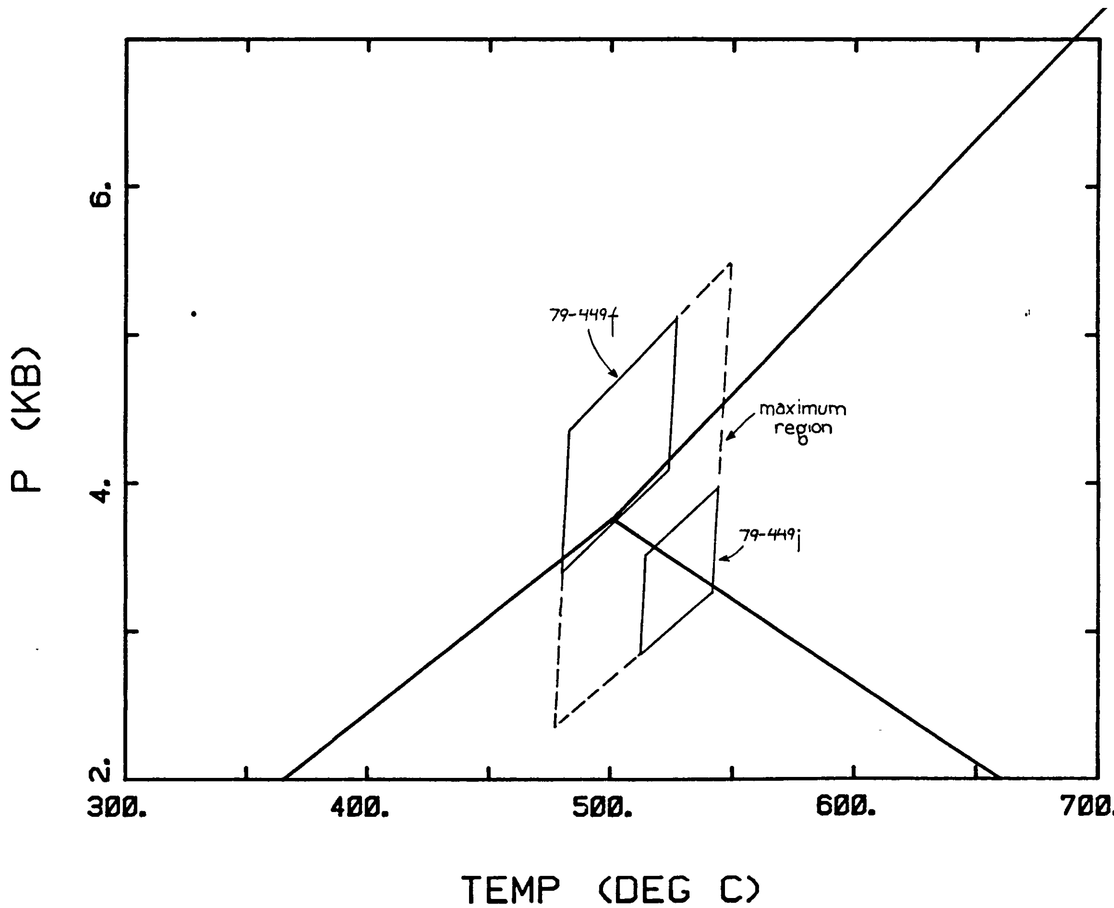

Figure 59: Baker Pond; Construction of extremal parallelogram using highest and lowest K_D lines from both Baker Pond samples.

region, containing the highest and lowest geothermometer and geobarometer of these samples is dashed in in Figure 59.

Since these two samples come from essentially the same outcrop, they must have experienced the same peak conditions. It is possible that sample 79-449J recorded a rim P-T farther along the P-T path than 79-449f. It is possible that the reactions in 79-449f stopped because no aluminosilicate was available to continue the plagioclase producing reaction (there is little matrix sillimanite and abundant kyanite inclusions). From the phase relationships and rim P-T conditions calculated from the Baker Pond samples, a reasonable estimate for peak metamorphic conditions would be at the higher temperature and in the sillimanite field; ie: 510-550°C and 3200-3900 bars.

Regional Cross-Section: P-T Space

Figure 60 shows the comparison of all the peak P-T conditions from the study area. Where multiple geobarometers were applied (e.g. Cottonstone Mountain, Archertown Brook west) the tetrahedron contains all possible geobarometers. Thus, the upper and lower boundaries are not parallel. Where aluminosilicate phase relationships were available, the polyhedra have been altered to be consistent with these data.

The Northey Hill Line, lying in the middle of the cross-section, is visibly low-grade and P-T relationships suggest a low pressure, medium temperature peak condition. It should be noted that these conditions are discussed only with respect to the other samples studied. To the west of the Northey Hill Line, pressure systematically increases by approximately 2.5 kilobars. Temperatures decrease slightly or remain the same.

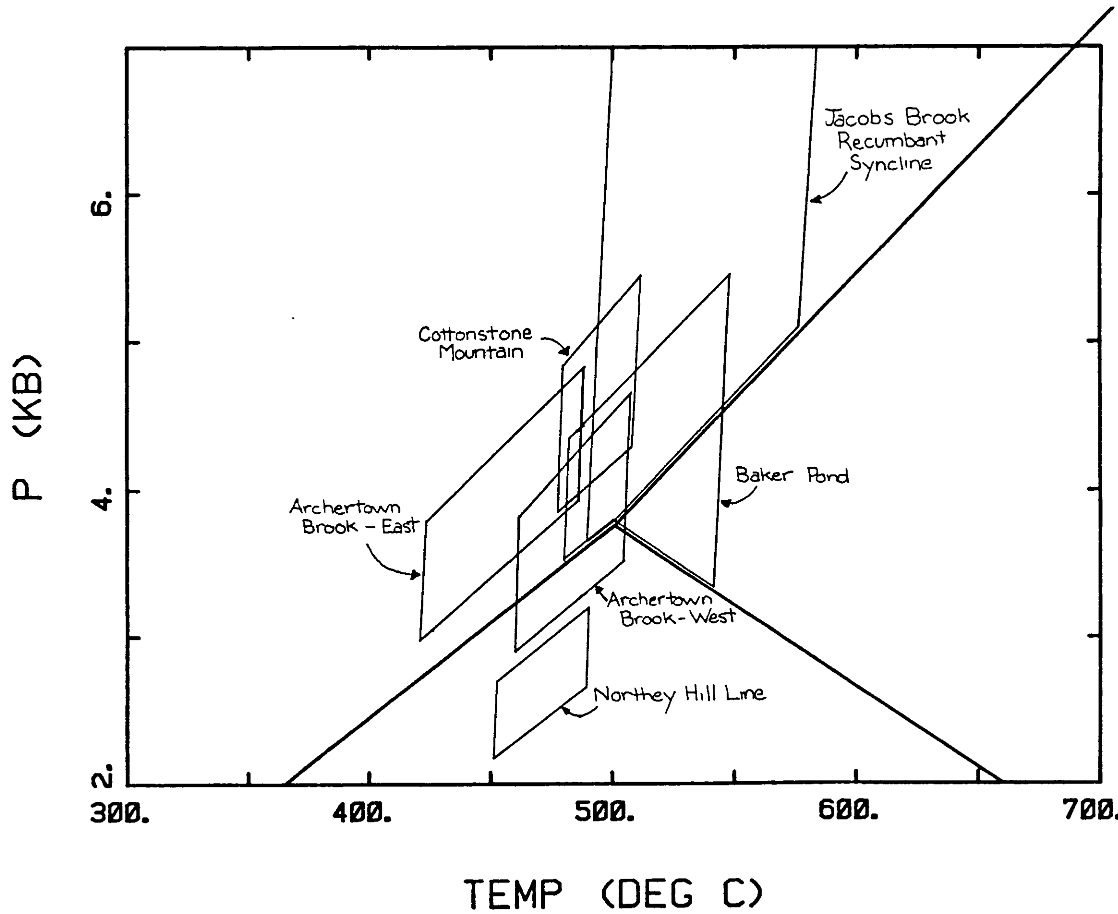

Figure 60: Regional cross section: P-T space. CM=Cottonstone Mountain, AB=Archertown Brook, NHL=Northey Hill Line, JBRS=Jacobs Brook Recumbant Syncline, BP=Baker Pond.

To the east of the Northey Hill Line, pressure and temperature increase. Rocks in the Jacobs Brook Recumbant Syncline are kyanite-bearing, indicative of higher pressures, and geothermometers suggest a mean temperature increase of 50°C. Baker Pond samples, farther to the east, have kyanite inclusions and matrix sillimanite, suggesting higher "peak" temperatures and pressures than the Northey Hill Line. The pressure-temperature relationship between the Jacobs Brook Recumbant Syncline and Baker Pond is less well constrained.

Chapter 8: PRESSURE-TEMPERATURE PATHS FROM GARNET ZONING

The quantitative determination of pressure-temperature (P-T) paths from mineral zoning (Spear and Selverstone, 1983) allows strong constraints to be put on the evolution of P-T conditions during prograde mineral growth. This information can be utilized to constrain tectonic and thermal processes during early portions of the metamorphic history.

The mineral zoning method involves the computation of ΔT and ΔP as functions of n compositional parameters, provided the mineral assemblage can be completely characterized with a variance of n. The input parameters for beginning the calculation are: the compositions all matrix phases, the molar entropies and volumes for all phases, the curvature of the Gibbs function for all phases, and a starting pressure and temperature.

Compositions for P-T path determinations are provided by microprobe analyses. All of the thermodynamic data used for computations are given by Selverstone, et al (1984). Rim temperatures are determined by geothermometry and geobarometry.

If the variance of the system is n, and if n independent compositional parameters can be determined by microprobe analysis of a zoned mineral, then the system is uniquely determined throughout the mineral's growth, assuming equilibrium has been maintained over the entire path and there have been no assemblage changes. In a uniquely determined system, when the independent compositional parameters are changed, the change in temperature, change in pressure, and change in compositions for all dependent compositional parameters are all determined as a result of the algebraic formulations. If more than one mineral is zoned, the observed zoning can be compared to the calculated zoning as a check on the accuracy of the calculations and assumptions.

If the variance is higher than the number of independent compositional parameters in a zoned mineral (ie: v=4 in garnet, 3 independent parameters), inclusions must serve to constrain the changes in an additional compositional parameter. In most cases plagioclase inclusions serve to constrain the additional parameter. In these situations, the change in plagioclase composition is assumed to be linear over distance from the inclusion to the rim (or to the next inclusion.

In the event that assemblage changes have taken place during the growth of the mineral, these must be pinpointed whithin the garnet grain and the assemblage changed accordingly before the P-T path computation is continued. Assemblage changes can be identified by incompatible mineral associations (ie: chlorite inclusion in garnet-cordierite-staurolite-sillimanite rocks) and textural relations. Assemblage changes can be pinpointed using inclusion compositions of the various phases.

Garnets have been used to produce all of the P-T paths from the study area. Garnets have the highest magnitude zoning, thus the least sensitivity to microprobe error. Additionally, garnets commonly have the most inclusions, which are useful for constaining high variance assemblages. Garnets grow over a relatively long stretch of the metamorphic history, and also have extremely slow rates of diffusion at temperatures less than 650°C (Yardley, 1977). The effects of diffusional re-equilibration are therefore minimal.

The starting conditions (T_0, P_0) for P-T paths are not considered to be the average points in the P-T parallelograms computed in chapter seven. Rather, the compositions of the matrix phases input initially into the P-T path computation are used to compute the initial temperatures and pressures. This initial P-T point lies inside of the parallelogram, but not necessarily at the average point.

Pressure-temperature paths are computed for four samples from the study area. Information is obtained from the Cottonstone Mountain locality (67-82e), Archertown Brook (PM-9B and D84-3d), and the Northey Hill Line (D84-1c and D84-1d-2). Due to varying numbers of constraints on these garnets, P-T paths present varying amounts of information.

COTTONSTONE MOUNTAIN

67-82e: The matrix assemblage identified in this sample is garnet + biotite + staurolite + kyanite + plagioclase + muscovite + quartz. In the system Si-Al-Mg-Fe-Mn-Ca-Na-K-H_2O, this assemblage is trivariant if water is considered as a phase. Plagioclase also occurs as inclusions in kyanite, staurolite, and garnet, and was used to constrain assemblage changes. Biotite and chlorite inclusions were also used to provide information on assemblage changes.

As was discussed earlier, the petrologic developement of the Cottonstone Mountain sample is interpreted to be from garnet-biotite-chlorite to garnet-biotite-chlorite-staurolite to garnet-biotite-staurolite-kyanite.

Plagioclase rim compositions vary from An_{20} to An_{23}; the initial plagioclase for the P-T path computations is taken to be An_{22}. The rim temperatures and pressures required by the garnet rim, this plagioclase, the presence of kyanite, and the initial biotite composition are 450°C and 4900 bars.

The traverse from this garnet is included along with a table listing the changes in garnet compositions, the inclusion compositions in porphyroblasts, and the assumed plagioclase zonings in Figure 61. All models for P-T path computations are listed in this figure.

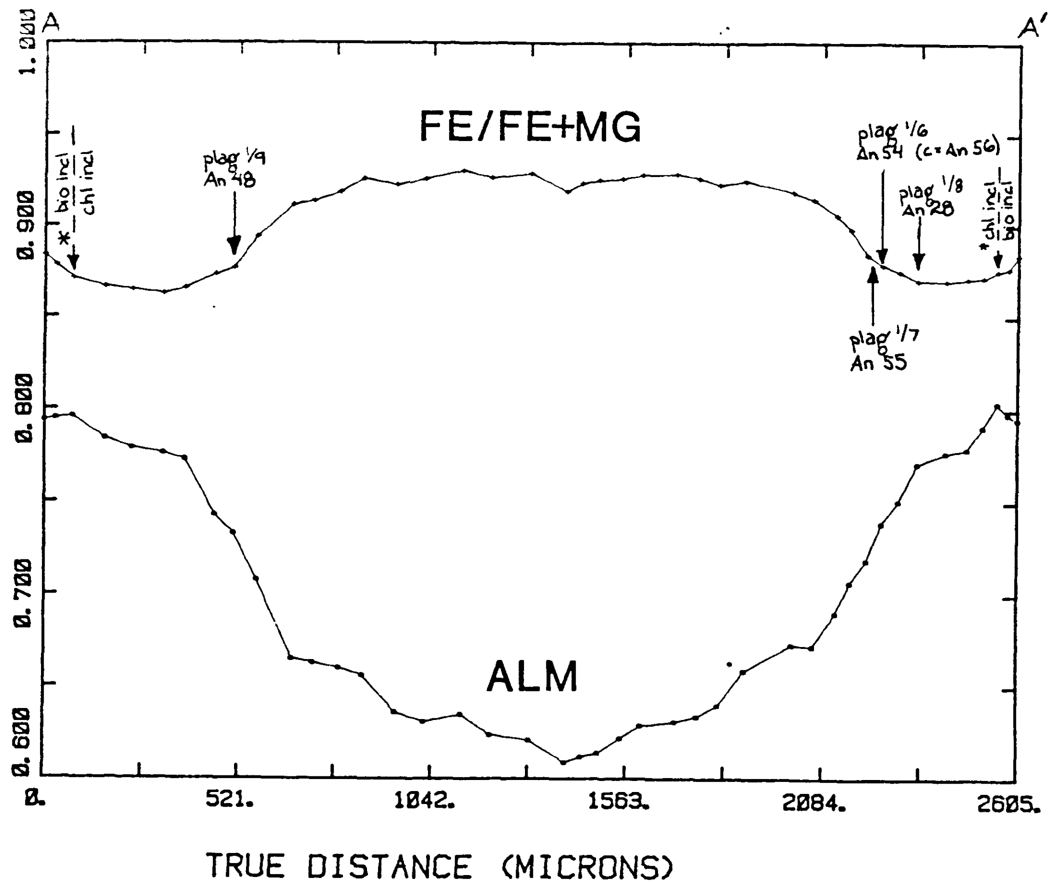

67-82e

	(rim)	1	2	3	4	5	6	7	8	9	10	11	12	13	14	15	16	17	18
ΔAlm	(.795)	.003	.006	-.013	-.012	-.002	-.006	-.020	-.012	-.017	-.003	-.012	-.017	-.018	.001	-.014	-.019	-.006	-.003
ΔSpess	(.039)	-.002	.002	.002	.004	.002	.004	.001	.002	.008	-.004	.013	.006	.019	.001	.021	.020	.006	.005
ΔGross	(.059)	-.008	-.010	.008	.010	-.001	.003	.028	.018	.015	.010	.011	.020	.008	.001	-.001	0	.002	0

Inclusions: (An22); chlorite inclusion (other garnet) at 3–4; An28 at 5; An48 at 7; An54 at 8; An55 at 9

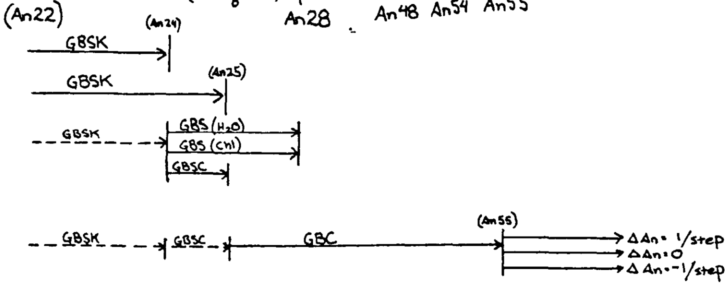

plag in Ky An20-23.5
plag in Strau An22.5-24

Figure 61: Cottonstone Mountain: Sample 67-82e; Garnet traverse and table listing compositions, assumptions, and models for P-T path calculations.

The closest plagioclase inclusion to the garnet rim has a composition of An_{28}. Plagioclase zoning between this inclusion and the matrix was assumed to be linear in composition and distance. Plagioclase inclusions in kyanite were analyzed and most values were found to lie in the range $An_{20.8}$ to $An_{23.5}$. One plagioclase inclusion had a higher value of An_{25}. For the sake of comparison, the kyanite bearing assemblage was modeled using two assumptions. The assemblage garnet-kyanite-staurolite-biotite was assumed to form over the range An_{22} (rim) to An_{24} or An_{25}. P-T path calculations made in the trivariant water bearing system produced plagioclase compositions that decreased from An_{22} (rim) to An_9. This is the opposite sense of zoning from what is observed. The assemblage was then modeled assuming fluid absent equilibria. The two plagioclase assumptions were found to make no difference on the shape of the P-T path. Since only one plagioclase analysis was above An_{24}, the former P-T path is felt to be more reliable. This near-rim P-T segment is show in Figure 62.

This segment shows a near isobaric decrease in temperature of approximately 60°C. This is very unusual, considering that the reaction

$$\text{staurolite} + \text{chlorite} + H_2O \rightarrow \text{kyanite} + \text{biotite}$$

is very steep in P-T space and kyanite occurs on the high temperature side. The reaction that garnet is growing by in this segment is unknown. The P-T segment computed has a flat slope and kyanite is being produce towards lower temperatures. By changing the activity of water in this sample, the equilibrium will shift in P-T space according to Le Chatelier's rule. The equilibrium shifts toward lower temperatures when the activity of water is decreased (J. Selverstone, pers. comm.). This allows for kyanite to be produced along a vector similar to the one computed, and also provides a possible explanation for why the fluid-present modeling was incorrect with respect to plagioclase zoning. Evidence of late stage fluid involvement is

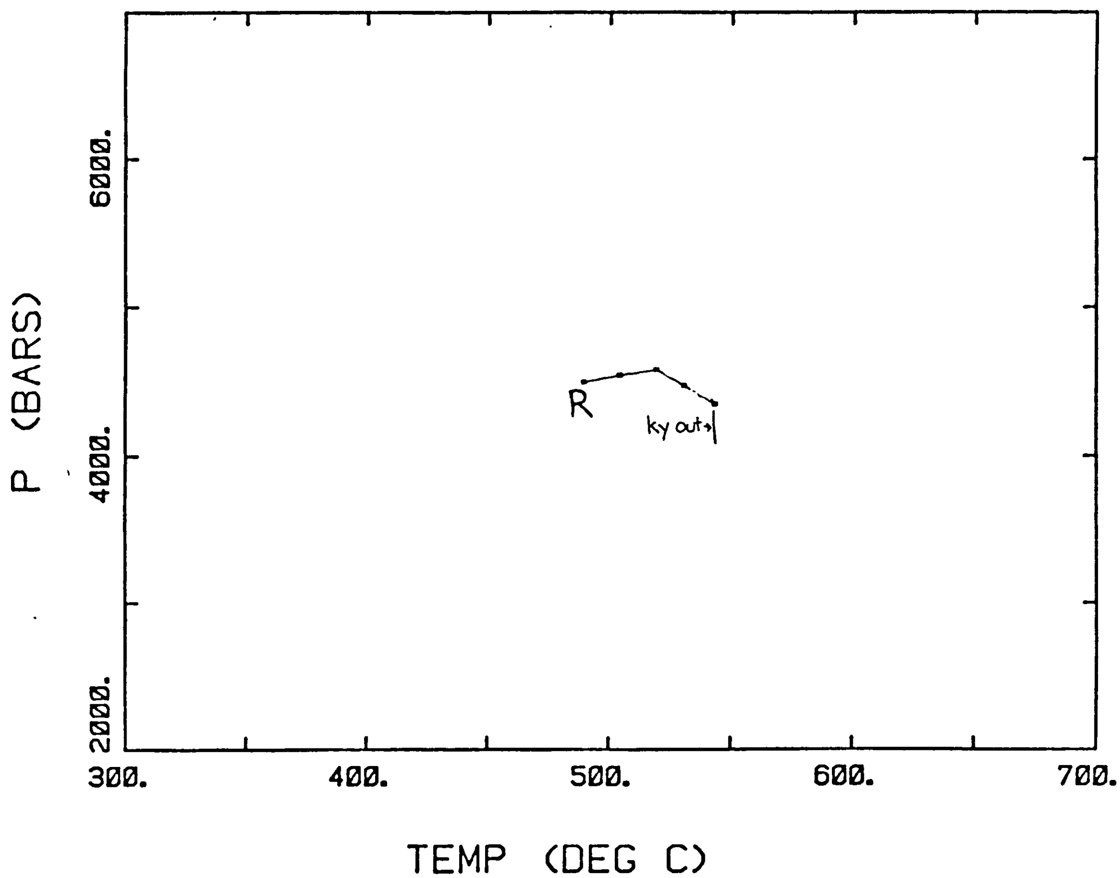

Figure 62: Cottonstone Mountain: Sample 67-82e; Near-rim P-T path using fluid absent equilibrium in the assemblage garnet-biotite-staurolite-kyanite.

seen in thin section, although it appears to post-date kyanite growth. The fluid involvement is seen as sericitization of kyanite, garnet, biotite, muscovite, plagioclase, and staurolite. One garnet in the sample is replaced 60% by sericite. This indicates a variable activity of water through time, which may be responsible for the observed P-T path geometry.

Staurolite contains plagioclase inclusions with rim compositions of $An_{22.5}$ and An_{24}, and core compositions as high as $An_{25.3}$. Because a definitive chlorite-biotite inclusion transition is seen in another garnet in this sample at a level correlative with the An_{28} inclusion in the mapped garnet (see discussion garnet map section), the staurolite-out reaction (producing the garnet-chlorite join) may have taken place as high as the An_{28} level. Since the garnet-biotite-staurolite system has a variance of five, the next P-T segment was modeled two ways. Chlorite was likely to be present during the staurolite bearing segment of the P-T path, so the quadrivariant system (fluid-absent) was modeled using staurolite present over the interval An_{24} to An_{28}. The composition of the chlorite inclusion nearest the rim of the neighboring garnet was used for the calculations. The fluid-absent assumption was investigated by including water in the assemblage and modeling the quadrivariant system (chlorite-absent) using the same plagioclase interval. Figure 63 compares the two garnet-biotite-staurolite paths. The paths are similar in shape and direction, and identical whithin the range of microprobe error (F. Spear, pers. comm.). This indicates that fluid was present at constant X_{H2O} throughout this segment of the path, and therefore it can be assumed that water was part of the prograde metamorphism up to the kyanite-present assemblage.

The least calcic plagioclase analysis from inclusions in staurolite was $An_{25.3}$. The staurolite-bearing assemblage was therefore modeled using

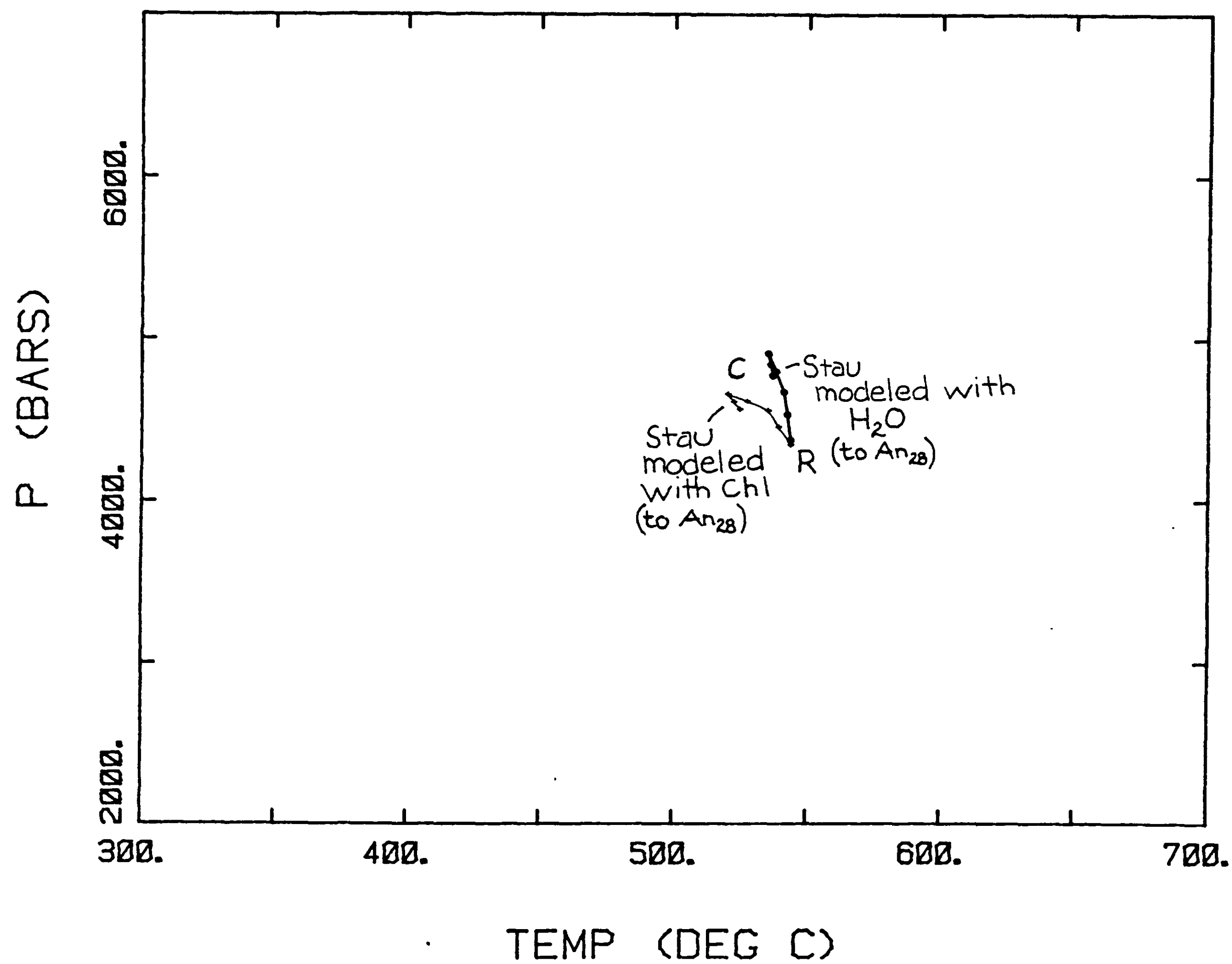

Figure 63: Cottonstone Mountain: Sample 67-82e; P-T segments computed for the staurolite-bearing assemblage assuming
a) chlorite-bearing, fluid absent
b) fluid present, chlorite absent

$An_{25.3}$ as the point where staurolite first joins the assemblage. This P-T segment is shown along with the near-rim kyanite-bearing segment in Figure 64. Because staurolite may or may not have been present when the chlorite inclusion was in equilibrium, the P-T segment for the segment An_{24} to $An_{25.3}$ is probably closer to the actual equilibrium range for this assemblage.

The two models are also similar in their final computed Fe/Fe+Mg ratios in staurolite, a value that can be also measured in the core of the slightly zoned phenocryst. The staurolite has a rim Fe/Fe+Mg ratio of 0.841, while the core has a value of 0.824. Both models have final Fe/Fe+Mg ratios of 0.832 to 0.834. Thus there is a similarity in zoning direction between the computed and the analyzed, but a minor discrepency in magnitude.

At the point where staurolite leaves the assemblage, garnet + biotite + chlorite are left. This assemblage has a variance of four in the presence of water. Actual and corelative inclusions in this garnet are more anorthitic toward the core of the garnet. The garnet-biotie-chlorite assemblage was modeled from the staurolite-out reaction at the $An_{25.3}$ level to the highest anorthite inclusion of An_{55}. This P-T segment is shown in Figure 65.

To travel the remainder of the way to the core (where no plagioclases occur as constraints), the garnet was modeled using three assumptions. The plagioclase was assumed to either increase, stay the same, or decrease at a rate of An_1 per step. Fortunately enough, there is little qualitative difference between these three models, as is evidenced by Figure 66.

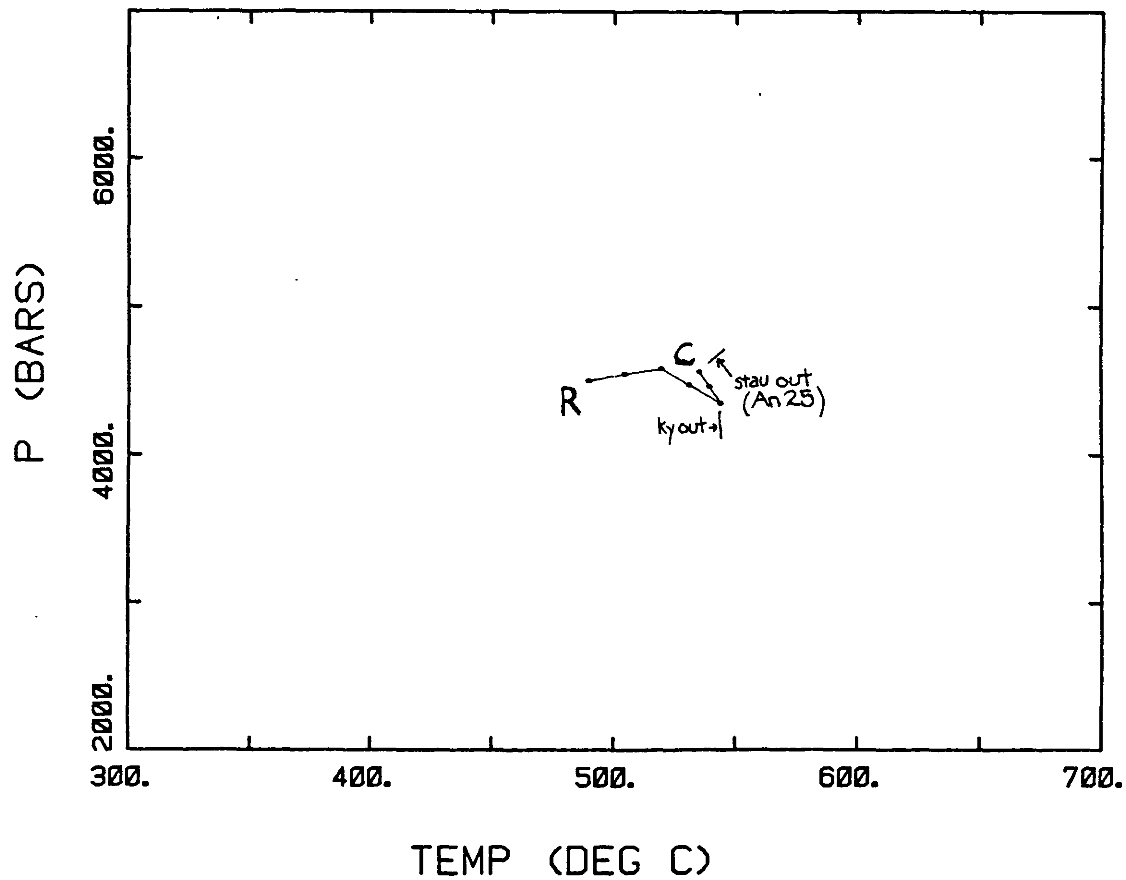

Figure 64: Cottonstone Mountain: Sample 67-82e; Near rim P-T paths, showing the kyanite-bearing path from Figure 62 as well as the staurolite-out path.

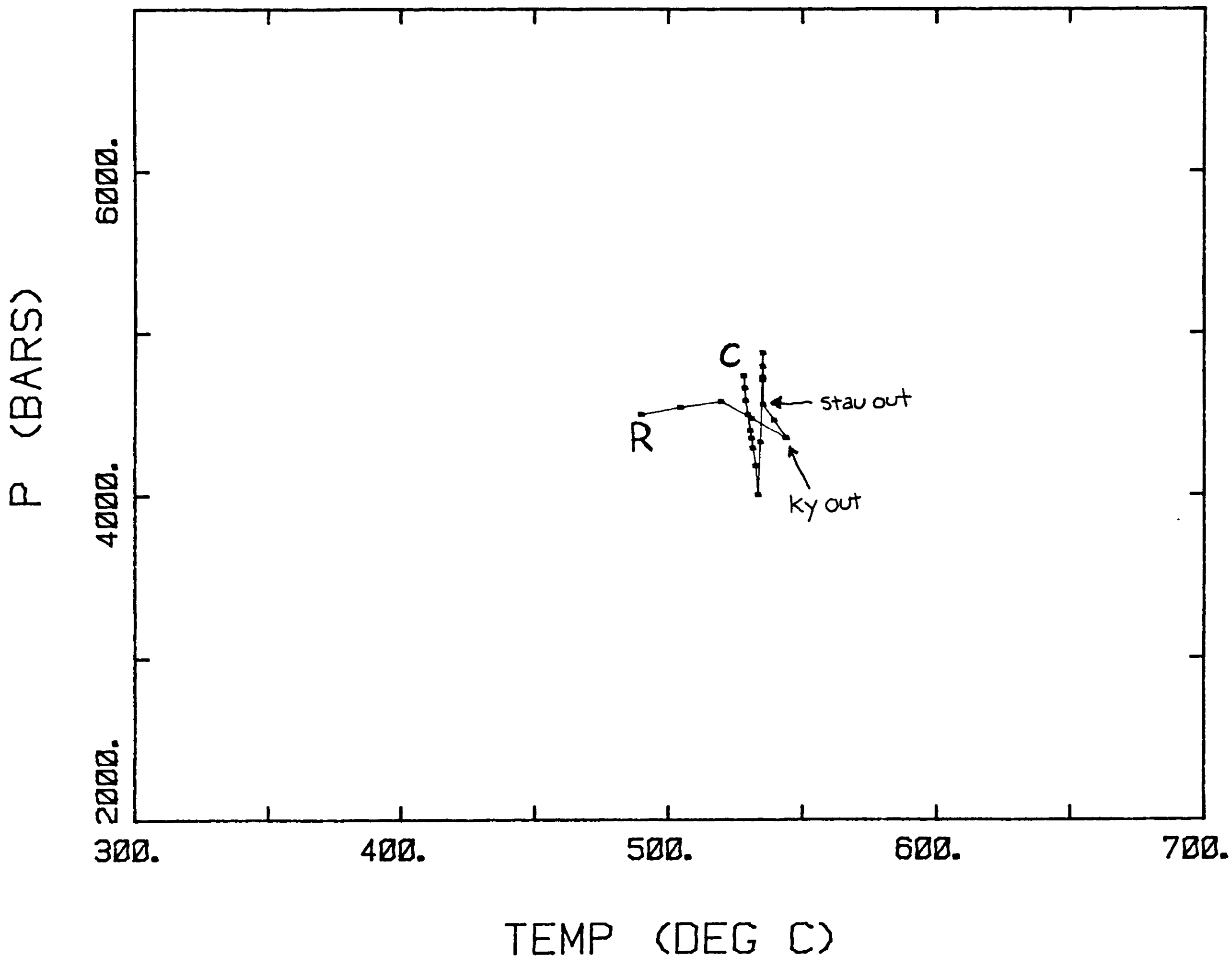

Figure 65: Cottonstone Mountain: Sample 67-82e; P-T path with kyanite-bearing assemblage, staurolite-bearing assemblage, and garnet-biotite-chlorite path modeled to the plagioclase inclusion nearest the core.

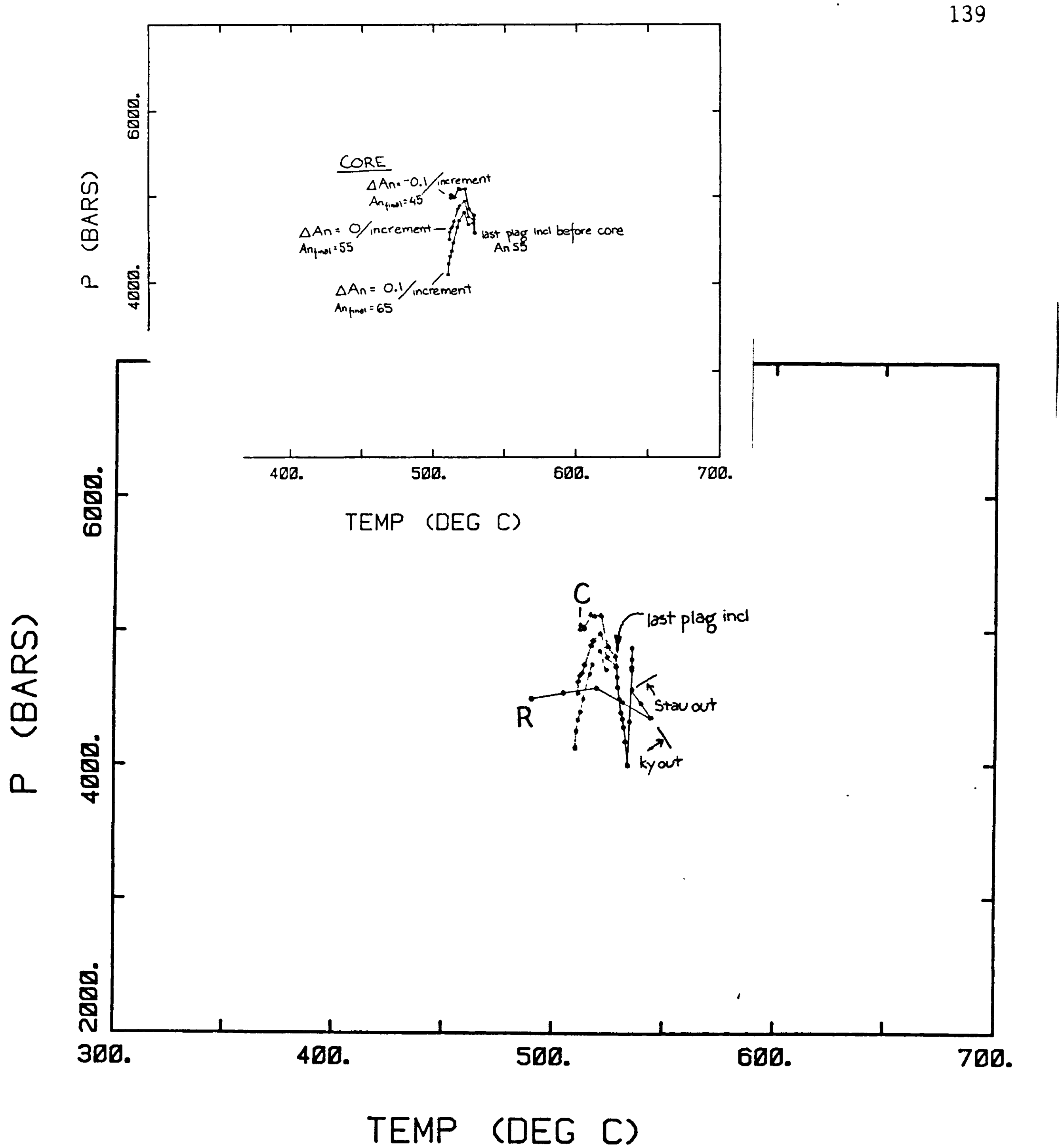

Figure 66: Cottonstone Mountain: Sample 67-82e; P-T path of kyanite-bearing assemblage, staurolite-bearing assemblage, and garnet-biotite-chlorite to the last plagioclase inclusion. Modeling from the last inclusion to the core using three assumptions: a) ΔAn=0.1, b) ΔAn=0, and c) ΔAn=-0.1 per increment.

Discussion

In the grossest possible sense, this garnet exhibits a clockwise P-T path. From core to rim, the details are interpreted as thus, with all interpretations having a foundation in the models of England and Richardson (1977). The initial growth of the garnet was in an increasing pressure-increasing temperature environment. This compressional event is followed by a segment of the P-T path which indicates decompression and mininor heating. This normal clockwise P-T path is interrupted by a dramatic isothermal increase in pressure. This compressional event is evident regardless of the assumed plagioclase gradients or even if the garnet-biotite-staurolite assemblage is modeled from An_{24} to An_{28}. This increase in pressure is interpreted to be due to the emplacement of one or more nappes. This is supported by the textural relations of this sample. The garnet has the dome stage foliation wrapping around it and is rotated. Because the Sunday Mountain cleavage belt is weak or non-existent in this area, the P-T path permits the quantitative investigation of the dome stage and nappe stage deformation.

The nappe stage compression is followed by an increase in temperature and a decrease in pressure. Regional and textural relations suggest that this decompression is due to dome stage uplift.

The final segment of the P-T path is essentially an isobaric decrease in temperature of approximately 60°C. As was discussed in the modeling section, this event is interpreted to be due to late stage fluid involvement resulting in the reduction of the activity of water and concommittant cooling. Rumble (1969) reports a high degree of fluid involved retrograde meatamorphism in the vicinity of the Ammonoosuc Fault. If the Ammonoosuc Fault is an east-dipping thrust fault, de-watering of the lower plate could provide the fluid necessary to cause the P-T path geometry found in the Cottonstone Mountain sample.

ARCHERTOWN BROOK

D84-3d: Sample D84-3d contains the same matrix assemblage as 67-82e: garnet + biotite + staurolite + kyanite + plagioclase + muscovite + quartz. The petrologic evolution of this sample is also identical to the Cottonstone Mountain sample; ie: garnet-biotite-chlorite to garnet-biotite-chlorite-staurolite to garnet-biotite-staurolite-kyanite. In contrast to 67-82e, however, the staurolites in D84-3d are rotated, contain inclusion trails that are 30° to the latest foliation, and also have the latest foliation wrapped around them. One kyanite crystal also exhibits deformation. This sample has also been deformed by the Sunday Mountain cleavage belt.

Plagioclase grains occurring at the garnet rim are zoned from An_{31} to An_{34}, with the cores more calcic than the rims. For this reason, the initial plagioclase composition for P-T path calculations is taken to be An_{31}. Geothermometry and geobarometry using this plagioclase, the presence of kyanite, the initial garnet rim composition, and the initial biotite composition yields 475°C and 3500 bars.

The traverse across this garnet is included along with a table listing the changes in garnet composition, the inclusion compositions, and the assumed plagioclase zoning in Figure 67. The P-T path models discussed in the text are also included in this figure.

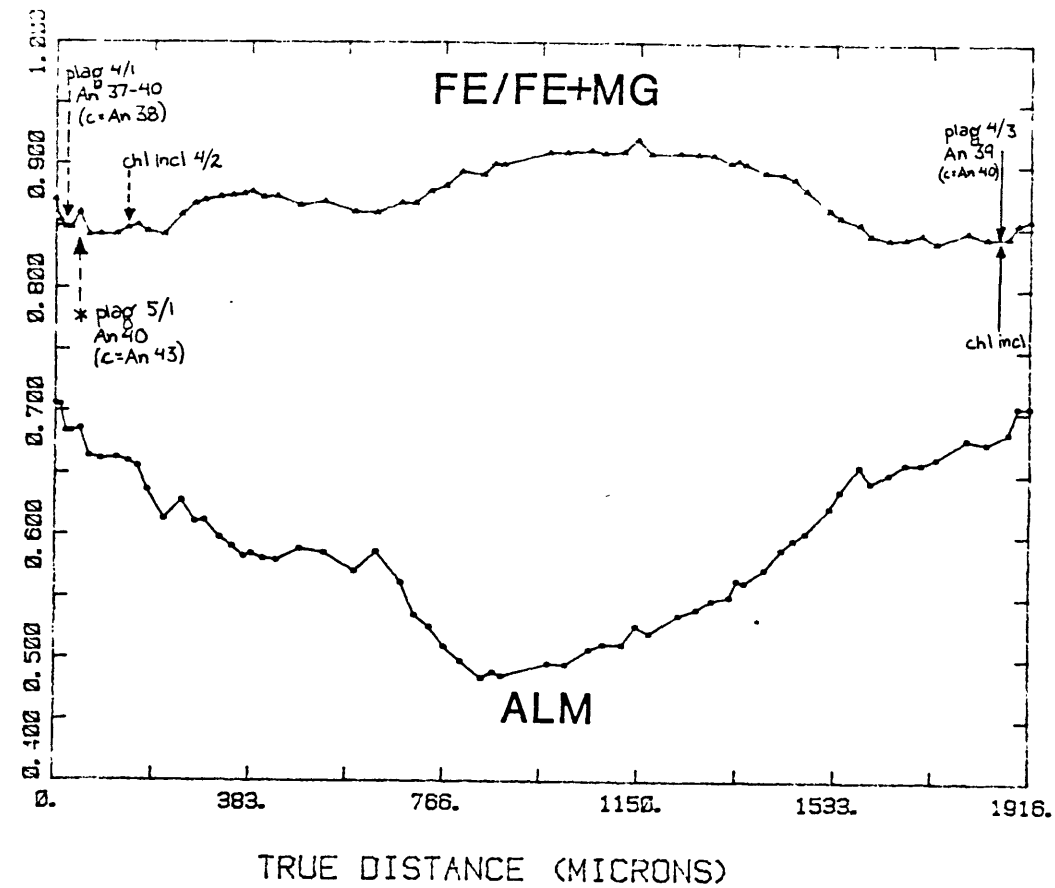

D84-3d

	(rim)	1a	1b	1c	2a	2b	2c
ΔAlm	(.706)	-.0004	-.0003	-.0003	-.007	-.007	-.007
ΔSpess	(.113)	-.0006	-.0007	-.0007	.002	.002	.002
ΔGross	(.074)	-.0036	-.0037	-.0037	.004	.004	.004
					↑ chl incl		
Inclusions	(An31)				An 39 (c=An40)		
ΔAn		2	2	2	3	1	

GBSK → | GBSH2O / GBSC → | GBC | Albite!

plag in Ky An 33-34
Ky incl in plag An 32-36
plag in stau An 35

Figure 67: Archertown Brook: Sample D84-3d; Garnet traverse and table listing compositions, assumptions, and models for P-T path calculations.

The nearest plagioclase inclusion to the rim of the garnet has a rim composition of An_{39} with a core of An_{40}. A chlorite inclusion occurs at the rim of this plagioclase inclusion. Plagioclase zoning between this inclusion and the garnet rim is assumed to be linear in both composition and distance. Plagioclase inclusions in kyanite vary from An_{33} to An_{34}. Kyanite is also found as an inclusion in a matrix plagioclase near the garnet rim. The plagioclase compositions adjacent to the kyanite are An_{32} to An_{36}. A plagioclase inclusion in staurolite was analyzed and found to have a composition of An_{35}.

The matrix assemblage in sample D84-3d is trivariant in the presence of water. When this system is modeled using the three independent garnet components as compositional parameters, problems are encountered that are identical to those discussed for the Cottonstone Mountain sample; ie: computed plagioclase zoning is in a sense opposite to that which is observed. As a result, the Gibbs-Duhem equation for water is removed and the system is modeled as quadravariant using the three independent garnet parameters and plagioclase. The kyanite-bearing assemblage is modeled over the range An_{31} to An_{36}, corresponding with the most calcic plagioclase analysis associated with kyanite. This produces a near rim decrease in pressure and temperature of 50 bars and 50°C. This segment, as well as the entire P-T path computed for this sample is shown in Figure 68. The composition at this point coincides with the inclusion-rich inclusion-free boundary in the garnet. Since the staurolite is more rotated than the kyanite, this makes sense texturally.

The garnet-staurolite-biotite assemblage is modeled as quadravariant as both fluid-absent and chlorite-absent. Again, the results are statistically identical. The fluid-absent path is modeled over the range

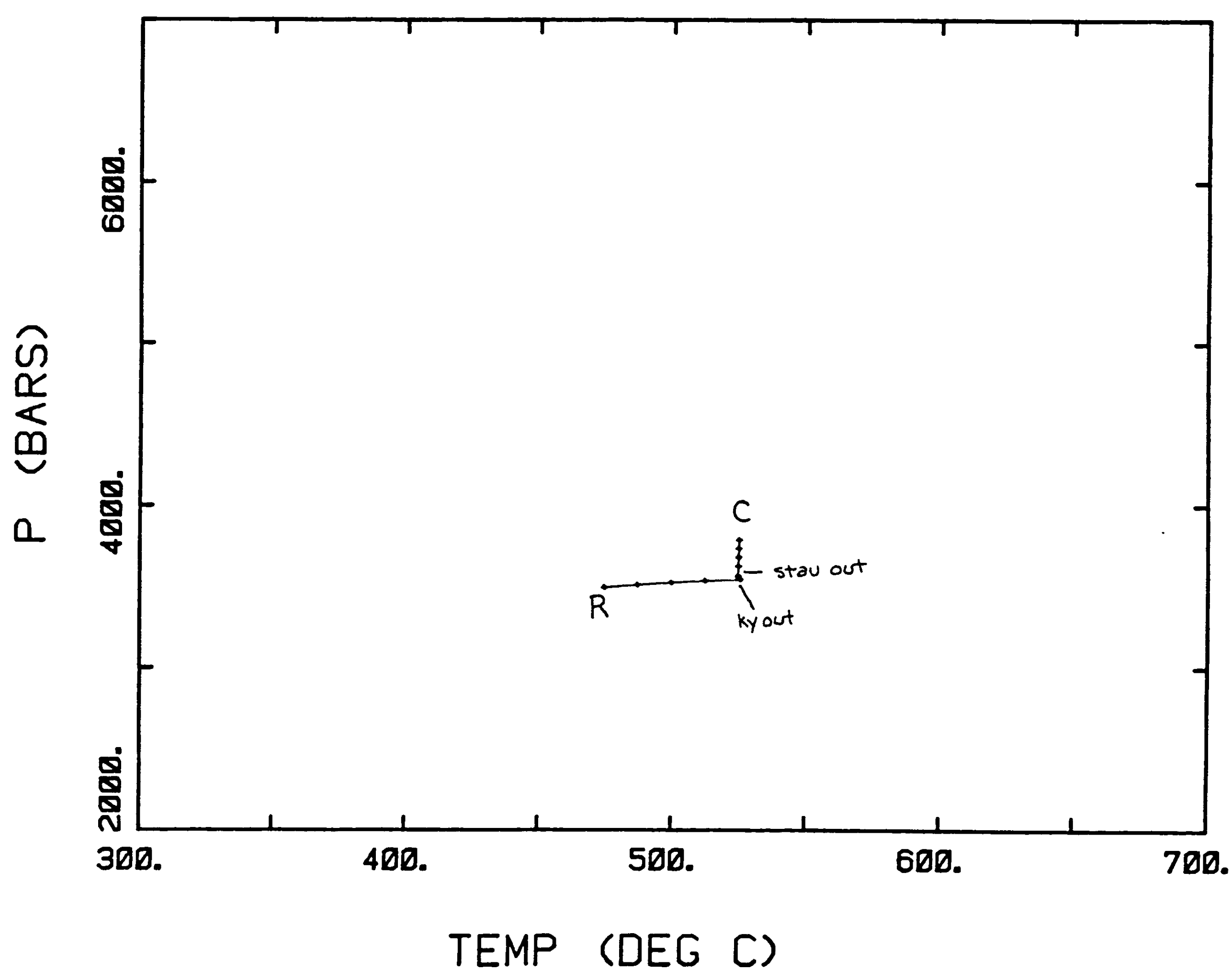

Figure 68: Archertown Brook: Sample D84-3d; P-T paths.

An_{36} to An_{39}, which corresponds to the plagioclase composition at the first chlorite inclusion. This plagioclase inclusion exhibits slight zoning, so the garnet-biotite-chlorite assemblage is modeled for one increment to the An_{40} level. The next plagioclase inclusion toward the garnet core has a composition of An_3. This suggests that the plagioclase in this garnet has crossed to the other side of the peristerite gap. The P-T path method is not able to account for this non-ideal character. Because of this, the garnet was not able to be modeled any further towards the core using plagioclase as the fourth independent compositional parameter. Several chlorite inclusions also occur in this garnet, yet these appear to be re-equilibrated along cracks in backscattered images taken using the electron microprobe.

Discussion

This P-T path is presented in Figure 68. It exhibits characteristics identical to those of 67-82e. The near rim isobaric cooling is present, as well as the beginning of the decompression. The kyanite in this sample pre-dates the Sunday Mountain schistosity, so the near-rim isobaric cooling event occurred after the dome stage deformation (from 67-82e P-T path) and before the Sunday Mountain deformation. The dome stage deformation, which is preserved as inclusion trails in rotated garnets and staurolites, is exhibited by the earliest P-T path determinations from this sample.

The zoning profile of this garnet, however, appears very similar to the traverse from 67-82e. Based on this observation, and the similar assemblages and bulk compositions in the two samples, the remainder of the P-T path for D84-3d probably has a similar geometry to 67-82e.

PM-9b: In contrast to the previous two samples, PM-9b has an equilibrium matrix assemblage of garnet + biotite + chlorite + plagioclase + muscovite + quartz. Due to biotite and plagioclase inclusions in garnet, this sample can be monitored with a variance of five, using both as monitor parameters, or as quadravariant (including H_2O in the assemblage) using either inclusion as a monitor. The latter technique can additionally test consistencies.

The matrix plagioclases have compositions ranging from An24-An30, with the cores more calcic than the rims. Because of this, the initial plagioclase composition was taken to be An_{24}. This was used with a biotite (Fe/Fe+Mg=0.445), muscovite, and garnet rim (X_{Gr}=0.057) to get rim conditions of 450°C and 3720 bars.

A rim to core traverse is shown in Figure 69, along with the garnet compositional changes per increment, the possible inclusion relationships, and all of the zoning models discussed in the text.

One plagioclase inclusion occurs in the mapped garnet, while one other occurs in another garnet. The mapped inclusion occurs at the X_{Gr} =0.136 level and has a rim value of An39 and a core of An42. The plagioclase in the other garnet has a value of An32 and corresponds to different points in the mapped garnet, depending on which garnet component is correlated. All correlations fall in the range X_{Gr}=0.103 to 0.115.

The first problem encountered when modeling this garnet was with biotite. Matrix biotites had Fe/Fe+Mg ratios ranging from 0.436 to 0.445; the biotite inclusion (analyzed at 20 points) had Fe/Fe+Mg ratios ranging from 0.425 to 0.454. No consistent zoning pattern was observed in the biotite inclusion. In the five-variant system (water absent), a range of biotite differences (ΔAn=0.002, 0, or -0.004 per step) were coupled with

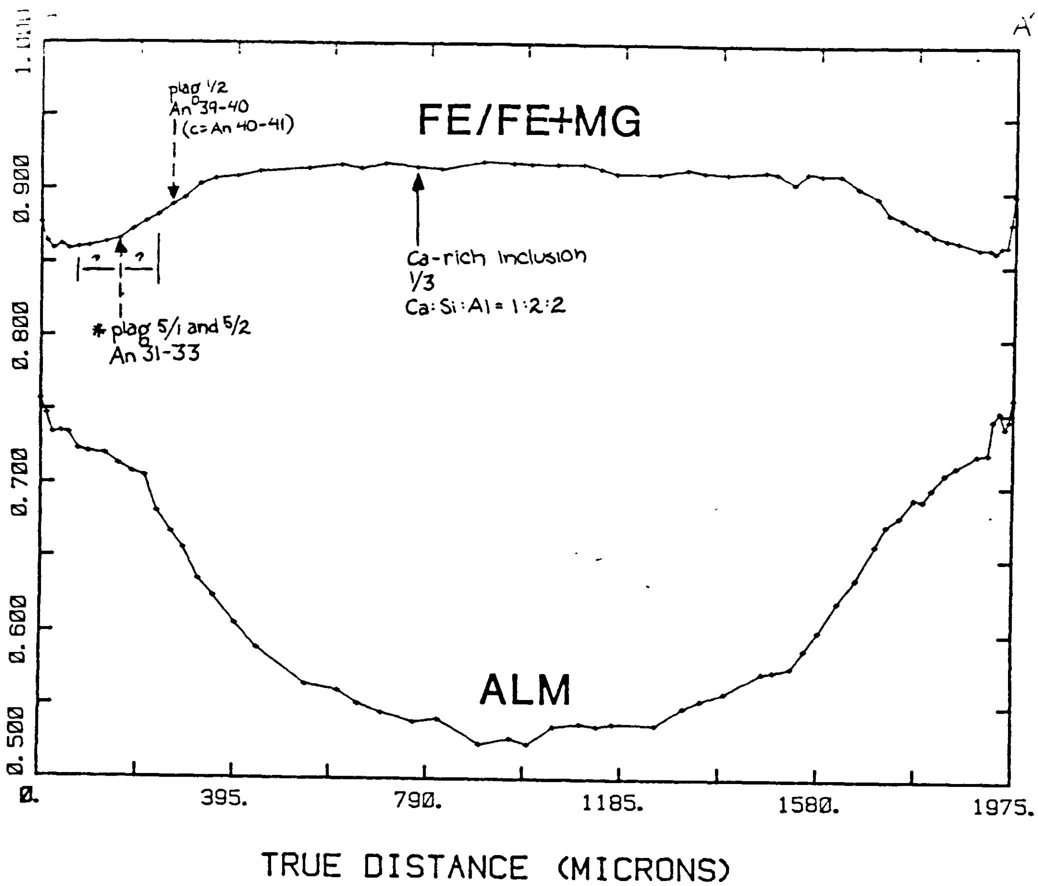

PM-9b

	(rim)	1	2	3	4	5	6	7	8	9	10	11	12	13
ΔAlm	(.757)	-.010	-.013	.001	-.001	-.011	-.002	-.001	-.007	-.005	-.003	-.024	-.014	-.011
ΔSpess	(.078)	.001	-.006	0	-.001	.003	-.002	-.003	.003	.004	.002	.012	.015	.006
ΔGross	(.057)	-.003	.016	.004	-.002	.011	.005	.008	.007	.006	.006	.021	.006	.010
Inclusions	(An 24)				Biotite incl				plag incl, other gar possible correlations An32				An 39 (c=An 42)	

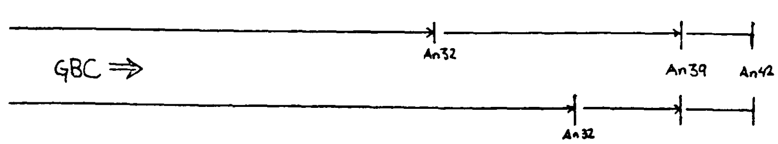

Figure 69: Archertown Brook: Sample PM-9b; Garnet traverse and table listing compositions, inclusions, assumptions, and models for P-T path calculations.

plagioclase inclusions. The three P-T paths produced were +20°C and +800 bars, +40°C and 1000 bars, and 60°C and 1200 bars from rim to biotite inclusion, respectively.

When modeled as quadrivariant system using biotite as a monitor parameter, the P-T path claculations produce a rim to core decrease in pressure of 10 kilobars. Several large cracks intersect this inclusion, and it looks somewhat altered in electron microprobe backscattered imagery. These textures suggest that the biotite may have re-equilibrated. Because of this, the sample will be modeled as a quadrivariant system using palgioclase as the fourth monitor parameter.

Using plagioclase as a monitor parameter, the results are far more reasonable. If the correlative plagioclase is brought in at the earliest possible moment (X_{Gr}=0.103), the P-T path exhibits a decompression of 620 bars preceded by a compressional event of 130 bars. If the plagioclase is brought in as late as possible (X_{Gr}=0.115), the path shows a near-rim decompression of 830 bars preceded by a compressional event of 330 bars. These P-T paths are shown graphically in Figure 70. The P-T path from these assumptions give biotite Fe/Fe+Mg ratios of 0.4081 to 0.4092 at the X_{Gr}=0.074 to 0.083 level. These are substantially lower than the values determined from the biotite inclusion. Quite a few large cracks exist in this garnet, and the range in biotite compositions, the inconsistent zoning, and the oddities in P-T path calculations are interpreted to be due to crack-induced re-equilibration.

The quadrivariant P-T path determined using plagioclase inclusions is then considered to be the P-T path from PM-9b. No further plagioclase inclusions were found in this garnet, although an inclusion of an unidentified Ca-Al silicate with anorthite or lawsonite stoichiometry is

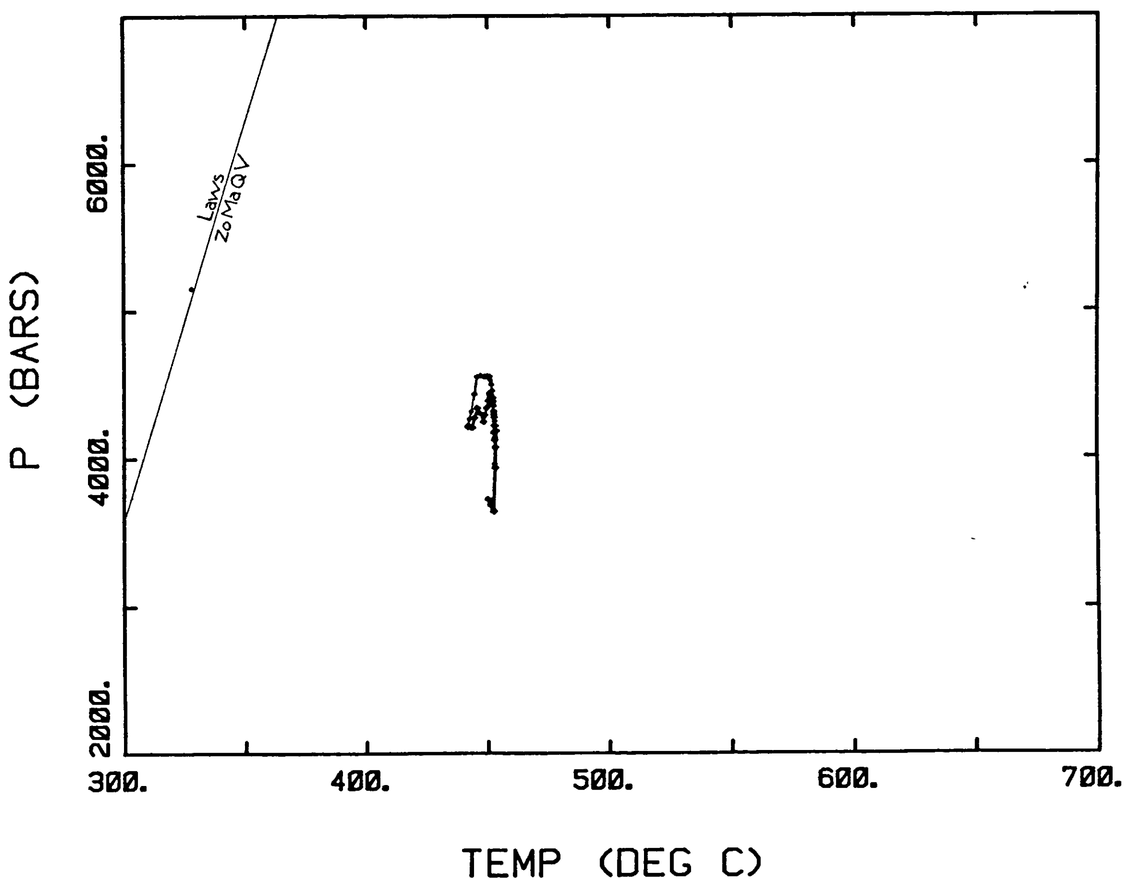

Figure 70: Archertown Brook: Sample PM-9b; P-T paths using quadrivariant assemblage garnet-biotite-chlorite with plagioclase as monitor parameter. Two models correspond to bringing correlative plagioclase inclusion in at different levels. Lawsonite stability curve from Chatterjee, et al. (1984).

found nearer the core. This inclusion suggests some assemblage change earlier on in the garnet's growth. Because of this, no assumption is valid for modeling plagioclase as a monitor parameter closer to the core of the garnet. If the inclusion is lawsonite, it places important constraints on the early P-T path of this sample. For reference, the lawsonite stability curve (from Chatterjee, et al. (1984) is also plotted on Figure 70.

Discussion

This sample contains the pervasive Sunday Mountain schistosity. The garnets in this sample are rotated and overprinted by this schistosity. This fabric relationship is quite consistent with the P-T path determine from this sample. The near-rim decompression (of 620 to 830 bars) visible in the P-T path correlates texturally with the dome stage deformation. A compressional event of 130 to 330 bars is visible in the core-most P-T path from this sample. It is impossible to tell quantitativley whether this is due to a normal clockwise P-T evolution or due to nappe stage deformation, because no plagioclase inclusions exist to constrain the early path.

The garnet zoning in PM-9b is very similar to the zoning seen in the other Archertown Brook sample and the Cottonstone Mountain sample. Qualitatively, then, the early P-T evolution of the PM-9b sample is probably similar to the other samples. This would suggest that the early decompression seen in this sample is due to post-nappe stage unloading following crustal thickening.

NORTHEY HILL LINE

D84-1d-2: Sample D84-1d-2 contains the matrix assemblage garnet + chloritoid + chlorite + plagioclase + quartz + muscovite. In the presence of fluid, this system is quadravariant in the system $CaO-Na_2O-K_2O-FeO-MnO-MgO-Al_2O_3-SiO_2-H_2O$. Unfortunately no inclusions of plagioclase, or any other monitor parameter for that matter, were found in this garnet. In order to gain some information from this sample, three plagioclase zoning assumptions were applied to the garnet zoning model. Plagioclase was assumed to increase at An_1 per step, stay the same, or decrease An_1 per step from rim to core.

The traverse from this garnet is included in Figure 71, along with a table showing garnet compositional changes per increment and P-T path models.

Fortunately enough, all three assumptions give very similar P-T paths. The directions are identical, and the three paths only differ in length, as is illustrated by Figure 72. When plagioclase is assumed to change by An1 each increment, the calculations suggest a maximum ΔP of 420 bars. Constant plagioclase composition give a maximum decompression of 730 bars, while a decreasing plagioclase composition gives a maximum ΔP of 1080 bars.

The initial conditions for this P-T path of 475°C and 3600 bars were taken from the average of the geothermometers and geobarometers from sample D84-1c. Since these two samples come from the same locality 50 meters apart, this assumption seems valid.

Texturally, the garnet from this sample is slightly rolled, although it overprints most of the S3 schistosity. This garnet is syn-/post-Sunday Mountain cleavage belt. The P-T path determined from this sample indicates that the Sunday Mountain deformation occurs during decompression in this locality.

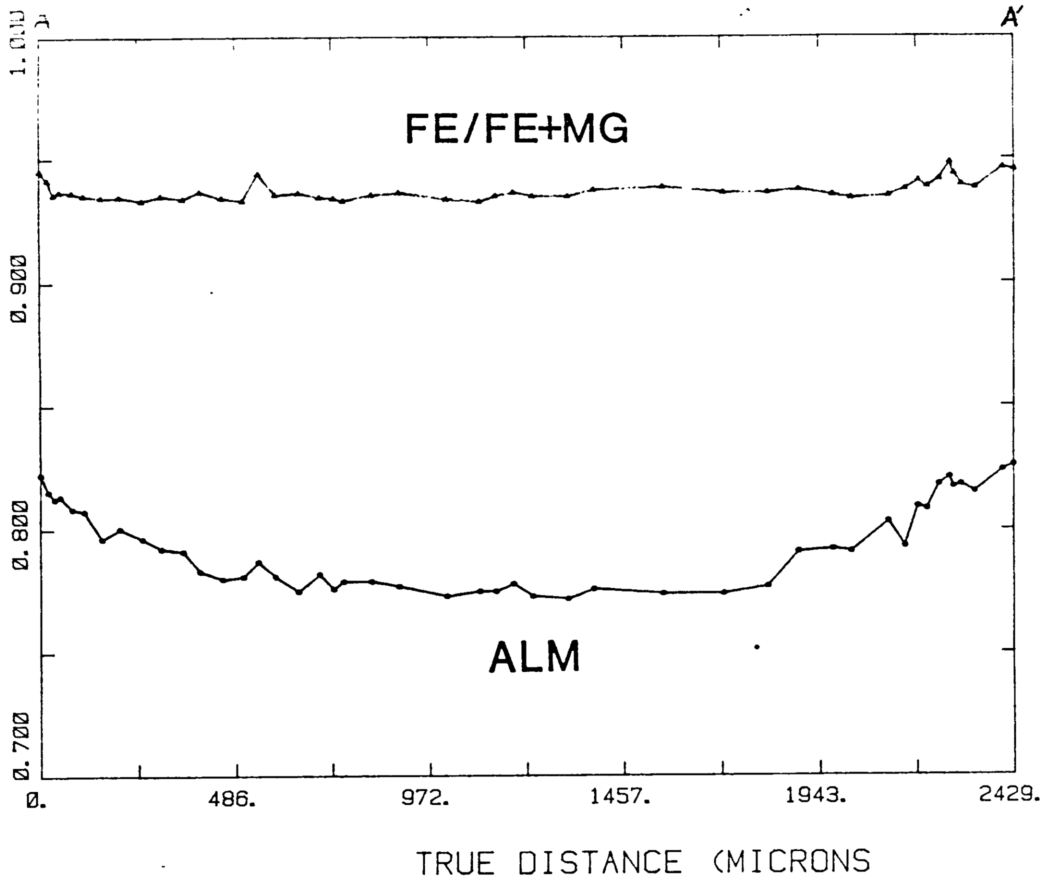

D84-1d-2

	(rim)	1	2	3	4	5	6	7
ΔAlm	(.837)	⁻.016	.005	⁻.005	⁻.016	⁻.014	⁻.014	⁻.004
ΔSpess	(.038)	.003	⁻.005	.001	.006	.010	.020	0
ΔGross	(.075)	.013	0	0	.004	.008	⁻.005	.004

(An 37)

→ ΔAn = 1/step

GChl Chlt'd → ΔAn = 0

→ ΔAn = -1/step

Figure 71: Northey Hill Line: Sample D84-1d-2; Garnet traverse and table listing compositions, assumptions, and models for P-T path calculations.

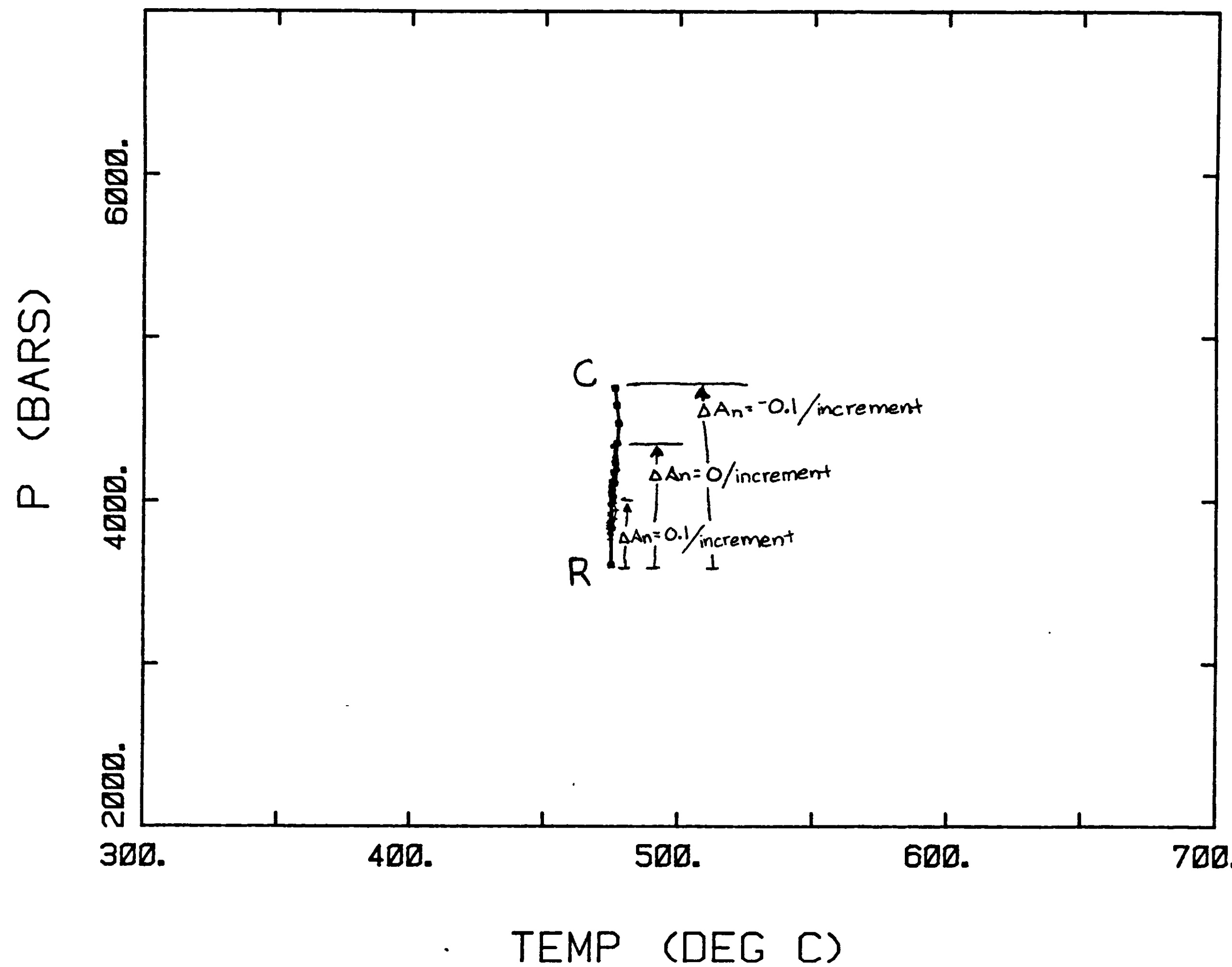

Figure 72: Northey Hill Line: Sample D84-1d-2; P-T paths using three different plagioclase assumptions.

D84-1c: Sample D84-1c contains the matrix assemblage garnet + biotite + chlorite + plagioclase + quartz + muscovite. In the presence of fluid, this system is quadravariant in the system $CaO-Na_2O-K_2O-FeO-MnO-MgO-Al_2O_3-SiO_2-H_2O$. Initial conditions were obtained using a matrix plagioclase rim of An13 and an average biotite (Fe/Fe+Mg=0.6003) along with muscovite and quartz, and the rim P-T was found to be 475°C and 4000 bars.

No inclusions that could be used as monitor parameters were found. As a result, this garnet was modeled identically to D84-1d-2, using plagioclase zoning assumptions of $+An_1$, An_0, and $-An_1$ per increment. It should be noted that matrix plagioclases span the range of An13 to An24, with the less calcic compositions more towards the rim. This adds a certain amount of credence to the increasing An content model.

Figure 73 contains a traverse across the garnet, as well as a table containing the garnet compositional changes per increment and the models used for determining P-T paths.

Similar to D84-1d-2, all three plagioclase models have identical directions and different magnitudes. This is illustrated in Figure 74. An assumption of ΔAn=+1 per increment gives a decompression of 580 bars accompanied by a decrease in temperature of 2.6°C. A constant plagioclase assumption yields a core to rim pressure decrease of 1200 bars and a temperature decrease of 3°C, while a decreasing plagioclase assumption gives a ΔP of 2020 bars and a ΔT of 3.6°C.

All plagioclase modeling assumptions were investigated for quantitative changes in biotite composition. It was found that all of the assumptions produced a decrease in Fe/Fe+Mg ratios from rim to core. The final ratios spanned the range of 0.5385-0.5430, with the original ratio being 0.6003. Matrix biotites are not zoned; these compositions are only investigated to see if P-T models produce unreasonable Fe/Fe+Mg ratios.

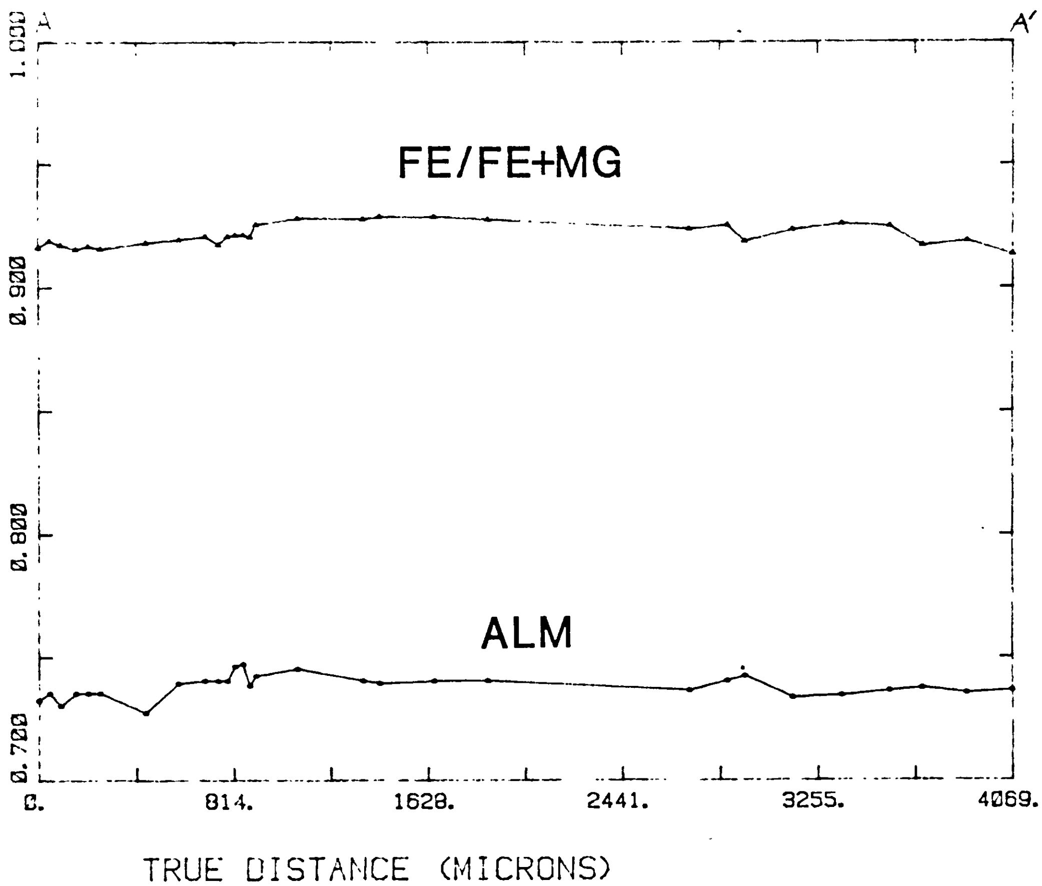

D84-1c

	(rim)	1	2	3	4
ΔAlm	(.739)	-.005	-.007	-.008	-.001
ΔSpess	(.159)	-.012	-.003	.003	-.005
ΔGross	(.045)	.006	.009	.002	.008

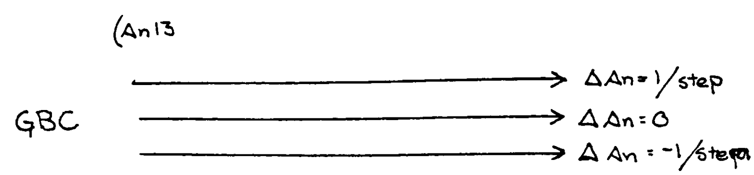

Figure 73: Northey Hill Line: Sample D84-1c; Garnet traverse and table listing compositions, assumptions, and models for P-T path calculations.

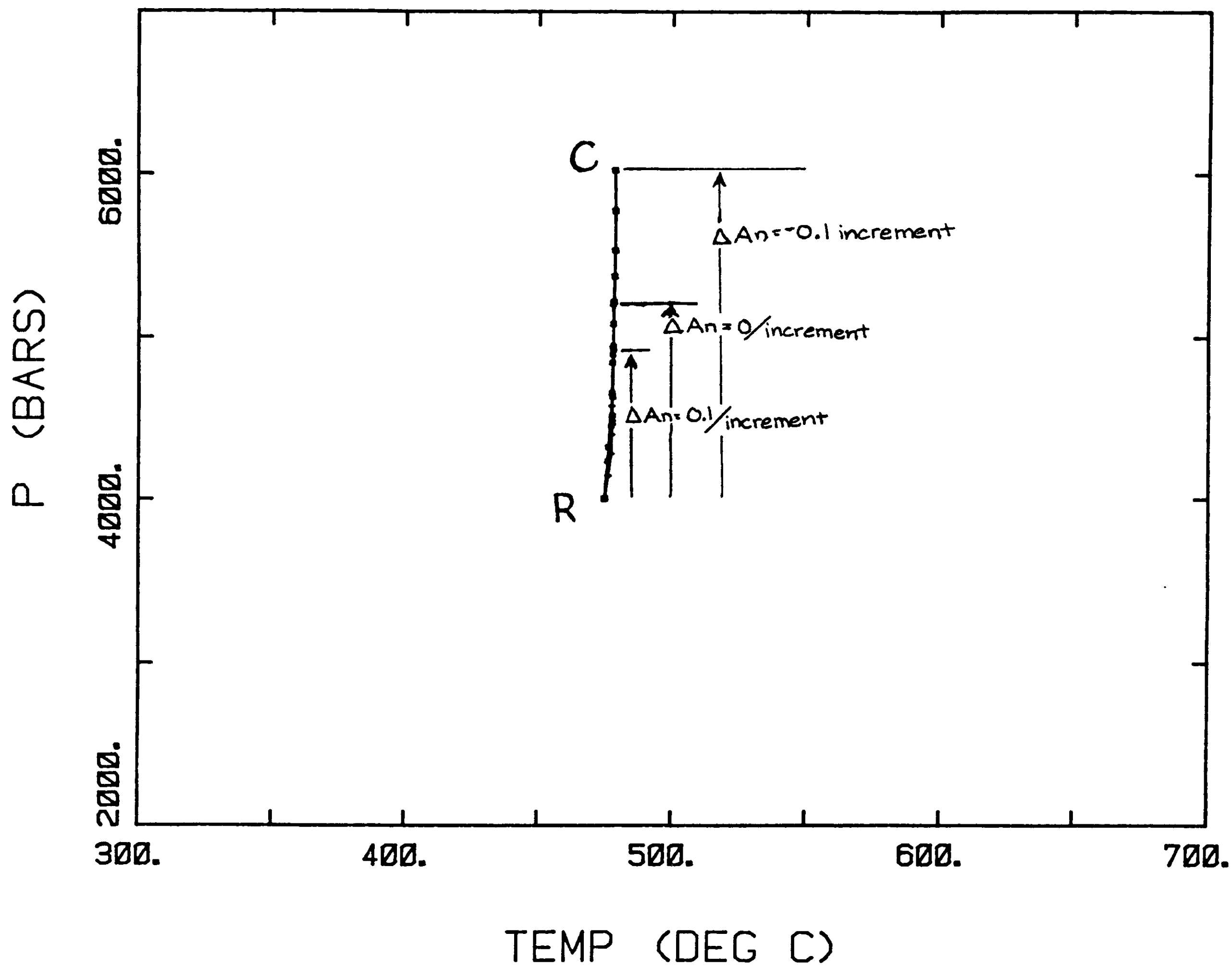

Figure 74: Northey Hill Line: Sample D84-1c; P-T paths using three different plagioclase assumptions.

Discussion

The garnet from D84-1c is rolled and has the Sunday Mountain schistosity wrapped around it. This garnet is interpreted to have formed during the dome stage deformation. Because of this, the isothermal decompression indicated by the P-T path from this sample quantitatively describes the dome stage uplft.

The P-T path from this sample also supports the interpretation presented in the geothermometry-geobarometry section that the wide range of plagioclase compositions present in this sample record different points along the P-T evolution.

Neither of the P-T paths from the Northey Hill Line garnets exhibits the near rim isobaric decrease in temperature evident in two of the other three samples. This may be due to the lower metamorphic conditions along the Northey Hill Line; the garnets in these samples may not have been able to re-equilibrate due to low temperatures.

All things considered, these garnets do not seem to present evidence for nappe stage compression evidenced in the Archertown Brook samples and the Orfordville belt farther to the west (Spear and Rumble, in press). They only seem to demonstrate dome-stage decompression.

JACOBS BROOK RECUMBANT SYNCLINE

D84-2e and D84-4k: The samples collected and analyzed from this locality had variances of four and five when water was assumed to be present. D84-2e (v=4) had no inclusions that could be used as monitor parameters. D84-4k (v=5) had a near rim inclusion of staurolite and further inclusions of margarite. It was therefore not possible to compute P-T paths for these samples.

Baker Pond--79-449f

Sample 79-449f contains a very low variance assemblage of garnet + biotite + sillimanite/kyanite + staurolite + cordierite + plagioclase + quartz. Inclusions of biotite, cordierite, and plagioclase occur near the rim of the garnet. Unfortunately, the modeling attempts for this garnet produced very unusual and geologically unreasonable results. This may be due to the fact that the garnet spans two different bulk compositions and exhibits very unusual zoning patterns. As a result, this garnet will not be discussed.

The most important P-T path information from this loclaity comes from the textural relationship of sillimanite after kyanite. When coupled with the geothermometry and geobarometry parallelograms from Chapter 7, this suggests a fairly steep slope in P-T space, as is evidenced by Figure 75. The zoning of plagioclase from the matrix (An_{13}) to the first inclusion (An_{20}) supports this morphology. This qualitative P-T path indicates a normal clockwise shape, suggesting decompression following crustal thickening (England and Richardson, 1977).

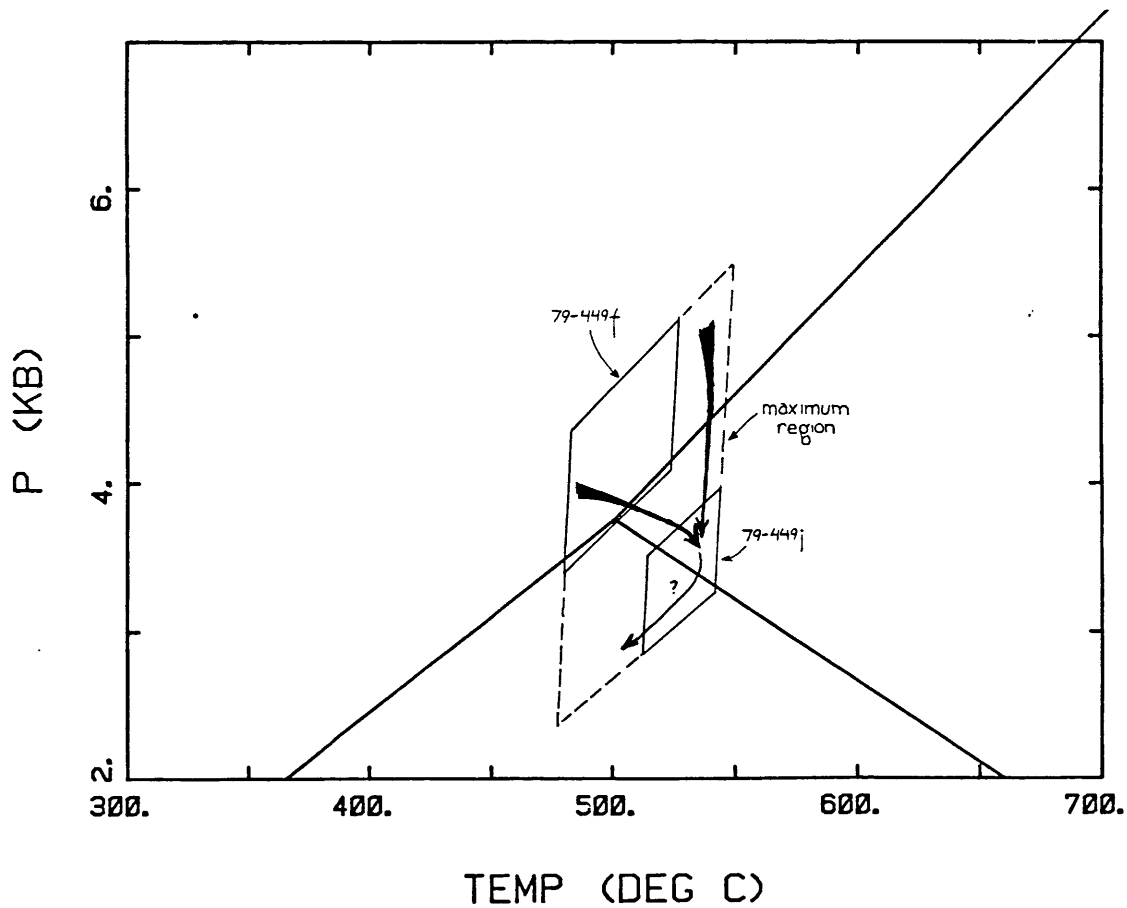

Figure 75: Baker Pond: Sample 79-449f; Qualitative P-T path from geothermometry and geobarometry calculations as well as textural relationships.

Chapter 9: DISCUSSION AND CONCLUSIONS

The relationship of P-T paths and peak meatamorphic conditions to structural and tectonic development are complex. Figure 76 contains the cross section from the study area with the locations and P-T paths of each locality sketched in.

The P-T path interpretations that will be discussed in this section are all in the framework of the studies of England and Richardson (1977), England and Thompson (1984), Thompson and England (1984), and Spear, at al. (1984).

COTTONSTONE MOUNTAIN

The P-T path from Cottonstone Mountain show an early compressional event. This part of the garnet growth is interpreted to have been in response to crustal thickening, which results in loading. The crustal thickening (which may be due to the early emplacement of nappes) is followed by uplift and erosion, causing a decrease in the overburden pressure. England and Richardson (1977) have shown that the thermal rebound is slower than the isostatic rebound, and therefore the temperature keeps increasing while the pressure is decreasing. The early decompressional event is interrupted by a nappe stage compressional event of one kilobar. The nappe stage overburden is followed by a second decompressional event, again in response to crustal thickening. The latest event seen in this sample is a near-rim cooling. The reason for this is less well constrained than the earlier interpretations, due to the fact that the features in the study area associated with this path (ie: fluid-involved metamorphism, Sunday Mountain Cleavage Belt) are not well understood tectonically. One possibility is that this locality lies in the

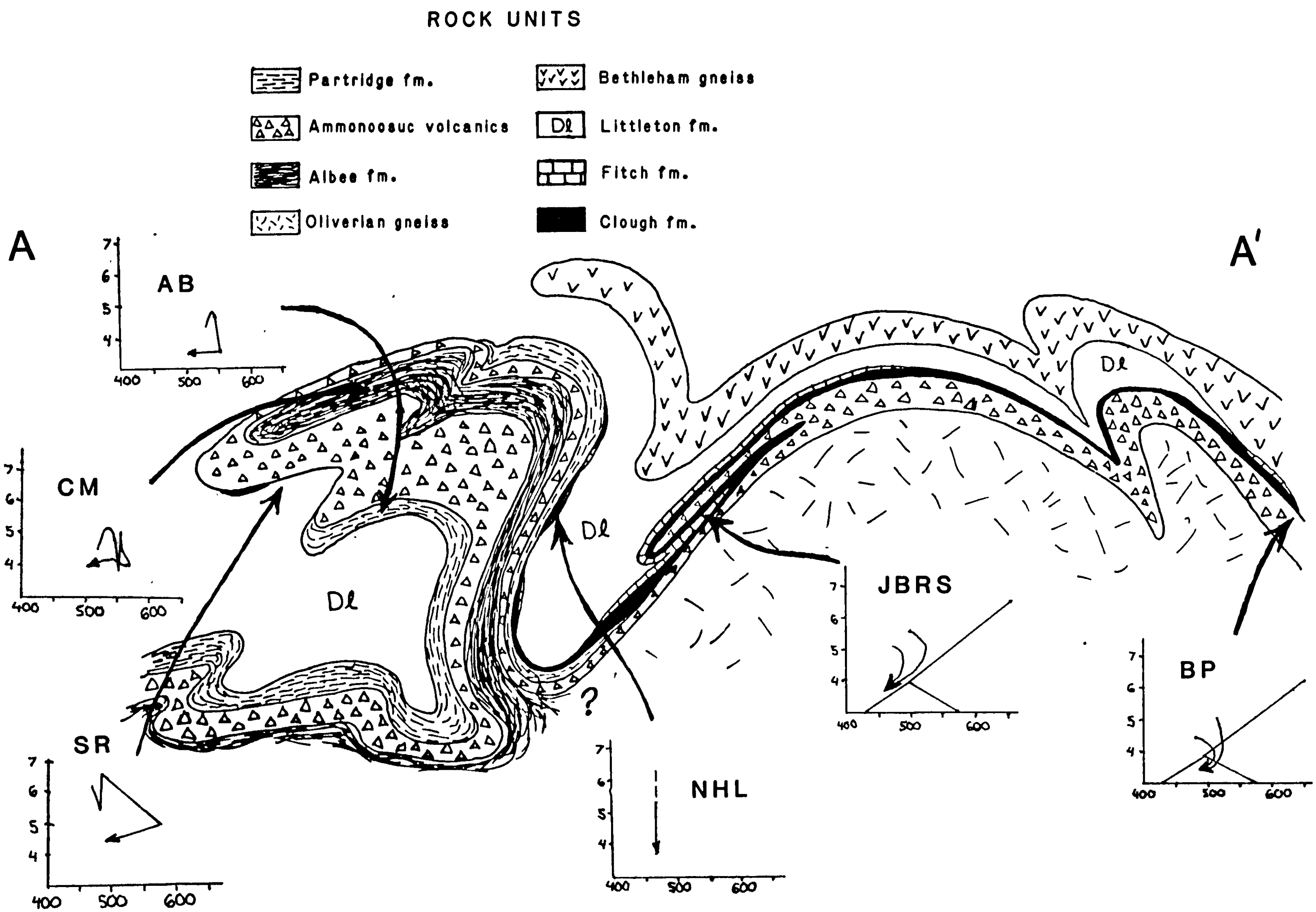

Figure 76: Cross-section of the study area (after Thompson, et al. (1968) containing structural locations of sample areas and computed P-T paths.

upper plate of a major thrust fault that places hot rocks over cold. The logical candidate in this region (although not the only one) is the Ammonoosuc Fault, since this east-dipping thrust places the garnet-grade rocks of the study area over the chlorite-grade rocks to the west. Thompson, et al. (1968), however, map this fault on strike into Mesozoic faulting in western Massachusetts. This would place the fault temporally as post-metamorphic and therefore all interpretations hinging on the Ammonoosuc Fault are problematic. Spear and Rumble (1985) suggeset an alternate possibility. They suggest that this near-rim event could be due to rapid uplift, resulting in folded isotherms. If this locality lay in the core of a thermal antiform, and the isotherms were allowed to relax with no subsequent unloading, this near rim isobaric cooling would be produced.

SPEAR AND RUMBLE (1985)

P-T paths reported from these samples are identical in shape to the path derived from the Cottonstone Mountain sample, although different in magnitude. The Spear and Rumble (1985) samples have a maximum pressure of 6 to 7 kilobars, while the Cottonstone Mountain sample has a maximum pressure of approximately 5 kilobars. This is consistent with the Spear and Rumble (1985) samples comming from the the Littleton Formation lying structurally below the Cottonstone Mountain sample, while both occur in the same overturned limb of a large nappe.

ARCHERTOWN BROOK

P-T paths from garnet zoning suggest that the Archertown Brook samples have evolved identically to those from Cottonstone Mountain. The Sunday Mounatain Cleavage Belt deformation aids in constraining the tectonic history. The isobaric cooling event, which is related to kyanite growth, occurs before or contemporaneous with the development of the Sunday Mountain Cleavage Belt.

NORTHEY HILL LINE

The Northey Hill Line samples have a P-T path that indicates growth during isothermal decompression. These garnets have textures indicative of formation during the development of the Sunday Mountain Cleavage Belt, with the possibility of some early dome stage growth. This P-T path contrasts markedly with the D3 paths from the localities to the west.

JACOBS BROOK RECUMBANT SYNCLINE

Due to the high variance assemblages, no P-T paths were determined for this locality. Aluminosilicate relationships, however, do constrain the thermal evolution somewhat. Kyanite is present in thin-section and abundant in the field, and no fibrolitic sillimanite is found. This suggests that the late-stage thermal trajectory of this locality did not intersect the sillimanite field. A possible trajectory is sketched in Figure 76.

BAKER POND

The only P-T path constraints from this locality are from the textural relations of aluminosilicate polymorphs. The presence of kyanite inclusions as well as prismatic and fibrolitic sillimanite suggest a clockwise P-T path through the kyanite and sillimanite fields. This path is constrained by the geothermometry and geobarometry discussed earlier, and is shown schematically in Figure 76.

DISCUSSION AND CONCLUSIONS

Pressure-temperature paths have been successfully determined from a variety of structural and stratigraphic units in the Mount Cube area. The relationship of tectonic processes to thermal evolution, as modeled and described by England and Richardson (1977), accurately predicts P-T path geometries, yet these models are simplistic. The interplay of tectonic forces that combine to influence the growth of a single crystal is complex. P-T paths from the study area dilineate two crustal thickening events separated by a decompressional event. The later thickening is followed by another decompression and an isobaric cooling event at the rim. These geometries correlate well with structural and field observations to show that there is evidence for regional scale structural evolution in P-T paths from zoned minerals.

In absolute terms, P-T paths from the region indicate a maximum pressure of 5 to 7 kilobars, corresponding to a maximum burial depth of 15 to 20 kilometers. If the sediment pile were initially 10 kilometers thick, this corresponds to an approximate doubling of the section during the initial crustal thickening event. The P-T paths indicate that approximately 3 kilometers of uplift followed this crustal thickening prior to the emplacement of a second nappe or nappe sequence. This one kilobar isothermal compression is the last crustal thickening event seen on the P-T path. This may correspond to the regional emplacement of the Fall Mountain nappe, which is the last known nappe emplaced in central New England (Thompson, et al., 1968).

The discrepency between the D3 P-T paths in the study area is quite puzzling. The samples collected along the Northey Hill Line, which were meatamorphosed during the deformation, record an isothermal folded by the Sunday Mountain Cleavage Belt schsitosity, and have a schistosity folded around them. These kyanites definitively overprint the dome stage fabric.

The two candidates for isobaric cooling, thrusting and folded thermal antiforms, can not accomodate for the P-T path geometry from the Northey Hill Line. One possible reason for this is that the D3 event is actually two events. The first would involve thrusting, with the Cottonstone Mountain, Archertown Brook, and Spear and Rumble (1985) localities riding in the upper plate of a thrust sheet moving over cold rocks. A possible candidate for this is the Ammonoosuc Fault, although more field work needs to be done to investigate this possibility.

The second D3 event would involve the rapid uplift of the Northey Hill Line samples. This decompression is not seen in the Archertown Brook samples, so a structural break must occur between them. Mapping along the Northey Hill Line show a massive amount of shearing, boudinage, and structural thinning of stratigraphic units. Rolled garnets (Rumble, 1969, Fig. 25) indicate an east-side up vergence. This structural evidence, coupled with the P-T path discrepency, suggests that the Northey Hill Line may be a zone of intense ductile deformation with a large normal component. In order to investigate this possiblity and constrain the structural evolution, and determine whether the D3 deformational event is one event or two, more regional mapping needs to be done along the Northey Hill Line and more samples need to be investigated for P-T paths. Detailed dating of porphyroblasts from the various localities is needed to constrain the temporal element of the metamorphic history.

REFERENCES

Albee, A.L. (1972) Metamorphism of pelitic schists: Reaction relations of chloritoid and staurolite. Geological Society of America Bulletin. v. 83, p. 3249-3268.

Billings, M.P. (1937) Regional metamorphism of the Littleton-Moosilauke area, New Hampshire, Geological Sciety of America Bulletin, 48, 463-566.

Billings, M.P. (1956) The geology of New Hampshire, part II: Bedrock Geology. New Hampshire State Planning and Development Commission, 203 p.

Chamberlain, C. P. (1981) Metamorphic zoning in south-central New Hampshire, unpub. M.A. thesis, Dartmouth College, New Hampshire.

Chamberlain, C.P., Lyons, J.B. (1982) Pressure, temperature and metamorphic zonation studies of pelitic schists in the Merrimack Synclinorum, south-central New Hampshire. Am. Min. 68:530-540.

Chatterjee, N. D., Johannes, W., and Leistner, H. (1984) The system CaO-Al2O3-SiO2-H2O: New phase equilibria data, some calculated phase relations, and their petrologic applications, Contrib. Mineral. and Petrol., 88, 1-13.

Crowley, P. D. and Hodges, K. V. (1983) Empirical calibrations of reactions in the assemblage Gt-Bio-Musc-Plag-Alsilicate-Qtz. EOS, v. 64, p. 347.

Dallmeyer, R.D. (1974) The role of crystal structure in controlling the partitioning of Mg and Fe2+ between coexisting garnet and biotite, American Mineralogist, 59, 201-203.

England, R.C. and Richardson, S.W. (1977) The influence of erosion upon the mineral facies of rocks from different metamorphic environments, Journal of the Geological Society of London, 134, 201-213.

England, P.C. and Richardson, S.W. (1980) Erosion and the age dependence of heat flow, Geophys. J. R. astr. Soc., 62, 421-437.

England, P.C., and Thompson, A.B., (1984) Pressure-temperature-time paths of regional metamorphism, Part I: Heat transfer during the evolution of regions of thickened continental crust: Journal of Petrology, submitted.

REFERENCES (cont'd)

Ferry, J.M. and Spear, F.S. (1978) Experimental califration of the partitioning of Fe and Mg between biotite and garnet, Contributions to Mineralogy and Petrology, v. 66, p. 113-117.

Frey, M. and Orville, P. M. (1974) Plagioclase in margarite-bearing rocks. Amer. J. Sci., 274, 31-47.

Ghent, E.C. (1976) Plagioclase-garnet-Al205 quartz: a potential geobarometer-geothermometer. American Mineralogist, 61, 710-714.

Ghent, E.D., Knitter, C.C., Raeside, R.P., and Stout, M.Z. (1982) Geothermometry and geobarometry of pelitic rocks, upper kyanite and sillimanite zones, Mica Creek area, British Colombia. Canadian Mineralogist, 20, 295-305.

Ghent, E.D. and Stout, M.Z. (1981) Geobarometry and geothermometry of plagioclase-biotite-garnet-muscovite assemblages. Contributions to Mineralogy and Petrology, v. 76,p. 92-97.

Grove, T.L., Baker, M.B., and Kinzler, R.J. (1984) Coupled CaAl-NaSi diffusion in plagioclase feldspar: Experiments and applications to cooling rate speedometry. Geochem. et Cosmo. Acta, v. 48, 2113-2121.

Hadley, J.B. (1938) Geologic map of the Mt. Cube quadrangle, New Hampshire, State of New Hampshire Highway Dept., Concord, N.H.

Hadley, J.B. (1942) Stratigraphy, structure and petrology of the Mt. Cube area, New Hampshire. G.S.A. Bull., 53,113-176.

Helgeson, H. C., Delany, J. M., Nesbitt H. W., and Bird, D. K. (1978) Summary and critique of the thermodynamic properties of rock-forming minerals. American Journal of Science, v. 278A, p. 1-299.

Hickmott, D.L. (1982) The mineralogy of the Betts Mine Area, Plainfield, Massachusetts. unpub. B.A. thesis, Amherst College, Mass.

Hodges, K.V. (1982) The tectonic evolution of the Aefjord-Sitas area, Norway-Sweden. unpub. P.H.D. thesis M.I.T. 192p.

Hodges, K.V. and Crowley, P.D. (1985) Error estimation and empirical geothermometry and geobarometry for pelitic systems. Amer. Mineral., in press.

REFERENCES (cont'd.)

Hodges, K.V. and Spear, F.S. (1982) Geothermometry, geobarometry, garnet closure temperatures and the Al2SiO5 triple point, Mt. Moosilauke, New Hampshire. Trans. Amer. Geophys. Union, 62, 1060.

Hodges, K. V. and Spear, F. S. (1982) Geothermometry, geobarometry and the Al2SiO5 triple point at Mt. Moosilauke, New Hampshire. American Mineralogist, v. 67, p. 1118-1134.

Holdaway, M.J. (1971) Stability of andalusite and the aluminum silicate phase diagram: American Journal of Science, V. 271, p. 97-131.

Malinconico, M.L. (1982) The stratigraphy and structure of the southeastern Rumney 15 minute quadrangle, New Hampshire. unpub. M.A. thesis, Dartmouth College, New Hampshire.

Naylor, R.S. (1968) Origin and regional relationships of the core rocks of the Oliverian domes. In E-an Zen, et al., eds., Studies of Appalacian Geology, Northern and Maritime, p. 231-240. John Wiley, New York.

Newton, R.C. and Haselton, H.T. (1981) Thermodynamics of the garnet-plagioclase-Al2SiO5-quartz geobarometer. In R.C. Newton, et al. Eds., Thermodynamics of Minerals and Melts, p. 131-147, Springer-Verlag, New York.

Robinson, P., and Hall L. (1979) Tectonic synthesis of southern New England in Wones D. ed. The Caledonides in the U.S.A.: Blacksburg, VA., Virginia Polytechnic Institute. p.73-82.

Robinson, P. , Thompson, J.B. Jr., and Rosenfeld, J.L. (1979) Nappes, gneiss domes, and regional metamorphism in western New Hampshire and central Massachusetts, in Skehan, J.W. and Osberg, P.H. eds., The Caledonides in the USA: Geologic excursions in the northeastern Appalacians, Weston Observatory, Department of Geology and Geophysics, Boston College, Mass., p. 93-175

Rumble, D. III (1969) Stratigraphic, structural and petrologic studies in the Mt. Cube area, New Hampshire. Ph.D Dissertation, Harvard University.

Rumble, D., III (1973) Andalusite, kyanite, and sillimanite from the Mount Moosilauke region, New Hampshire. Geological Society of American Bulletin, 84, 2423-2430.

Selverstone, J., Spear, F. S., Franz, G., and Morteani, G. (1984) High pressure metamorphism in the SW Tauern window, Austria: P-T paths from hornblende-kyanite-staurolite schists. Journal of Petrology, v. 25, p. 501-531.

REFERENCES (cont'd.)

Spear, F.S. (1980) Plotting steroscopic phase diagrams. American Mineralogist, 65, 1291-1293.

Spear, F. S., Ferry, J. M. and Rumble, D. (1982) Analytical formulation of phase equilibria: The Gibbs method. in: J. M. Ferry, ed. Characterization of Metamorphism through Mineral Equilibria. Mineralogical Society of America Reviews in Mineralogy, v. 10, p. 105-152.

Spear, F.S., Hickmott, D.D., Selverstone, J. (1983) Petrologic evidence for a metamorphic discontinuity- Bellows Falls area, New Hampshire and Vermont. EOS (A.G.U Transactions) 64:878.

Spear, F.S. and Rumble, D. III (1985) Pressure, temperature and structural evolution of the Orfordville Belt, west-central New Hampshire, in preparation.

Spear, F. S. and Selverstone, J. (1983) Quantitative P-T paths from zoned minerals: Theory and tectonic applications. Contributions to Mineralogy and Petrology, v. 83, p. 348-357.

Spear, F. S., Selverstone, J., Hickmott, D., Crowley, P., and Hodges, K. V. (1984) P-T paths from garnet zoning: A new technique for deciphering tectonic processes in crystalline terranes. Geology, v. 12, p. 87-90.

Thompson, A.B., Tracy, R.J., Lyttle, P., and Thompson, J.B., (1977) Prograde reaction histories deduced from compositional zonation and mineral inclusions in garnet from the Gassetts schist, Vermont: American Journal of Science, v. 277, p. 1152-1167.

Thompson, A.B. (1981), The pressure-temperature (P,T) plane viewed by geophysicists and petrologists: Terra Cognita, V. 1, p. 1-20.

Thompson, A.B. and England, P., (1984) Pressure-temperature-time paths of regional metamorphism of the continental crust, II: Some petrological constraints from ineral assemblages in metamorphic rocks: submitted, Journal of Petrology.

Thompson, J.B. Jr. (1956) Skitchewaug Nappe, a major recumbant fold in the area near Claremont, New Hampshire. G.S.A. Bull., v. 67, p. 1826 (abs.)

Thompson, J.B. Jr. (1957) Graphical analysis fo mineral assemblages in pelitic schists. Amer. Mineralogist, 42, 842-858.

REFERENCES (cont'd.)

Thompson, J.B., Jr., and Norton, S.A. (1968) Paleozoic regional metamorphism in New England and adjacent areas. In E-an Zen et al., Eds., Studies of Appalachian Geology, Northern and Maritime p. 319-327. John Wiley, New York.

Thompson, J. B. Jr., Robinson, P., Clifford, T. N., and Trask, N. J. (1968) Nappes and gneiss domes in west-central New England. In E-an Zen et al., Eds., Studies of Appalachian Geology, Northern and Maritime, p. 203-218. John Wiley, New York.

Tracy, R.J., Robinson, P., and Thompson, A.B. (1976) Garnet composition and zoning in the determination of temperature and pressure of metamorphism, central Massachusetts: American Mineralogist, v. 61, p. 762-775.

Tracy, R.J. and Robinson, P. (1980) Evolution of metamorphic belts: Information from detailed petrologic studies, in Wones, D., ed., The Caledonides in the USA: Virginia Polytechnic University Geology Department Memoir, v. 2, p. 189-195.

Yardley, B.W.D. (1977) An empirical study of diffusion in garnet. Amer. Min., 62, p. 793-800.

Appendix 1: Estimated modal abundances, Cottonstone Mountain, Albee Formation

	67-82e
Quartz	10
Plagioclase	10
Muscovite	35
Biotite	5
Garnet	20
Staurolite	5
Kyanite	15
Opaques (undiff)	tr.

Appendix 2: Estimated modal abundances, Archertown Brook, Partridge Formation

	D84-3a	D84-3b	D84-3c	D84-3d	D84-3e	D84-3g	D84-3h	D84-3i
Quartz	72	35	55	45	40	29	39	50
Plagioclase	2	2		3	2	1		3
Muscovite	3	30	20	25	30	40	35	10
Biotite	10	15	15	10	10	10	5	15
Chlorite	1	2	2		1	5	5	
Garnet	7	5	5	5	3	3	5	7
Staurolite		2	2	7	7		tr.	
Kyanite				3				
Graphite		5			5	7		20
Tourmaline		1					tr.	tr.
Opaques (undiff)	5	3	1	2	2	5	10	5
Carbonate							1	

Appendix 2: Estimated modal abundances, Archertown Brook, Partridge Formation (cont'd.)

	D84-3j	PM-9b	PM-11c	67-78a
Quartz	38	33	43	30
Plagioclase	3	2		1
Muscovite	30	35	25	25
Biotite	15	20	20	50
Chlorite		2	7	10
Garnet	7	5	15	7
Staurolite				7
Kyanite				
Graphite		8		10
Tourmaline				
Opaques (undiff)	7	5	tr.	5
Carbonate				
Apatite	tr.			

Appendix 3: Estimated modal abundances, Northey Hill Line, Partridge and Littleton Formations

	D84-1c	D84-1d	D84-1e	D84-6a	D84-6b
Quartz	48	35	34	55	34
Plagioclase	2	2	10	2	1
Muscovite	30	5	40	25	35
Biotite	15	10			
Chlorite	2	5	2	2	
Garnet	2	10	1	3	10
Chloritoid		3	tr.	3	
Graphite		28	10	7	15
Tourmaline				tr.	tr.
Opaques (undiff)	1	2	5	3	5

Appendix 4: Estimated modal abundances, Jacobs Brook Recumbant Syncline
Clough Formation

	D84-2a	D84-2b	D84-2c	D84-2d	D84-2e	D84-4d (catacule)	D84-4f	D84-4g
Quartz	80	80	23	68	50	24	52	60
Plagioclase			tr.	2		14	2	2
Muscovite	10	15	30	15	20	5	25	20
Biotite			10	2	5	15	15	15
Chlorite			tr.	2	2	5		
Garnet			35	5	10	35	1	3
Staurolite				5	10			
Kyanite		1						
Tourmaline	3	1						
Opaques (undiff)	7	3	2	1	3	2	5	tr.

Appendix 4: Estimated modal abundances, Jacobs Brook Recumbant Syncline
Clough Formation (cont'd.)

	D84-4i	D84-4j	D84-4k	D84-4l	D84-4m	D84-4n	D84-4o
Quartz	26	50	47	51	54	65	85
Plagioclase	25	1				tr.	1
Muscovite	20	25	18	20	25	20	7
Biotite	7	10	12	1	5	10	3
Chlorite		1	1	2	1		
Garnet	10	10	15	15	10	5	3
Staurolite	5	2	5	10	5		
Kyanite							
Tourmaline				tr.			
Opaques (undiff)	7	1	2	1	tr.	tr.	1

Appendix 5: Estimated modal abundances, Baker Pond, Ammonoosuc Volcanics.

	79-449f	79-449g	79-449h	79-449i	79-449j	79-449k
Quartz	55	35	49	54	50	46
Plagioclase	tr.	5			2	
Muscovite						
Biotite	10	5	10	15	10	20
Chlorite		2	3	2		3
Garnet	5	20		3	10	
Staurolite	5		3	3	3	3
Kyanite	3	5	tr.			
Sillimanite	1	5	15	3	5	3
Cordierite	20	23	20	20	20	25
Opaques (undiff)	1		tr.	tr.		tr.

Appendix 6: Cottonstone Mountain: Microprobe Analyses; Sample 67-82e

--------------------GARNET RIM ANALYSES--------------------

	6782E 1/12 GAR A	6782E 1/14 GAR R	6782E 1/58 GAR R	6782E 1/61 GAR R	6782E 1/71 GAR R	6782E 1/80 GAR R	6782E 1/142 GAR R	6782E 1/145 GAR R
SiO2	37.67	37.83	37.69	37.47	37.80	37.75	37.73	37.91
Al2O3	21.30	21.39	21.32	21.19	21.37	21.35	21.34	21.44
MgO	2.88	2.64	2.63	2.46	2.56	2.63	2.66	2.67
FeO	36.22	35.96	35.79	35.97	36.11	36.02	36.23	36.35
MnO	1.73	1.74	1.60	1.64	1.61	1.65	1.74	1.75
CaO	1.44	2.08	2.25	2.13	2.22	2.08	1.83	1.84
Total	101.25	101.65	101.28	100.86	101.67	101.49	101.52	101.95
Si	3.000	3.000	3.000	3.000	3.000	3.000	3.000	3.000
Al	2.000	2.000	2.000	2.000	2.000	2.000	2.000	2.000
Mg	0.342	0.312	0.312	0.294	0.303	0.312	0.315	0.315
Fe2+	2.412	2.385	2.382	2.409	2.397	2.394	2.409	2.406
Mn	0.117	0.117	0.108	0.111	0.108	0.111	0.117	0.117
Ca	0.123	0.177	0.192	0.183	0.189	0.177	0.156	0.156
Fe/Fe+Mg	0.876	0.884	0.884	0.891	0.888	0.885	0.884	0.884
Pyrope	0.114	0.104	0.104	0.098	0.101	0.104	0.105	0.105
Alman	0.806	0.797	0.796	0.804	0.800	0.800	0.804	0.804
Spess	0.039	0.039	0.036	0.037	0.036	0.037	0.039	0.039
Gross	0.041	0.059	0.064	0.061	0.063	0.059	0.052	0.052

------------GARNET RIM AT BIOTITE------------

	6782E 1/123 GAR@B	6782E 1/124 GAR@B	6782E 1/125 GAR@B	6782E 1/126 GAR@B	6782E 1/127 GAR@B	6782E 1/128 GAR@B
SiO2	37.81	37.77	37.71	37.74	37.66	38.01
Al2O3	21.38	21.36	21.33	21.34	21.29	21.49
MgO	2.89	2.89	2.86	2.71	2.45	2.73
FeO	35.26	35.63	35.90	36.15	36.20	36.81
MnO	2.37	2.18	2.00	1.83	1.87	1.75
CaO	1.80	1.62	1.55	1.73	1.93	1.49
Total	101.50	101.45	101.35	101.49	101.40	102.28
Si	3.000	3.000	3.000	3.000	3.000	3.000
Al	2.000	2.000	2.000	2.000	2.000	2.000
Mg	0.342	0.342	0.339	0.321	0.291	0.321
Fe2+	2.340	2.367	2.388	2.403	2.412	2.430
Mn	0.159	0.147	0.135	0.123	0.126	0.117
Ca	0.153	0.138	0.132	0.147	0.165	0.126
Fe/Fe+Mg	0.872	0.874	0.876	0.882	0.892	0.883
Pyrope	0.114	0.114	0.113	0.107	0.097	0.107
Alman	0.782	0.791	0.798	0.803	0.806	0.812
Spess	0.053	0.049	0.045	0.041	0.042	0.039
Gross	0.051	0.046	0.044	0.049	0.055	0.042

Appendix 6: Cottonstone Mountain: Sample 67-82e (cont.)

	----MATRIX BIOTITE---			--BIO AT GARNET RIM--			------BIOTITE INCLUSION------			
	6782E 3/1B MXBIO	6782E 3/1C MXBIO	6782E 3/1D MXBIO	6782E 1/1A BIO @	6782E 1/1B BIO @	6782E 1/1AV BIO @	6782E 1/2A BIO I	6782E 1/2B BIO I	6782E 1/2C BIO I	6782E 1/2D BIO I
SiO2	35.88	35.85	36.10	36.02	36.41	36.22	36.32	36.14	35.87	36.22
Al2O3	19.63	19.62	19.59	19.61	19.60	19.60	19.53	19.22	19.22	19.48
TiO2	1.59	1.49	1.57	1.41	1.41	1.42	1.39	1.42	1.46	1.59
MgO	10.78	10.73	10.85	10.52	10.56	10.54	10.53	10.50	10.11	10.48
FeO	20.41	19.49	19.83	19.72	19.57	19.64	18.95	19.52	19.47	19.09
MnO	0.00	0.01	0.00	0.00	0.08	0.02	0.04	0.08	0.07	0.05
CaO	0.00	0.00	0.00	0.00	0.00	0.00	0.00	0.01	0.00	0.00
Na2O	0.28	0.27	0.23	0.41	0.23	0.32	0.45	0.49	0.26	0.27
K2O	8.39	8.46	8.22	8.56	8.59	8.57	8.19	8.12	8.15	8.51
Total	96.96	95.93	96.38	96.26	96.44	96.34	95.40	95.50	94.61	95.69
Si	5.347	5.379	5.387	5.395	5.431	5.414	5.453	5.441	5.449	5.435
Aliv	2.653	2.621	2.613	2.605	2.569	2.586	2.547	2.559	2.551	2.565
Alvi	0.796	0.849	0.833	0.857	0.877	0.868	0.910	0.853	0.892	0.880
Ti	0.180	0.170	0.178	0.161	0.160	0.161	0.159	0.162	0.169	0.181
Mg	2.393	2.400	2.412	2.348	2.347	2.348	2.357	2.356	2.290	2.343
Fe2+	2.543	2.446	2.474	2.470	2.441	2.455	2.379	2.458	2.474	2.396
Mn	0.000	0.001	0.000	0.000	0.010	0.003	0.005	0.010	0.009	0.006
Sum Oct	5.912	5.866	5.897	5.836	5.835	5.835	5.810	5.839	5.834	5.806
Ca	0.000	0.000	0.000	0.000	0.000	0.000	0.000	0.002	0.000	0.000
Na	0.081	0.079	0.066	0.119	0.066	0.093	0.130	0.142	0.076	0.080
K	1.595	1.620	1.564	1.636	1.635	1.635	1.568	1.559	1.579	1.628
Sum A	1.676	1.699	1.630	1.755	1.701	1.728	1.698	1.703	1.655	1.708
(OH)	0.000	0.000	0.000	0.000	0.000	0.000	0.000	0.000	0.000	0.000
Fe/Fe+Mg	0.515	0.505	0.506	0.513	0.510	0.511	0.502	0.511	0.519	0.506
X(Ca)	0.000	0.000	0.000	0.000	0.000	0.000	0.000	0.001	0.000	0.000
X(Na)	0.048	0.046	0.040	0.068	0.039	0.054	0.077	0.083	0.046	0.047
X(K)	0.952	0.954	0.960	0.932	0.961	0.946	0.923	0.915	0.954	0.953

Appendix 6: Sample 67-82e (cont.)

	BIO INCL (AVG) 6782E 1/2AV BIO I	-------MATRIX MUSCOVITE------ 6782E 3/4A MX MU	6782E 3/4B MX MU	6782E 3/4C MX MU	6782E 3/4AV MX MU
SiO2	36.13	45.75	46.69	46.60	46.35
Al2O3	19.36	35.72	36.06	35.83	35.87
TiO2	1.47	0.55	0.36	0.38	0.43
MgO	10.41	0.63	0.63	0.66	0.64
FeO	19.26	1.16	1.25	1.35	1.25
MnO	0.06	0.00	0.00	0.00	0.00
CaO	0.00	0.00	0.01	0.00	0.00
Na2O	0.37	1.38	1.23	1.27	1.29
K2O	8.24	9.13	8.88	8.87	8.96
Total	95.30	94.32	95.11	94.95	94.79
Si	5.444	6.116	6.168	6.171	6.152
Aliv	2.556	1.884	1.832	1.829	1.848
Alvi	0.883	3.746	3.784	3.764	3.765
Ti	0.168	0.056	0.036	0.038	0.043
Mg	2.337	0.125	0.124	0.131	0.127
Fe2+	2.427	0.130	0.138	0.149	0.139
Mn	0.008	0.000	0.000	0.000	0.000
Sum Oct	5.823	4.057	4.082	4.082	4.074
Ca	0.000	0.000	0.001	0.000	0.000
Na	0.107	0.357	0.315	0.325	0.332
K	1.583	1.558	1.496	1.498	1.517
Sum A	1.690	1.915	1.812	1.823	1.849
(OH)	0.000	0.000	0.000	0.000	0.000
Fe/Fe+Mg	0.509	0.510	0.527	0.532	0.523
X(Ca)	0.000	0.000	0.001	0.000	0.000
X(Na)	0.063	0.186	0.174	0.178	0.180
X(K)	0.937	0.814	0.826	0.822	0.820

Appendix 6: Sample 67-82e (cont.)

	---MATRIX PLAGIOCLASE---								
			(--------RIM--------)			(AVG)	(----RIM----)		(CORE)
	6782E 3/2A MX PL	6782E 3/2B MX PL	6782E 3/2C PL RI	6782E 3/2D PL RI	6782E 3/2E PL RI	6782E 3/2AV MX PL	6782E 3/3A PL RI	6782E 3/3B PL RI	6782E 3/3C PL CO
SiO2	61.85	62.45	62.92	62.86	63.10	62.62	63.43	63.42	62.98
Al2O3	24.69	24.14	24.01	23.43	23.61	23.98	23.57	23.46	23.67
FeO	0.00	0.00	0.14	0.05	0.11	0.05	0.25	0.00	0.03
CaO	6.26	6.03	5.38	5.30	5.21	5.64	5.13	4.77	5.25
Na2O	8.81	8.88	8.97	8.95	8.95	8.91	9.24	9.32	8.84
K2O	0.07	0.07	0.07	0.11	0.07	0.09	0.07	0.11	0.05
Total	101.68	101.58	101.49	100.71	101.05	101.30	101.69	101.08	100.81
Si	2.709	2.734	2.752	2.776	2.768	2.746	2.769	2.779	2.767
Al	1.275	1.246	1.238	1.220	1.221	1.240	1.213	1.212	1.226
Fe2+	0.000	0.000	0.005	0.002	0.004	0.002	0.009	0.000	0.001
Ca	0.294	0.283	0.252	0.251	0.245	0.265	0.240	0.224	0.247
Na	0.748	0.754	0.761	0.766	0.761	0.758	0.782	0.792	0.753
K	0.004	0.004	0.004	0.006	0.004	0.005	0.004	0.006	0.003
Ca/Ca+Na	0.282	0.273	0.249	0.247	0.244	0.259	0.235	0.220	0.247
Al*/SiAl	0.279	0.251	0.240	0.221	0.223	0.243	0.217	0.214	0.228
An	0.281	0.272	0.248	0.245	0.243	0.258	0.234	0.219	0.246
Ab	0.715	0.724	0.748	0.749	0.753	0.737	0.762	0.775	0.751
Or	0.004	0.004	0.004	0.006	0.004	0.005	0.004	0.006	0.003

	(CORE)	(RIM?)	(----RIM----)			(RIM?)	(RIM)
	6782E 1/14A MX P	6782E 1/14B MX PL	6782E 1/14C PL RI	6782E 1/14D PL RI	6782E 1/14E PLAG	6782E 1/14F PL RI	6782E 1/14G PL RI
SiO2	61.29	67.16	61.45	61.82	62.49	61.31	62.15
Al2O3	23.95	19.91	23.92	23.90	23.40	24.13	23.28
FeO	0.05	0.08	0.11	0.11	0.05	0.05	0.05
CaO	4.98	0.30	4.89	4.78	4.28	4.63	4.53
Na2O	8.57	10.95	8.76	8.87	9.13	8.85	8.96
K2O	0.07	0.90	0.07	0.09	0.07	0.07	0.07
Total	98.92	99.30	99.20	99.56	99.42	99.05	99.05
Si	2.744	2.967	2.745	2.751	2.779	2.741	2.776
Al	1.264	1.037	1.260	1.254	1.227	1.272	1.226
Fe2+	0.002	0.003	0.004	0.004	0.002	0.002	0.002
Ca	0.239	0.014	0.234	0.228	0.204	0.222	0.217
Na	0.744	0.938	0.759	0.765	0.787	0.767	0.776
K	0.004	0.051	0.004	0.005	0.004	0.004	0.004
Ca/Ca+Na	0.243	0.015	0.236	0.230	0.206	0.224	0.219
Al*/SiAl	0.262	0.037	0.259	0.253	0.226	0.269	0.226
An	0.242	0.014	0.235	0.228	0.205	0.224	0.218
Ab	0.754	0.935	0.761	0.767	0.791	0.772	0.778
Or	0.004	0.051	0.004	0.005	0.004	0.004	0.004

Appendix 6: Sample 67-82e (cont.)

	------MATRIX	STAUROLITE------		
	(AT GAR RIM)	(CORE)	(RIM)	(AVG)
	6782E 1/3A ST@GA	6782E 1/3B ST CO	6782E 1/3C ST RI	6782E 1/3AV STAU
SiO2	28.38	27.70	28.24	28.11
Al2O3	55.63	55.15	55.50	55.43
TiO2	0.59	0.62	0.95	0.72
MgO	1.40	1.62	1.33	1.45
FeO	12.80	13.46	12.53	12.93
MnO	0.14	0.08	0.11	0.11
ZnO	0.76	0.69	0.92	0.79
CaO	0.00	0.00	0.00	0.00
Total	99.71	99.32	99.58	99.54
Si	3.851	3.790	3.837	3.826
Al	8.898	8.895	8.889	8.894
Ti	0.061	0.064	0.098	0.074
Mg	0.284	0.330	0.269	0.294
Fe2+	1.453	1.540	1.424	1.472
Mn	0.016	0.009	0.013	0.013
Zn	0.076	0.070	0.092	0.079
Ca	0.000	0.000	0.000	0.000
Fe/Fe+Mg	0.836	0.824	0.841	0.834

Appendix 6: Sample 67-82e (cont.)

	-----------PLAGIOCLASE INCLUSION IN GARNET-----------						
	(CORE)	(----RIM----)		(1/2 WAY)	(RIM)		(RIM)
	6782E 1/4A PL IN	6782E 1/4B PL IN	6782E 1/4D PL IN	6782E 1/4E PL IN	6782E 1/4F PL IN	6782E 1/4G PL IN	6782E 1/4H PL IN
SiO2	66.86	65.85	63.86	66.33	64.34	64.11	65.09
Al2O3	21.37	20.42	20.99	20.40	21.14	21.38	20.04
FeO	0.47	0.76	0.98	0.57	0.56	0.54	1.04
CaO	1.86	1.14	1.80	1.10	1.92	2.32	1.10
Na2O	9.56	11.10	10.03	11.21	10.42	10.49	10.91
K2O	0.07	0.05	0.07	0.05	0.05	0.05	0.03
Total	100.19	99.31	97.73	99.67	98.43	98.89	98.22
Si	2.919	2.919	2.880	2.926	2.879	2.862	2.920
Al	1.100	1.067	1.116	1.061	1.115	1.125	1.060
Fe2+	0.017	0.028	0.037	0.021	0.021	0.020	0.039
Ca	0.087	0.054	0.087	0.052	0.092	0.111	0.053
Na	0.809	0.954	0.877	0.959	0.904	0.908	0.949
K	0.004	0.003	0.004	0.003	0.003	0.003	0.002
Ca/Ca+Na	0.097	0.054	0.090	0.051	0.092	0.109	0.053
Al*/SiAl	0.098	0.068	0.116	0.062	0.116	0.127	0.061
An	0.097	0.053	0.090	0.051	0.092	0.109	0.053
Ab	0.899	0.944	0.906	0.946	0.905	0.888	0.945
Or	0.004	0.003	0.004	0.003	0.003	0.003	0.002

	(CORE)	(RIM)	(CORE)	(--------RIM--------)			(CORE)
	6782E 1/5A PL IN	6782E 1/5B PL IN	6782E 1/5C PL IN	6782E 1/5E PL IN	6782E 1/6B PL IN	6782E 1/6D PL IN	6782E 1/6E PL IN
SiO2	63.49	64.87	62.73	66.13	53.77	51.24	52.30
Al2O3	22.02	21.49	23.33	21.46	29.16	26.92	29.81
FeO	0.43	0.68	0.30	0.74	0.74	1.70	0.81
CaO	2.93	2.55	4.15	1.88	11.09	10.03	11.76
Na2O	9.99	10.15	9.20	10.78	5.15	5.13	4.75
K2O	0.07	0.05	0.07	0.07	0.05	0.03	0.05
Total	98.92	99.79	99.77	101.07	99.96	95.05	99.48
Si	2.835	2.868	2.782	2.885	2.435	2.451	2.387
Al	1.159	1.120	1.220	1.104	1.557	1.518	1.604
Fe2+	0.016	0.025	0.011	0.027	0.028	0.068	0.031
Ca	0.140	0.121	0.197	0.088	0.538	0.514	0.575
Na	0.865	0.870	0.791	0.912	0.452	0.476	0.420
K	0.004	0.003	0.004	0.004	0.003	0.002	0.003
Ca/Ca+Na	0.139	0.122	0.199	0.088	0.543	0.519	0.578
Al*/SiAl	0.160	0.121	0.220	0.105	0.561	0.535	0.609
An	0.139	0.122	0.199	0.088	0.542	0.518	0.576
Ab	0.857	0.875	0.797	0.908	0.455	0.480	0.421
Or	0.004	0.003	0.004	0.004	0.003	0.002	0.003

Appendix 6: Sample 67-82e (cont.)

	--------PLAGIOCASE	INCLUSION	IN GARNET--------			
	(CORE)	(----RIM	----)	(CORE)	(----RIM----)	
	6782E 1/7A PL IN	6782E 1/7B PL IN	6782E 1/8B PL IN	6782E 1/9A PL IN	6782E 1/9B PL IN	6782E 1/9C PL IN
SiO2	52.09	53.42	60.05	53.29	53.39	54.59
Al2O3	29.79	29.31	24.45	27.39	27.50	27.97
FeO	0.57	0.92	0.83	0.80	0.85	1.45
CaO	11.81	11.23	5.74	9.89	10.31	9.68
Na2O	4.57	4.99	8.20	5.82	5.57	5.78
K2O	0.03	0.03	0.07	0.05	0.12	0.03
Total	98.87	99.91	99.34	97.23	97.74	99.51
Si	2.388	2.423	2.696	2.479	2.474	2.483
Al	1.610	1.567	1.294	1.502	1.502	1.500
Fe2+	0.022	0.035	0.031	0.031	0.033	0.055
Ca	0.580	0.546	0.276	0.493	0.512	0.472
Na	0.406	0.439	0.714	0.525	0.500	0.510
K	0.002	0.002	0.004	0.003	0.007	0.002
Ca/Ca+Na	0.588	0.554	0.279	0.484	0.506	0.481
Al*/SiAl	0.611	0.573	0.297	0.512	0.514	0.509
An	0.587	0.553	0.278	0.483	0.502	0.480
Ab	0.411	0.445	0.718	0.514	0.491	0.518
Or	0.002	0.002	0.004	0.003	0.007	0.002

Appendix 6: Sample 67-82e (cont.)

	---------PLAGIOCLASE	INCLUSION IN KYANITE	------------				
		(RIM?)					(AVG)
	6782E 2/1A PL:KY	6782E 2/1B PL:KY	6782E 2/1C PL:KY	6782E 2/1D PL:KY	6782E 2/1E PL:KY	6782E 2/2F PL:KY	6782E 2/1AV PL:KY
SiO2	62.48	62.36	62.09	61.41	62.15	63.63	62.36
Al2O3	23.74	23.69	24.43	24.45	24.42	23.61	24.06
FeO	0.03	0.05	0.11	0.08	0.08	0.03	0.05
CaO	4.63	4.40	4.70	5.43	5.92	4.91	5.00
Na2O	9.62	9.27	9.04	8.85	8.82	9.03	9.10
K2O	0.07	0.05	0.23	0.11	0.07	0.07	0.11
Total	100.57	99.82	100.60	100.33	101.46	101.28	100.68
Si	2.757	2.766	2.738	2.721	2.725	2.780	2.748
Al	1.235	1.239	1.270	1.277	1.262	1.216	1.250
Fe2+	0.001	0.002	0.004	0.003	0.003	0.001	0.002
Ca	0.219	0.209	0.222	0.258	0.278	0.230	0.236
Na	0.823	0.797	0.773	0.760	0.750	0.765	0.778
K	0.004	0.003	0.013	0.006	0.004	0.004	0.006
Ca/Ca+Na	0.210	0.208	0.223	0.253	0.270	0.231	0.233
Al*/SiAl	0.237	0.238	0.268	0.278	0.265	0.217	0.251
An	0.209	0.207	0.220	0.252	0.269	0.230	0.231
Ab	0.787	0.790	0.767	0.742	0.727	0.766	0.763
Or	0.004	0.003	0.013	0.006	0.004	0.004	0.006

	-----------PLAGIOCLASE			INCLUSIONS------------		
	IN KYANITE		IN STAU	AT STAU RIM	IN KYANITE	
						(RIM)
	6782E 1/15A PL IN	6782E 1/15B PL IN	6782E 1/16A PL IN	6782E 1/17A PL@ST	6782E 1/18A PL IN	6782E 1/18B PL IN
SiO2	61.04	61.91	61.59	61.35	61.12	60.70
Al2O3	24.07	23.46	24.05	23.91	23.66	23.74
FeO	0.19	0.40	0.38	0.27	0.05	0.08
CaO	5.13	4.66	4.98	4.95	4.83	4.70
Na2O	8.63	8.89	8.88	8.62	8.71	8.46
K2O	0.09	0.07	0.05	0.07	0.05	0.21
Total	99.14	99.40	99.93	99.16	98.43	97.88
Si	2.732	2.762	2.737	2.743	2.750	2.746
Al	1.270	1.234	1.260	1.260	1.255	1.266
Fe2+	0.007	0.015	0.014	0.010	0.002	0.003
Ca	0.246	0.223	0.237	0.237	0.233	0.228
Na	0.749	0.769	0.765	0.747	0.760	0.742
K	0.005	0.004	0.003	0.004	0.003	0.012
Ca/Ca+Na	0.247	0.225	0.237	0.241	0.235	0.235
Al*/SiAl	0.269	0.235	0.261	0.259	0.254	0.263
An	0.246	0.224	0.236	0.240	0.234	0.232
Ab	0.749	0.772	0.761	0.756	0.763	0.756
Or	0.005	0.004	0.003	0.004	0.003	0.012

Appendix 6: Sample 67-82e (cont.)

CHLORITE INCLUSION

	6782E 1/2A CHL I	6782E 1/2B CHL I
SiO2	23.35	23.52
Al2O3	21.80	21.96
MgO	7.04	6.99
FeO	34.80	34.42
MnO	0.59	0.49
CaO	0.00	0.04
Total	87.58	87.43
Si	2.235	2.248
Al	2.460	2.474
Mg	1.005	0.996
Fe2+	2.786	2.751
Mn	0.048	0.040
Ca	0.000	0.004
Fe/Fe+Mg	0.735	0.734

Appendix 7: Archertown Brook: Microprobe Analyses; Sample D84-3d

	MATRIX PLAGIOCLASE (CORE)	(RIM)			(CORE)		(RIM)		(AVG)
	D84-3 D/3/1 A PLA	D84-3 D/3/1 C PLA	D84-3 D/3/1 B PLA	D84-3 D/3/1 D PLA	D84-3 E/3/1 E PLA	D84-3 F/3/1 F PLA	D84-3 G/3/1 G PLA	D84-3 H/3/1 H PLA	D84-3 D/3/1 PLAG
SiO2	59.80	59.78	59.49	59.77	57.76	59.64	60.44	58.83	59.45
Al2O3	26.16	26.00	26.12	26.02	25.91	26.03	25.43	25.78	25.93
FeO	0.03	0.24	0.11	0.00	0.08	0.11	0.05	0.05	0.08
CaO	7.57	7.46	7.59	7.53	7.27	7.17	6.68	7.33	7.32
Na2O	7.88	7.66	7.43	7.83	7.96	7.78	7.89	7.44	7.74
K2O	0.07	0.09	0.05	0.05	0.07	0.09	0.04	0.05	0.07
Total	101.51	101.24	100.79	101.21	99.05	100.82	100.53	99.49	100.58
Si	2.633	2.639	2.635	2.638	2.611	2.641	2.675	2.638	2.639
Al	1.358	1.353	1.364	1.354	1.381	1.359	1.327	1.363	1.357
Fe2+	0.001	0.009	0.004	0.000	0.003	0.004	0.002	0.002	0.003
Ca	0.357	0.353	0.360	0.356	0.352	0.340	0.317	0.352	0.348
Na	0.673	0.656	0.638	0.670	0.698	0.668	0.677	0.647	0.666
K	0.004	0.005	0.003	0.003	0.004	0.005	0.002	0.003	0.004
CA/CA+NA	0.347	0.350	0.361	0.347	0.335	0.337	0.319	0.352	0.343
Al*/SiAl	0.361	0.356	0.364	0.357	0.384	0.359	0.326	0.363	0.358
An	0.345	0.348	0.360	0.346	0.334	0.336	0.318	0.351	0.342
Ab	0.651	0.647	0.637	0.651	0.662	0.659	0.680	0.646	0.654
Or	0.004	0.005	0.003	0.003	0.004	0.005	0.002	0.003	0.004

	MATRIX PLAG		PLAGIOCLASE AT GARNET RIM					
	D843D 5/1A MX PL	D843D 5/1B MX PL	D843D 4/5B PL@GA	D843D 4/2A PL@GA	D843D 4/2B PL@@G	D843D 4/2C PL@@G	D843D 4/2D PL@GA	D843D 4/2AV PL@GA
SiO2	60.08	59.38	60.01	58.90	59.44	57.76	59.06	58.80
Al2O3	27.26	27.04	26.70	25.93	24.60	25.86	25.00	25.34
FeO	0.17	0.27	0.00	0.40	0.58	0.24	0.50	0.42
CaO	7.41	7.44	7.18	7.36	6.51	7.59	6.47	6.99
Na2O	7.75	7.57	7.42	8.03	7.55	7.27	7.42	7.57
K2O	0.07	0.07	0.05	0.09	0.10	0.10	0.42	0.17
Total	102.73	101.77	101.37	100.71	98.79	98.81	98.88	99.30
Si	2.612	2.608	2.635	2.622	2.683	2.615	2.667	2.647
Al	1.397	1.400	1.382	1.361	1.309	1.380	1.331	1.345
Fe2+	0.006	0.010	0.000	0.015	0.022	0.009	0.019	0.016
Ca	0.345	0.350	0.338	0.351	0.315	0.368	0.313	0.337
Na	0.653	0.645	0.632	0.693	0.661	0.638	0.650	0.661
K	0.004	0.004	0.003	0.005	0.006	0.006	0.024	0.010
Ca/Ca+Na	0.346	0.352	0.348	0.336	0.323	0.366	0.325	0.338
Al*/SiAl	0.393	0.397	0.376	0.367	0.311	0.382	0.332	0.348
An	0.344	0.350	0.347	0.335	0.321	0.364	0.317	0.334
Ab	0.652	0.646	0.650	0.661	0.673	0.630	0.659	0.656
Or	0.004	0.004	0.003	0.005	0.006	0.006	0.024	0.010

Appendix 7: Sample D84-3d (cont.)

	PLAGIOCLASE INCLUSIONS IN GARNET							
	(RIM)	(CORE)	(----RIM----)		(AVG)	(----RIM----)		(AVG)
	D843D 4/1B PL RI	D843D 4/1A PL CO	D843D 4/1C PL IN	D843D 4/1E PL IN	D843D 4/1AV PL IN	D843D 4/3A PL IN	D843D 4/3B PL IN	D843D 4/3AV PL IN
SiO2	57.91	58.72	57.40	58.52	57.85	57.18	58.59	57.86
Al2O3	26.08	26.63	26.47	26.25	26.07	25.34	26.37	25.86
FeO	1.09	0.84	0.82	1.10	0.98	2.75	0.89	1.84
CaO	7.71	8.13	8.43	7.86	7.79	7.95	8.16	8.06
Na2O	7.23	7.32	6.85	7.43	7.22	6.73	7.14	6.94
K2O	0.17	0.09	0.07	0.07	0.14	0.10	0.18	0.14
Total	100.20	101.74	100.05	101.23	100.06	100.05	101.33	100.70
Si	2.599	2.594	2.579	2.600	2.599	2.590	2.599	2.594
Al	1.380	1.387	1.402	1.375	1.381	1.353	1.379	1.367
Fe2+	0.041	0.031	0.031	0.041	0.037	0.104	0.033	0.069
Ca	0.371	0.385	0.406	0.374	0.375	0.386	0.388	0.387
Na	0.629	0.627	0.597	0.640	0.629	0.591	0.614	0.603
K	0.010	0.005	0.004	0.004	0.008	0.006	0.010	0.008
Ca/Ca+Na	0.371	0.380	0.405	0.369	0.374	0.395	0.387	0.391
Al*/SiAl	0.388	0.394	0.410	0.385	0.389	0.374	0.388	0.382
An	0.367	0.379	0.403	0.367	0.371	0.393	0.383	0.388
Ab	0.623	0.617	0.593	0.629	0.622	0.601	0.607	0.604
Or	0.010	0.005	0.004	0.004	0.008	0.006	0.010	0.008

	(RIM)			(AVG)
	D843D 4/4A PL IN	D843D 4/4B PL IN	D843D 4/4C PL IN	D843D 4/4AV PL IN
SiO2	67.34	68.08	67.78	67.72
Al2O3	20.89	20.36	19.69	20.31
FeO	0.97	0.83	0.76	0.85
CaO	0.49	0.75	0.72	0.66
Na2O	11.48	11.22	11.02	11.24
K2O	0.60	0.09	0.14	0.29
Total	101.76	101.33	100.12	101.07
Si	2.920	2.950	2.970	2.947
Al	1.068	1.040	1.017	1.042
Fe2+	0.035	0.030	0.028	0.031
Ca	0.023	0.035	0.034	0.031
Na	0.965	0.943	0.936	0.948
K	0.033	0.005	0.008	0.016
Ca/Ca+Na	0.023	0.036	0.035	0.032
Al*/SiAl	0.069	0.040	0.017	0.042
An	0.023	0.036	0.035	0.031
Ab	0.945	0.959	0.957	0.953
Or	0.032	0.005	0.008	0.016

Appendix 7: Sample D84-3d (cont.)

	-----BIOTITE NEAR GARNET-----				--------MATRIX BIOTITE-------			
	D84-3 D/1/2 B BIO	D84-3 D/1/2 D BIO	D84-3 E/1/2 E BIO	D84-3 D/1/2 BIO	D84-3 D/2/2 A MAT	D84-3 D/2/2 C MAT	D84-3 D/2/2 D MAT	D84-3 D/2/2 AVG
SiO2	34.93	34.73	36.51	34.25	36.12	36.91	36.98	36.49
Al2O3	19.66	19.48	19.10	19.76	19.18	19.36	19.59	19.32
TiO2	1.43	1.34	1.49	1.25	1.22	1.29	1.26	1.27
MgO	14.08	13.32	12.79	14.07	12.43	12.52	12.50	12.54
FeO	18.47	18.14	17.74	18.41	16.56	16.24	16.90	16.50
MnO	0.06	0.09	0.04	0.07	0.09	0.08	0.06	0.07
CaO	0.00	0.00	0.00	0.00	0.00	0.00	0.00	0.00
Na2O	0.06	0.08	0.08	0.06	0.13	0.11	0.13	0.12
K2O	5.92	7.58	8.16	6.06	8.67	8.45	8.62	8.43
Total	94.63	94.76	95.92	93.92	94.40	94.96	96.05	94.74
Si	5.223	5.235	5.417	5.172	5.438	5.494	5.462	5.457
Aliv	2.777	2.765	2.583	2.828	2.562	2.506	2.538	2.543
Alvi	0.689	0.697	0.759	0.690	0.843	0.891	0.873	0.863
Ti	0.163	0.153	0.168	0.143	0.139	0.146	0.141	0.144
Mg	3.138	2.993	2.829	3.167	2.789	2.778	2.752	2.794
Fe2+	2.310	2.287	2.202	2.325	2.086	2.021	2.088	2.064
Mn	0.008	0.011	0.005	0.009	0.012	0.010	0.008	0.009
Sum Oct	6.308	6.141	5.963	6.334	5.869	5.846	5.862	5.874
Ca	0.000	0.000	0.000	0.000	0.000	0.000	0.000	0.000
Na	0.017	0.023	0.024	0.017	0.039	0.033	0.036	0.036
K	1.130	1.458	1.544	1.167	1.665	1.604	1.625	1.609
Sum A	1.147	1.481	1.568	1.184	1.704	1.637	1.661	1.645
(OH)	0.000	0.000	0.000	0.000	0.000	0.000	0.000	0.000
Fe/Fe+Mg	0.424	0.433	0.438	0.423	0.428	0.421	0.431	0.425
X(Ca)	0.000	0.000	0.000	0.000	0.000	0.000	0.000	0.000
X(Na)	0.015	0.016	0.015	0.014	0.023	0.020	0.022	0.022
X(K)	0.985	0.984	0.985	0.986	0.977	0.980	0.978	0.978

Appendix 7: Sample D84-3d (cont.)

	----MATRIX BIOTITE---			-------MATRIX MUSCOVITE------			
	D84-3 D/3/2 A BIO	D84-3 D/3/2 B BIO	D84-3 D/3/2 BIO	D84-3 D/*/* MUSC	D84-3 D/*/* MUSC	D84-3 D/*/* MUSC	D84-3 D/*/* MUSC
SiO2	35.84	36.26	36.05	46.61	46.20	46.37	46.39
Al2O3	19.23	19.14	19.19	35.60	35.16	35.06	35.27
TiO2	1.32	1.37	1.34	0.58	0.58	0.44	0.53
MgO	13.01	13.07	13.04	0.76	0.75	0.70	0.74
FeO	17.35	17.08	17.22	0.89	0.89	0.87	0.88
MnO	0.04	0.06	0.05	0.00	0.00	0.00	0.00
CaO	0.00	0.00	0.00	0.00	0.01	0.13	0.05
Na2O	0.13	0.12	0.12	1.43	1.40	1.61	1.48
K2O	8.08	8.06	8.07	9.24	9.19	8.74	9.06
Total	95.00	95.15	95.07	95.09	94.18	93.93	94.40
Si	5.367	5.408	5.388	6.170	6.177	6.202	6.183
Aliv	2.633	2.592	2.612	1.830	1.823	1.798	1.817
Alvi	0.763	0.774	0.769	3.726	3.719	3.731	3.725
Ti	0.150	0.155	0.152	0.058	0.059	0.045	0.054
Mg	2.904	2.905	2.904	0.149	0.149	0.140	0.146
Fe2+	2.173	2.130	2.152	0.098	0.100	0.097	0.098
Mn	0.005	0.008	0.006	0.000	0.000	0.000	0.000
Sum Oct	5.995	5.972	5.983	4.031	4.027	4.013	4.023
Ca	0.000	0.000	0.000	0.000	0.001	0.019	0.007
Na	0.038	0.034	0.036	0.368	0.362	0.418	0.382
K	1.544	1.533	1.538	1.560	1.567	1.492	1.540
Sum A	1.582	1.567	1.574	1.928	1.930	1.929	1.929
(OH)	0.000	0.000	0.000	0.000	0.000	0.000	0.000
Fe/Fe+Mg	0.428	0.423	0.426	0.397	0.402	0.409	0.402
X(Ca)	0.000	0.000	0.000	0.000	0.001	0.010	0.004
X(Na)	0.024	0.022	0.023	0.191	0.188	0.217	0.198
X(K)	0.976	0.978	0.977	0.809	0.812	0.773	0.798

Appendix 7: Sample D84-3d (cont.)

	MATRIX CHLORITE (RETROGRADE)				-CHLORITE INCLUSION--		
	D843D 0/1A MX CH	D843D 0/1B MX CH	D843D 0/1C MX CH	D843D 0/1AV MX CH	D843D 4/2A CHL I	D843D 4/2B CHL I	D843D 4/2AV CHL I
SiO2	25.48	25.81	12.38	25.52	24.15	23.91	24.03
Al2O3	25.29	23.90	30.43	24.84	24.30	24.11	24.21
TiO2	0.09	0.16	0.10	0.11	0.28	0.19	0.24
MgO	17.87	17.83	21.49	17.86	14.40	13.84	14.12
FeO	21.47	21.42	24.94	21.22	24.79	25.63	25.21
MnO	0.10	0.17	0.18	0.14	0.78	0.82	0.80
CaO	0.00	0.00	0.00	0.00	0.00	0.01	0.01
Na2O	0.00	0.00	0.00	0.00	0.00	0.00	0.00
K2O	0.00	0.00	0.00	0.00	0.00	0.00	0.00
Total	90.30	89.30	89.52	89.70	88.71	88.51	88.61
Si	5.079	5.208	2.067	5.118	5.025	5.013	5.019
Aliv	2.921	2.792	1.933	2.882	2.975	2.987	2.981
Alvi	3.021	2.894	4.056	2.991	2.987	2.974	2.980
Ti	0.013	0.025	0.013	0.017	0.045	0.031	0.038
Mg	5.307	5.362	5.347	5.338	4.465	4.326	4.396
Fe2+	3.578	3.615	3.482	3.558	4.314	4.495	4.404
Mn	0.017	0.029	0.026	0.024	0.137	0.145	0.141
Sum Oct	11.936	11.925	12.924	11.928	11.948	11.971	11.959
Ca	0.001	0.000	0.000	0.000	0.001	0.002	0.002
Na	0.000	0.000	0.000	0.000	0.000	0.000	0.000
K	0.000	0.000	0.000	0.000	0.000	0.000	0.000
Sum A	0.001	0.000	0.000	0.000	0.001	0.002	0.002
(OH)	0.000	0.000	0.000	0.000	0.000	0.000	0.000
Fe/Fe+Mg	0.403	0.403	0.394	0.400	0.491	0.510	0.500

Appendix 7: Sample D84-3d (cont.)

	MATRIX STAUROLITE			(RIM)		(CORE)	(AVG)
	D84-3 D/2/1 A STA	D84-3 D/2/1 B STA	D84-3 D/2/1 STAU	D843D 2/1D STAU	D843D 2/1E STAU	D843D 2/1F STAU	D843D 2/1AV STAU
SiO2	28.93	28.45	28.51	28.17	27.64	27.90	27.77
Al2O3	54.96	54.55	54.22	57.86	57.64	56.31	56.96
TiO2	0.68	0.62	0.64	0.55	0.61	0.56	0.59
MgO	1.35	1.31	1.30	1.22	1.26	1.31	1.28
FeO	10.92	10.71	10.71	10.65	10.48	10.83	10.65
MnO	0.37	0.33	0.32	0.26	0.27	0.31	0.29
ZnO	1.96	1.92	1.81	1.94	1.58	1.40	1.50
CaO	0.00	0.00	0.00	0.00	0.01	0.00	0.01
Total	99.17	97.88	97.51	100.65	99.49	98.62	99.05
Si	3.938	3.920	3.941	3.769	3.735	3.808	3.772
Al	8.820	8.863	8.838	9.127	9.183	9.059	9.122
Ti	0.070	0.065	0.067	0.056	0.063	0.058	0.061
Mg	0.273	0.269	0.268	0.244	0.254	0.266	0.260
Fe2+	1.243	1.234	1.238	1.192	1.184	1.236	1.210
Mn	0.043	0.038	0.038	0.029	0.031	0.036	0.033
Zn	0.197	0.195	0.185	0.192	0.158	0.141	0.150
Ca	0.000	0.000	0.000	0.000	0.001	0.000	0.001
Fe/Fe+Mg	0.820	0.821	0.822	0.830	0.823	0.823	0.823

Appendix 7: Sample D84-3d (cont.)

GARNET TRAVERSE

(RIM)

	D84-3 D/1/1 A GAR	D84-3 D/1/1 B GAR	D84-3 D/1/1 C GAR	D84-3 D/1/1 D GAR	D84-3 D/1/1 E GAR	D84-3 D/1/1 F GAR	D84-3 D/1/1 G GAR	D84-3 D/1/1 H GAR
SiO2	38.22	37.69	36.52	35.85	36.79	37.12	35.01	35.10
Al2O3	21.28	20.64	21.57	21.88	20.17	20.46	21.55	21.66
MgO	3.49	3.36	3.17	3.18	3.10	3.23	3.23	3.32
FeO	30.99	31.52	30.77	31.00	32.08	32.06	31.01	31.26
MnO	5.02	4.96	5.26	4.74	4.65	4.90	4.77	5.09
CaO	2.92	2.38	2.96	2.85	3.18	3.07	2.39	2.17
Total	101.93	100.55	100.25	99.50	99.98	100.84	97.97	98.60
Si	2.004	2.010	1.957	1.936	1.988	1.987	1.925	1.920
Al	1.315	1.298	1.363	1.393	1.285	1.291	1.397	1.397
Mg	0.273	0.267	0.253	0.256	0.250	0.258	0.265	0.271
Fe2+	1.359	1.406	1.379	1.400	1.450	1.435	1.426	1.430
Mn	0.223	0.224	0.239	0.217	0.213	0.222	0.222	0.236
Ca	0.164	0.136	0.170	0.165	0.184	0.176	0.141	0.127
Fe/Fe+Mg	0.833	0.840	0.845	0.845	0.853	0.848	0.843	0.841
Pyrope	0.135	0.131	0.124	0.126	0.119	0.123	0.129	0.131
Alman	0.673	0.692	0.676	0.687	0.691	0.686	0.694	0.693
Spess	0.110	0.110	0.117	0.106	0.102	0.106	0.108	0.114
Gross	0.081	0.067	0.083	0.081	0.088	0.084	0.069	0.062

(CORE)

	D84-3 D/1/1 I GAR	D84-3 D/1/1 J GAR	D84-3 D/1/1 K GAR	D84-3 D/1/1 L GAR	D84-3 D/1/1 M GAR	D84-3 D/1/1 O GAR	D84-3 D/1/1 P GAR	D84-3 D/1/1 Q GAR
SiO2	35.00	37.54	36.27	37.24	35.03	35.56	35.68	36.35
Al2O3	21.48	21.14	21.27	20.97	20.84	21.64	21.38	21.26
MgO	3.35	3.50	1.48	1.42	2.42	3.37	3.32	2.47
FeO	30.69	31.18	22.34	22.44	27.34	30.28	30.44	27.14
MnO	4.95	4.93	10.16	10.45	6.96	5.85	5.53	8.02
CaO	2.22	2.91	7.31	7.49	5.29	2.99	2.77	4.34
Total	97.68	101.19	98.83	100.01	97.89	99.68	99.13	99.58
Si	1.928	1.988	2.951	2.993	2.900	2.986	2.908	2.945
Al	1.395	1.320	2.040	1.987	2.034	2.070	2.054	2.030
Mg	0.275	0.276	0.190	0.170	0.299	0.407	0.403	0.298
Fe2+	1.414	1.381	1.520	1.508	1.893	2.055	2.075	1.839
Mn	0.231	0.221	0.700	0.711	0.488	0.402	0.382	0.550
Ca	0.131	0.165	0.637	0.645	0.469	0.260	0.242	0.377
Fe/Fe+Mg	0.837	0.833	0.894	0.899	0.864	0.835	0.837	0.861
Pyrope	0.134	0.135	0.059	0.056	0.095	0.130	0.130	0.097
Alman	0.689	0.676	0.500	0.497	0.601	0.658	0.669	0.600
Spess	0.113	0.108	0.230	0.234	0.155	0.129	0.123	0.180
Gross	0.064	0.081	0.210	0.213	0.149	0.083	0.078	0.123

Appendix 7: Sample D84-3d (cont.)

	D84-3 D/1/1 R GAR	D84-3 D/1/1 S GAR	D84-3 D/1/1 T GAR	D84-3 D/1/1 U GAR	D84-3 D/1/1 V GAR	D84-3 D/1/1 W GAR	D84-3 D/1/1 X GAR	D84-3 D/1/1 Y GAR
SiO2	36.70	36.50	37.08	36.61	36.80	37.05	36.15	36.17
Al2O3	21.24	21.44	21.38	21.20	21.42	21.43	21.74	21.58
MgO	1.56	1.44	1.70	1.71	2.61	3.28	3.38	3.28
FeO	23.02	21.92	24.06	25.19	29.13	29.52	29.64	29.77
MnO	10.99	10.94	10.60	9.67	5.97	4.73	4.70	5.00
CaO	5.67	7.33	5.86	5.49	4.95	3.85	3.68	3.51
Total	99.18	99.57	100.69	99.87	100.88	99.85	99.29	99.32
Si	2.977	2.949	2.969	2.960	2.942	2.970	2.921	2.927
Al	2.031	2.042	2.018	2.021	2.019	2.025	2.071	2.059
Mg	0.189	0.174	0.203	0.206	0.311	0.392	0.407	0.396
Fe2+	1.562	1.481	1.611	1.703	1.948	1.979	2.003	2.015
Mn	0.755	0.749	0.719	0.662	0.404	0.321	0.322	0.343
Ca	0.493	0.635	0.503	0.476	0.424	0.331	0.319	0.304
Fe/Fe+Mg	0.892	0.895	0.888	0.892	0.862	0.835	0.831	0.836
Pyrope	0.063	0.057	0.067	0.068	0.101	0.130	0.133	0.129
Alman	0.521	0.487	0.531	0.559	0.631	0.655	0.657	0.659
Spess	0.252	0.246	0.237	0.217	0.131	0.106	0.106	0.112
Gross	0.164	0.209	0.166	0.156	0.137	0.109	0.105	0.099

	D84-3 D/1/1 Z GAR	D84-3 D/1/1 A' GA	D84-3 D/1/1 B' GA	D84-3 D/1/1 GAR	D84-3 D/1/1 GAR	D84-3 D/1/1 GAR
SiO2	35.11	37.30	37.09	35.96	36.48	37.19
Al2O3	21.71	21.29	21.33	21.14	21.18	21.31
MgO	3.35	2.18	1.55	2.74	3.29	1.87
FeO	30.53	25.53	23.61	26.09	31.26	24.57
MnO	4.85	8.84	10.87	7.16	4.93	9.86
CaO	2.93	5.55	5.75	4.59	2.70	5.65
Total	98.48	100.70	100.20	97.69	99.85	100.45
Si	2.878	2.978	2.981	2.952	1.965	2.979
Al	2.098	2.004	2.021	2.046	1.345	2.012
Mg	0.409	0.260	0.186	0.335	0.264	0.223
Fe2+	2.093	1.705	1.587	1.791	1.408	1.646
Mn	0.337	0.598	0.740	0.498	0.225	0.669
Ca	0.257	0.475	0.495	0.404	0.156	0.485
Fe/Fe+Mg	0.837	0.868	0.895	0.842	0.842	0.881
Pyrope	0.132	0.086	0.062	0.111	0.129	0.074
Alman	0.676	0.561	0.528	0.591	0.686	0.544
Spess	0.109	0.197	0.246	0.164	0.110	0.221
Gross	0.083	0.156	0.165	0.133	0.076	0.160

Appendix 7: Sample D84-3d (cont.)

----GARNET RIM ANALYSES-----

	D843D 4/90 GAR R	D843D 4/177 GAR R	D843D 4/166 GAR R	D843D 4/51 GAR R
SiO2	37.55	37.64	37.69	37.83
Al2O3	21.23	21.29	21.32	21.39
MgO	3.10	3.11	3.14	3.00
FeO	31.11	31.69	31.77	31.89
MnO	5.14	4.71	4.63	5.05
CaO	2.31	2.25	2.32	2.19
Total	100.44	100.68	100.87	101.34
Si	3.000	3.000	3.000	3.000
Al	2.000	2.000	2.000	2.000
Mg	0.369	0.369	0.372	0.354
Fe2+	2.079	2.112	2.115	2.115
Mn	0.348	0.318	0.312	0.339
Ca	0.198	0.192	0.198	0.186
Fe/Fe+Mg	0.849	0.851	0.850	0.857
Pyrope	0.123	0.123	0.124	0.118
Alman	0.694	0.706	0.706	0.706
Spess	0.116	0.106	0.104	0.113
Gross	0.066	0.064	0.066	0.062

-----GARNET RIMS-----

	D843D 4/203 GAR R	D843D 4/205 GAR R	D843D 4/123 GAR R
SiO2	37.94	37.68	37.77
Al2O3	21.46	21.31	21.36
MgO	3.26	3.08	2.86
FeO	31.49	31.81	31.12
MnO	5.20	4.80	4.73
CaO	2.09	2.18	3.17
Total	101.43	100.86	101.02
Si	3.000	3.000	3.000
Al	2.000	2.000	2.000
Mg	0.384	0.366	0.339
Fe2+	2.082	2.118	2.067
Mn	0.348	0.324	0.318
Ca	0.177	0.186	0.270
Fe/Fe+Mg	0.844	0.853	0.859
Pyrope	0.128	0.122	0.113
Alman	0.696	0.707	0.690
Spess	0.116	0.108	0.106
Gross	0.059	0.062	0.090

Appendix 7: Sample D84-3d (cont.)

	---PLAGIOCLASE (CORE)	INCLUSIONS (RIM)	IN GARNET (RIM)	--- (RIM)	(CORE)	-MATRIX	PLAG- (CORE)
	D843D 1/3A PL CO	D843D 1/3B PL RI	D843D 1/3C PL RI	D843D 1/3D PL RI	D843D 1/4B PL CO	D843D 1/5A PL NR	D843D 1/5B PL CO
SiO2	53.27	61.69	52.83	55.15	54.18	59.94	59.10
Al2O3	29.37	23.30	28.66	27.34	28.75	25.44	25.72
FeO	0.82	2.06	0.96	1.10	0.74	0.11	0.11
CaO	11.42	4.05	11.17	9.39	10.65	6.76	6.96
Na2O	5.05	8.52	5.06	5.91	5.55	7.85	7.69
K2O	0.02	0.00	0.00	0.00	0.02	0.04	0.04
Total	99.93	99.62	98.69	98.90	99.88	100.13	99.61
Si	2.417	2.758	2.428	2.515	2.454	2.666	2.645
Al	1.571	1.228	1.553	1.470	1.535	1.334	1.357
Fe2+	0.031	0.077	0.037	0.042	0.028	0.004	0.004
Ca	0.555	0.194	0.550	0.459	0.517	0.322	0.334
Na	0.444	0.739	0.451	0.523	0.487	0.677	0.667
K	0.001	0.000	0.000	0.000	0.001	0.002	0.002
Ca/Ca+Na	0.556	0.208	0.549	0.467	0.515	0.322	0.334
Al*/SiAl	0.578	0.231	0.564	0.477	0.541	0.334	0.356
An	0.555	0.208	0.549	0.467	0.514	0.322	0.333
Ab	0.444	0.792	0.451	0.533	0.485	0.676	0.665
Or	0.001	0.000	0.000	0.000	0.001	0.002	0.002

Appendix 7: Sample D84-3d (cont.)

	-MATRIX PLAG-		------PALGIOCLASE AT GARNET RIM------ (AT KYANITE INCL)				
	D843D 1/6A PL MX	D843D 1/6B PL MX	D843D 1/9A PL@GA	D843D 1/9B PL@GA	D843D 1/9C PL@GA	D843D 1/9D PL@GA	D843D 1/9E PL@GA
SiO2	59.11	55.41	58.43	58.36	57.54	59.49	58.57
Al2O3	25.58	28.80	26.35	26.23	26.23	25.00	25.50
FeO	0.05	0.05	0.50	0.21	0.13	0.11	0.11
CaO	7.14	6.95	4.39	7.47	7.37	6.60	7.27
Na2O	7.52	6.61	7.90	7.48	7.15	7.73	7.58
K2O	0.02	0.07	0.78	0.05	0.03	0.03	0.03
Total	99.43	97.89	98.35	99.71	98.46	98.96	99.06
Si	2.650	2.523	2.645	2.613	2.609	2.676	2.640
Al	1.352	1.546	1.406	1.387	1.402	1.326	1.355
Fe2+	0.002	0.002	0.019	0.008	0.005	0.004	0.004
Ca	0.343	0.339	0.213	0.359	0.358	0.318	0.351
Na	0.654	0.584	0.693	0.650	0.629	0.674	0.662
K	0.001	0.004	0.045	0.003	0.002	0.002	0.002
Ca/Ca+Na	0.344	0.367	0.235	0.356	0.363	0.321	0.346
Al*/SiAl	0.351	0.511	0.386	0.387	0.398	0.325	0.357
An	0.344	0.366	0.224	0.355	0.362	0.320	0.346
Ab	0.655	0.630	0.729	0.642	0.636	0.678	0.652
Or	0.001	0.004	0.047	0.003	0.002	0.002	0.002

Appendix 7: Sample D84-3d (cont.)

	MATRIX PLAGIOCLASE							
	(CORE)	(RIM)	(RIM)	(CORE)	(RIM			)
	D843D V/1A MX PL	D843D V/1B MX PL	D843D 4/7A MX PL	D843D 4/7B MX PL	D843D 4/8A MX PL	D843D 4/9A MX PL	D843D 4/9B MX PL	D843D 4/9C MX PL
SiO2	57.73	57.93	58.38	58.57	58.81	60.41	65.10	66.23
Al2O3	25.85	25.71	25.63	25.78	25.70	24.38	23.38	20.50
FeO	0.08	0.16	0.08	0.08	0.03	0.40	0.22	0.22
CaO	7.47	7.12	7.02	7.15	7.24	5.72	3.37	1.03
Na2O	7.35	7.41	7.62	7.48	7.56	8.18	8.91	10.65
K2O	0.05	0.07	0.03	0.05	0.03	0.07	0.13	0.07
Total	98.53	98.40	98.76	99.13	99.37	99.16	101.11	98.70
Si	2.618	2.628	2.637	2.636	2.640	2.709	2.829	2.938
Al	1.382	1.375	1.365	1.368	1.360	1.289	1.198	1.072
Fe2+	0.003	0.006	0.003	0.003	0.001	0.015	0.008	0.008
Ca	0.363	0.346	0.340	0.345	0.348	0.275	0.157	0.049
Na	0.646	0.652	0.667	0.653	0.658	0.711	0.751	0.916
K	0.003	0.004	0.002	0.003	0.002	0.004	0.007	0.004
Ca/Ca+Na	0.360	0.347	0.338	0.346	0.346	0.279	0.173	0.051
Al*/SiAl	0.382	0.374	0.364	0.367	0.360	0.290	0.193	0.071
An	0.359	0.345	0.337	0.345	0.345	0.278	0.172	0.051
Ab	0.638	0.651	0.661	0.652	0.653	0.718	0.821	0.945
Or	0.003	0.004	0.002	0.003	0.002	0.004	0.008	0.004

Appendix 7: Sample D84-3d (cont.)

	--PLAGIOCLASE AT GARNET RIM--			
	(CORE)	(--------RIM--------)		
	D843D 4/2E PL@GA	D843D 4/2F PL@GA	D843D 4/6A PL@GA	D843D 4/6B PL@@G
SiO2	57.02	58.87	59.07	58.98
Al2O3	25.30	24.85	25.52	25.77
FeO	0.23	0.61	0.16	0.43
CaO	7.43	6.42	6.99	6.96
Na2O	7.29	8.04	7.18	7.55
K2O	0.03	0.05	0.05	0.05
Total	97.31	98.84	98.98	99.75
Si	2.621	2.662	2.656	2.640
Al	1.371	1.325	1.353	1.360
Fe2+	0.009	0.023	0.006	0.016
Ca	0.366	0.311	0.337	0.334
Na	0.650	0.705	0.626	0.655
K	0.002	0.003	0.003	0.003
Ca/Ca+Na	0.360	0.306	0.350	0.338
Al*/SiAl	0.374	0.329	0.350	0.360
An	0.360	0.305	0.349	0.337
Ab	0.639	0.692	0.648	0.660
Or	0.002	0.003	0.003	0.003

Appendix 7: Sample D84-3d (cont.)

	PLAG INCL IN: KYANITE	STAUROLITE
	D843D 1/7A PL IN	D843D V/2A PL IN
SiO2	58.69	58.06
Al2O3	25.63	25.65
FeO	0.05	0.18
CaO	7.08	7.29
Na2O	7.42	7.34
K2O	0.07	0.05
Total	98.94	98.59
Si	2.644	2.630
Al	1.361	1.370
Fe2+	0.002	0.007
Ca	0.342	0.354
Na	0.648	0.645
K	0.004	0.003
Ca/Ca+Na	0.345	0.354
Al*/SiAl	0.359	0.370
An	0.344	0.353
Ab	0.652	0.644
Or	0.004	0.003

Appendix 7: Sample D84-3d (cont.)

	-PLAGIOCLASE INCLUSION IN GARNET-			
	(RIM)	(CORE)	(CORE)	(RIM)
	D843D 4/3B PL IN	D843D 4/3C PL IN	D943D IV/1A PL IN	D843D IV/1B PL IN
SiO2	57.21	54.75	55.55	56.44
Al2O3	26.51	24.55	26.57	26.14
FeO	0.61	0.75	0.65	1.07
CaO	8.04	7.60	8.72	7.87
Na2O	6.95	6.48	6.46	6.58
K2O	0.05	0.07	0.07	0.09
Total	99.37	94.20	98.03	98.20
Si	2.583	2.607	2.550	2.582
Al	1.411	1.378	1.438	1.410
Fe2+	0.023	0.030	0.025	0.041
Ca	0.389	0.388	0.429	0.386
Na	0.608	0.598	0.575	0.584
K	0.003	0.004	0.004	0.005
Ca/Ca+Na	0.390	0.394	0.427	0.398
Al*/SiAl	0.413	0.384	0.443	0.413
An	0.389	0.392	0.426	0.396
Ab	0.608	0.604	0.570	0.599
Or	0.003	0.004	0.004	0.005

Appendix 7: Sample PM-9b

	---------GARNET RIM ANALYSES---------									
	PM9B/ 1/64 GAR R	PM9B/ 1/63 GAR N	PM9B/ 1/65 GAR R	PM9B/ 1/66 GAR R	PM9B/ 1/87 GAR R	PM9B/ 1/118 GAR R	PM9B/ 1/145 GAR R	PM9B/ 1/175 GAR R	PM9B/ 1/169 GAR P	PM9B/ 1/194 GAR P
SiO2	37.76	37.89	37.27	37.49	37.37	37.92	37.51	37.73	37.50	37.55
Al2O3	21.35	21.43	21.08	21.20	21.13	21.44	21.21	21.33	21.21	21.24
MgO	3.04	2.97	2.93	2.67	2.66	3.03	2.52	2.89	2.26	1.71
FeO	33.14	33.30	33.29	33.94	33.43	33.60	33.59	33.65	30.85	27.79
MnO	3.25	3.27	3.48	3.45	3.40	3.18	3.54	3.43	4.38	6.47
CaO	2.47	2.62	1.88	1.99	2.34	2.37	2.42	2.18	4.20	5.78
Total	101.02	101.48	99.92	100.74	100.33	101.53	100.79	101.21	100.40	100.55
Si	3.000	3.000	3.000	3.000	3.000	3.000	3.000	3.000	3.000	3.000
Al	2.000	2.000	2.000	2.000	2.000	2.000	2.000	2.000	2.000	2.000
Mg	0.360	0.351	0.351	0.318	0.318	0.357	0.300	0.342	0.270	0.204
Fe2+	2.202	2.205	2.241	2.271	2.244	2.223	2.247	2.238	2.064	1.857
Mn	0.219	0.219	0.237	0.234	0.231	0.213	0.240	0.231	0.297	0.438
Ca	0.210	0.222	0.162	0.171	0.201	0.201	0.207	0.186	0.360	0.495
Fe/Fe+Mg	0.859	0.863	0.865	0.877	0.876	0.862	0.882	0.867	0.884	0.901
Pyrope	0.120	0.117	0.117	0.106	0.106	0.119	0.100	0.114	0.090	0.068
Alman	0.736	0.736	0.749	0.759	0.749	0.742	0.751	0.747	0.690	0.620
Spess	0.073	0.073	0.079	0.078	0.077	0.071	0.080	0.077	0.099	0.146
Gross	0.070	0.074	0.054	0.057	0.067	0.067	0.069	0.062	0.120	0.165

Appendix 7: Sample PM-9b (cont.)

	---PLAGIOCLASE INCLUSION IN GARNET---					------MATRIX PLAGIOCLASE-----			
	PM9B/ 1/2A PLAG	PM9B/ 1/2B PL IN	PM9B/ 1/2C PLAG	PM9B/ 1/2D PLAG	PM9B/ 1/2 A VG PL	PM9B/ 3/1A MX PL	PM9B/ 3/1B MX PL	PM9B/ 3/1C MX PL	PM9B/ 3/1AV MX PL
SiO2	57.90	55.81	56.02	56.39	56.53	62.16	60.61	60.03	60.93
Al2O3	26.66	25.86	25.78	26.29	26.15	25.13	24.80	23.91	24.62
FeO	0.97	0.88	0.80	0.97	0.89	0.11	0.11	0.11	0.11
CaO	8.35	8.55	8.39	8.22	8.39	6.04	6.41	5.81	6.09
Na2O	7.35	6.62	6.48	6.98	6.87	8.54	7.78	8.05	8.12
K2O	0.09	0.09	0.09	0.09	0.09	0.13	0.12	0.26	0.18
Total	101.32	97.81	97.56	98.94	98.91	102.11	99.84	98.17	100.04
Si	2.575	2.570	2.581	2.567	2.573	2.707	2.699	2.719	2.708
Al	1.398	1.404	1.400	1.411	1.403	1.290	1.302	1.277	1.290
Fe2+	0.036	0.034	0.031	0.037	0.034	0.004	0.004	0.004	0.004
Ca	0.398	0.422	0.414	0.401	0.409	0.282	0.306	0.282	0.290
Na	0.634	0.591	0.579	0.616	0.606	0.721	0.672	0.707	0.700
K	0.005	0.005	0.005	0.005	0.005	0.007	0.007	0.015	0.010
Ca/Ca+Na	0.386	0.417	0.417	0.394	0.403	0.281	0.313	0.285	0.293
Al*/SiAl	0.409	0.415	0.408	0.420	0.413	0.291	0.302	0.278	0.291
An	0.384	0.415	0.415	0.392	0.401	0.279	0.311	0.281	0.290
Ab	0.611	0.581	0.580	0.603	0.594	0.714	0.682	0.704	0.700
Or	0.005	0.005	0.005	0.005	0.005	0.007	0.007	0.015	0.010

Appendix 7: Sample PM-9b (cont.)

	BIOTITE INCLUSION IN GARNET							
	PM9B/ 1/1A BIO I	PM9B/ 1/1B BIO I	PM9B/ 1/1D BIO I	PM9B/ 1/1E BIO I	PM9B/ 1/1F BIO I	PM9B/ 1/1G BIO I	PM9B/ 1/1H BIO I	PM9B/ 1/1K BIO I
SiO2	37.49	38.00	38.21	14.87	37.16	38.22	37.21	36.58
Al2O3	19.44	19.93	20.28	26.34	19.72	20.17	19.76	19.24
TiO2	1.37	1.44	1.49	2.07	1.48	1.47	1.55	1.35
MgO	12.15	12.49	12.75	16.37	12.44	12.51	12.50	11.98
FeO	15.99	16.56	16.38	23.59	17.07	16.63	17.25	15.99
MnO	0.03	0.10	0.03	0.13	0.09	0.07	0.09	0.11
CaO	0.06	0.11	0.02	0.00	0.06	0.06	0.00	0.04
Na2O	0.35	0.23	0.22	0.37	0.31	0.31	0.31	0.27
K2O	8.34	8.52	8.62	11.65	8.24	8.24	8.59	8.42
Total	95.23	97.39	98.01	95.39	96.58	97.67	97.26	93.98
Si	5.548	5.508	5.494	1.625	5.452	5.511	5.435	5.503
Aliv	2.452	2.492	2.506	2.375	2.548	2.489	2.565	2.497
Alvi	0.939	0.914	0.932	1.019	0.863	0.939	0.838	0.915
Ti	0.154	0.159	0.163	0.172	0.165	0.161	0.172	0.154
Mg	2.679	2.699	2.731	2.667	2.720	2.689	2.720	2.685
Fe2+	1.979	2.008	1.970	2.156	2.095	2.005	2.107	2.012
Mn	0.004	0.012	0.004	0.012	0.011	0.009	0.011	0.014
Sum Oct	5.755	5.792	5.800	6.026	5.854	5.803	5.848	5.780
Ca	0.010	0.017	0.003	0.000	0.010	0.009	0.000	0.007
Na	0.101	0.064	0.060	0.079	0.088	0.086	0.089	0.079
K	1.575	1.576	1.581	1.625	1.542	1.515	1.601	1.617
Sum A	1.686	1.657	1.644	1.704	1.640	1.610	1.690	1.703
(OH)	0.000	0.000	0.000	0.000	0.000	0.000	0.000	0.000
Fe/Fe+Mg	0.425	0.427	0.419	0.447	0.435	0.427	0.437	0.428
X(Ca)	0.006	0.010	0.002	0.000	0.006	0.006	0.000	0.004
X(Na)	0.060	0.039	0.036	0.046	0.054	0.053	0.053	0.046
X(K)	0.934	0.951	0.962	0.954	0.940	0.941	0.947	0.950

Appendix 7: Sample PM-9b (cont.)

	----BIOTITE INCLUSION IN GARNET------					BIO NEAR GARNET	
	PM9B/ 1/1L BIO I	PM9B 1/1AV BIO	PM9B/ 1/3B BIO I	PM9B/ 1/3C BIO I	PM9B/ 1/3D BIO I	PM9B/ 1/4A BIO N	PM9B/ 1/4C BIO N
SiO2	36.02	36.85	36.42	37.18	36.25	38.20	35.61
Al2O3	18.90	19.36	19.38	19.55	19.15	20.58	19.37
TiO2	1.44	1.44	1.29	1.31	1.29	1.24	1.33
MgO	11.50	12.13	12.26	12.58	12.14	10.99	12.41
FeO	16.51	16.58	16.46	16.71	16.40	16.40	17.33
MnO	0.01	0.06	0.00	0.06	0.05	0.02	0.07
CaO	0.08	0.05	0.06	0.07	0.08	0.00	0.00
Na2O	0.26	0.27	0.32	0.16	0.26	0.33	0.18
K2O	8.37	8.39	8.21	8.76	8.34	8.83	8.24
Total	93.10	95.14	94.39	96.37	93.96	96.60	94.53
Si	5.492	5.485	5.462	5.471	5.469	5.574	5.367
Aliv	2.508	2.515	2.538	2.529	2.531	2.426	2.633
Alvi	0.890	0.883	0.888	0.863	0.875	1.114	0.809
Ti	0.167	0.163	0.147	0.146	0.148	0.138	0.152
Mg	2.614	2.690	2.739	2.759	2.730	2.391	2.787
Fe2+	2.105	2.064	2.064	2.056	2.069	2.002	2.184
Mn	0.001	0.008	0.000	0.007	0.006	0.003	0.009
Sum Oct	5.777	5.808	5.838	5.831	5.828	5.648	5.941
Ca	0.013	0.008	0.010	0.011	0.013	0.000	0.000
Na	0.076	0.079	0.093	0.047	0.076	0.094	0.052
K	1.629	1.593	1.570	1.644	1.605	1.644	1.585
Sum A	1.718	1.680	1.673	1.702	1.694	1.738	1.637
(OH)	0.000	0.000	0.000	0.000	0.000	0.000	0.000
Fe/Fe+Mg	0.446	0.434	0.430	0.427	0.431	0.456	0.439
X(Ca)	0.008	0.005	0.006	0.006	0.008	0.000	0.000
X(Na)	0.044	0.047	0.056	0.028	0.045	0.054	0.032
X(K)	0.948	0.948	0.938	0.966	0.947	0.946	0.968

Appendix 7: Sample PM-9b (cont.)

	-------MATRIX BIOTITE--------			
	PM9B/ 2/1A MX BI	PM9B/ 2/1B MX BI	PM9B/ 2/1C MX BI	(AVG) PM9B/ 2/1MX BI AV
SiO2	37.58	37.20	36.29	37.03
Al2O3	19.72	19.55	19.27	19.52
TiO2	1.38	1.36	1.32	1.35
MgO	12.34	11.95	11.77	12.02
FeO	16.92	16.90	15.82	16.55
MnO	0.09	0.07	0.05	0.07
CaO	0.00	0.00	0.00	0.00
Na2O	0.32	0.41	0.26	0.33
K2O	8.92	8.77	9.02	8.90
Total	97.28	96.21	93.82	95.77
Si	5.484	5.492	5.487	5.488
Aliv	2.516	2.508	2.513	2.512
Alvi	0.877	0.895	0.922	0.898
Ti	0.153	0.152	0.152	0.152
Mg	2.684	2.630	2.653	2.656
Fe2+	2.065	2.086	2.001	2.051
Mn	0.011	0.009	0.007	0.009
Sum Oct	5.790	5.772	5.735	5.766
Ca	0.000	0.000	0.000	0.000
Na	0.091	0.117	0.077	0.095
K	1.660	1.652	1.740	1.683
Sum A	1.751	1.769	1.817	1.778
(OH)	0.000	0.000	0.000	0.000
Fe/Fe+Mg	0.435	0.442	0.430	0.436
X(Ca)	0.000	0.000	0.000	0.000
X(Na)	0.052	0.066	0.042	0.053
X(K)	0.948	0.934	0.958	0.947

Appendix 7: Sample PM-9b (cont.)

	-------MATRIX MUSCOVITE-------			
				(AVG)
	PM9B/ 3/2A MX MU	PM9B/ 3/2B MX MU	PM9B/ 3/2C MX MU	PM9B/ 3/2AV MX MU
SiO2	49.01	47.40	47.56	47.99
Al2O3	37.57	36.41	36.12	36.70
TiO2	0.37	0.36	0.40	0.38
MgO	0.71	0.79	0.84	0.78
FeO	0.89	0.93	0.96	0.93
MnO	0.03	0.00	0.00	0.00
CaO	0.00	0.00	0.00	0.00
Na2O	1.18	1.26	1.05	1.17
K2O	9.36	9.15	9.27	9.26
Total	99.12	96.31	96.21	97.20
Si	6.198	6.179	6.206	6.195
Aliv	1.802	1.821	1.794	1.805
Alvi	3.799	3.775	3.763	3.780
Ti	0.036	0.036	0.040	0.037
Mg	0.134	0.154	0.164	0.150
Fe2+	0.094	0.101	0.105	0.100
Mn	0.003	0.000	0.000	0.000
Sum Oct	4.066	4.066	4.072	4.067
Ca	0.000	0.000	0.000	0.000
Na	0.290	0.319	0.266	0.292
K	1.510	1.522	1.544	1.525
Sum A	1.800	1.841	1.810	1.817
(OH)	0.000	0.000	0.000	0.000
Fe/Fe+Mg	0.412	0.396	0.390	0.400
X(Ca)	0.000	0.000	0.000	0.000
X(Na)	0.161	0.173	0.147	0.161
X(K)	0.839	0.827	0.853	0.839

Appendix 7: Sample PM-9b (cont.)

	-----MATRIX PLAGIOCLASES-----			
	(CORE)	(--------RIM-------)		
	PM9B 1/5A MX PL	PM9B 1/5B MX PL	PM9B 1/5C PL RI	PM9B 1/5D PL RI
SiO2	58.08	60.67	58.08	58.82
Al2O3	25.78	24.55	24.69	24.95
FeO	0.08	0.08	0.10	0.11
CaO	7.14	5.89	6.35	5.75
Na2O	7.52	7.98	7.50	7.95
K2O	0.03	0.07	0.09	0.40
Total	98.63	99.24	96.81	97.97
Si	2.628	2.712	2.672	2.674
Al	1.375	1.294	1.339	1.337
Fe2+	0.003	0.003	0.004	0.004
Ca	0.346	0.282	0.313	0.280
Na	0.660	0.692	0.669	0.701
K	0.002	0.004	0.005	0.023
Ca/Ca+Na	0.344	0.290	0.319	0.285
Al*/SiAl	0.374	0.292	0.335	0.333
An	0.343	0.288	0.317	0.279
Ab	0.655	0.708	0.678	0.698
Or	0.002	0.004	0.005	0.023

Appendix 7: Sample PM-9b (cont.)

	PLAGIOCLASE INCLUSIONS IN GARNETS								
	(CORE)				(RIM)		(OTHER GARNET---RIMS)		
	PM9B 1/2E PL IN	PM9B 1/2F CORE	PM9B 1/2G PL IN	PM9B 1/2H PL IN	PM9B 1/2I RIM P	PM9B 1/2J PL IN	PM9B V/1A PL IN	PM9B V/1B PL IN	PM9B V/2A PL IN
SiO2	56.55	57.61	56.82	58.17	57.03	54.78	56.95	55.44	57.42
Al2O3	26.40	26.36	26.72	26.60	26.31	25.03	24.76	23.53	24.56
FeO	0.53	0.49	0.48	0.48	0.82	0.68	0.33	1.05	0.47
CaO	8.40	8.15	8.42	8.26	8.05	7.82	6.63	5.99	6.72
Na2O	6.89	6.70	6.85	7.17	6.77	6.52	7.31	7.00	7.17
K2O	0.07	0.17	0.07	0.05	0.05	0.17	0.08	0.03	0.07
Total	98.83	99.47	99.36	100.73	99.03	95.00	96.07	93.04	96.40
Si	2.571	2.653	2.568	2.591	2.585	2.590	2.645	2.662	2.657
Al	1.415	1.431	1.424	1.397	1.406	1.395	1.356	1.332	1.340
Fe2+	0.020	0.019	0.018	0.018	0.031	0.027	0.013	0.042	0.018
Ca	0.409	0.402	0.408	0.394	0.391	0.396	0.330	0.308	0.333
Na	0.607	0.598	0.600	0.619	0.595	0.598	0.658	0.652	0.643
K	0.004	0.010	0.004	0.003	0.003	0.010	0.005	0.002	0.004
Ca/Ca+Na	0.403	0.402	0.405	0.389	0.397	0.398	0.334	0.321	0.341
Al*/SiAl	0.421	0.398	0.427	0.402	0.410	0.401	0.356	0.334	0.341
An	0.401	0.398	0.403	0.388	0.395	0.394	0.332	0.320	0.340
Ab	0.595	0.592	0.593	0.609	0.602	0.596	0.663	0.678	0.656
Or	0.004	0.010	0.004	0.003	0.003	0.010	0.005	0.002	0.004

	MATRIX PLAGIOCLASES						
	PM9B 1/4A MX PL	PM9B 1/4D MX PL	PM9B 1/4E MX PL	PM9B 1/4F MX PL	PM9B 1/4G MX PL	PM9B 1/4H MX PL	PM9B 1/4I MX PL
SiO2	61.47	61.08	61.10	62.66	60.57	61.85	60.13
Al2O3	23.19	23.55	23.45	25.00	25.43	24.45	24.14
FeO	0.27	0.37	0.24	0.19	0.24	0.33	0.42
CaO	4.63	4.67	4.87	5.14	6.28	5.01	5.49
Na2O	9.06	8.88	8.66	9.38	8.30	8.85	8.44
K2O	0.05	0.07	0.07	0.05	0.07	0.14	0.09
Total	98.68	98.62	98.39	102.42	100.89	100.63	98.71
Si	2.763	2.748	2.753	2.719	2.675	2.729	2.711
Al	1.229	1.249	1.246	1.279	1.324	1.272	1.283
Fe2+	0.010	0.014	0.009	0.007	0.009	0.012	0.016
Ca	0.223	0.225	0.235	0.239	0.297	0.237	0.265
Na	0.790	0.775	0.757	0.789	0.711	0.757	0.738
K	0.003	0.004	0.004	0.003	0.004	0.008	0.005
Ca/Ca+Na	0.220	0.225	0.237	0.232	0.295	0.238	0.264
Al*/SiAl	0.231	0.250	0.246	0.280	0.324	0.272	0.285
An	0.219	0.224	0.236	0.232	0.293	0.237	0.263
Ab	0.778	0.772	0.760	0.765	0.703	0.755	0.732
Or	0.003	0.004	0.004	0.003	0.004	0.008	0.005

Appendix 7: Sample PM-9b (cont.)

LAWSONITE INCLUSION (?)

	PM9B 1/3A	PM9B 1/3B
SiO2	41.65	43.60
Al2O3	33.08	34.31
FeO	0.46	0.50
CaO	18.26	17.20
Na2O	1.06	1.39
K2O	0.10	0.13
Total	94.60	97.13
Si	2.046	2.074
Al	1.916	1.924
Fe2+	0.019	0.020
Ca	0.961	0.877
Na	0.101	0.128
K	0.006	0.008
Ca/Ca+Na	0.905	0.873
Al*/SiAl	0.952	0.926
An	0.900	0.866
Ab	0.095	0.126
Or	0.006	0.008

Appendix 7: Sample PM-9b (cont.)

	---MATRIX CHLORITE---		
	PM9B 3/1A MX CH	PM9B 3/1B MX CH	PM9B 3/1C MX CH
SiO2	24.56	24.42	25.53
Al2O3	23.61	24.02	24.36
MgO	17.36	16.86	18.00
FeO	21.27	20.88	21.10
MnO	0.05	0.08	0.05
CaO	0.00	0.00	0.00
Total	86.86	86.26	89.04
Si	2.190	2.199	2.209
Al	2.482	2.550	2.485
Mg	2.307	2.263	2.322
Fe2+	1.586	1.573	1.527
Mn	0.004	0.006	0.004
Ca	0.000	0.000	0.000
Fe/Fe+Mg	0.407	0.410	0.397

Appendix 7: Sample PM-11c

--------------GARNET AT PLAGIOCLASE INCLUSIONS------------

	PM11C 2/5A GAR@P	PM11C 2/5B GAR@P	PM11C 2/5C GAR@P	PM11C 2/5D GAR@P	PM11C 2/6A GAR@P	PM11C 2/6B GAR@P	PMM1C 2/6C GAR@P	PM11C 2/6D GAR@P
SiO2	36.86	37.25	36.98	36.69	37.07	37.02	36.83	37.13
Al2O3	21.43	20.97	21.26	21.18	21.46	21.47	21.24	21.60
MgO	2.22	2.40	2.19	2.05	2.69	2.25	2.54	2.89
FeO	26.93	26.48	27.32	26.24	31.33	31.90	31.66	31.96
MnO	8.20	7.54	8.34	8.19	4.46	4.99	4.70	4.35
CaO	4.35	4.52	4.14	4.62	3.14	2.79	3.10	3.07
Total	99.98	99.15	100.22	99.15	100.14	100.42	100.06	101.00
Si	2.967	3.010	2.975	2.989	2.976	2.976	2.970	2.961
Al	2.034	1.997	2.016	2.023	2.031	2.035	2.019	2.031
Mg	0.266	0.289	0.262	0.247	0.322	0.270	0.305	0.344
Fe2+	1.813	1.789	1.838	1.778	2.104	2.145	2.135	2.132
Mn	0.559	0.516	0.568	0.562	0.303	0.340	0.321	0.294
Ca	0.375	0.391	0.357	0.401	0.270	0.240	0.268	0.262
Fe/Fe+Mg	0.872	0.861	0.875	0.878	0.867	0.888	0.875	0.861
Pyrope	0.088	0.097	0.087	0.083	0.107	0.090	0.101	0.113
Alman	0.602	0.599	0.608	0.595	0.702	0.716	0.705	0.703
Spess	0.186	0.173	0.188	0.188	0.101	0.114	0.106	0.097
Gross	0.124	0.131	0.118	0.134	0.090	0.080	0.088	0.086

--------GARNET AT PLAG INCLUSIONS------------

	PM11C 2/7A GAR@P	PM11C 2/7B GAR@P	PM11C 2/8A GAR@P	PM11C 2/8BG AR@PL	PM11C 2/8C GAR@P	PM11C 2/8AV GAR@P
SiO2	36.82	36.99	38.38	35.77	38.46	37.53
Al2O3	21.20	21.32	21.30	20.44	21.63	21.12
MgO	2.72	2.76	3.03	2.81	2.81	2.88
FeO	28.13	29.63	30.19	30.00	30.33	30.17
MnO	6.60	6.47	6.33	7.10	7.02	6.82
CaO	2.95	2.89	3.31	3.09	3.00	3.14
Total	98.42	100.05	102.54	99.21	103.26	101.67
Si	2.996	2.976	3.008	2.934	2.999	2.981
Al	2.034	2.022	1.968	1.977	1.988	1.973
Mg	0.330	0.331	0.354	0.344	0.327	0.341
Fe2+	1.914	1.994	1.979	2.058	1.978	2.004
Mn	0.455	0.441	0.420	0.493	0.464	0.459
Ca	0.257	0.249	0.278	0.272	0.251	0.267
Fe/Fe+Mg	0.853	0.858	0.848	0.857	0.858	0.855
Pyrope	0.112	0.110	0.117	0.109	0.108	0.111
Alman	0.647	0.661	0.653	0.650	0.655	0.653
Spess	0.154	0.146	0.139	0.156	0.154	0.149
Gross	0.087	0.083	0.092	0.086	0.083	0.087

Appendix 7: Sample PM-11c (cont.)

-----------------GARNET RIM ANALYSES-----------------

	PM11C 1/10 GAR R	PM11C 1/44 GAR R	PM11C 1/60 GAR R	PM11C 1/73 GAR R	PM11C 1/78 GAR R	PM11C 1/81 GAR R	PM11C 1/45 GAR R
SiO2	37.62	37.67	37.84	37.63	37.76	37.58	37.48
Al2O3	21.27	21.30	21.40	21.28	21.36	21.25	21.19
MgO	2.90	2.83	3.00	2.75	2.91	3.00	2.77
FeO	32.61	32.75	32.35	33.48	32.87	33.02	32.76
MnO	3.78	3.87	3.98	3.86	3.66	3.59	3.58
CaO	2.56	2.53	2.66	2.04	2.61	2.21	2.66
Total	100.75	100.95	101.24	101.04	101.17	100.65	100.43
Si	3.000	3.000	3.000	3.000	3.000	3.000	3.000
Al	2.000	2.000	2.000	2.000	2.000	2.000	2.000
Mg	0.345	0.336	0.354	0.327	0.345	0.357	0.330
Fe2+	2.175	2.181	2.145	2.232	2.184	2.205	2.193
Mn	0.255	0.261	0.267	0.261	0.246	0.243	0.243
Ca	0.219	0.216	0.228	0.174	0.222	0.189	0.228
Fe/Fe+Mg	0.863	0.867	0.858	0.872	0.864	0.861	0.869
Pyrope	0.115	0.112	0.118	0.109	0.115	0.119	0.110
Alman	0.726	0.728	0.716	0.745	0.729	0.736	0.732
Spess	0.085	0.087	0.089	0.087	0.082	0.081	0.081
Gross	0.073	0.072	0.076	0.058	0.074	0.063	0.076

-----GARNET RIM ANALYSES-----

	PM11C 1/99 GAR R	PM11C 1/51 GAR R	PM11C 1/62 GAR R	PM11C 1/92 GAR R
SiO2	38.02	37.52	37.09	37.61
Al2O3	21.50	21.22	20.97	21.27
MgO	3.06	3.07	2.49	2.90
FeO	32.41	32.80	33.17	33.37
MnO	3.99	3.63	3.94	3.46
CaO	2.70	2.24	2.08	2.18
Total	101.69	100.48	99.74	100.80
Si	3.000	3.000	3.000	3.000
Al	2.000	2.000	2.000	2.000
Mg	0.360	0.366	0.300	0.345
Fe2+	2.139	2.193	2.244	2.226
Mn	0.267	0.246	0.270	0.234
Ca	0.228	0.192	0.180	0.186
Fe/Fe+Mg	0.856	0.857	0.882	0.866
Pyrope	0.120	0.122	0.100	0.115
Alman	0.714	0.732	0.749	0.744
Spess	0.089	0.082	0.090	0.078
Gross	0.076	0.064	0.060	0.062

Appendix 7: Sample PM-11c (cont.)

	PLAGIOCLASE INCLUSIONS IN GARNET								
	PM11C 2/1A PL IN	PM11C 2/1B PL IN	PM11C 2/1C PL IN	PM11C 2/1D PL IN	PM11C 2/2A PL IN	PM11C 2/2B PL IN	PM11C 2/2C PL IN	PM11C 2/2D PL IN	PM11C 2/2E PL IN
SiO2	53.76	56.41	60.08	54.22	57.08	61.59	56.94	57.56	59.64
Al2O3	25.02	26.29	23.77	25.14	26.46	24.67	26.77	26.73	24.74
FeO	0.67	0.44	0.34	0.70	0.71	0.44	0.42	0.69	0.29
CaO	8.31	8.48	7.39	8.21	8.25	7.85	8.45	8.33	7.96
Na2O	6.04	6.48	6.22	6.14	6.61	6.46	6.54	6.67	6.47
K2O	0.07	0.05	0.09	0.07	0.07	0.07	0.07	0.07	0.07
Total	93.87	98.16	97.90	94.48	99.19	101.08	99.19	100.05	99.17
Si	2.573	2.577	2.723	2.577	2.582	2.708	2.573	2.581	2.678
Al	1.412	1.416	1.270	1.409	1.411	1.279	1.426	1.413	1.310
Fe2+	0.027	0.017	0.013	0.028	0.027	0.016	0.016	0.026	0.011
Ca	0.426	0.415	0.359	0.418	0.400	0.370	0.409	0.400	0.383
Na	0.561	0.574	0.547	0.566	0.580	0.551	0.573	0.580	0.563
K	0.004	0.003	0.005	0.004	0.004	0.004	0.004	0.004	0.004
Ca/Ca+Na	0.432	0.420	0.396	0.425	0.408	0.402	0.416	0.408	0.405
Al*/SiAl	0.418	0.419	0.272	0.415	0.414	0.283	0.426	0.415	0.314
An	0.430	0.418	0.394	0.423	0.407	0.400	0.415	0.407	0.403
Ab	0.566	0.579	0.600	0.573	0.589	0.596	0.581	0.589	0.593
Or	0.004	0.003	0.005	0.004	0.004	0.004	0.004	0.004	0.004

	PLAGIOCLASE INCLUSIONS IN GARNET								
	(CORE)	(----RIM----	----)	(CORE)	(RIM)	(CORE)	(RIM)		
	PM11C 2/3A PL IN	PM11C 2/3B PL IN	PM11C 2/3C PL IN	PM11C 2/4A PL IN	PM11C 2/4B PL IN	PM11C 2/4C PL IN	PM11C 2/4D PL IN	PM11C 1/4B PL IN	PM11C 1/4C PL IN
SiO2	59.20	54.99	58.64	58.11	58.10	57.14	55.73	60.86	57.35
Al2O3	25.12	23.91	24.84	25.44	25.14	24.60	22.51	26.31	25.71
FeO	0.96	3.81	1.40	0.58	0.89	0.59	1.14	0.94	4.15
CaO	6.44	5.65	6.20	6.91	6.56	6.79	5.41	6.75	5.96
Na2O	7.79	7.36	7.74	7.34	7.44	7.27	7.36	8.15	7.01
K2O	0.03	0.03	0.03	0.09	0.03	0.05	0.05	0.07	0.05
Total	99.54	95.75	98.85	98.46	98.17	96.44	92.19	103.07	100.23
Si	2.659	2.608	2.657	2.637	2.646	2.648	2.699	2.643	2.594
Al	1.330	1.337	1.327	1.361	1.350	1.344	1.285	1.347	1.371
Fe2+	0.036	0.151	0.053	0.022	0.034	0.023	0.046	0.034	0.157
Ca	0.310	0.287	0.301	0.336	0.320	0.337	0.281	0.314	0.289
Na	0.678	0.677	0.680	0.646	0.657	0.653	0.691	0.686	0.615
K	0.002	0.002	0.002	0.005	0.002	0.003	0.003	0.004	0.003
Ca/Ca+Na	0.314	0.298	0.307	0.342	0.328	0.340	0.289	0.314	0.320
Al*/SiAl	0.334	0.357	0.332	0.362	0.351	0.347	0.290	0.351	0.384
An	0.313	0.297	0.306	0.340	0.327	0.339	0.288	0.313	0.319
Ab	0.685	0.701	0.692	0.655	0.671	0.658	0.709	0.683	0.678
Or	0.002	0.002	0.002	0.005	0.002	0.003	0.003	0.004	0.003

Appendix 7: Sample PM-11c (cont.)

	PLAG INCL (RIM)	IN OTHER GAR (CORE)
	PM11C 2/7A PL IN	PM11C 2/7C PL IN
SiO2	58.19	59.53
Al2O3	25.54	25.63
FeO	0.88	0.83
CaO	7.10	7.09
Na2O	7.77	7.23
K2O	0.09	0.07
Total	99.56	100.37
Si	2.623	2.650
Al	1.357	1.345
Fe2+	0.033	0.031
Ca	0.343	0.338
Na	0.679	0.624
K	0.005	0.004
Ca/Ca+Na	0.336	0.351
Al*/SiAl	0.364	0.347
An	0.334	0.350
Ab	0.661	0.646
Or	0.005	0.004

Appendix 7: Sample PM-11c (cont.)

	MATRIX PLAGIOCLASE							
					(AVG)	(CORE)	(RIM)	(AVG)
	PM11C 1/3A PLAG	PM11C 1/3B PLAG	PM11C 1/3C PLAG	PM11C 1/3D PLAG	PM11C 1/3AV PLAG	PM11C MX/6A PL CO	PM11C MX/6B PL RI	PM11C M/6AV PLAG
SiO2	60.93	62.24	62.24	60.93	61.57	62.15	61.99	62.06
Al2O3	23.77	24.47	24.13	24.06	24.12	24.32	24.41	24.37
FeO	0.45	0.44	0.30	0.32	0.38	0.11	0.11	0.11
CaO	5.53	5.66	5.80	5.91	5.72	5.77	5.84	5.81
Na2O	8.22	8.33	8.03	8.13	8.18	8.53	8.15	8.34
K2O	0.07	0.09	0.09	0.09	0.09	0.12	0.07	0.11
Total	98.97	101.23	100.58	99.44	100.05	101.00	100.58	100.79
Si	2.735	2.731	2.744	2.724	2.733	2.733	2.733	2.733
Al	1.258	1.266	1.254	1.268	1.262	1.261	1.269	1.265
Fe2+	0.017	0.016	0.011	0.012	0.014	0.004	0.004	0.004
Ca	0.266	0.266	0.274	0.283	0.272	0.272	0.276	0.274
Na	0.715	0.709	0.686	0.705	0.704	0.727	0.697	0.712
K	0.004	0.005	0.005	0.005	0.005	0.007	0.004	0.006
Ca/Ca+Na	0.271	0.273	0.285	0.286	0.279	0.272	0.284	0.278
Al*/SiAl	0.260	0.267	0.255	0.270	0.263	0.263	0.268	0.266
An	0.270	0.271	0.284	0.285	0.277	0.270	0.282	0.276
Ab	0.726	0.723	0.711	0.710	0.718	0.723	0.713	0.718
Or	0.004	0.005	0.005	0.005	0.005	0.007	0.004	0.006

Appendix 7: Sample PM-11c (cont.)

	-----BIOTITE NEAR GARNET-----				--------MATRIX BIOTITE-------			
	PM11C 1/1A BIO N	PM11C 1/1B BIO N	PM11C 1/1D BIO N	PM11C 1/1AV BIO N	PM11C MX/5A BIO	PM11C MX/5B BIO	PM11C MX/5C BIO	PM11C M/5AV BIO
SiO2	36.27	36.23	37.57	36.29	37.62	37.41	37.89	37.64
Al2O3	19.57	19.48	19.64	19.20	19.59	19.71	19.80	19.69
TiO2	1.23	1.40	1.40	1.32	1.35	1.47	1.42	1.41
MgO	12.73	12.58	12.41	12.38	12.62	12.35	12.56	12.51
FeO	16.77	16.68	16.79	16.58	16.66	16.13	16.78	16.52
MnO	0.10	0.01	0.08	0.06	0.08	0.09	0.09	0.09
CaO	0.04	0.01	0.00	0.05	0.01	0.04	0.05	0.03
Na2O	0.17	0.16	0.09	0.15	0.14	0.12	0.43	0.23
K2O	8.27	8.84	9.11	8.67	8.80	8.73	8.54	8.69
Total	95.14	95.40	97.09	94.69	96.88	96.04	97.55	96.82
Si	5.407	5.402	5.492	5.444	5.499	5.501	5.496	5.499
Aliv	2.593	2.598	2.508	2.556	2.501	2.499	2.504	2.501
Alvi	0.847	0.825	0.876	0.840	0.875	0.918	0.881	0.891
Ti	0.139	0.159	0.156	0.150	0.150	0.164	0.156	0.157
Mg	2.829	2.795	2.704	2.768	2.749	2.706	2.714	2.723
Fe2+	2.091	2.080	2.052	2.080	2.037	1.984	2.036	2.019
Mn	0.012	0.001	0.010	0.008	0.010	0.011	0.011	0.011
Sum Oct	5.918	5.860	5.798	5.846	5.821	5.783	5.798	5.801
Ca	0.006	0.002	0.000	0.008	0.002	0.007	0.007	0.005
Na	0.049	0.047	0.026	0.043	0.041	0.034	0.121	0.066
K	1.573	1.682	1.698	1.660	1.641	1.638	1.580	1.619
Sum A	1.628	1.731	1.724	1.711	1.684	1.679	1.708	1.690
(OH)	0.000	0.000	0.000	0.000	0.000	0.000	0.000	0.000
Fe/Fe+Mg	0.425	0.427	0.431	0.429	0.426	0.423	0.429	0.426
X(Ca)	0.004	0.001	0.000	0.005	0.001	0.004	0.004	0.003
X(Na)	0.030	0.027	0.015	0.025	0.024	0.020	0.071	0.039
X(K)	0.966	0.972	0.985	0.970	0.974	0.976	0.925	0.958

Appendix 7: Sample PM-11c (cont.)

	-------MATRIX MUSCOVITE------			
	PM11C MX/4A MUSC	PM11C MX/4B MUSC	PM11C MX/4C MUSC	PM11C MX/4 AV MU
SiO2	47.31	47.53	47.97	47.61
Al2O3	36.51	36.57	36.81	36.63
TiO2	0.38	0.36	0.52	0.43
MgO	0.59	0.58	0.58	0.58
FeO	0.83	0.79	0.63	0.75
MnO	0.02	0.00	0.00	0.00
CaO	0.01	0.00	0.02	0.01
Na2O	1.68	1.61	1.64	1.64
K2O	8.80	8.60	8.67	8.69
Total	96.13	96.04	96.84	96.33
Si	6.173	6.193	6.195	6.187
Aliv	1.827	1.807	1.805	1.813
Alvi	3.789	3.811	3.799	3.800
Ti	0.038	0.036	0.051	0.042
Mg	0.115	0.112	0.112	0.113
Fe2+	0.091	0.086	0.068	0.081
Mn	0.002	0.000	0.000	0.000
Sum Oct	4.035	4.045	4.030	4.036
Ca	0.001	0.000	0.003	0.001
Na	0.424	0.407	0.410	0.413
K	1.465	1.430	1.428	1.441
Sum A	1.890	1.837	1.841	1.855
(OH)	0.000	0.000	0.000	0.000
Fe/Fe+Mg	0.442	0.434	0.378	0.418
X(Ca)	0.001	0.000	0.002	0.001
X(Na)	0.224	0.222	0.223	0.223
X(K)	0.775	0.778	0.776	0.777

Appendix 7: Sample PM-11c (cont.)

	PM11C 1/2A CHL 1	PM11C 1/2B CHL	PM11C 1/2C CHL	PM11C 1/2AV CHL
	-------MATRIX CHLORITE-------			
SiO2	24.99	26.45	25.88	25.77
Al2O3	23.94	24.60	24.21	24.26
TiO2	0.00	0.00	0.00	0.00
MgO	18.26	18.35	18.34	18.32
FeO	21.49	21.02	21.26	21.26
MnO	0.00	0.00	0.00	0.00
CaO	0.00	0.00	0.00	0.00
Na2O	0.00	0.00	0.00	0.00
K2O	0.00	0.00	0.00	0.00
Total	88.68	90.42	89.69	89.60
Si	5.088	5.240	5.187	5.172
Aliv	2.912	2.760	2.813	2.828
Alvi	2.836	2.986	2.908	2.911
Ti	0.000	0.000	0.000	0.000
Mg	5.542	5.419	5.480	5.479
Fe2+	3.660	3.482	3.564	3.568
Mn	0.000	0.000	0.000	0.000
Sum Oct	12.038	11.887	11.952	11.958
Ca	0.000	0.000	0.000	0.000
Na	0.000	0.000	0.000	0.000
K	0.000	0.000	0.000	0.000
Sum A	0.000	0.000	0.000	0.000
(OH)	0.000	0.000	0.000	0.000
Fe/Fe+Mg	0.398	0.391	0.394	0.394

Appendix 7: Sample 67-78a

	-GARNET IN STAUROLITE-			-----MATRIX GARNET-----		
	(RIM)	(RIM)	(CORE)	(--------RIM--------)		
	6778A 1/1A GAR R	6778A 1/1B GAR R	6778A 1/1D GAR C	6778A 2/1A MXGAR	6778A 2/1B MXGAR	6778A 2/1AV GAR R
SiO2	37.35	37.20	37.09	37.54	37.25	37.40
Al2O3	21.34	21.55	20.90	21.24	21.24	21.24
MgO	2.47	2.72	1.49	2.48	2.63	2.55
FeO	35.04	34.36	26.24	34.71	34.66	34.69
MnO	3.09	2.79	8.65	3.16	3.18	3.17
CaO	2.70	3.12	6.19	2.58	2.38	2.48
Total	101.99	101.75	100.56	101.71	101.34	101.53
Si	2.969	2.956	2.982	2.987	2.976	2.982
Al	2.000	2.019	1.981	1.992	2.000	1.996
Mg	0.293	0.322	0.179	0.294	0.313	0.303
Fe2+	2.330	2.283	1.764	2.310	2.316	2.313
Mn	0.208	0.188	0.589	0.213	0.215	0.214
Ca	0.230	0.266	0.533	0.220	0.204	0.212
Fe/Fe+Mg	0.888	0.876	0.908	0.887	0.881	0.884
Pyrope	0.096	0.105	0.058	0.097	0.103	0.100
Alman	0.761	0.746	0.576	0.761	0.760	0.760
Spess	0.068	0.061	0.192	0.070	0.071	0.070
Gross	0.075	0.087	0.174	0.072	0.067	0.070

Appendix 7: Sample 67-78a (cont.)

	--STAUROLITE WITH	GARNET	INCLUSION--	
	(AT GAR)	(CORE)	(RIM)	(AVG)
	6778A 1/2A ST@GA	6778A 1/2B ST CO	6778A 1/2C ST RI	6778A 1/2AV STAU
SiO2	27.21	26.40	27.29	26.97
Al2O3	53.71	55.23	53.54	54.16
TiO2	0.59	0.45	0.51	0.52
MgO	1.55	1.73	1.89	1.72
FeO	13.47	13.03	13.09	13.20
MnO	0.20	0.22	0.19	0.20
ZnO	1.15	1.29	1.18	1.21
CaO	0.00	0.00	0.00	0.00
Na2O	0.00	0.00	0.00	0.00
K2O	0.00	0.00	0.00	0.00
Total	97.88	98.35	97.69	97.98
Si	3.796	3.663	3.808	3.756
Al	8.832	9.033	8.806	8.891
Ti	0.063	0.047	0.054	0.055
Mg	0.322	0.358	0.393	0.358
Fe2+	1.571	1.512	1.527	1.537
Mn	0.024	0.026	0.022	0.024
Zn	0.118	0.132	0.122	0.124
Ca	0.000	0.000	0.000	0.000
Na	0.000	0.000	0.000	0.000
K	0.000	0.000	0.000	0.000
Fe/Fe+Mg	0.830	0.809	0.795	0.811

Appendix 7: Sample 67-78a (cont.)

MATRIX BIOTITE

	6778A 2/2A MX BIO
SiO2	35.18
Al2O3	18.70
TiO2	1.50
MgO	11.44
FeO	18.22
MnO	0.00
CaO	0.00
Na2O	0.18
K2O	8.40
Total	93.62
Si	5.392
Aliv	2.608
Alvi	0.771
Ti	0.175
Mg	2.613
Fe2+	2.336
Mn	0.000
Sum Oct	5.895
Ca	0.000
Na	0.054
K	1.642
Sum A	1.696
(OH)	0.000
Fe/Fe+Mg	0.472
X(Ca)	0.000
X(Na)	0.032
X(K)	0.968

Appendix 8: Northey Hill Line: Microprobe Analyses; Sample D84-1c

-----------------GARNET RIM ANALYSES----------------

	D841C 1/111 GAR R	D841C 1/176 GAR R	D841C 1/185 GAR R	D841C 1/253 GAR R	D841C 1/254 GAR R	D841C 1/263 GAR R	D841C 1/190 GAR R
SiO2	36.84	37.02	37.01	36.65	36.70	36.61	36.69
Al2O3	20.83	20.94	20.93	20.73	20.75	20.70	20.75
MgO	1.43	1.44	1.49	1.60	1.58	1.50	1.48
FeO	32.47	32.98	32.88	32.25	32.25	32.35	32.47
MnO	6.87	6.60	6.51	6.40	6.54	6.48	6.63
CaO	1.55	1.49	1.59	1.68	1.64	1.64	1.54
Total	100.00	100.47	100.42	99.31	99.47	99.27	99.55
Si	3.000	3.000	3.000	3.000	3.000	3.000	3.000
Al	2.000	2.000	2.000	2.000	2.000	2.000	2.000
Mg	0.174	0.174	0.180	0.195	0.192	0.183	0.180
Fe2+	2.211	2.235	2.229	2.208	2.205	2.217	2.220
Mn	0.474	0.453	0.447	0.444	0.453	0.450	0.459
Ca	0.135	0.129	0.138	0.147	0.144	0.144	0.135
Fe/Fe+Mg	0.927	0.928	0.925	0.919	0.920	0.924	0.925
Pyrope	0.058	0.058	0.060	0.065	0.064	0.061	0.060
Alman	0.738	0.747	0.744	0.737	0.736	0.740	0.741
Spess	0.158	0.151	0.149	0.148	0.151	0.150	0.153
Gross	0.045	0.043	0.046	0.049	0.048	0.048	0.045

Appendix 8: Sample D84-1c (cont.)

	-----BIOTITE NEAR GARNET-----				---MATRIX BIOTITE---		
	D841C 1/1A BIO N	D841C 1/1B BIO N	D841C 1/1C BIO N	D841C 1/1AV BIO N	D841C 2/1A MX BI	D841C 2/1B MX BI	D841C 2/1AV MX BI
SiO2	35.68	35.35	35.09	35.37	34.85	35.66	35.25
Al2O3	19.05	18.57	18.67	18.76	19.16	19.30	19.23
TiO2	1.71	1.57	1.68	1.65	1.77	1.78	1.78
MgO	8.34	7.98	8.47	8.27	7.89	7.98	7.94
FeO	22.16	21.36	22.84	22.12	22.47	22.48	22.47
MnO	0.13	0.13	0.16	0.14	0.14	0.11	0.12
CaO	0.00	0.00	0.00	0.00	0.00	0.00	0.00
Na2O	0.10	0.10	0.05	0.08	0.12	0.11	0.11
K2O	8.55	8.25	8.35	8.39	8.57	8.63	8.60
Total	95.73	93.31	95.31	94.78	94.97	96.04	95.50
Si	5.441	5.509	5.399	5.449	5.380	5.427	5.404
Aliv	2.559	2.491	2.601	2.551	2.620	2.573	2.596
Alvi	0.866	0.921	0.786	0.857	0.867	0.889	0.878
Ti	0.198	0.186	0.196	0.193	0.207	0.206	0.207
Mg	1.896	1.854	1.943	1.898	1.816	1.810	1.813
Fe2+	2.826	2.784	2.939	2.850	2.901	2.861	2.881
Mn	0.017	0.017	0.021	0.018	0.018	0.014	0.016
Sum Oct	5.803	5.762	5.885	5.816	5.809	5.780	5.795
Ca	0.000	0.000	0.000	0.000	0.000	0.000	0.000
Na	0.029	0.031	0.015	0.025	0.035	0.033	0.034
K	1.663	1.640	1.640	1.648	1.688	1.675	1.681
Sum A	1.692	1.671	1.655	1.673	1.723	1.708	1.715
(OH)	0.000	0.000	0.000	0.000	0.000	0.000	0.000
Fe/Fe+Mg	0.598	0.600	0.602	0.600	0.615	0.613	0.614
X(Ca)	0.000	0.000	0.000	0.000	0.000	0.000	0.000
X(Na)	0.017	0.019	0.009	0.015	0.020	0.019	0.020
X(K)	0.983	0.981	0.991	0.985	0.980	0.981	0.980

Appendix 8: Sample D84-1c (cont.)

	------MATRIX MUSCOVITE-------			
	D841C 1/2A MUS N	D841C 1/2B MUS N	D841C 1/2C MUS N	D841C 1/2AV MUS N
SiO2	47.28	46.69	46.32	46.77
Al2O3	34.73	34.63	35.53	34.96
TiO2	0.34	0.33	0.31	0.33
MgO	0.73	0.63	0.53	0.63
FeO	1.38	1.28	1.30	1.32
MnO	0.00	0.00	0.00	0.00
CaO	0.00	0.00	0.00	0.00
Na2O	0.74	0.84	0.84	0.80
K2O	9.44	9.49	9.49	9.47
Total	94.63	93.90	94.31	94.28
Si	6.287	6.263	6.188	6.246
Aliv	1.713	1.737	1.812	1.754
Alvi	3.731	3.740	3.784	3.751
Ti	0.034	0.034	0.031	0.033
Mg	0.145	0.126	0.106	0.126
Fe2+	0.153	0.144	0.145	0.147
Mn	0.000	0.000	0.000	0.000
Sum Oct	4.063	4.044	4.066	4.057
Ca	0.000	0.000	0.000	0.000
Na	0.190	0.218	0.217	0.208
K	1.601	1.624	1.617	1.614
Sum A	1.791	1.842	1.834	1.822
(OH)	0.000	0.000	0.000	0.000
Fe/Fe+Mg	0.513	0.533	0.578	0.538
X(Ca)	0.000	0.000	0.000	0.000
X(Na)	0.106	0.118	0.118	0.114
X(K)	0.894	0.882	0.882	0.886

Appendix 8: Sample D84-1c (cont.)

	MATRIX PLAGIOCLASE							
			(RIM)			(RIM)		
	D841C 2/2A MX PL	D841C 2/2B PLAG	D841C 2/2C PL RI	D841C 2/2AV PL CO	D841C 2/2D PLAG	D841C 2/2E PL RI	D841C 2/2F PLAG	D841C 2/2G PLAG
SiO2	61.75	61.46	62.09	61.76	62.86	63.33	62.08	63.07
Al2O3	24.06	23.61	23.50	23.73	23.58	23.53	23.74	23.81
FeO	0.05	0.00	0.05	0.03	0.22	0.11	0.13	0.08
CaO	5.32	5.00	4.95	5.10	4.97	4.70	5.37	4.92
Na2O	9.38	8.88	8.73	8.99	9.28	9.16	8.74	9.02
K2O	0.11	0.11	0.14	0.12	0.11	0.09	0.11	0.11
Total	100.67	99.07	99.46	99.73	101.01	100.92	100.17	101.00
Si	2.730	2.751	2.765	2.749	2.763	2.778	2.751	2.766
Al	1.254	1.246	1.234	1.245	1.222	1.217	1.240	1.231
Fe2+	0.002	0.000	0.002	0.001	0.008	0.004	0.005	0.003
Ca	0.252	0.240	0.236	0.243	0.234	0.221	0.255	0.231
Na	0.804	0.771	0.754	0.776	0.791	0.779	0.751	0.767
K	0.006	0.006	0.008	0.007	0.006	0.005	0.006	0.006
Ca/Ca+Na	0.239	0.237	0.238	0.238	0.228	0.221	0.253	0.231
Al*/SiAl	0.258	0.247	0.234	0.246	0.225	0.218	0.242	0.232
An	0.237	0.236	0.236	0.237	0.227	0.220	0.252	0.230
Ab	0.757	0.758	0.756	0.756	0.767	0.775	0.742	0.764
Or	0.006	0.006	0.008	0.007	0.006	0.005	0.006	0.006

	(RIM)		(CORE)				
	D841C 2/2H PLAG	D841C 2/2I PLAG	D841C 2/2J PLAG	D841C 2/2K PLAG	D841C 2/2L PLAG	D841C 2/2M PLAG	D841C 2/2AV PLAG
SiO2	63.46	62.92	62.02	63.69	64.03	62.82	63.01
Al2O3	22.72	23.80	23.73	23.21	23.01	23.75	23.48
FeO	0.08	0.05	0.30	0.11	0.14	0.24	0.16
CaO	3.98	4.99	5.28	4.31	4.44	5.06	4.81
Na2O	9.30	8.94	8.62	9.18	9.42	8.99	9.06
K2O	0.12	0.09	0.14	0.11	0.11	0.14	0.11
Total	99.66	100.79	100.09	100.60	101.14	101.00	100.64
Si	2.812	2.765	2.751	2.798	2.802	2.760	2.775
Al	1.187	1.233	1.241	1.202	1.187	1.230	1.219
Fe2+	0.003	0.002	0.011	0.004	0.005	0.009	0.006
Ca	0.189	0.235	0.251	0.203	0.208	0.238	0.227
Na	0.799	0.762	0.741	0.782	0.799	0.766	0.774
K	0.007	0.005	0.008	0.006	0.006	0.008	0.006
Ca/Ca+Na	0.191	0.236	0.253	0.206	0.207	0.237	0.227
Al*/SiAl	0.187	0.233	0.243	0.202	0.189	0.232	0.220
An	0.190	0.235	0.251	0.205	0.205	0.235	0.225
Ab	0.803	0.760	0.741	0.789	0.789	0.757	0.769
Or	0.007	0.005	0.008	0.006	0.006	0.008	0.006

Appendix 8: Sample D84-1c (cont.)

	----------MATRIX PLAGIOCLASE NEAR GARNET----------						
	(CORE)	(RIM)	(AVG)	(RIM)		(CORE)	(AVG)
	D841C 1/1A PL NR	D841C 1/1B PL NR	D841C 1/1AV PL NR	D841C 1/2A PL NR	D841C 1/2B PL NR	D841C 1/2C PL NR	D841C 1/2AV PL NR
SiO2	63.55	65.61	64.60	67.26	63.79	63.70	64.93
Al2O3	23.95	22.40	23.17	21.47	24.01	23.94	23.16
FeO	0.11	0.25	0.17	0.11	0.22	0.14	0.14
CaO	4.94	3.42	4.17	1.64	4.97	4.93	3.85
Na2O	9.48	9.85	9.67	10.79	9.08	8.90	9.60
K2O	0.13	0.16	0.14	0.22	0.14	0.13	0.16
Total	102.15	101.69	101.92	101.49	102.22	101.74	101.84
Si	2.762	2.848	2.805	2.910	2.767	2.772	2.816
Al	1.227	1.146	1.186	1.095	1.228	1.228	1.184
Fe2+	0.004	0.009	0.006	0.004	0.008	0.005	0.005
Ca	0.230	0.159	0.194	0.076	0.231	0.230	0.179
Na	0.799	0.829	0.814	0.905	0.764	0.751	0.807
K	0.007	0.009	0.008	0.012	0.008	0.007	0.009
Ca/Ca+Na	0.224	0.161	0.192	0.077	0.232	0.234	0.182
Al*/SiAl	0.230	0.147	0.188	0.095	0.229	0.228	0.184
An	0.222	0.159	0.191	0.077	0.230	0.233	0.180
Ab	0.771	0.831	0.801	0.911	0.762	0.760	0.811
Or	0.007	0.009	0.008	0.012	0.008	0.007	0.009

	(--------RIM--------)			(---CORE----)	
	D841C 1/3A PL RI	D841C 1/3CP L RIM	D841C 1/3E PL RI	D841C 1/3B PL CO	D841C 1/3D PL CO
SiO2	63.42	63.37	64.58	63.65	61.49
Al2O3	22.08	22.35	21.03	22.35	22.98
FeO	2.02	0.51	0.11	0.49	0.37
CaO	2.88	3.11	2.59	3.01	3.84
Na2O	10.10	10.11	9.93	10.10	9.17
K2O	0.05	0.09	0.04	0.07	0.16
Total	100.56	99.54	99.27	99.67	98.00
Si	2.811	2.818	2.889	2.824	2.778
Al	1.154	1.172	1.109	1.169	1.224
Fe2+	0.075	0.019	0.004	0.018	0.014
Ca	0.137	0.148	0.124	0.143	0.186
Na	0.868	0.872	0.861	0.869	0.803
K	0.003	0.005	0.002	0.004	0.009
Ca/Ca+Na	0.136	0.145	0.126	0.141	0.188
Al*/SiAl	0.160	0.174	0.109	0.170	0.224
An	0.136	0.144	0.126	0.141	0.186
Ab	0.861	0.851	0.872	0.855	0.805
Or	0.003	0.005	0.002	0.004	0.009

Appendix 8: Sample D84-1d-2

	GARNET RIM ANALYSES						
	D841D 1/36 GAR R	D841D 1/82 GAR R	D841D 1/92 GAR R	D841D 1/131 GAR R	D841D 1/134 GAR R	D841D 1/146 GAR R	D841D 1/154 GAR R
SiO2	36.75	36.85	36.38	36.95	36.47	36.67	37.03
Al2O3	20.78	20.84	20.57	20.89	20.62	20.73	20.94
MgO	1.18	1.24	1.22	1.19	1.15	1.11	1.24
FeO	36.12	36.13	35.84	36.27	36.50	36.48	36.75
MnO	1.74	1.70	1.55	1.61	1.64	1.60	1.57
CaO	3.02	3.06	2.95	3.03	2.55	2.87	2.83
Total	99.58	99.80	98.51	99.95	98.93	99.46	100.36
Si	3.000	3.000	3.000	3.000	3.000	3.000	3.000
Al	2.000	2.000	2.000	2.000	2.000	2.000	2.000
Mg	0.144	0.150	0.150	0.144	0.141	0.135	0.150
Fe2+	2.466	2.460	2.472	2.463	2.511	2.496	2.490
Mn	0.120	0.117	0.108	0.111	0.114	0.111	0.108
Ca	0.264	0.267	0.261	0.264	0.225	0.252	0.246
Fe/Fe+Mg	0.945	0.943	0.943	0.945	0.947	0.949	0.943
Pyrope	0.048	0.050	0.050	0.048	0.047	0.045	0.050
Alman	0.824	0.822	0.826	0.826	0.840	0.834	0.832
Spess	0.040	0.039	0.036	0.037	0.038	0.037	0.036
Gross	0.088	0.089	0.087	0.089	0.075	0.084	0.082

Appendix 8: Sample D84-1d-2 (cont.)

	MATRIX PLAGIOCLASE								
	(CORE)		(--------RIM--------)				(CORE)		(AVG)
	D841D 5/1A PL CO	D841D 5/1B PLAG	D841D 5/1C PL RI	D841D 5/1D PL RI	D841D 5/1E PL RI	D841D 5/1G PLAG	D841D 5/1H PL CO	D841D 5/1I PLAG	D841D 5/1AV PLAG
SiO2	59.50	59.88	60.44	60.14	60.36	59.94	59.67	58.21	59.75
Al2O3	26.51	25.88	25.69	25.28	25.79	25.80	26.37	25.01	25.78
FeO	0.03	0.14	0.08	0.13	0.14	0.14	0.08	0.08	0.11
CaO	8.07	7.46	7.12	7.13	7.17	7.45	7.93	7.27	7.46
Na2O	7.71	7.76	7.94	7.80	8.00	7.62	7.30	7.27	7.68
K2O	0.07	0.07	0.07	0.05	0.09	0.07	0.05	0.05	0.07
Total	101.89	101.18	101.35	100.53	101.55	101.02	101.40	97.89	100.85
Si	2.614	2.644	2.660	2.668	2.654	2.649	2.628	2.652	2.646
Al	1.373	1.347	1.333	1.322	1.337	1.344	1.369	1.343	1.346
Fe2+	0.001	0.005	0.003	0.005	0.005	0.005	0.003	0.003	0.004
Ca	0.380	0.353	0.336	0.339	0.338	0.353	0.374	0.355	0.354
Na	0.657	0.664	0.678	0.671	0.682	0.653	0.623	0.642	0.659
K	0.004	0.004	0.004	0.003	0.005	0.004	0.003	0.003	0.004
Ca/Ca+Na	0.366	0.347	0.331	0.336	0.331	0.351	0.375	0.356	0.349
Al*/SiAl	0.378	0.350	0.335	0.325	0.340	0.346	0.370	0.345	0.349
An	0.365	0.346	0.330	0.335	0.330	0.350	0.374	0.355	0.348
Ab	0.631	0.650	0.666	0.662	0.665	0.647	0.623	0.642	0.648
Or	0.004	0.004	0.004	0.003	0.005	0.004	0.003	0.003	0.004

	(CORE)	(RIM)	(RIM?)		(RIM)	(AVG)	(CORE)
	D841D 2/3A PL CO	D843D 2/3B PL RI	D841D 2/3C PLAG	D841D 2/3D PLAG	D841D 2/3E PL RI	D841D 2/3AV PLAG	D841D 1/1B PL CO
SiO2	57.57	57.90	58.52	57.27	57.85	57.82	59.05
Al2O3	25.65	25.63	25.60	25.49	25.41	25.57	25.23
FeO	0.13	0.11	0.03	0.05	0.16	0.08	0.05
CaO	7.68	7.81	7.50	7.88	7.64	7.71	7.11
Na2O	7.30	7.16	7.35	7.14	6.77	7.14	7.53
K2O	0.07	0.09	0.10	0.09	0.07	0.09	0.10
Total	98.40	98.69	99.09	97.93	97.90	98.40	99.08
Si	2.618	2.623	2.637	2.617	2.636	2.626	2.658
Al	1.375	1.369	1.360	1.373	1.365	1.369	1.339
Fe2+	0.005	0.004	0.001	0.002	0.006	0.003	0.002
Ca	0.374	0.379	0.362	0.386	0.373	0.375	0.343
Na	0.644	0.629	0.642	0.633	0.598	0.629	0.657
K	0.004	0.005	0.006	0.005	0.004	0.005	0.006
Ca/Ca+Na	0.367	0.376	0.361	0.379	0.384	0.374	0.343
Al*/SiAl	0.378	0.372	0.361	0.377	0.365	0.371	0.340
An	0.366	0.374	0.358	0.377	0.383	0.372	0.341
Ab	0.630	0.621	0.636	0.618	0.613	0.623	0.653
Or	0.004	0.005	0.006	0.005	0.004	0.005	0.006

Appendix 8: Sample D84-ld-2 (cont.)

	MATRIX PLAGIOCLASE					
	RIM				CORE	
	D841D 6/1B PL RI	D841D 6/1C PL RI	D841D 6/1D PL RI	D841D 6/1E PL RI	D841D 6/1A PL CO	D841D 6/1F PL CO
SiO2	56.90	58.43	58.42	58.89	58.55	57.77
Al2O3	25.90	26.19	26.08	26.97	26.33	26.21
FeO	0.18	0.27	0.27	0.30	0.19	0.19
CaO	6.90	7.56	7.44	7.34	7.43	7.70
Na2O	6.95	7.29	7.26	7.37	7.30	7.16
K2O	0.31	0.05	0.05	0.25	0.05	0.07
Total	97.14	99.79	99.52	101.12	99.86	99.09
Si	2.615	2.617	2.622	2.604	2.618	2.606
Al	1.403	1.383	1.380	1.406	1.388	1.394
Fe2+	0.007	0.010	0.010	0.011	0.007	0.007
Ca	0.340	0.363	0.358	0.348	0.356	0.372
Na	0.619	0.633	0.632	0.632	0.633	0.626
K	0.018	0.003	0.003	0.014	0.003	0.004
Ca/Ca+Na	0.355	0.364	0.362	0.355	0.360	0.373
Al*/SiAl	0.396	0.383	0.379	0.402	0.386	0.394
An	0.348	0.363	0.361	0.350	0.359	0.371
Ab	0.634	0.634	0.636	0.636	0.638	0.625
Or	0.018	0.003	0.003	0.014	0.003	0.004

Appendix 8: Sample D84-1d-2 (cont.)

	------MATRIX MUSCOVITE-------			
	D841D 3/1A MX MU	D841D 3/1B MUSC	D841D 3/1C MUSC	D841D 3/1AV MUSC
SiO2	46.67	46.83	47.66	47.05
Al2O3	35.76	35.88	36.16	35.93
TiO2	0.18	0.18	0.21	0.19
MgO	0.43	0.48	0.47	0.46
FeO	1.23	1.22	1.09	1.18
MnO	0.02	0.01	0.03	0.02
CaO	0.00	0.00	0.00	0.00
Na2O	1.19	1.11	1.23	1.18
K2O	8.72	8.64	8.44	8.60
Total	94.19	94.34	95.28	94.60
Si	6.213	6.218	6.249	6.227
Aliv	1.787	1.782	1.751	1.773
Alvi	3.826	3.834	3.839	3.833
Ti	0.018	0.018	0.021	0.019
Mg	0.086	0.094	0.091	0.090
Fe2+	0.137	0.135	0.119	0.131
Mn	0.002	0.001	0.003	0.002
Sum Oct	4.069	4.082	4.073	4.075
Ca	0.000	0.000	0.000	0.000
Na	0.306	0.286	0.313	0.302
K	1.481	1.464	1.411	1.452
Sum A	1.787	1.750	1.724	1.754
(OH)	0.000	0.000	0.000	0.000
Fe/Fe+Mg	0.614	0.590	0.567	0.593
X(Ca)	0.000	0.000	0.000	0.000
X(Na)	0.171	0.163	0.182	0.172
X(K)	0.829	0.837	0.818	0.828

Appendix 8: Sample D84-1d-2 (cont.)

	CHLORITE NEAR GARNET			----MATRIX CHLORITE--- (CORE)	(RIM)	(AVG)
	D841D 1/2A CHL N	D841D 1/2B CHL N	D841D 1/2AV CHL N	D841D 1/3A CHL C	D841D 1/3B CHL R	D841D 1/3AV CHL
SiO2	22.58	23.39	22.99	23.08	23.38	23.23
Al2O3	22.15	22.94	22.55	23.13	25.20	24.17
TiO2	0.08	0.06	0.07	0.07	0.04	0.05
MgO	8.60	8.68	8.64	8.93	8.05	8.49
FeO	33.25	31.84	32.55	32.65	31.69	32.17
MnO	0.11	0.18	0.14	0.07	0.14	0.10
CaO	0.00	0.00	0.00	0.00	0.00	0.00
Na2O	0.00	0.00	0.00	0.00	0.00	0.00
K2O	0.00	0.00	0.00	0.00	0.00	0.00
Total	86.77	87.10	86.94	87.93	88.50	88.22
Si	5.052	5.151	5.102	5.055	5.035	5.044
Al	5.841	5.956	5.899	5.973	6.400	6.189
Ti	0.013	0.010	0.011	0.012	0.007	0.009
Mg	2.867	2.848	2.857	2.915	2.583	2.747
Fe2+	6.220	5.864	6.041	5.980	5.708	5.843
Mn	0.021	0.033	0.027	0.013	0.026	0.019
Ca	0.000	0.000	0.000	0.000	0.000	0.000
Na	0.000	0.000	0.000	0.000	0.000	0.000
K	0.000	0.000	0.000	0.000	0.000	0.000
Fe/Fe+Mg	0.684	0.673	0.679	0.672	0.688	0.680

	------------------MATRIX CHLORITE-------------------						
	D841D 2/2A MX CH	D841D 2/2B MX CH	D841D 2/2C MX CH	D841D 2/2AV MX CH	D841D 4/1A MX CH	D841D 4/1B MX CH	D841D 4/1AV CHL
SiO2	23.15	23.20	23.28	23.21	22.95	23.34	23.15
Al2O3	23.35	22.94	23.42	23.24	23.04	22.89	22.97
TiO2	0.10	0.05	0.07	0.07	0.10	0.07	0.08
MgO	9.14	8.89	8.99	9.01	8.95	8.96	8.95
FeO	32.45	32.52	32.31	32.43	33.16	33.24	33.20
MnO	0.15	0.11	0.13	0.13	0.15	0.16	0.15
CaO	0.00	0.00	0.00	0.00	0.00	0.00	0.00
Na2O	0.00	0.00	0.00	0.00	0.00	0.00	0.00
K2O	0.00	0.00	0.00	0.00	0.00	0.00	0.00
Total	88.35	87.70	88.19	88.08	88.34	88.66	88.50
Si	5.039	5.092	5.069	5.067	5.021	5.084	5.053
Al	5.993	5.935	6.011	5.980	5.942	5.877	5.910
Ti	0.017	0.008	0.011	0.012	0.016	0.012	0.014
Mg	2.964	2.908	2.917	2.930	2.917	2.908	2.912
Fe2+	5.908	5.969	5.883	5.920	6.068	6.054	6.061
Mn	0.028	0.020	0.024	0.024	0.027	0.029	0.028
Ca	0.000	0.000	0.000	0.000	0.000	0.000	0.000
Na	0.000	0.000	0.000	0.000	0.000	0.000	0.000
K	0.000	0.000	0.000	0.000	0.000	0.000	0.000
Fe/Fe+Mg	0.666	0.672	0.669	0.669	0.675	0.676	0.675

Appendix 8: Sample D84-1d-2 (cont.)

	------MATRIX CHLORITOID------			
	D841D 2/1A CLTD	D841D 2/1B CLTD	D841D 2/1C CLTD	D841D 2/1AV CLTD
SiO2	24.08	23.84	24.11	24.02
Al2O3	40.24	40.40	40.48	40.36
TiO2	0.00	0.00	0.00	0.00
MgO	1.74	1.81	1.76	1.77
FeO	25.22	25.31	25.23	25.27
MnO	0.11	0.15	0.13	0.13
Total	91.39	91.52	91.70	91.54
Si	2.019	2.001	2.014	2.012
Al	3.978	3.998	3.987	3.985
Ti	0.000	0.000	0.000	0.000
Mg	0.218	0.226	0.219	0.221
Fe2+	1.769	1.777	1.763	1.770
Mn	0.008	0.011	0.009	0.009
Fe/Fe+Mg	0.890	0.887	0.890	0.889

Appendix 9: Jacobs Brook Recumbant Syncline: Microprobe Analyses; Sample D84-2e

	GARNET RIM ANALYSIS						
	D842E 1/24 GAR R	D842E 1/34 GAR R	D842E 1/35 GAR R	D842E 1/88 GAR R	D842E 1/97 GAR R	D842E 1/100 GAR R	D842E 1/116 GAR R
SiO2	37.61	36.61	37.16	36.85	37.12	37.47	37.51
Al2O3	21.27	20.70	21.01	20.84	20.99	21.19	21.21
MgO	2.83	2.68	2.82	3.09	3.06	2.97	3.07
FeO	34.05	33.32	34.04	32.87	33.38	33.74	33.42
MnO	4.00	3.76	3.69	3.39	3.73	3.94	3.68
CaO	1.37	1.44	1.21	1.34	1.32	1.33	1.68
Total	101.12	98.51	99.93	98.88	99.60	100.64	100.57
Si	3.000	3.000	3.000	3.000	3.000	3.000	3.000
Al	2.000	2.000	2.000	2.000	2.000	2.000	2.000
Mg	0.336	0.327	0.339	0.375	0.369	0.354	0.366
Fe2+	2.271	2.283	2.298	2.238	2.256	2.259	2.235
Mn	0.270	0.261	0.252	0.268	0.255	0.267	0.249
Ca	0.117	0.126	0.105	0.117	0.114	0.114	0.144
Fe/Fe+Mg	0.871	0.875	0.871	0.856	0.859	0.865	0.859
Pyrope	0.112	0.109	0.113	0.125	0.123	0.118	0.122
Alman	0.759	0.762	0.768	0.746	0.754	0.755	0.746
Spess	0.090	0.087	0.084	0.089	0.085	0.089	0.083
Gross	0.039	0.042	0.035	0.039	0.038	0.038	0.048

Appendix 9: Sample D84-2e (cont.)

	--------MATRIX	BIOTITE-------		
		(CORE)	(RIM)	(AVG)
	D842E 3/1A BIO	D842E 3/1B BIO C	D842E 3/1C BIO R	D842E 3/1AV MX BI
SiO2	33.95	34.84	35.26	34.68
Al2O3	18.97	18.91	18.91	18.93
TiO2	1.28	1.30	1.31	1.30
MgO	11.07	11.36	10.93	11.12
FeO	21.08	21.12	20.85	21.02
MnO	0.14	0.09	0.09	0.11
CaO	0.01	0.00	0.00	0.00
Na2O	0.17	0.14	0.19	0.17
K2O	6.93	7.07	7.01	7.00
Total	93.59	94.83	94.56	94.33
Si	5.251	5.308	5.371	5.310
Aliv	2.749	2.692	2.629	2.690
Alvi	0.710	0.704	0.767	0.727
Ti	0.151	0.150	0.152	0.151
Mg	2.552	2.580	2.482	2.538
Fe2+	2.727	2.691	2.656	2.691
Mn	0.018	0.011	0.012	0.014
Sum Oct	6.158	6.136	6.069	6.121
Ca	0.001	0.000	0.000	0.000
Na	0.052	0.042	0.057	0.050
K	1.367	1.374	1.363	1.368
Sum A	1.420	1.416	1.420	1.418
(OH)	0.000	0.000	0.000	0.000
Fe/Fe+Mg	0.517	0.511	0.517	0.515
X(Ca)	0.001	0.000	0.000	0.000
X(Na)	0.037	0.030	0.040	0.035
X(K)	0.963	0.970	0.960	0.965

Appendix 9: Sample D84-2e (cont.)

	-------MATRIX	MUSCOVITE------		
	D842E 1/3A MUSC	D842E 1/3B MUSC	D842E 1/3C MUSC	D842E 1/3AV MUSC
SiO2	46.68	46.98	46.11	46.59
Al2O3	34.11	34.29	34.25	34.21
TiO2	0.41	0.41	0.40	0.41
MgO	0.84	0.75	0.79	0.79
FeO	2.11	2.33	2.23	2.22
MnO	0.00	0.07	0.00	0.02
CaO	0.00	0.00	0.00	0.00
Na2O	1.17	0.93	0.95	1.02
K2O	9.33	9.16	9.02	9.17
Total	94.65	94.92	93.75	94.43
Si	6.246	6.261	6.219	6.242
Aliv	1.754	1.739	1.781	1.758
Alvi	3.627	3.648	3.664	3.646
Ti	0.042	0.042	0.041	0.042
Mg	0.168	0.148	0.159	0.158
Fe2+	0.236	0.260	0.252	0.249
Mn	0.000	0.008	0.000	0.002
Sum Oct	4.073	4.106	4.116	4.097
Ca	0.000	0.000	0.000	0.000
Na	0.303	0.240	0.248	0.264
K	1.592	1.557	1.552	1.567
Sum A	1.895	1.797	1.800	1.831
(OH)	0.000	0.000	0.000	0.000
Fe/Fe+Mg	0.584	0.637	0.613	0.612
X(Ca)	0.000	0.000	0.000	0.000
X(Na)	0.160	0.134	0.138	0.144
X(K)	0.840	0.866	0.862	0.856

Appendix 9: Sample D84-2e (cont.)

	---STAUROLITE NEAR GARNET----				------MATRIX STAUROLITE------			
	D842E 1/2A ST NR	D842E 1/2B ST NR	D842E 1/2C ST NR	D842E 1/2AV ST NR	D842E 4/1A MX ST	D842E 4/1B MX ST	D842E 4/1D MX ST	D842E 4/1AV MX ST
SiO2	27.79	28.42	28.36	28.19	28.05	28.31	28.56	28.30
Al2O3	54.50	54.97	54.15	54.54	54.29	53.90	54.31	54.16
TiO2	0.49	0.57	0.53	0.53	0.58	0.46	0.51	0.52
MgO	1.15	1.21	1.01	1.12	1.59	1.71	1.57	1.62
FeO	13.32	13.20	12.86	13.12	13.92	14.11	13.56	13.87
MnO	0.32	0.27	0.29	0.29	0.27	0.27	0.26	0.27
ZnO	0.06	0.17	0.16	0.13	0.21	0.08	0.21	0.17
CaO	0.00	0.00	0.00	0.00	0.00	0.00	0.00	0.00
Total	97.63	98.81	97.35	97.93	98.91	98.83	98.98	98.90
Si	3.853	3.888	3.932	3.891	3.854	3.893	3.910	3.885
Al	8.908	8.866	8.851	8.875	8.793	8.738	8.766	8.766
Ti	0.052	0.059	0.056	0.056	0.061	0.048	0.053	0.054
Mg	0.238	0.247	0.208	0.231	0.326	0.350	0.320	0.332
Fe2+	1.545	1.510	1.491	1.515	1.600	1.623	1.553	1.592
Mn	0.037	0.031	0.034	0.034	0.031	0.031	0.030	0.031
Zn	0.006	0.017	0.016	0.013	0.021	0.008	0.021	0.017
Ca	0.000	0.000	0.000	0.000	0.000	0.000	0.000	0.000
Fe/Fe+Mg	0.867	0.859	0.878	0.868	0.831	0.823	0.829	0.827

Appendix 9: Sample D84-2e (cont.)

	---------------MATRIX CHLORITE---------------					
	(CORE)			(RIM)	(CORE)	(AVG)
	D842E 2/1A CHL C	D842E 2/1B CHL	D842E 2/1C CHL	D842E 2/1D CHL R	D842E 2/1E CHL C	D842E 2/1AV CHL
SiO2	24.29	24.93	25.03	24.91	24.87	24.80
Al2O3	23.15	23.09	23.16	23.02	23.31	23.15
TiO2	0.06	0.08	0.10	0.08	0.08	0.08
MgO	15.99	15.98	16.07	15.79	15.15	15.80
FeO	24.06	25.26	24.75	25.44	24.93	24.88
MnO	0.11	0.14	0.13	0.15	0.15	0.14
CaO	0.00	0.00	0.00	0.00	0.00	0.00
Na2O	0.00	0.00	0.00	0.00	0.00	0.00
K2O	0.00	0.00	0.00	0.00	0.00	0.00
Total	87.65	89.48	89.24	89.38	88.49	88.85
Si	5.088	5.137	5.155	5.144	5.172	5.139
Aliv	2.912	2.863	2.845	2.856	2.828	2.861
Alvi	2.806	2.747	2.780	2.748	2.887	2.793
Ti	0.009	0.012	0.015	0.013	0.013	0.013
Mg	4.994	4.909	4.934	4.859	4.694	4.878
Fe2+	4.215	4.353	4.263	4.394	4.336	4.312
Mn	0.019	0.025	0.023	0.026	0.027	0.024
Sum Oct	12.043	12.046	12.015	12.040	11.957	12.020
Ca	0.000	0.000	0.000	0.000	0.000	0.000
Na	0.000	0.000	0.000	0.000	0.000	0.000
K	0.000	0.000	0.000	0.000	0.000	0.000
Sum A	0.000	0.000	0.000	0.000	0.000	0.000
(OH)	0.000	0.000	0.000	0.000	0.000	0.000
Fe/Fe+Mg	0.458	0.470	0.464	0.475	0.480	0.469

Appendix 9: Sample D84-4k

D84-4K JACOB'S BROOK RECUMBANT SYNCLINE D.ORANGE

	GARNET RIM ANALYSES							
	D844K 1/34 GAR R	D844K 1/35 GAR R	D844K 1/96 GAR R	D844K 1/97 GAR R	D844K 1/151 GAR R	D844K 1/134 GAR R	D844K 1/135 GAR R	D844K 1/136 GAR R
SiO2	37.03	37.28	36.96	36.72	37.34	37.72	37.80	37.44
Al2O3	20.94	21.08	20.90	20.77	21.11	21.33	21.38	21.17
MgO	2.51	2.30	2.65	2.54	2.73	2.81	2.74	2.61
FeO	34.40	35.30	34.30	34.25	34.74	35.32	35.39	34.92
MnO	2.62	2.55	2.62	2.69	2.51	2.40	2.37	2.61
CaO	2.07	1.95	1.90	1.78	1.92	1.76	1.87	1.92
Total	99.58	100.46	99.33	98.75	100.35	101.35	101.55	100.68
Si	3.000	3.000	3.000	3.000	3.000	3.000	3.000	3.000
Al	2.000	2.000	2.000	2.000	2.000	2.000	2.000	2.000
Mg	0.303	0.276	0.321	0.309	0.327	0.333	0.324	0.312
Fe2+	2.331	2.376	2.328	2.340	2.334	2.349	2.349	2.340
Mn	0.180	0.174	0.180	0.186	0.171	0.162	0.159	0.177
Ca	0.180	0.168	0.165	0.156	0.165	0.150	0.159	0.165
Fe/Fe+Mg	0.885	0.896	0.879	0.883	0.877	0.876	0.879	0.882
Pyrope	0.101	0.092	0.107	0.103	0.109	0.111	0.108	0.104
Alman	0.779	0.794	0.778	0.782	0.779	0.785	0.785	0.782
Spess	0.060	0.058	0.060	0.062	0.057	0.054	0.053	0.059
Gross	0.060	0.056	0.055	0.052	0.055	0.050	0.053	0.055

Appendix 9: Sample D84-4k (cont.)

	----BIOTITE NEAR CHLORITE----			
	D844K 2/4A BIO N	D844K 2/4B BIO N	D844K 2/4AV BIO N	D844K 1/2A BIO N
SiO2	35.16	35.29	35.23	35.27
Al2O3	18.26	18.80	18.53	18.99
TiO2	1.72	1.45	1.59	1.41
MgO	9.89	9.99	9.94	9.75
FeO	21.12	21.30	21.20	20.33
MnO	0.05	0.12	0.08	0.03
CaO	0.00	0.00	0.00	0.00
Na2O	0.11	0.25	0.18	0.36
K2O	7.34	8.87	8.10	8.51
Total	93.65	96.08	94.86	94.65
Si	5.430	5.364	5.397	5.404
Aliv	2.570	2.636	2.603	2.596
Alvi	0.754	0.733	0.744	0.833
Ti	0.202	0.168	0.185	0.164
Mg	2.277	2.263	2.270	2.225
Fe2+	2.727	2.707	2.717	2.605
Mn	0.006	0.016	0.011	0.004
Sum Oct	5.966	5.887	5.927	5.831
Ca	0.000	0.000	0.000	0.000
Na	0.032	0.073	0.053	0.108
K	1.447	1.719	1.584	1.663
Sum A	1.479	1.792	1.637	1.771
(OH)	0.000	0.000	0.000	0.000
Fe/Fe+Mg	0.545	0.545	0.545	0.539
X(Ca)	0.000	0.000	0.000	0.000
X(Na)	0.022	0.041	0.032	0.061
X(K)	0.978	0.959	0.968	0.939

Appendix 9: Sample D84-4k (cont.)

	--BIOTITE RIMS NEAR GARNET---				--MATRIX MUSCOVITE---		
	D844K 1/2B BIO N	D844K 1/2C BIO N	D844K 1/2D BIO N	D844K 1/2AV BIO N	D844K 2/3A MUSC	D844K 2/3B MUSC	D844K 2/3AV MUSC
SiO2	35.98	34.56	33.87	34.92	46.51	46.51	46.51
Al2O3	19.36	18.95	18.21	18.88	34.37	34.00	34.19
TiO2	1.46	1.29	1.37	1.38	0.31	0.37	0.34
MgO	9.86	9.31	9.84	9.69	0.72	0.69	0.71
FeO	19.73	20.29	21.08	20.36	2.51	2.37	2.44
MnO	0.12	0.05	0.09	0.07	0.01	0.04	0.03
CaO	0.00	0.00	0.01	0.00	0.00	0.00	0.00
Na2O	0.34	0.25	0.24	0.30	1.07	1.15	1.11
K2O	8.54	8.71	8.66	8.60	9.05	9.04	9.04
Total	95.39	93.41	93.37	94.21	94.56	94.18	94.37
Si	5.441	5.381	5.317	5.386	6.229	6.252	6.241
Aliv	2.559	2.619	2.683	2.614	1.771	1.748	1.759
Alvi	0.892	0.859	0.687	0.819	3.656	3.641	3.649
Ti	0.168	0.153	0.163	0.162	0.032	0.038	0.035
Mg	2.222	2.161	2.303	2.227	0.143	0.139	0.141
Fe2+	2.495	2.642	2.767	2.626	0.281	0.267	0.274
Mn	0.015	0.007	0.012	0.009	0.001	0.005	0.003
Sum Oct	5.792	5.822	5.932	5.843	4.113	4.090	4.102
Ca	0.000	0.000	0.001	0.000	0.000	0.000	0.000
Na	0.101	0.076	0.073	0.090	0.279	0.300	0.289
K	1.647	1.731	1.734	1.693	1.547	1.550	1.548
Sum A	1.748	1.807	1.808	1.783	1.825	1.850	1.837
(OH)	0.000	0.000	0.000	0.000	0.000	0.000	0.000
Fe/Fe+Mg	0.529	0.550	0.546	0.541	0.663	0.658	0.660
X(Ca)	0.000	0.000	0.001	0.000	0.000	0.000	0.000
X(Na)	0.058	0.042	0.040	0.050	0.152	0.162	0.157
X(K)	0.942	0.958	0.959	0.950	0.848	0.838	0.843

Appendix 9: Sample D84-4k (cont.)

	------MATRIX STAUROLITE------				---STAUROLITE NEAR GARNET----			
		(CORE)	(RIM)	(AVG)	(RIM)		(CORE)	(AVG)
	D844K 2/1A MX ST	D844K 2/1B ST CO	D844K 2/1C ST RI	D844K 2/1AV STAU	D844K 1/3A ST NR	D844K 1/3B ST NR	D844K 1/3C ST NR	D844K 1/3AV ST NR
SiO2	28.01	27.88	28.15	27.96	28.28	27.89	27.53	27.90
Al2O3	54.44	54.22	54.81	54.58	54.69	55.01	54.67	54.79
TiO2	0.54	0.54	0.55	0.54	0.48	0.49	0.55	0.50
MgO	1.50	1.55	0.92	1.32	1.06	1.12	1.11	1.09
FeO	14.04	14.03	12.42	13.47	12.79	13.54	13.16	13.16
MnO	0.15	0.20	0.09	0.15	0.21	0.15	0.18	0.18
ZnO	0.35	0.32	0.20	0.28	0.12	0.35	0.24	0.24
CaO	0.00	0.01	0.00	0.00	0.00	0.00	0.00	0.00
Total	99.03	98.76	97.13	98.31	97.62	98.55	97.44	97.87
Si	3.847	3.841	3.876	3.854	3.905	3.837	3.825	3.856
Al	8.814	8.808	8.899	8.871	8.904	8.922	8.953	8.927
Ti	0.056	0.057	0.058	0.057	0.050	0.051	0.058	0.053
Mg	0.308	0.319	0.189	0.272	0.218	0.229	0.229	0.225
Fe2+	1.612	1.617	1.430	1.553	1.477	1.558	1.529	1.521
Mn	0.018	0.023	0.010	0.017	0.025	0.017	0.021	0.021
Zn	0.035	0.033	0.020	0.029	0.012	0.036	0.025	0.024
Ca	0.000	0.001	0.000	0.000	0.000	0.000	0.000	0.000
Fe/Fe+Mg	0.840	0.835	0.883	0.851	0.871	0.872	0.870	0.871

Appendix 9: Sample D84-4k (cont.)

	-------MATRIX	CHLORITE------- (RIM)		(AVG)
	D844K 2/2A CHL	D844K 2/2B MX CH	D844K 2/2C CHL R	D844K 2/2AV CHL
SiO2	24.61	24.37	24.67	24.55
Al2O3	22.98	22.82	23.26	23.02
TiO2	0.06	0.09	0.05	0.06
MgO	15.23	15.01	15.08	15.11
FeO	25.56	26.37	25.68	25.87
MnO	0.10	0.14	0.10	0.12
CaO	0.00	0.00	0.00	0.00
Na2O	0.00	0.00	0.00	0.00
K2O	0.00	0.00	0.00	0.00
Total	88.53	88.81	88.84	88.73
Si	5.138	5.101	5.132	5.124
Aliv	2.862	2.899	2.868	2.876
Alvi	2.795	2.732	2.836	2.788
Ti	0.009	0.014	0.008	0.010
Mg	4.738	4.681	4.677	4.699
Fe2+	4.463	4.616	4.468	4.516
Mn	0.018	0.025	0.018	0.021
Sum Oct	12.023	12.068	12.007	12.034
Ca	0.000	0.000	0.000	0.000
Na	0.000	0.000	0.000	0.000
K	0.000	0.000	0.000	0.000
Sum A	0.000	0.000	0.000	0.000
(OH)	0.000	0.000	0.000	0.000
Fe/Fe+Mg	0.485	0.497	0.489	0.490

Appendix 9: Sample D84-4k (cont.)

----------------MARGARITE INCLUSIONS IN GARNET---------------
(LOCATIONS ON MAPPED GARNET)

	(CORE)	(RIM)	(CORE)		(CORE)	(RIM)	(CORE)	(RIM)
	D844K 1/4A CO MA	D844K 1/4B RI MA	D844K 1/5A CO MA	D844K 1/5B MARG	D844K 1/6A CO MA	D844K 1/6B RI MA	D844K 1/7A CO MA	D844K 1/7B RI MA
SiO2	30.09	29.48	30.23	29.93	30.08	29.54	29.82	29.47
Al2O3	49.83	49.47	44.73	48.63	49.05	49.28	48.68	49.11
FeO	1.30	1.35	1.61	1.39	1.30	1.52	1.10	1.37
CaO	12.45	12.41	9.95	11.80	10.57	11.26	11.46	11.58
Na2O	0.95	0.77	1.93	1.11	1.37	1.34	1.26	1.26
K2O	0.00	0.02	0.27	0.06	0.05	0.02	0.08	0.02
Total	94.62	93.50	88.72	92.93	92.92	92.96	92.40	92.81
Si	1.471	1.459	1.574	1.489	1.493	1.469	1.489	1.468
Al	2.872	2.886	2.746	2.852	2.870	2.889	2.865	2.884
Fe2+	0.053	0.056	0.070	0.058	0.054	0.063	0.046	0.057
Ca	0.652	0.658	0.555	0.629	0.562	0.600	0.613	0.618
Na	0.090	0.074	0.195	0.107	0.180	0.129	0.122	0.122
K	0.000	0.001	0.018	0.004	0.003	0.001	0.005	0.001
Fe/Fe+Mg	1.000	1.000	1.000	1.000	1.000	1.000	1.000	1.000

	(RIM)	(CORE)	(RIM)	(CORE)				
	D844K 1/9A RI MA	D844K 1/9B CO MA	D844K 1/10A RI MA	D844K 1/10B CO MA	D844K 1/11A MARG	D844K 1/11B MARG	D844K 1/12A MARG	D844K 1/13A MARG
SiO2	29.31	30.28	29.13	29.50	28.63	28.66	29.08	29.88
Al2O3	49.78	48.79	49.70	49.03	48.67	49.52	48.99	48.39
FeO	1.06	1.13	1.16	1.37	1.28	1.25	1.15	1.44
CaO	12.47	11.19	12.76	12.64	12.54	12.94	12.48	11.50
Na2O	0.79	1.36	0.46	0.45	0.66	0.52	0.64	1.14
K2O	0.02	0.05	0.16	0.24	0.02	0.02	0.17	0.17
Total	93.43	92.79	93.37	93.22	91.79	92.91	92.50	92.52
Si	1.450	1.503	1.444	1.466	1.445	1.430	1.455	1.493
Al	2.904	2.855	2.905	2.873	2.896	2.913	2.890	2.851
Fe2+	0.044	0.047	0.048	0.057	0.054	0.052	0.048	0.060
Ca	0.661	0.595	0.678	0.673	0.678	0.692	0.669	0.616
Na	0.076	0.131	0.044	0.043	0.065	0.050	0.062	0.110
K	0.001	0.003	0.010	0.015	0.001	0.001	0.011	0.011
Fe/Fe+Mg	1.000	1.000	1.000	1.000	1.000	1.000	1.000	1.000

Appendix 9: Sample D84-2c

	GAR RIM	GARNET TRAVERSE...							
	D84-2 C/1/4 A GAR	D84-2 C/1/4 B GAR	D84-2 C/1/4 C GAR	D84-2 C/1/4 D GAR	D84-2 C/1/4 E GAR	D84-2 C/1/4 G GAR	D84-2 C/1/4 F GAR	D84-2 C/1/4 H GAR	D84-2 C/1/4 GAR
SiO2	35.14	37.18	36.53	37.40	37.17	37.20	36.61	37.36	36.83
Al2O3	22.24	21.17	21.97	21.73	21.66	21.51	22.03	21.73	21.75
MgO	2.34	1.95	1.96	1.79	1.83	1.65	1.72	1.92	1.90
FeO	37.73	36.59	35.99	36.13	35.72	35.18	35.75	35.76	36.11
MnO	0.39	0.56	0.63	0.71	0.78	1.27	1.27	0.61	0.78
CaO	2.56	4.11	3.99	4.10	4.22	4.70	4.27	4.64	4.08
Total	100.40	101.56	101.08	101.87	101.38	101.52	101.65	102.02	101.44
Si	2.854	2.971	2.927	2.970	2.965	2.967	2.923	2.961	2.943
Al	2.130	1.994	2.076	2.035	2.037	2.023	2.073	2.030	2.049
Mg	0.283	0.232	0.234	0.212	0.217	0.196	0.205	0.227	0.226
Fe2+	2.563	2.445	2.412	2.400	2.383	2.347	2.387	2.370	2.413
Mn	0.027	0.038	0.043	0.048	0.053	0.086	0.086	0.041	0.053
Ca	0.223	0.352	0.343	0.349	0.361	0.402	0.365	0.394	0.349
Fe/Fe+Mg	0.901	0.913	0.912	0.919	0.917	0.923	0.921	0.913	0.914
Pyrope	0.091	0.076	0.077	0.070	0.072	0.065	0.067	0.075	0.074
Alman	0.828	0.797	0.796	0.798	0.791	0.774	0.784	0.782	0.793
Spess	0.009	0.012	0.014	0.016	0.018	0.028	0.028	0.014	0.017
Gross	0.072	0.115	0.113	0.116	0.120	0.133	0.120	0.130	0.115

Appendix 9: Sample D84-2c (cont.)

	---MATRIX BIOTITE----		
	D84-2 C/1/1 A BIO	D84-2 C/1/1 B BIO	D84-2 C/1/1 C BIO
SiO2	34.31	34.43	34.30
Al2O3	18.53	18.60	18.72
TiO2	1.63	1.56	1.48
MgO	7.90	7.69	7.63
FeO	23.76	23.34	23.68
MnO	0.12	0.14	0.11
CaO	0.01	0.00	0.00
Na2O	0.22	0.19	0.12
K2O	9.22	8.99	9.05
Total	95.71	94.93	95.08
Si	5.326	5.367	5.348
Aliv	2.674	2.633	2.652
Alvi	0.717	0.785	0.788
Ti	0.192	0.185	0.175
Mg	1.828	1.786	1.773
Fe2+	3.085	3.043	3.087
Mn	0.016	0.018	0.014
Sum Oct	5.838	5.817	5.837
Ca	0.002	0.000	0.000
Na	0.066	0.056	0.035
K	1.826	1.789	1.801
Sum A	1.894	1.845	1.836
(OH)	0.000	0.000	0.000
Fe/Fe+Mg	0.628	0.630	0.635
X(Ca)	0.001	0.000	0.000
X(Na)	0.035	0.030	0.019
X(K)	0.964	0.970	0.981

Appendix 9: Sample D84-2c (cont.)

	----------MATRIX MUSCOVITE----------				
	D84-2 C/1/3 A MUS	D84-2 C/1/3 B MUS	D84-2 C/1/3 C MUS	D84-2 C/1/3 D MUS	D84-2 C/1/3 MUSC
SiO2	45.31	45.25	45.12	45.00	45.17
Al2O3	35.64	36.03	35.78	35.00	35.61
TiO2	0.35	0.31	0.32	0.29	0.32
MgO	0.60	0.54	0.49	0.53	0.54
FeO	2.26	2.18	2.17	2.11	2.18
MnO	0.00	0.02	0.04	0.03	0.02
CaO	0.00	0.00	0.00	0.00	0.00
Na2O	1.24	1.16	1.20	0.92	1.13
K2O	9.42	9.68	9.60	9.81	9.63
Total	94.83	95.17	94.73	93.69	94.60
Si	6.071	6.047	6.056	6.109	6.071
Aliv	1.929	1.953	1.944	1.891	1.929
Alvi	3.702	3.723	3.719	3.710	3.714
Ti	0.036	0.031	0.033	0.030	0.033
Mg	0.120	0.108	0.099	0.107	0.109
Fe2+	0.253	0.244	0.244	0.240	0.245
Mn	0.000	0.002	0.004	0.003	0.002
Sum Oct	4.111	4.108	4.099	4.090	4.103
Ca	0.000	0.000	0.000	0.000	0.000
Na	0.323	0.300	0.313	0.241	0.294
K	1.611	1.651	1.644	1.699	1.651
Sum A	1.934	1.951	1.957	1.940	1.945
(OH)	0.000	0.000	0.000	0.000	0.000
Fe/Fe+Mg	0.678	0.693	0.711	0.692	0.692
X(Ca)	0.000	0.000	0.000	0.000	0.000
X(Na)	0.167	0.154	0.160	0.124	0.151
X(K)	0.833	0.846	0.840	0.876	0.849

Appendix 9: Sample D84-2c (cont.)

	-----------MATRIX CHLORITE-----------				
	D84-2 C/1/2 A CHL	D84-2 C/1/2 B CHL	D84-2 C/1/2 C CHL	D84-2 C/1/2 D CHL	D84-2 C/1/2 CHL
SiO2	23.10	23.66	23.43	23.66	23.46
Al2O3	23.53	23.36	23.40	23.57	23.46
TiO2	0.07	0.13	0.08	0.07	0.09
MgO	11.66	11.68	11.73	11.55	11.65
FeO	30.15	30.59	29.77	30.37	30.22
MnO	0.08	0.07	0.09	0.08	0.08
CaO	0.00	0.03	0.00	0.00	0.00
Na2O	0.00	0.00	0.00	0.00	0.00
K2O	0.00	0.00	0.00	0.00	0.00
Total	88.58	89.52	88.50	89.31	88.97
Si	4.953	5.023	5.014	5.027	5.005
Aliv	3.047	2.977	2.986	2.973	2.995
Alvi	2.901	2.868	2.919	2.930	2.905
Ti	0.012	0.021	0.013	0.012	0.014
Mg	3.726	3.696	3.742	3.657	3.705
Fe2+	5.407	5.430	5.329	5.396	5.391
Mn	0.014	0.013	0.017	0.015	0.014
Sum Oct	12.060	12.028	12.020	12.010	12.029
Ca	0.001	0.006	0.000	0.000	0.001
Na	0.000	0.000	0.000	0.000	0.000
K	0.000	0.000	0.000	0.000	0.000
Sum A	0.001	0.006	0.000	0.000	0.001
(OH)	0.000	0.000	0.000	0.000	0.000
Fe/Fe+Mg	0.592	0.595	0.587	0.596	0.593

Appendix 10: Baker Pond: Microprobe Analyses; Sample 79-449f

	--------------------GARNET RIM ANALYSES---------------------							
	-449F /1/50 PIGAR	-449F /1/51 PIGAR	-449F /1/71 PIGAR	-449F /1/72 PIGAR	-449F /1/77 PIGAR	-449F /1/78 PIGAR	-449F /1/92 PIGAR	-449F /1/95 PIGAR
SiO2	37.47	38.33	37.81	37.90	38.04	38.19	37.62	37.80
Al2O3	21.74	22.16	21.81	21.85	21.41	21.26	21.55	21.37
MgO	4.48	4.50	4.66	4.50	4.88	4.86	4.30	4.69
FeO	29.96	28.47	29.38	29.36	29:79	30.36	29.31	29.87
MnO	7.31	6.40	5.98	6.98	6.06	6.40	6.83	6.61
CaO	0.94	0.90	1.13	0.88	0.84	0.96	1.03	0.99
Total	101.90	100.77	100.78	101.47	101:03	102.03	100.64	101.33
Si	2.952	3.011	2.985	2.981	3.000	2.994	2.987	2.984
Al	2.019	2.052	2.030	2.026	1.990	1.965	2.017	1.989
Mg	0.526	0.527	0.548	0.528	0.574	0.568	0.509	0.552
Fe2+	1.974	1.870	1.940	1.931	1.965	1.991	1.946	1.972
Mn	0.488	0.426	0.400	0.465	0.405	0.425	0.459	0.442
Ca	0.079	0.076	0.096	0.074	0.071	0.081	0.088	0.084
Fe/Fe+Mg	0.790	0.780	0.780	0.785	0.774	0.778	0.793	0.781
Pyrope	0.172	0.182	0.184	0.176	0.190	0.185	0.170	0.181
Alman	0.644	0.645	0.650	0.644	0.652	0.650	0.648	0.647
Spess	0.159	0.147	0.134	0.155	0.134	0.139	0.153	0.145
Gross	0.026	0.026	0.032	0.025	0.024	0.026	0.029	0.028

	----GARNET RIM ANALYSES-----			
	-449F 1/108 GAR N	-449F 1/109 GAR N	-449F 1/110 GAR N	-449F ^1^ GRAVG
SiO2	37.61	37.43	37.15	37.39
Al2O3	22.13	21.95	21.87	21.98
MgO	4.84	4.81	4.85	4.83
FeO	29.25	30.05	29.48	29.60
MnO	5.77	5.72	5.87	5.78
CaO	0.86	0.83	0.83	0.84
Total	100.45	100.77	100.05	100.42
Si	2.972	2.961	2.958	2.964
Al	2.062	2.047	2.053	2.054
Mg	0.570	0.567	0.575	0.571
Fe2+	1.933	1.988	1.963	1.962
Mn	0.386	0.383	0.396	0.388
Ca	0.073	0.070	0.071	0.071
Fe/Fe+Mg	0.772	0.778	0.773	0.775
Pyrope	0.192	0.188	0.191	0.191
Alman	0.653	0.661	0.653	0.656
Spess	0.130	0.127	0.132	0.130
Gross	0.025	0.023	0.024	0.024

Appendix 10: Sample 79-449f (cont.)

	PLAG IN GAR		MATRIX PLAGIOCLASE NEAR GARNET RIM					
			(CORE)	(RIM)	(RIM)	(RIM)	(CORE)	(RIM)
	449F 1/26A PL IN	449F 1/26B PL IN	449F 1/27A CO PL	449F 1/27B RI PL	449F 1/27C RI PL	449F 1/28A RI PL	449F 1/28B CO PL	449F 1/28C RI PL
SiO2	63.35	64.45	61.02	60.99	58.99	61.30	60.11	61.01
Al2O3	19.78	19.51	22.93	22.97	23.13	22.11	23.08	22.83
FeO	0.36	0.47	0.45	0.69	1.42	0.37	0.24	0.45
CaO	0.59	0.31	4.29	4.10	4.12	2.42	4.37	4.09
Na2O	11.23	11.55	9.29	9.21	8.91	10.14	9.13	9.38
K2O	0.07	0.05	0.10	0.10	0.10	0.10	0.12	0.10
Total	95.39	96.34	98.09	98.06	96.68	96.44	97.04	97.86
Si	2.920	2.940	2.763	2.763	2.724	2.810	2.750	2.768
Al	1.075	1.049	1.224	1.227	1.259	1.195	1.245	1.221
Fe2+	0.014	0.018	0.017	0.026	0.055	0.014	0.009	0.017
Ca	0.029	0.015	0.208	0.199	0.204	0.119	0.214	0.199
Na	1.004	1.022	0.816	0.809	0.798	0.901	0.810	0.825
K	0.004	0.003	0.006	0.006	0.006	0.006	0.007	0.006
Ca/Ca+Na	0.028	0.014	0.203	0.197	0.204	0.117	0.209	0.194
Al4/SiAl	0.075	0.050	0.227	0.229	0.263	0.194	0.246	0.223
An	0.028	0.014	0.202	0.196	0.202	0.116	0.208	0.193
Ab	0.968	0.983	0.792	0.798	0.792	0.878	0.786	0.801
Or	0.004	0.003	0.006	0.006	0.006	0.006	0.007	0.006

Appendix 10: Sample 79-449f (cont.)

	---------MATRIX	PLAGIOCLASE-----------			
	79-44 9F/2/ 1 PLA	79-44 9F/2/ 2 PLA	79-44 9F/2/ 3 PLA	79-44 9F/2/ 4 PLA	79-44 9F/2/ 5 PLA
SiO2	62.05	62.84	65.05	65.21	63.96
Al2O3	22.30	22.50	23.02	22.81	23.19
FeO	0.00	0.00	0.00	0.06	0.00
CaO	3.34	3.41	3.41	3.38	3.99
Na2O	10.81	10.33	10.58	10.51	9.90
K2O	0.07	0.11	0.11	0.09	0:05
Total	98.56	99.18	102.16	102.06	101.09
Si	2.795	2.805	2.816	2.825	2.798
Al	1.184	1.184	1.175	1.165	1.196
Fe2+	0.000	0.000	0.000	0.002	0.000
Ca	0.161	0.163	0.158	0.157	0.187
Na	0.944	0.894	0.888	0.883	0.840
K	0.004	0.006	0.006	0.005	0.003
Ca/Ca+Na	0.146	0.154	0.151	0.151	0.182
Al*/SiAl	0.188	0.186	0.177	0.167	0.197
An	0.145	0.153	0.150	0.150	0.182
Ab	0.851	0.841	0.844	0.845	0.816
Or	0.004	0.006	0.006	0.005	0.003

Appendix 10: Sample 79-449 f(cont.)

	-MATRIX PLAG- (CORE)	(RIM)	-PLAG IN BIO-	
	449F 1/29A CO MX	449F 1/29B RI MX	449F 1/30A PL IN	449F 1/30B PL IN
SiO2	61.67	62.02	65.52	66.97
Al2O3	21.85	21.67	21.52	21.56
FeO	0.05	0.10	0.14	0.22
CaO	2.92	2.49	1.82	1.62
Na2O	9.85	10.27	10.85	11.19
K2O	0.09	0.05	0.05	0.05
Total	96.41	96.61	99.90	101.61
Si	2.823	2.833	2.884	2.898
Al	1.179	1.167	1.117	1.100
Fe2+	0.002	0.004	0.005	0.008
Ca	0.143	0.122	0.086	0.075
Na	0.874	0.910	0.926	0.939
K	0.005	0.003	0.003	0.003
Ca/Ca+Na	0.141	0.118	0.085	0.074
Al*/SiAl	0.179	0.167	0.117	0.100
An	0.140	0.118	0.085	0.074
Ab	0.855	0.879	0.912	0.923
Or	0.005	0.003	0.003	0.003

Appendix 10: Sample 79-449f (cont.)

PLAGIOCLASE INCLUSIONS IN GARNET

	(CORE)	(RIM)	(CORE)		(CORE)	(CORE)	
	79-44 9F/1/ 16A P	79-44 9F/1/ 16B P	79-44 9F/1/ 16C P	-449F 1/10A PLAG	-449F 1/10B PL IN	-449F 1/10C PL IN	-449F 1/10D PL IN
SiO2	65.92	63.87	65.91	63.43	62.95	62.78	62.55
Al2O3	20.95	21.58	20.97	24.13	23.79	23.53	23.95
FeO	0.33	0.38	0.24	0.19	0.16	0.16	0.24
CaO	1.92	2.66	2.04	4.56	4.70	4.74	4.56
Na2O	12.22	10.50	11.08	10.09	9.49	9.75	9.35
K2O	0.09	0.11	0.11	0.09	0.11	0.30	0.16
Total	101.43	99.09	100.35	102.49	101.20	101.26	100.80
Si	2.880	2.849	2.896	2.752	2.761	2.759	2.754
Al	1.079	1.135	1.086	1.234	1.230	1.219	1.243
Fe2+	0.012	0.014	0.009	0.007	0.006	0.006	0.009
Ca	0.090	0.127	0.096	0.212	0.221	0.223	0.215
Na	1.035	0.908	0.944	0.849	0.807	0.831	0.798
K	0.005	0.006	0.006	0.005	0.006	0.017	0.009
Ca/Ca+Na	0.080	0.123	0.092	0.200	0.215	0.212	0.212
Al*/SiAl	0.082	0.137	0.088	0.237	0.232	0.224	0.244
An	0.080	0.122	0.092	0.199	0.214	0.208	0.210
Ab	0.916	0.872	0.902	0.796	0.780	0.776	0.781
Or	0.004	0.006	0.006	0.005	0.006	0.016	0.009

	(RIM?)					(RIM)	(RIM)	(CORE)
	-449F 1/10E PL IN	-449F 1/10F PLAG	-449F 1/10G PL IN	-449F 1/10H PL IN	-449F 1/10I PL IN	-449F 1/10J PL IN	-449F 1/10K PL IN	-449F 1/10L PLAG
SiO2	65.69	66.40	70.11	67.14	63.90	67.88	66.98	63.62
Al2O3	22.14	21.58	20.16	21.09	23.77	21.04	21.65	23.67
FeO	0.19	0.22	0.17	0.39	0.25	0.47	0.47	0.22
CaO	2.81	1.89	2.12	1.68	4.12	0.28	0.37	4.37
Na2O	10.55	10.94	10.84	10.97	9.44	10.59	11.13	9.70
K2O	0.11	0.11	0.13	0.09	0.23	0.72	0.67	0.14
Total	101.49	101.14	103.53	101.36	101.70	100.98	101.26	101.72
Si	2.856	2.889	2.970	2.913	2.782	2.945	2.908	2.774
Al	1.135	1.107	1.007	1.079	1.220	1.076	1.108	1.217
Fe2+	0.007	0.008	0.006	0.014	0.009	0.017	0.017	0.008
Ca	0.131	0.088	0.096	0.078	0.192	0.013	0.017	0.204
Na	0.889	0.923	0.890	0.923	0.797	0.891	0.937	0.820
K	0.006	0.006	0.007	0.005	0.013	0.040	0.037	0.008
Ca/Ca+Na	0.128	0.087	0.097	0.078	0.194	0.014	0.018	0.199
Al*/SiAl	0.136	0.107	0.007	0.080	0.220	0.074	0.106	0.219
An	0.128	0.087	0.097	0.078	0.192	0.014	0.017	0.198
Ab	0.866	0.908	0.896	0.917	0.795	0.944	0.946	0.795
Or	0.006	0.006	0.007	0.005	0.013	0.042	0.037	0.008

Appendix 10: Sample 79-449f (cont.)

	--PL IN GAR--		------PLAGIOCLASE AT GARNET RIM------				
	-449F 1/10M PL IN	-449F /1/10 PL AV	-449F 1/11A PL @	-449F 1/11B PL @	-449F 1/11C PL@RI	-449F 1/11D PL @R	-449F /1/11 PLAVG
SiO2	63.33	65.07	63.96	65.12	62.14	63.36	63.54
Al2O3	23.68	22.65	22.87	22.82	23.88	22.76	23.16
FeO	0.16	0.25	0.27	0.64	0.08	0.03	0.25
CaO	4.42	3.17	3.66	3.17	4.49	3.29	3.65
Na2O	9.76	10.19	10.04	10.80	9.43	10.40	10.20
K2O	0.11	0.22	0.14	0.09	0.11	0.11	0.11
Total	101.46	101.54	100.95	102.64	100.12	99.94	100.91
Si	2.770	2.832	2.806	2.815	2.753	2.806	2.791
Al	1.221	1.162	1.183	1.163	1.247	1.188	1.199
Fe2+	0.006	0.009	0.010	0.023	0.003	0.001	0.009
Ca	0.207	0.148	0.172	0.147	0.213	0.156	0.172
Na	0.828	0.860	0.854	0.905	0.810	0.893	0.869
K	0.006	0.012	0.008	0.005	0.006	0.006	0.006
Ca/Ca+Na	0.200	0.147	0.168	0.140	0.208	0.149	0.165
Al*/SiAl	0.223	0.163	0.185	0.167	0.247	0.189	0.201
An	0.199	0.145	0.166	0.139	0.207	0.148	0.164
Ab	0.795	0.843	0.826	0.856	0.787	0.846	0.830
Or	0.006	0.012	0.008	0.005	0.006	0.006	0.006

	------PLAGIOCLASE INCLUSION IN GARNET--------					
	(RIM)	(---CORE?---)		(RIM?)	(CORE?)	—
	-449F 1/16D PL IN	-449F 1/16E PL IN	-449F 1/16F PL IN	-449F 1/16G PL IN	-449F 1/16H PL IN	-449F /1/16 AVGPL
SiO2	68.48	66.80	68.26	65.92	66.42	66.18
Al2O3	20.21	20.99	20.35	21.80	21.49	21.63
FeO	0.61	0.44	0.28	0.55	0.17	0.36
CaO	0.24	1.71	0.58	2.51	2.19	2.36
12.67	10.96	11.85	10.66	11.35	11.01	
K2O	0.05	0.11	0.05	0.05	0.09	0.07
Total	102.26	101.01	101.37	101.50	101.71	101.61
Si	2.949	2.910	2.954	2.867	2.882	2.875
Al	1.026	1.078	1.038	1.118	1.099	1.108
Fe2+	0.022	0.016	0.010	0.020	0.006	0.013
Ca	0.011	0.080	0.027	0.117	0.102	0.110
Na	1.058	0.926	0.994	0.899	0.955	0.927
K	0.003	0.006	0.003	0.003	0.005	0.004
Ca/Ca+Na	0.010	0.080	0.026	0.115	0.096	0.106
Al*/SiAl	0.027	0.079	0.038	0.120	0.101	0.110
An	0.010	0.079	0.026	0.115	0.096	0.106
Ab	0.987	0.915	0.971	0.882	0.899	0.890
Or	0.003	0.006	0.003	0.003	0.005	0.004

Appendix 10: Sample 79-449f (cont.)

	-------------PLAGIOCLASE INCLUSIONS IN GARNET---------------							
	(RIM?)		(CORE)		(RIM)		(CORE)	
	-449F 1/17B PL IN	-449F 1/17C PL IN	-449F 1/17D PL IN	-449F /1/17 AVGPL	-449F 1/18A PL IN	-449F 1/18B PL IN	-449F 1/18C PL IN	-449F /1/18 AVGPL
SiO2	68.72	68.66	68.44	66.97	69.13	68.86	68.82	68.94
Al2O3	20.11	20.26	20.35	20.09	20.36	20.10	20.02	20.15
FeO	0.61	0.47	0.44	0.49	0.31	0.28	0.44	0.33
CaO	0.32	0.28	0.32	0.32	0.33	0.37	0.26	0.33
Na2O	11.91	12.02	12.17	11.98	12.48	12.29	12.28	12.35
K2O	0.02	0.04	0.04	0.04	0.04	0.02	0.04	0.04
Total	101.69	101.73	101.76	99.89	102.64	101.92	101.86	102.14
Si	2.965	2.961	2.953	2.946	2.958	2.964	2.966	2.963
Al	1.023	1.030	1.035	1.042	1.027	1.020	1.017	1.021
Fe2+	0.022	0.017	0.016	0.018	0.011	0.010	0.016	0.012
Ca	0.015	0.013	0.015	0.015	0.015	0.017	0.012	0.015
Na	0.996	1.005	1.018	1.022	1.035	1.026	1.026	1.029
K	0.001	0.002	0.002	0.002	0.002	0.001	0.002	0.002
Ca/Ca+Na	0.015	0.013	0.015	0.014	0.014	0.016	0.012	0.014
Al*/SiAl	0.023	0.030	0.035	0.043	0.027	0.020	0.017	0.021
An	0.015	0.013	0.014	0.014	0.014	0.016	0.012	0.014
Ab	0.984	0.985	0.984	0.984	0.984	0.983	0.987	0.984
Or	0.001	0.002	0.002	0.002	0.002	0.001	0.002	0.002

	-------------PLAGIOCLASE INCLUSIONS IN GARNET---------------							
	(CORE)	(RIM)			(RIM)		(RIM)	
	-449F 1/19A PL IN	-449F 1/19B PL IN	-449F 1/19C PL IN	-449F 1/19D PL IN	-449F 1/19E PL IN	-449F /1/19 PLAVG	-449F 1/20A PL IN	-449F 1/20B PL IN
SiO2	59.73	66.79	59.16	59.22	60.15	59.50	63.11	62.52
Al2O3	26.09	20.87	26.80	25.57	25.92	25.98	24.38	24.27
FeO	0.27	1.06	0.30	1.02	0.68	0.70	0.55	0.33
CaO	7.76	5.77	8.43	7.04	6.95	7.44	5.04	5.06
Na2O	7.86	6.49	7.36	7.76	8.28	7.84	9.73	8.81
K2O	0.04	0.04	0.00	0.04	0.04	0.04	0.05	0.05
Total	101.75	101.02	102.06	100.64	102.02	101.50	102.86	101.04
Si	2.629	3.632	2.599	2.638	2.641	2.628	2.734	2.745
Al	1.354	1.338	1.388	1.343	1.342	1.353	1.245	1.256
Fe2+	0.010	0.048	0.011	0.038	0.025	0.026	0.020	0.012
Ca	0.366	0.336	0.397	0.336	0.327	0.352	0.234	0.238
Na	0.671	0.684	0.627	0.670	0.705	0.671	0.817	0.750
K	0.002	0.003	0.000	0.002	0.002	0.002	0.003	0.003
Ca/Ca+Na	0.353	0.329	0.388	0.334	0.317	0.344	0.223	0.241
Al*/SiAl	0.360	0.172	0.393	0.350	0.348	0.360	0.250	0.256
An	0.352	0.328	0.388	0.333	0.316	0.343	0.222	0.240
Ab	0.646	0.669	0.612	0.665	0.682	0.655	0.775	0.757
Or	0.002	0.003	0.000	0.002	0.002	0.002	0.003	0.003

Appendix 10: Sample 79-449f (cont.)

	---PLAGIOCLASE INCLUSION IN GARNET--- (CORE)					--PLAG AT GARNET RIM--		
	-449F 1/20C PL IN	-449F /1/20 PLAVG	-449F 1/21A PL IN	-449F 1/21B PL IN	-449F /1/21 PLAVG	-449F 1/22A PL@GA	-449F 1/22B PL@GA	-449F /1/22 PLAVG
SiO2	62.29	62.64	62.83	63.15	62.98	64.79	64.90	64.84
Al2O3	24.43	24.35	23.98	23.84	23.91	22.73	22.10	22.41
FeO	0.35	0.41	0.33	0.38	0.36	0.47	0.27	0.38
CaO	5.45	5.19	4.76	4.81	4.79	2.94	2.83	2.88
Na2O	8.88	9.14	9.89	9.71	9.80	10.96	10.50	10.73
K2O	0.05	0.05	0.07	0.07	0.07	0.05	0.05	0.05
Total	101.46	101.79	101.86	101.96	101.91	101.94	100.66	101.30
Si	2.729	2.736	2.745	2.755	2.750	2.817	2.847	2.832
Al	1.262	1.254	1.235	1.226	1.231	1.165	1.143	1.154
Fe2+	0.013	0.015	0.012	0.014	0.013	0.017	0.010	0.014
Ca	0.256	0.243	0.223	0.225	0.224	0.137	0.133	0.135
Na	0.754	0.774	0.838	0.821	0.830	0.924	0.893	0.909
K	0.003	0.003	0.004	0.004	0.004	0.003	0.003	0.003
Ca/Ca+Na	0.253	0.239	0.210	0.215	0.213	0.129	0.130	0.129
Al*/SiAl	0.264	0.257	0.240	0.230	0.235	0.168	0.144	0.156
An	0.253	0.238	0.209	0.214	0.212	0.129	0.129	0.129
Ab	0.744	0.759	0.787	0.782	0.784	0.868	0.868	0.868
Or	0.003	0.003	0.004	0.004	0.004	0.003	0.003	0.003

Appendix 10: Sample 79-449f (cont.)

PLAGIOCLASE INCLUSIONS IN GARNET

	(CORE)	(RIM)	(RIM)	(CORE)	(RIM)	(RIM)		
	449F 1/16D CO PL	449F 1/16E RI PL	449F 1/18A RI PL	449F 1/24A CO PL	449F 1/24C RI PL	449F 1/24B RI PL	449F 1/24D PL IN	449F 1/25A PL I
SiO2	63.62	66.16	65.77	59.32	58.63	57.81	58.36	63.90
Al2O3	21.24	19.71	19.69	23.83	23.31	24.92	23.87	19.67
FeO	0.29	0.13	0.35	0.42	0.80	0.52	0.28	0.63
CaO	2.17	0.21	0.50	5.32	4.92	6.48	5.23	0.57
Na2O	10.33	11.70	11.64	8.65	8.71	7.83	8.58	11.21
K2O	0.07	0.04	0.03	0.09	0.12	0.09	0.10	0.05
Total	97.73	97.95	97.98	97.61	96.49	97.64	96.43	96.03
Si	2.868	2.958	2.947	2.707	2.712	2.647	2.696	2.927
Al	1.129	1.039	1.040	1.282	1.271	1.345	1.300	1.062
Fe2+	0.011	0.005	0.013	0.016	0.031	0.020	0.011	0.024
Ca	0.105	0.010	0.024	0.260	0.244	0.318	0.259	0.028
Na	0.903	1.014	1.011	0.765	0.781	0.695	0.769	0.996
K	0.004	0.002	0.002	0.005	0.007	0.005	0.006	0.003
Ca/Ca+Na	0.104	0.010	0.023	0.254	0.238	0.314	0.252	0.027
AlA/SiAl	0.129	0.039	0.041	0.285	0.276	0.348	0.301	0.063
An	0.104	0.010	0.023	0.252	0.236	0.312	0.250	0.027
Ab	0.892	0.988	0.975	0.743	0.757	0.683	0.744	0.970
Or	0.004	0.002	0.002	0.005	0.007	0.005	0.006	0.003

Appendix 10: Sample 79-449f (cont.)

	CHLORITE INCLUSIONS IN GARNET							
	(CORE)	(RIM)	(CORE)	(RIM)	(CORE)	(RIM)	(RIM)	(RIM)
	449F 1/37A CO CH	449F 1/37B RI CH	449F 1/38A CO CH	449F 1/38B RI CH	449F 1/39A CO CH	449F 1/39B RI CH	449F 1/41A RI CH	449F 1/42A RI CH
SiO2	24.69	24.11	25.18	24.99	24.15	23.65	24.08	23.56
Al2O3	21.82	21.66	21.40	21.44	22.02	22.30	21.67	22.36
MgO	15.62	12.14	16.43	16.47	14.57	10.97	13.71	10.53
FeO	23.38	27.81	23.04	23.65	25.07	28.83	26.26	29.71
MnO	0.63	1.33	0.53	0.69	0.78	1.65	0.97	1.36
CaO	0.03	0.04	0.03	0.03	0.03	0.05	0.04	0.03
Total	86.18	87.09	86.62	87.27	86.62	87.45	86.74	87.55
Si	2.255	2.242	2.281	2.258	2.218	2.206	2.227	2.202
Al	2.349	2.374	2.286	2.283	2.385	2.452	2.363	2.464
Mg	2.126	1.682	2.219	2.217	1.994	1.525	1.890	1.466
Fe2+	1.786	2.163	1.746	1.787	1.926	2.249	2.031	2.322
Mn	0.049	0.105	0.041	0.053	0.061	0.130	0.076	0.108
Ca	0.003	0.004	0.003	0.003	0.003	0.005	0.004	0.003
Fe/Fe+Mg	0.457	0.563	0.440	0.446	0.491	0.596	0.518	0.613

Appendix 10: Sample 79-449f (cont.)

	CHLORITE INCLUSIONS IN GARNET							
	(CORE)	(RIM)	(RIM)	(CORE)	(RIM)	(CORE)	(RIM)	
	449F 1/32A CO CH	449F 1/32B RI CH	449F 1/32C RI CH	449F 1/33A CO CH	449F 1/33B RI CH	449F 1/35A CO CH	449F 1/35B RI CH	449F 1/36A CHL I
SiO2	23.64	23.67	23.97	25.09	25.14	24.73	23.99	23.82
Al2O3	23.49	23.49	24.01	20.18	20.73	21.86	21.76	21.04
MgO	18.08	18.59	18.71	15.84	14.77	16.66	13.39	12.75
FeO	18.45	18.91	18.65	23.94	25.89	22.20	26.33	26.32
MnO	0.25	0.29	0.25	0.54	0.85	0.49	1.13	0.95
CaO	0.00	0.03	0.03	0.04	0.05	0.04	0.05	0.06
Total	83.91	84.97	85.62	85.63	87.43	85.98	86.65	84.93
Si	2.159	2.141	2.144	2.316	2.296	2.249	2.224	2.255
Al	2.529	2.504	2.532	2.196	2.232	2.343	2.378	2.349
Mg	2.460	2.505	2.495	2.179	2.011	2.258	1.850	1.799
Fe2+	1.409	1.430	1.395	1.848	1.978	1.688	2.041	2.084
Mn	0.019	0.022	0.019	0.042	0.066	0.038	0.089	0.076
Ca	0.000	0.003	0.003	0.004	0.005	0.004	0.005	0.006
Fe/Fe+Mg	0.364	0.363	0.359	0.459	0.496	0.428	0.525	0.537

Appendix 10: Sample 79-449f (cont.)

	CHLORITE INCLUSIONS IN GARNET								
	(CORE)	(RIM)	(CORE)	(RIM)	(CORE)	(RIM)			
	449F 1/43A CO CH	449F 1/43B RI CH	449F 1/44A CO CH	449F 1/44B RI CH	449F 1/23E CO CH	449F 1/23F RI CH	449F 1/23G CHL I	449F 1/23H CHL I	449F 1/23I CHL I
SiO2	25.13	23.69	22.60	22.71	23.71	23.76	23.35	24.81	21.65
Al2O3	21.10	21.77	22.78	23.05	21.98	21.79	21.82	21.71	24.68
MgO	16.75	11.63	8.46	7.41	11.51	11.38	11.19	16.77	4.88
FeO	22.62	28.69	31.73	33.36	27.44	27.33	28.44	21.86	34.69
MnO	0.52	1.53	1.31	1.83	1.32	1.53	1.46	0.49	1.97
CaO	0.04	0.06	0.06	0.05	0.04	0.05	0.05	0.02	0.04
Total	86.15	87.36	86.94	88.41	86.00	85.84	86.31	85.66	87.90
Si	2.285	21..211	256	2.150	2.231	2.241	2.205	2.260	2.079
Al	2.262	2.395	2.562	2.573	2.438	2.423	2.430	2.331	2.794
Mg	2.270	1.617	1.202	1.046	1.614	1.600	1.575	2.276	0.699
Fe2+	1.720	2.239	2.531	2.642	2.159	2.156	2.246	1.665	2.786
Mn	0.040	0.121	0.106	0.147	0.105	0.122	0.117	0.038	0.160
Ca	0.004	0.006	0.006	0.005	0.004	0.005	0.005	0.002	0.004
Fe/Fe+Mg	0.431	0.581	0.678	0.716	0.572	0.574	0.588	0.422	0.799

Appendix 10: Sample 79-449f (cont.)

	-----------CHLORITE INCLUSION IN GARNET		(----CORE---)		(RIM)	--------------	(AVG)
	-449F /1/7A /CHL	-449F /1/7B CHL I	-449F /1/7C CHL C	-449F /1/7C CHL C	-449F /1/7E CHL R	-449F /1/7E CHL R	-449F /1/7 CHL A
SiO2	25.03	25.12	25.17	25.41	24.60	24.66	25.00
Al2O3	21.61	21.46	21.34	22.11	22.02	22.13	21.79
TiO2	0.08	0.08	0.07	0.09	0.13	0.11	0.09
MgO	12.83	15.94	15.02	15.65	12.23	12.88	14.11
FeO	28.11	25.27	25.56	25.06	28.14	28.17	26.73
MnO	1.07	0.63	0.74	0.57	1.32	1.16	0.91
CaO	0.00	0.00	0.00	0.00	0.02	0.00	0.00
Total	88.73	88.50	87.91	88.89	88.45	89.11	88.63
Si	5.312	5.260	5.316	5.277	5.248	5.216	5.270
Al	5.407	5.297	5.313	5.414	5.539	5.520	5.414
Ti	0.013	0.012	0.012	0.014	0.021	0.018	0.015
Mg	4.058	4.973	4.726	4.843	3.889	4.060	4.433
Fe2+	4.990	4.425	4.515	4.353	5.022	4.985	4.712
Mn	0.192	0.112	0.133	0.101	0.238	0.207	0.163
Ca	0.000	0.000	0.000	0.000	0.004	0.001	0.000
Fe/Fe+Mg	0.552	0.471	0.489	0.473	0.564	0.551	0.515

	----CHLORITE INCLUSIONS IN GARNET----				
	-449F 1/23A CHL I	-449F 1/23B CHL I	-449F 1/23C CHL I	-449F 1/23D CHL I	-449F /1/23 CHAVG
SiO2	24.82	24.54	25.20	24.02	24.64
Al2O3	22.15	22.18	22.68	22.22	22.31
TiO2	0.03	0.08	0.03	0.07	0.06
MgO	13.92	11.89	13.10	11.04	12.50
FeO	26.49	29.36	27.23	29.40	28.13
MnO	0.99	1.31	1.03	1.54	1.22
CaO	0.01	0.01	0.01	0.01	0.01
Total	88.41	89.38	89.27	88.30	88.86
Si	5.241	5.213	5.276	5.182	5.227
Al	5.513	5.554	5.598	5.652	5.578
Ti	0.005	0.013	0.005	0.012	0.009
Mg	4.380	3.765	4.087	3.548	3.951
Fe2+	4.678	5.216	4.769	5.305	4.989
Mn	0.177	0.235	0.183	0.281	0.219
Ca	0.003	0.002	0.002	0.002	0.002
Fe/Fe+Mg	0.516	0.581	0.539	0.599	0.558

Appendix 10: Sample 79-449f (cont.)

	-----BIOTITE INCLUSION IN GARNET----- (RIM)	(---CORE---)			
	-449F /1/8A BIO I	-449F /1/8B BIO I	-449F /1/8C BIO I	-449F /1/8D BIO I	-449F /1/8 BIO A
SiO2	38.03	37.65	37.38	36.83	37.48
Al2O3	20.15	19.99	20.78	20.10	20.26
TiO2	1.31	1.35	1.26	1.17	1.27
MgO	15.55	14.90	14.83	15.59	15.22
FeO	13.01	12.86	12.97	13.14	12.99
MnO	0.17	0.10	0.11	0.07	0.11
CaO	0.00	0.00	0.00	0.00	0.00
Na2O	0.54	0.54	0.48	0.35	0.48
K2O	8.21	8.04	6.85	7.54	7.66
Total	96.98	95.44	94.66	94.79	95.47
Si	5.445	5.471	5.435	5.387	5.435
Aliv	2.555	2.529	2.565	2.613	2.565
Alvi	0.846	0.896	0.998	0.853	0.899
Ti	0.143	0.149	0.139	0.130	0.140
Mg	3.319	3.226	3.213	3.399	3.289
Fe2+	1.558	1.563	1.577	1.607	1.576
Mn	0.021	0.012	0.014	0.009	0.014
Sum Oct	5.887	5.846	5.941	5.998	5.918
Ca	0.000	0.000	0.000	0.000	0.000
Na	0.150	0.153	0.135	0.099	0.134
K	1.500	1.491	1.271	1.408	1.418
Sum A	1.650	1.644	1.406	1.507	1.552
(OH)	0.000	0.000	0.000	0.000	0.000
Fe/Fe+Mg	0.319	0.326	0.329	0.321	0.324
X(Ca)	0.000	0.000	0.000	0.000	0.000
X(Na)	0.091	0.093	0.096	0.066	0.086
X(K)	0.909	0.907	0.904	0.934	0.914

Appendix 10: Sample 79-449 f(cont.)

	MATRIX CORDIERITE					
	(CORE)	(RIM)	(RIM)	(1/2)		(RIM)
	449F 1/31A CD CO	449F 1/31B CD RI	449F 1/31C CD RI	449F 1/31D CD HA	449F 1/31E CORD	449F 1/31F CD RI
SiO2	47.79	47.06	47.02	47.36	47.12	46.66
Al2O3	32.89	32.81	32.68	32.79	32.83	33.14
MgO	9.77	9.82	9.75	9.98	9.85	9.84
FeO	5.59	5.49	5.65	5.51	5.55	5.48
MnO	0.24	0.29	0.25	0.24	0.25	0.25
CaO	0.03	0.01	0.03	0.00	0.03	0.03
Total	96.31	95.47	95.38	95.88	95.63	95.41
Si	3.310	3.290	3.293	3.296	3.290	3.266
Al	2.686	2.704	2.698	2.691	2.702	2.735
Mg	1.009	1.023	1.018	1.035	1.025	1.027
Fe2+	0.324	0.321	0.331	0.321	0.324	0.321
Mn	0.014	0.017	0.015	0.014	0.015	0.015
Ca	0.002	0.001	0.002	0.000	0.002	0.002
Fe/Fe+Mg	0.243	0.239	0.245	0.237	0.240	0.238

Appendix 10: Sample 79-449f (cont.)

	MATRIX CORDIERITE	(RIM)	(---CORE?---)		
	79-44 9F/3/ 2A MA	79-44 9F/3/ 2B CO	79-44 9F/3/ 2C MA	79-44 9F/3/ 2D MA	79-44 9F/3/ 2 AVG
SiO2	48.75	49.07	48.78	49.21	48.95
Al2O3	32.28	33.27	33.12	33.28	32.99
TiO2	0.00	0.00	0.00	0.00	0.00
MgO	10.11	10.37	10.54	10.36	10.34
FeO	5.48	5.56	5.40	5.50	5.48
MnO	0.31	0.33	0.29	0.35	0.32
Total	97.20	98.79	98.51	99.14	98.41
Si	5.021	4.975	4.962	4.975	4.983
Al	3.920	3.976	3.972	3.967	3.959
Ti	0.000	0.000	0.000	0.000	0.000
Mg	1.552	1.567	1.597	1.561	1.569
Fe2+	0.472	0.471	0.459	0.465	0.467
Mn	0.027	0.028	0.025	0.030	0.028
Fe/Fe+Mg	0.233	0.231	0.223	0.230	0.229

	CORDIERITE INCLUSION IN GARNET	(RIM?)	(CORE)	
	-449F /1/9A CORD	-449F /1/9B CD IN	-449F /1/9C CD IN	-449F 1/9CD INAVG
SiO2	49.76	49.57	49.44	49.58
Al2O3	33.51	33.69	33.93	33.71
TiO2	0.00	0.00	0.00	0.00
MgO	10.48	10.30	10.46	10.41
FeO	5.50	5.64	5.53	5.56
MnO	0.28	0.35	0.32	0.32
Total	99.53	99.55	99.67	99.58
Si	4.997	4.982	4.962	4.980
Al	3.968	3.992	4.014	3.992
Ti	0.000	0.000	0.000	0.000
Mg	1.568	1.543	1.564	1.558
Fe2+	0.462	0.474	0.464	0.467
Mn	0.024	0.030	0.027	0.027
Fe/Fe+Mg	0.228	0.235	0.229	0.231

Appendix 10: Sample 79-449f (cont.)

	---BIO AT GAR RIM----			MATRIX BIO NEAR CORD	
	79-44 9F/1/ 4B BI	79-44 9F/1/ 5B BI	79-44 9F/1/ 6B BI	79-44 9F/3/ 1B MA	79-44 9F/3/ 1C MA
SiO2	37.51	37.08	37.89	37.33	37.37
Al2O3	19.56	19.27	19.13	19.59	19.76
TiO2	1.34	1.37	1.32	1.11	1.08
MgO	14.60	14.48	14.95	14.73	14.73
FeO	12.98	13.10	13.11	13.05	12.72
MnO	0.05	0.10	0.04	0.08	0.03
CaO	0.00	0.00	0.00	0.00	0.00
Na2O	0.40	0.38	0.44	0.42	0.53
K2O	8.66	8.65	8.73	8.61	8.51
Total	95.11	94.44	95.61	94.93	94.73
Si	5.494	5.481	5.525	5.482	5.485
Aliv	2.506	2.519	2.475	2.518	2.515
Alvi	0.872	0.839	0.814	0.873	0.905
Ti	0.149	0.154	0.146	0.124	0.120
Mg	3.187	3.190	3.249	3.223	3.223
Fe2+	1.590	1.620	1.598	1.603	1.561
Mn	0.006	0.013	0.005	0.010	0.004
Sum Oct	5.804	5.816	5.812	5.833	5.813
Ca	0.000	0.000	0.000	0.000	0.000
Na	0.113	0.109	0.124	0.120	0.151
K	1.619	1.631	1.623	1.613	1.594
Sum A	1.732	1.740	1.747	1.733	1.745
(OH)	0.000	0.000	0.000	0.000	0.000
Fe/Fe+Mg	0.333	0.337	0.330	0.332	0.326
X(Ca)	0.000	0.000	0.000	0.000	0.000
X(Na)	0.065	0.063	0.071	0.069	0.087
X(K)	0.935	0.937	0.929	0.931	0.913

Appendix 10: Sample 79-449f (cont.)

	------MATRIX STAUROLITE------			
	(CORE)	(----RIM----)		(AVG)
	79-44 9F/4/ 1A MA	79-44 9F/4/ 1B MA	79-44 9F/4/ 1C MA	79-44 9F/4/ 1 MAT
SiO2	27.21	27.06	27.36	27.21
Al2O3	54.91	54.10	54.55	54.53
TiO2	0.48	0.50	0.44	0.47
MgO	2.82	2.62	2.73	2.72
FeO	11.72	11.36	11.36	11.48
MnO	0.42	0.40	0.35	0.38
ZnO	0.84	0.87	0.84	0.85
CaO	0.00	0.00	0.02	0.00
Total	98.40	96.91	97.66	97.65
Si	3.742	3.773	3.783	3.766
Al	8.903	8.893	8.891	8.896
Ti	0.050	0.053	0.046	0.049
Mg	0.579	0.545	0.562	0.562
Fe2+	1.348	1.325	1.314	1.329
Mn	0.049	0.047	0.041	0.045
Zn	0.085	0.090	0.086	0.087
Ca	0.000	0.000	0.003	0.000
Fe/Fe+Mg	0.700	0.709	0.700	0.703

Appendix 10: Sample 79-449j

	GAR RIM	GARNET TRAVERSE.........................								
	79-44 9J/3/ 1A GA	79-44 9J/3/ 1B GA	79-44 9J/3/ 1C GA	79-44 9J/3/ 1D GA	79-44 9J/3/ 1E GA	79-44 9J/3/ 1F GA	79-44 9J/3/ 1J GA	79-44 9J/3/ 1H GA	79-44 9J/3/ 1G GA	79-44 9J/3/ 1K GA
SiO2	34.61	34.81	37.25	36.63	37.43	37.68	37.44	34.90	36.44	36.80
Al2O3	22.44	22.25	22.72	22.65	22.80	22.43	22.40	22.49	22.49	21.26
MgO	5.05	4.92	5.01	5.06	4.80	4.70	4.18	3.66	3.96	3.74
FeO	28.62	27.65	27.90	28.40	27.90	27.54	25.37	24.24	25.89	24.32
MnO	7.85	7.55	8.18	8.05	8.67	9.52	11.18	10.75	10.98	10.76
CaO	0.77	0.66	0.67	0.69	0.71	0.72	1.42	2.67	1.55	1.10
Total	99.34	97.85	101.73	101.49	102.30	102.60	101.99	98.70	101.31	97.99
Si	2.809	2.851	2.919	2.889	2.921	2.938	2.938	2.844	2.893	2.996
Al	2.147	2.148	2.099	2.106	2.098	2.062	2.072	2.161	2.105	2.040
Mg	0.611	0.600	0.585	0.595	0.558	0.546	0.489	0.444	0.468	0.454
Fe2+	1.943	1.894	1.828	1.873	1.821	1.796	1.665	1.652	1.719	1.656
Mn	0.540	0.524	0.543	0.538	0.573	0.629	0.743	0.742	0.738	0.742
Ca	0.067	0.058	0.056	0.058	0.059	0.060	0.119	0.233	0.132	0.096
Fe/Fe+Mg	0.761	0.759	0.758	0.759	0.765	0.767	0.773	0.788	0.786	0.785
Pyrope	0.193	0.195	0.194	0.194	0.185	0.180	0.162	0.145	0.153	0.154
Alman	0.615	0.616	0.607	0.611	0.605	0.593	0.552	0.538	0.562	0.562
Spess	0.171	0.170	0.180	0.176	0.190	0.208	0.246	0.242	0.241	0.252
Gross	0.021	0.019	0.019	0.019	0.020	0.020	0.039	0.076	0.043	0.033

Appendix 10: Sample 79-449j (cont.)

	GARNET CORE		.........GARNET TRAVERSE..........						GAR RIM	
	79-44 9J/3/ 1L GA	79-44 9J/3/ 1M GA	79-44 9J/3/ 1O GA	79-44 9J/3/ 1N GA	79-44 9J/3/ 1P GA	79-44 9J/3/ 1Q GA	79-44 9J/3/ 1R GA	79-44 9J/3/ 1S GA	79-44 9J/3/ 1T GA	79-44 9J/3/ 1 GAR
SiO2	38.03	37.13	37.48	37.82	37.94	37.33	37.38	37.48	37.85	36.97
Al2O3	21.85	22.50	22.23	22.43	22.01	22.48	22.36	22.20	22.31	22.33
MgO	4.27	4.56	4.42	4.59	4.57	4.85	4.73	4.85	4.77	4.57
FeO	26.68	27.03	27.31	27.07	27.58	27.09	28.17	27.84	28.01	27.08
MnO	10.71	9.92	9.46	9.13	8.86	8.57	8.48	8.62	8.06	9.23
CaO	0.83	0.84	0.87	0.81	0.85	0.95	0.94	0.88	0.86	0.99
Total	102.38	101.99	101.77	101.85	101.81	101.27	102.06	101.88	101.87	101.17
Si	2.976	2.917	2.946	2.959	2.974	2.936	2.930	2.940	2.960	2.923
Al	2.016	2.084	2.060	2.069	2.034	2.084	2.066	2.053	2.057	2.082
Mg	0.498	0.534	0.518	0.535	0.534	0.568	0.553	0.567	0.556	0.538
Fe2+	1.746	1.776	1.795	1.771	1.808	1.782	1.847	1.826	1.832	1.791
Mn	0.710	0.660	0.630	0.605	0.588	0.571	0.563	0.573	0.534	0.618
Ca	0.070	0.071	0.073	0.068	0.071	0.080	0.079	0.074	0.072	0.084
Fe/Fe+Mg	0.778	0.769	0.776	0.768	0.772	0.758	0.770	0.763	0.767	0.769
Pyrope	0.165	0.176	0.172	0.180	0.178	0.189	0.182	0.187	0.186	0.177
Alman	0.577	0.584	0.595	0.594	0.602	0.594	0.607	0.601	0.612	0.591
Spess	0.235	0.217	0.209	0.203	0.196	0.190	0.185	0.188	0.178	0.204
Gross	0.023	0.023	0.024	0.023	0.024	0.027	0.026	0.024	0.024	0.028

Appendix 10: Sample 79-449j (cont.)

	MATRIX BIOTITE							
	79-44 9J/5/ 3A BI	79-44 9J/5/ 3B BI	79-44 9J/5/ 3C BI	79-44 9J/5/ 3 BIO	79-44 9J/4/ 2A BI	79-44 9J/4/ 2B BI	79-44 9J/4/ 2D BI	79-44 9J/4/ 2 BIO
SiO2	38.25	38.30	37.96	38.17	37.52	36.98	37.15	37.22
Al2O3	19.36	19.37	19.71	19.48	19.67	19.72	19.25	19.55
TiO2	1.40	1.29	1.27	1.32	1.35	1.39	1.30	1.34
MgO	15.07	14.85	15.19	15.03	14.99	14.84	14.92	14.92
FeO	13.56	13.28	13.74	13.52	12.87	13.52	12.82	13.07
MnO	0.20	0.15	0.22	0.20	0.21	0.18	0.19	0.19
CaO	0.00	0.00	0.00	0.00	0.00	0.01	0.02	0.01
Na2O	0.60	0.50	0.54	0.55	0.56	0.64	0.64	0.61
K2O	8.32	8.33	8.08	8.24	8.59	8.27	8.20	8.35
Total	96.77	96.07	96.72	96.52	95.76	95.55	94.50	95.27
Si	5.510	5.544	5.469	5.508	5.461	5.408	5.473	5.447
Aliv	2.490	2.456	2.531	2.492	2.539	2.592	2.527	2.553
Alvi	0.798	0.849	0.816	0.822	0.836	0.809	0.817	0.821
Ti	0.153	0.142	0.139	0.145	0.149	0.154	0.145	0.149
Mg	3.235	3.203	3.262	3.233	3.252	3.235	3.276	3.254
Fe2+	1.634	1.608	1.656	1.632	1.566	1.654	1.579	1.600
Mn	0.024	0.019	0.027	0.024	0.026	0.022	0.024	0.024
Sum Oct	5.844	5.821	5.900	5.856	5.829	5.874	5.841	5.848
Ca	0.000	0.000	0.000	0.000	0.000	0.002	0.003	0.001
Na	0.168	0.140	0.151	0.153	0.158	0.181	0.184	0.174
K	1.529	1.538	1.485	1.517	1.595	1.543	1.542	1.560
Sum A	1.697	1.678	1.636	1.670	1.753	1.726	1.729	1.735
(OH)	0.000	0.000	0.000	0.000	0.000	0.000	0.000	0.000
Fe/Fe+Mg	0.336	0.334	0.337	0.335	0.325	0.338	0.325	0.330
X(Ca)	0.000	0.000	0.000	0.000	0.000	0.001	0.002	0.001
X(Na)	0.099	0.083	0.092	0.092	0.090	0.105	0.106	0.100
X(K)	0.901	0.917	0.908	0.908	0.910	0.894	0.892	0.899

Appendix 10: Sample 79-449j (cont.)

	---------------------------MATRIX PALGIOCLASE---------------------------									
	79-44 9J/5/ 4A PL	79-44 9J/5/ 4B PL	79-44 9J/5/ 4C PL	79-44 9J/5/ 4 PLA	79-44 9J/4/ 1A PL	79-44 9J/4/ 1B PL	79-44 9J/4/ 1C PL	79-44 9J/4/ 1D PL	79-44 9J/4/ 1 PLA	79- 9J/ 3B
SiO2	64.78	64.70	64.40	64.63	64.67	62.58	65.00	64.29	64.12	63.
Al2O3	23.20	23.21	23.16	23.19	23.19	23.00	23.03	23.09	23.08	23.
FeO	0.00	0.00	0.00	0.00	0.00	0.05	0.00	0.03	0.03	0.
CaO	3.39	3.54	3.44	3.45	3.41	3.26	3.32	3.47	3.36	3.
Na2O	10.06	9.82	9.74	9.88	10.30	9.81	9.70	9.73	9.89	10.
K2O	0.09	0.09	0.09	0.09	0.11	0.12	0.09	0.16	0.13	0.
Total	101.52	101.36	100.83	101.24	101.68	98.82	101.14	100.78	100.60	100.
Si	2.816	2.816	2.816	2.816	2.810	2.797	2.830	2.815	2.813	2.
Al	1.189	1.191	1.194	1.191	1.188	1.212	1.182	1.192	1.194	1.
Fe2+	0.000	0.000	0.000	0.000	0.000	0.002	0.000	0.001	0.001	0.
Ca	0.158	0.165	0.161	0.161	0.159	0.156	0.155	0.163	0.158	0.1
Na	0.848	0.829	0.826	0.835	0.868	0.850	0.819	0.826	0.841	0.
K	0.005	0.005	0.005	0.005	0.006	0.007	0.005	0.009	0.007	0.
Ca/Ca+Na	0.157	0.166	0.163	0.162	0.155	0.155	0.159	0.165	0.158	0.1
Al*/SiAl	0.188	0.190	0.192	0.190	0.188	0.210	0.180	0.191	0.193	0.
An	0.156	0.165	0.162	0.161	0.154	0.154	0.158	0.163	0.157	0.1
Ab	0.839	0.830	0.833	0.834	0.840	0.839	0.837	0.828	0.836	0.
Or	0.005	0.005	0.005	0.005	0.006	0.007	0.005	0.009	0.007	0.

Appendix 10: Sample 79-449j (cont.)

	----------MATRIX PALGIOCLASE----------									
	79-44 9J/5/ 4A PL	79-44 9J/5/ 4B PL	79-44 9J/5/ 4C PL	79-44 9J/5/ 4 PLA	79-44 9J/4/ 1A PL	79-44 9J/4/ 1B PL	79-44 9J/4/ 1C PL	79-44 9J/4/ 1D PL	79-44 9J/4/ 1 PLA	79-44 9J/3/ 3B PL
SiO2	64.78	64.70	64.40	64.63	64.67	62.58	65.00	64.29	64.12	63.3
Al2O3	23.20	23.21	23.16	23.19	23.19	23.00	23.03	23.09	23.08	23.2
FeO	0.00	0.00	0.00	0.00	0.00	0.05	0.00	0.03	0.03	0.0
CaO	3.39	3.54	3.44	3.45	3.41	3.26	3.32	3.47	3.36	3.3
Na2O	10.06	9.82	9.74	9.88	10.30	9.81	9.70	9.73	9.89	10.0
K2O	0.09	0.09	0.09	0.09	0.11	0.12	0.09	0.16	0.13	0.1
Total	101.52	101.36	100.83	101.24	101.68	98.82	101.14	100.78	100.60	100.1
Si	2.816	2.816	2.816	2.816	2.810	2.797	2.830	2.815	2.813	2.79
Al	1.189	1.191	1.194	1.191	1.188	1.212	1.182	1.192	1.194	1.20
Fe2+	0.000	0.000	0.000	0.000	0.000	0.002	0.000	0.001	0.001	0.00
Ca	0.158	0.165	0.161	0.161	0.159	0.156	0.155	0.163	0.158	0.15
Na	0.848	0.829	0.826	0.835	0.868	0.850	0.819	0.826	0.841	0.86
K	0.005	0.005	0.005	0.005	0.006	0.007	0.005	0.009	0.007	0.00
Ca/Ca+Na	0.157	0.166	0.163	0.162	0.155	0.155	0.159	0.165	0.158	0.15
Al*/SiAl	0.188	0.190	0.192	0.190	0.188	0.210	0.180	0.191	0.193	0.20
An	0.156	0.165	0.162	0.161	0.154	0.154	0.158	0.163	0.157	0.15
Ab	0.839	0.830	0.833	0.834	0.840	0.839	0.837	0.828	0.836	0.83
Or	0.005	0.005	0.005	0.005	0.006	0.007	0.005	0.009	0.007	0.00

Appendix 10: Sample 79-449j (cont.)

	MATRIX PLAGIOCLASE							
	79-44 9J/3/ 3C PL	79-44 9J/3/ 3 PLA	79-44 9J/3/ 3A PL	79-44 9J/3/ 2A PL	79-44 9J/5/ 2A PL	79-44 9J/5/ 2B PL	79-44 9J/5/ 2 PLA	79-44 9J/2/ 3A PO
SiO2	62.70	63.28	63.87	64.50	61.10	62.12	61.60	62.43
Al2O3	23.27	23.22	23.17	20.19	22.79	22.45	22.62	23.47
FeO	0.08	0.08	0.11	1.03	0.00	0.11	0.05	0.03
CaO	3.42	3.38	3.38	0.68	3.39	3.28	3.33	3.27
Na2O	9.98	10.08	10.23	10.80	10.16	9.59	9.87	10.14
K2O	0.00	0.11	0.09	0.12	0.10	0.07	0.09	0.09
Total	99.45	100.14	100.85	97.32	97.54	97.62	97.57	99.43
Si	2.786	2.795	2.801	2.918	2.777	2.809	2.793	2.778
Al	1.219	1.209	1.198	1.077	1.221	1.197	1.209	1.231
Fe2+	0.003	0.003	0.004	0.039	0.000	0.004	0.002	0.001
Ca	0.163	0.160	0.159	0.033	0.165	0.159	0.162	0.156
Na	0.860	0.863	0.870	0.947	0.895	0.841	0.868	0.875
K	0.000	0.006	0.005	0.007	0.006	0.004	0.005	0.005
Ca/Ca+Na	0.159	0.156	0.155	0.034	0.156	0.159	0.157	0.151
Alλ/SiAl	0.218	0.208	0.198	0.077	0.221	0.196	0.209	0.229
An	0.159	0.155	0.154	0.033	0.155	0.158	0.157	0.151
Ab	0.841	0.839	0.841	0.959	0.840	0.838	0.839	0.845
Or	0.000	0.006	0.005	0.007	0.006	0.004	0.005	0.005

Appendix 10: Sample 79-449j (cont.)

	MATRIX STAUROLITE						
	79-44 9J/4/ 3A ST	79-44 9J/4/ 3B ST	79-44 9J/4/ 3C ST	79-44 9J/4/ 3 STA	79-44 9J/1/ 1A ST	79-44 9J/1/ 1B ST	79-44 9J/1/ 1C ST
SiO2	27.58	27.87	27.64	27.70	28.16	28.07	28.21
Al2O3	56.96	56.38	55.94	56.42	56.08	56.38	56.16
TiO2	0.63	0.62	0.63	0.63	0.49	0.55	0.60
MgO	2.72	2.74	2.60	2.69	2.65	2.50	2.55
FeO	11.87	12.20	11.59	11.88	11.91	11.89	12.22
MnO	0.51	0.53	0.54	0.53	0.52	0.49	0.47
ZnO	1.13	1.19	0.90	1.08	1.00	0.99	0.84
CaO	0.01	0.01	0.00	0.01	0.00	0.00	0.01
Total	101.42	101.53	99.84	100.93	100.81	100.87	101.05
Si	3.686	3.727	3.743	3.718	3.781	3.764	3.780
Al	8.974	8.887	8.929	8.930	8.876	8.914	8.870
Ti	0.064	0.063	0.065	0.064	0.050	0.056	0.061
Mg	0.542	0.546	0.525	0.538	0.530	0.499	0.509
Fe2+	1.327	1.364	1.312	1.334	1.337	1.334	1.369
Mn	0.058	0.060	0.062	0.060	0.059	0.056	0.053
Zn	0.112	0.117	0.090	0.107	0.099	0.098	0.083
Ca	0.002	0.001	0.000	0.001	0.000	0.000	0.001
Fe/Fe+Mg	0.710	0.714	0.714	0.713	0.716	0.728	0.729

Appendix 10: Sample 79-449j (cont.)

----MATRIX CHLORITE (RETROGRADE)-----

	79-44 9J/2/ 1A CH	79-44 9J/2/ 1B CH	79-44 9J/2/ 1C CH	79-44 9J/2/ 1 CHL	79-44 9J/2/ 2A MO
SiO2	25.43	25.95	25.93	25.77	25.81
Al2O3	24.43	24.82	24.36	24.53	24.30
TiO2	0.05	0.11	0.13	0.10	0.11
MgO	21.33	21.45	21.23	21.33	20.74
FeO	17.36	17.06	17.24	17.22	17.15
MnO	0.24	0.23	0.19	0.22	0.25
CaO	0.00	0.01	0.00	0.00	0.01
Na2O	0.00	0.00	0.00	0.00	0.00
K2O	0.00	0.00	0.00	0.00	0.00
Total	88.83	89.62	89.09	89.18	88.37
Si	5.063	5.104	5.136	5.101	5.153
Al	5.734	5.754	5.688	5.725	5.721
Ti	0.008	0.016	0.020	0.015	0.017
Mg	6.328	6.285	6.265	6.292	6.170
Fe2+	2.890	2.805	2.856	2.850	2.863
Mn	0.040	0.038	0.032	0.037	0.043
Ca	0.000	0.002	0.001	0.001	0.002
Na	0.000	0.000	0.000	0.000	0.000
K	0.000	0.000	0.000	0.000	0.000
Fe/Fe+Mg	0.314	0.309	0.313	0.312	0.317

Appendix 10: Sample 79-449j (cont.)

	------MATRIX CORDIERITE-------			
	79449J 5/1A CORD	79449J 5/1B CORD	79449J 5/1C CORD	79449J 5/1 CD AVG
SiO2	31.32	49.22	48.84	49.04
Al2O3	21.83	34.06	33.98	34.08
TiO2	0.00	0.00	0.00	0.00
MgO	6.54	10.04	10.09	10.13
FeO	39.13	5.50	5.39	5.35
MnO	0.24	0.39	0.28	0.35
CaO	0.00	0.00	0.00	0.00
Na2O	0.00	0.00	0.00	0.00
K2O	0.00	0.00	0.00	0.00
Total	99.06	99.22	98.58	98.95
Si	4.948	4.962	4.951	4.953
Al	4.065	4.048	4.061	4.058
Ti	0.000	0.000	0.000	0.000
Mg	1.539	1.509	1.525	1.524
Fe2+	5.170	0.464	0.457	0.452
Mn	0.032	0.033	0.024	0.030
Ca	0.000	0.000	0.000	0.000
Na	0.000	0.000	0.000	0.000
K	0.000	0.000	0.000	0.000
Fe/Fe+Mg	0.771	0.235	0.231	0.229